CRANFIELD UNIVERSITY

ADRIAN DE LA MORENA DIAZ

DEVELOPMENT OF A BIO-INSPIRED GNS METHODOLOGY IN THE DARK ENVIRONMENT

CRANFIELD UNIVERSITY

AEROSPACE DYNAMICS

MSc

Academic Year: 2020 - 2021

Supervisor: Linghai Lu

Co-supervisor: Juan Carlos Aguado Chao

08/2021

CRANFIELD UNIVERSITY

SCHOOL OF AEROSPACE, TRANSPORT & MANUFACTURING AEROSPACE DYNAMICS

MSc

Academic Year 2020 - 2021

ADRIAN DE LA MORENA DIAZ

Development of a Bio-inspired GNS Methodology in the Dark Environment

Supervisor: Linghai Lu

Co-supervisor: Juan Carlos Aguado Chao

08/2021

This thesis is submitted in partial fulfilment of the requirements for the degree of MSc Aerospace Dynamics

ABSTRACT

The current research explores the connection between gazing and locomotion of acoustic guided animals and the application of this in autonomous vehicles guidance and navigation strategies. Research groups worldwide are currently investigating different technologies and autonomous guidance algorithm-based strategies. The use of nature inspired innovations ensures both the efficiency and the robustness of guidance strategies. The current research looks to fill the lack of research of those methodologies using bio-inspired techniques for acoustic guided animals as only visual based methodologies have been implemented for a variety of task. Also, to connect the results from bat's flight experiments of Moss et al. with the Tau Theory of David Lee. The connection between the Tau Theory and flight dynamics and manoeuvring is another interesting topic not only for autonomous navigation but also for handling qualities and safety improvement. After carrying out a data analysis of Bat's flight experiments through the cluttering of environment and connecting the flight behaviour with the extensive research done upon environmental cues perception guiding locomotion action for visual and acoustic cues. This concept is in an early phase of development and therefore, the aim is to set the baseline for further research in the topic. Results showed that bats perform a controlled braking manoeuvre when closing gaps, this in which is coined the term "Energised Approach". However, biased errors were found in some cases hence the results were negatively impacted, causing the results to be inaccurate in certain phases of the analysis. Despite the error found post-analysis, the results found in this research can still be considered insightful however artificial intelligence algorithms should be incorporated in future studies in order to achieve a more accurate result and finding.

Keywords:

Guidance, Bio-inspired, Tau theory, Bat, UAV

ACKNOWLEDGEMENTS

First and foremost, I would like to thank my individual research project supervisor Mr. Linghai Lu for guiding me and providing the needed support to me during the write-up of research thesis. I would also like to thank all the staffs at Cranfield University who have provided me with the support and knowledge over the course of the academic year, especially considering how the COVID-19 pandemic has affected us students, the efforts of the staff in trying to make our lives easier is greatly appreciated. Not to forget I would like to thank my friends and family in Spain for giving me the strength and mental support throughout this tough journey from a distance, without them I would not have been able to complete this masters course. Finally, I would also like to thank the friends I have made here in Cranfield especially my roommate, who has provided me support during the stressful period leading up to the end of the thesis.

Thank you, Cranfield, for this amazing year!

Adrian De La Morena Diaz

TABLE OF CONTENTS

LIST OF FIGURES

LIST OF TABLES

LIST OF EQUATIONS

1 Introduction

1.1 The industry

Although some people still associate military Unmanned Aerial Vehicles, also known as UAVs with military use, however UAVs are no longer limited to the defence industry only [19]. Investor are looking for Air mobility solutions from vertiports to green electric vertical take-off and landing vehicles (eVTOL) as business opportunities for the next decade [21]. Stakeholders are also interested in other market solutions related with UAV's such as cargo delivery and infrastructure [20].

The market side of the infrastructure, such as air-traffic control technology and physical infrastructures to land VTOLs, has been indeed recognised as a viable market to help private and public investors deal with the significant problems and enormous costs of this revolutionary technology [20,21]. On the other hand, the UAV market has grown from 40$ million in 2012 to almost $1 billion in 2017 in the United States alone, and the estimations for 2026 goes within the range from $31 to $46 billion for the country's GDP [20].

Aside from economic concerns, law regulations and public acceptability are two critical themes to grasp in order to propel the UAV business forward in the coming years. New-age technologies have always had a big impact on the society. The future of this technology is heavily reliant on the public acceptance or on the contrary, the absolute rejection of it. The deployment of autonomous vehicles particularly aerial vehicles is a hot topic of public discussion in the society. Researchers have identified that the perceived trade-off between advantages and downsides need to be balanced among the former in order for it to be publicly accepted [19]. Most notably, transparency and inclusiveness are two of the most prevalent themes for societal acceptance [19]. Ethical and security concerns on the other hand, are two of the most prevalent among the general population; particularly with regards to drones as the technology has been used in defence projects. Furthermore, studies discovered that the general public accepts the introduction of UAV in a risk-free environment, for instance a 60 percent of the general public are in favour of the use of drones for freight operations when a risk-free environment can is assured [19].

To summarise, the usage of unmanned aerial vehicles has the potential to provide a huge economic impact as well as alter the perception of the general public on the transportation business for both deliveries and people relocation. To accomplish the proper deployment of UAVs into the society, one of the most crucial things to consider is safety. New disruptive technologies within the autonomous guidance and navigation field, developed mostly in the research community are yielding promising results [11]. One filed that has produced great results is product design influenced by nature's inventiveness, often known as bio-inspired design. Nature has created wonderful designs that not even the finest designer in the world could have ever imagined. Bio-inspired ideas have created aerodynamic designs based on wings of owls to minimise flight noise to aerodynamic efficiency gained in the train industry by modelling the form of the train's cockpit after the head of a duck.

Bio-inspired innovations and designs has been applied in the field of autonomous guidance and navigation, but solely in optic flow navigation [11]. Researchers have focused their attention on the insect world [22]. Insects has been used as inspiration to derive optic flow based autonomous guidance strategies to perform a series of task from visual odometry to terrain following or flight speed regulation [11].

Extensive research has been conducted on gazing as a direct locomotion guidance. First, using visual guidance as a primary motor to obtain environmental cues but those theories has been generally implemented for other sensor motor such as acoustic cues or even magnetic field variations to sense altitude [2]. In particular, David Lee's study in the field has resulted in the Tau Theory, a generic locomotion theory. This idea has been utilised to benefit human piloting in rotorcraft vehicles [10]. As a result, the inspirations arise to apply the same concepts for the guidance and navigation of autonomous flying vehicles.

1.2 Research Aims & Objectives

The primary aim of this research is to develop an early concept of a guidance strategy based on an idea inspired by sound guided animals. It is known that bats move primarily guided by ultrasound; thus, bats execute fly navigation based on auditory flow generated by echoes from their surroundings rather than visual flow.

In addition, the goal of this research is to broaden the study of bio-inspired guidance technology in the UAV field.

Prior to the beginning of the research, four main objectives were set out and are to be achieved by the end of the research. The objectives can be found in the list below. The primary objectives are:

1. Understand and summarize how bat's sensory motor works.
2. Connect the bat's sensory motor to the animal locomotion theory, tau theory.
3. Introduce the bat's dynamic performance using tau theory to flight dynamics.
4. Derive a preliminary design of the autonomous guidance.

1.3 Scope of Research

Considering that the current bio-inspired navigation strategy is still a fresh and new concept, the background literature is limited. Due to the limited availability of existing literature, this research takes a global view in trying to uncover information on the connection of a series of unrelated hypothesis. Data analysis of the flight experiments conducted by professor Moss et al. [5,6,7,8,9] at the John Hopkins university Bat lab.

2 LITERATURE REVIEW

2.1 Moss Study and Bat Data

2.1.1 Introduction

Cynthia F. Moss is a researcher and professor of Psychological and Brain Sciences, with joint appointments in Neuroscience and Mechanical Engineering. At Johns Hopkins, she directs the Comparative Neural Systems and Behaviour Laboratory also known as 'the Bat Lab'. [Johns Hopkins University, department of Psychological and brain sciences]

Professor Moss has studied extensively the behaviour of echolocating Bats within the Johns Hopkins research group where they have a laboratory specifically to study the flight behaviour of Bats. I have acquired the knowledge in bat flight behaviour based on the papers her research group has published. Moss has provided the data, obtained from the Bat lab, used in her work to Linghai Lu as part of a research collaboration. The data has been used to derive the analysis of the current work. A summary of the Moss's work has been done and it will guide the guidance strategy methodology. The importance of the review of Moss's work lies in the inspiration on the animal, or bio-inspired, to create a guidance strategy. Therefore, the bat behaviour was the baseline to derive the GNS methodology.

The data analysed was obtained through a series of flight recording of different bat from the same species in the Bat lab, located in Johns Hopkins university. The lab is a dark room of 7.3x6.4x2 m3 used for flight experiments with trained bat. This lab has been used to study the flight of echolocating animals (Bats from the species Eptesicus Fuscus) for a variety of purposes, the author recommends looking directly in the Bat lab webpage for more information about the different project of the research team. The lab is equipped with microphones and high-speed infrared cameras and the walls are covered with sound absorbent material to reduce the reverberation. To study the bat flight's behaviour under different circumstances the bat includes an artificial forest to study the animal in cluttered environment.

The equipment of the lab allows the researchers to obtain both the video of the bat's flight path and the sounds emitted by the animal to guide itself during the flight.

2.1.2 Terminology

To ease the understanding of the research the terminology used by the cited researcher is introduced. The most importance terms used by Moss is cited and introduced in the followings paragraphs.

The sound beam call is defined as the sound vector pattern emitted by the bat to guide echolocated themselves using echolocation. The echolocation technique guides the flight of the animal and a numerous of studies suggest it is based on doppler effect, binaural differentiation of sound intensity [1].

The bat creates a sound beam by emitting brief, intermittent calls, which allows the bat to receive information from the direction of the beam [7]. A sound beam call is made up of vectors pointing in different directions, each with a certain variable intensity. The combination of all call vectors enables the bat to receive echoes from its surroundings similarly as visual animals receive information from light beams perceived by their eyes. The intensity of each vector calls for this particular species, E. fuscus, is symmetrically centred on its head, with the maximum sound intensity on the centre point. This fact ease the study of the bat guidance.

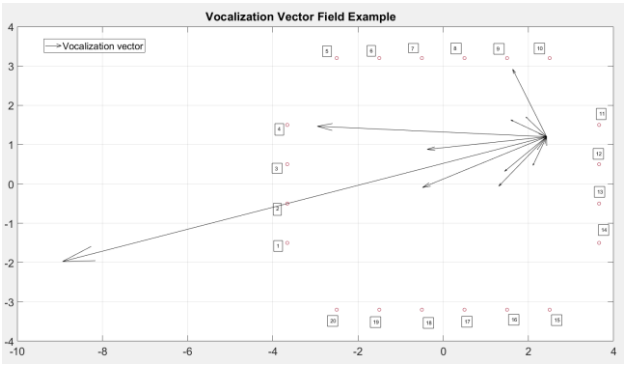

Figure 1 Schematic Sound Vector Field

The bat's acoustic gaze is the area of space from which it perceives information from its surroundings for guidance. Therefore, the bat's environment is sampled by the acoustic gaze. The same happens with visual guided animals as they receive information sampling their current spatial state with their eyes.

The bat will direct its acoustic gaze flow to receive navigational cues by moving the sonar beam [7]. It's similar to how visual-based animals use their visual sensing motor to guide their locomotion output.

The sound beam call and the rate of turn delayed in time have a linear relationship according to Moss et al [5,6,7,8]. This is a significant finding because it implies that, like visual-guided animals, bats use echo information to guide their movement using auditory signals received before from the environment [2].

This finding suggests that an echolocating bat's locomotion motor is derived from acoustic gaze information. Therefore, the locomotion is a task guided action delayed a time τ from the perception cues obtained from the environment using acoustic

beam. In the current research as the symbol tau, τ, is used to express the time to close a gap or time to contact, the delay in time is expressed as ‘delay’.

The research of C. Moss indicate that the bat would adjust its sonar beam to first sense the environment and then guide its locomotion motor to navigate through a cluttered environment, according to Moss' research. The linear relationship between the sensor motor and the delayed locomotion motor can be written mathematically as:

$$\dot{\boldsymbol{\theta}}_{\boldsymbol{flight}}(\boldsymbol{t}+\boldsymbol{delay}) = \boldsymbol{k}\boldsymbol{\theta}_{\boldsymbol{gaze}}(\boldsymbol{t})$$

2.1 Delayed Linear model Turn rate and Gazing angle

$\dot{\theta}_{flight}(t + delay)$, is the turn rate at time $(t + delay)$. This rate is the derivative of heading angle with time.

$\theta_{gaze}(t)$ is the acoustic gaze angle between the sonar beam axis and the flight vector at time t. The k value is the slope or the linear term relating both parameters. The relationship is always satisfied with a positive value of delay. A positive value for the delay term means that the motor output is delayed in time with respect to the sensory motor.

The linear relationship established a path planning by creating a link between the bat's sensing process and its movement. The linear relationship is found to change as the bat navigate and perform different task. As the environmental state of the animal changes the slope, k value, change therefore, the link between sensor motor and locomotion is an adaptative process developed by the animal [7].

2.1.3 Environmental Behavioural Adaptation

Moss et al [5,6,7,8] analysis how the linear connection between the gazing angle and the turn rate will change based on the task and the environmental situation. The animal adapts its flight behaviour depending on the phase of task. The bat will change its patter of flight while foraging depending on if it is looking for a prey if the prey is localized or if the prey is being capture. The environment conditioned the flight

as the bat will modify its behaviour comparing a flight in open or cluttered space. The parameter k variation is as follows:

The parameter k will vary during different steps of the navigation task. The higher the term k the more pronounced the turn, resulting in sharper change of direction. As previously explained the k parameter is a result of the environment-dependency adaptative behaviour of the animal.[7]

The slope k is bigger for open space than for cluttered environments. This indicates that, as expected, the bat navigates more cautiously in a room surrounded by obstacles than in an obstacle-free, or open space.

The k will be smaller in the search/approach phase than in pursuit and capture phase, named as ‘terminal buzz’. In the searching phase the animal manoeuvre gently gathering acoustic cues from the environment. Once a prey is located, the buzz stage involves quicker corrections of the flight path to capture the prey [7]. It has been discovered that the bat's speed is reduced to facilitate the final steps of prey capture as well as when navigating through a cluttered environment. This speed change is a good example of an adaptative process as flying in slow speed regimes involves a higher energy consumption for the bat. For that reason, the bat will decrease the speed only for the last step of the process.[8]

2.1.4 Open vs Cluttered Environment

Moss’s work has evaluated the flight in open and cluttered space and how bats change their active gazing between those two. Moss has proven that the bat modifies the main characteristics of the acoustic sensor motor (sonar call structure and temporal patterning) and its flight speed when flying in open space and artificial forest.

Moss’s results have verified that bats modify both its sensing motor and motion output based on the environment. adaptative behaviour with the environment is a well-known characteristic of visual guided animals. For instance, humans adapt its sensing and motion motor for different situations. Nevertheless, Moss’ result clarify that acoustic guided animals also have adaptative navigation behaviour base on its surrounding [8].

Moss' results indicate that in cluttered environments the vocalizations produced by the animal are shorter. The explanation for this behaviour is that the animal reduces the echo overlap when the vocalization has shorter length in time. By reducing the echo overlap the animal perceive clearer the cues from the environment.

Flying in cluttered environment demand higher cues to navigate without collision, for that reason bats vocalize at higher repetition rate. Approach manoeuvres have also higher frequency of vocalization. In general, bats have higher call emissions when flying close to objects to perceive more information from the surroundings and improve the quality of the model they create from the environment to navigate through it.

Moreover, the temporal pattern of the calls changes as bats emits higher rate of sounds groups. To maximize the quality of the cues from the environment perceived by bats they emit a group of call instead of a single vocalization. The group of calls helps bats to gather new information at high frequency rates while flying making possible to compare structure more efficiently the spatial mapping of the surrounding.

More sound groups are emitted in cluttered environments for collision avoidance, as navigate through obstacles demand a higher resolution of the environment. To obtain more cues and to have more time to react bat's flight speed is reduced when navigating through cluttered environment. As seen previously the reduction of the flight speed demand higher energy consuming but it is a necessary behaviour adaptation as occurs with prey capture. Flying at a slower flight range leave more time to bat's path planning to process the echo information and control the flight path.

For cluttered environment both the bat's pulse density, that is defined as the number of vocalizations per meter travelled, and the sound group density, that is defined as the sound groups emitted per meter travelled, increases. Similarly, then for the group of calls the more pulse and group density the more information's flow is perceived as the number of echoes received by the animal from its surrounding increase.

To sum up, it is fundamental to slow the flight speed and increase the pulse and group density to navigate through obstacles as those adaptative process in sensory motor allows the bat to obtain higher information flow that improves the resolution of

the spatial model of the environment needed for possible preys and obstacles around it.

2.1.5 Call Patterns, Frequency & Sonar Groups

The bat emits not only individual calls, but a group of calls that change depending on the stage of the foraging task. The temporal length of the call, the number of individual or groups of call, the period of each call and the temporal shift of calls varies between the stages of hunting.

When navigating around obstacles, the sensor motor emission of sound groups in temporal patterns has been found to be linked flight planning. [5,6,7,8]. This behaviour change includes a broad range of frequency calls, group of sounds density. The group of calls density is the number of calls emitted per meter travelled.

The bat duty cycle will change along foraging phases. During the terminal buzz the duty cycle was reduced. Bat's call emitted are characterize for being short frequency modulated calls. This adaptative behaviour have been examined to be found for both prey capture and navigation through highly cluttered environment. Those two situations have similar performance of their sensor motor as both manoeuvres demands higher information flow to be perceived by the animal compared with open space navigation or prey searching. The explanation lies on the fact the bat avoid echo overlapping that difficult the processing of echo information and increases the bandwidth of its calls in both situations to improve the resolution of the spatial map by obtaining more and clearer echoes or sound cues about the near objects.

The sonar pulse is frequency modulated. The sonar pulse is composed by of multiple harmonics that adapt to the phase of the foraging task. During approach stage of insect pursuit, the frequency sweep between 25 to 60Khz. While flying in open space the pulse production rate (PPR) can be as low as 4Khz and the duration of the calls reach up to 20 milliseconds.

During the phases of prey detection and approach the PPR rise and in final approach phase and capture the PPR rise to 150-200 Kilohertz and the duration of 0.5 milliseconds [7].

The PPR is drastically increased during the last stages of prey pursuit. Moss's results have proven that PPR is highly sensible to behavioural states. PPR varies and its

performance is divided into the four stages of the foraging task. For search/approach PPR is less than 50 Hz, approach is 20-50 Hz, tracking is 50<PPR<100 Hz and attacking phase is bigger than 100 Hz reaching up to 200 Hz. [5,6,7,8]

2.1.6 Stereotypy vs Active Sensing

The results of several studies have concluded with coherent data to validate that bat´s flights paths follow specific patterns comparing different consecutive number of experiment flights with trained bats. The results suggest that bats weather creates a spatial model of the environment based on echolocation or using a mixed sensory motor relying on echolocation and limited visual cues. Both models are developed and connected with spatial memory. Once the environment is known and the spatial model is saved in the memory of the bat results have suggested a reduction on active sensing, sound calls or group of calls, as navigation rely also in spatial memory [9].

Professor Moss has verified this stereotypy flight path on her experiments, but Moss has not reach coherent data to verify the bat's change of its sonar pattern neither reducing the number of individual or group of calls. Moss has gathered data to successfully represent the bat flight´s path histogram over the days and correlate them between flight experiments of the same bat in different days. Successfully, their correlated the number of points over 60% and search for maximum over the histograms. Moss's conclusions proposed that the bat could rely on its spatial model but depending on the environmental state. Moss' results has not correlate the use of spatial memory over flights and a reduction of active sonar motor as primary guidance. The explanation relies on the fact that Moss's studies are centred in foraging or cluttered environment navigation and those activities demands clear and fast response to the environment to successfully capture the prey her results [8].

2.1.7 Visual vs Acoustic Cues

Previous studies have found that visual guided predators and how they guide its movement based on visual cues sensed from its environment [1]. An important contribution of Moss et al [1,5,6,7,8] is that echolocating animals based its motion similarly to visual guided animals using the information sensed from the environment but guided through sound cues. The animal mission planner obtains an optimal path to the prey based on the cues whether visual, auditory, haptic or others [4]. It is

important to underline that in all cases the animal has a clear task guiding the locomotion, in this case capture a prey.

Moss's work has helped to understand how sonar-based navigation animals use their sensory motor and the relation of her results with the broad knowledge for visual guided animals.

David Lee has developed the tau theory and verified for both visual and echolocating animals [1,2,3]. A review of his research is done in the following pages.

Nevertheless, one of the main differences between the visual gathered information and the echo-based cues is that the latter is an intermittent source of information. The echolocating animal will gather snapshots of its environment based on processing the echo information received. Therefore, the surrounding environment that will be constantly change as the bats flight need to be refreshed constantly to successfully achieve its task while navigating through obstacles. The echolocation technique can be understood as a discrete function while the visual based navigation is a continues flow of information. The bat will create a certain number of environment models that will be updating with each call [7].

2.1.8 Data Analysis & Result

The data recorded is a U shape array of 16 microphones later extended to square set of 20 microphones. This is the data analysed to obtain the linear connection. The sound intensity of each call reaches each microphone with I_j intensity. Data already been correct for spherical and atmospheric looses so we are using already filtered data. The bat's velocity direction θ_{flight} is the tangential vector to its flight path and it is computed by differentiation between two points. The rate of turn or $\dot{\theta}_{flight}$ is the time derivative of the flight path. It can be computed by simple numerically differentiation of the changes in the angle of the tangent to bat's flight for each videoframe. The bat flight path and gaze angle is adjusted during the flight before and after the prey were released.

They correlated the acoustic gaze (sonar beam direction) and turn rate for different time delays. When they found the biggest correlation, they plotted the data using the gain for this time delay.

A comparison between search/approach and buzz (terminal state before prey capture) phases is done to compare the time delay.

2.2 Tau Theory

2.2.1 Introduction

The possibility of a linear relationship between the sensor and the locomotion motor based purely in echolocating techniques has been extensively study since the early 1900's with their beginning dated around the 1800's. The knowledge on the use of sound cues guiding bats of how bats use hearing had been documented by Lazzaro Spallanzani in the 1800's. Since the findings of Spallanzani, two main researchers, the French naturalist George Cuvier had published in 1800's and Hahn, American zoologist in the 1900's, had experiment with bats to derive a theory of their guidance based on echolocating techniques [11].

Nevertheless, it was Donal R. Griffin the pioneer in the study of echolocating techniques used for guidance as his book Listening in the Dark, published in 1958, analysed and explained bat's sonar mechanism and how it is used for a variety of tasks from planning and guiding their flight trajectories avoiding obstacles at high-speed ranges to locate, track and capture preys.

In the 1900's, the psychologist James J. Gibson had contributed with his extensive work in locomotion guided by perception. Gibson had analysed how visual flow information from the environment guide locomotion. Gibson correlate the active visual gazing and the connection with the locomotion motor in humans. His results confirm that active perception, in this case visual cues, drive the action of a predetermine task. This correlation established the baseline tenets for a perception guiding locomotion theory fully developed later by David Lee.

David Lee has absorbed the previous work of Gibson to extend the results an create a broader theory called Tau-theory. His work from the mid to the end of the 20th century not only expand the theory for other sensory motor, echolocating, haptic, magnetoreception, from different animals but set a mathematical formula that generalised the connection between the perception of cues from environment and the dynamic performance of the animal conducting a specific task.

In the field of echolocation, David Lee has been publishing conclusive results from his experiments that clarifies not only that Bats guide their movements by obtaining information of their surroundings from sound cues, echo, and intensity information, but He has linked it with his general locomotion theory.

David Lee was inspired by Gibson's ideas and that motivates him to develop the general Tau theory. Lee had developed the principles of the theory while working in the Ithaca Airport Perception Lab and continue extending the theory later in Edinburgh university. First, visual information guiding the motion was studied and as a result the initial research paper [2,13] on tau theory was created followed by another published paper two years later when Lee has moved to Edinburgh University [2,3].

The perception theory of Tau is based on a simple concept. The term tau (τ) refers to the time to contact or time to close a gap. Lee was enlightened while studying the manoeuvre to park a car. A car driver knows how to park a car perfectly after reasonable amount of training. The way the mind of the driver works is not based on newton's law, the mind doesn't compute the speed of the car and derive the time needed to park while adjusting the breaking. Mainly, parking the car is considered as a gap to close or action to finish. The distance gap must be controlled to avoid a collision. For that reason, the driver adjusts the speed of the manoeuvre while the car is closing the physical space to be parked. Note that not only the speed but direction, angle, is adjusted to properly leave the car inside the parking space.

Tau theory stablished that τ_x is the tau-function, or tau margin, for the gap $X(t)$. Tau theory generalised the name gap to any measurable physical gap, from angle or linear distance to applied force, hapticresponse [4]. The parameter τ_x, time to close the gap $X(t)$, is stablished to be negative when the gap is closing, and it is defined as follows:

$$\boldsymbol{\tau(x) \equiv \tau_x = \frac{X}{\dot{X}}}$$

2.2 Tau function of the Gap X

The value of τ_x, will vary as the dynamics of the movement change affecting the rate of change of the time to close the action. Therefore, for a continuous evaluation of the system to guide the motion the perception motor of the driver needs to sense not

the τ_x but how this parameter varies with time, $\dot{\tau}_x$. If the action speed of closing is changing the tau margin could be used for a first approximation.

Thus, for a controlled action guided by perception animals keep the rate of change of the time to close the gap at a constant value, $\dot{\tau}_x(t) = b$ [2]. Lee has stablished a series of kinematic profiles connecting the constant value of the rate of change of τ_x and the kinematic performance of the action of closing the gap $X(t)$. The following picture from [2] shows the how looks the kinematic profiles of a motion closing a distance gap normalising time (A) and distance(B).

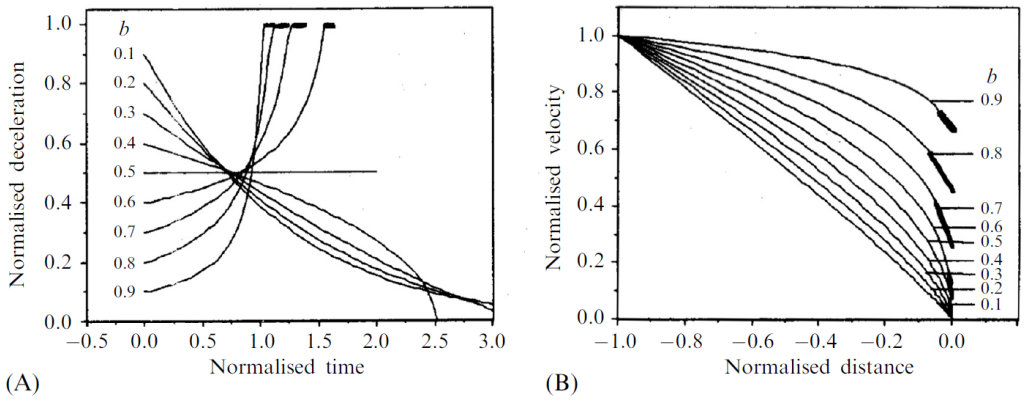

Figure 2 Kinematic Profiles of Motion [4]

To ease the understanding of the previous graphs the following table based on [1] is presented. In the table below it is explained the way the kinematics of the action will vary depending on the constant value of $\dot{\tau}_x(t)$.

$\dot{\tau}_x$	***Kinematic Performance***	***Action Output***
$\dot{\tau}_x > 1$	*Accelerated movement*	*The gap closure end in collision.* *At closure* $\dot{\tau}_x = 1$
$\dot{\tau}_x = 1$	*Movement with constant velocity*	*The gap closure end in collision. Increasing Braking*
$0.5 < \dot{\tau}_x < 1$	*Decelerated movement*	*The gap closure end in a controlled collision adjusts.*

$\dot{\tau}_x = 0.5$	*Decelerated movement*	*Action stops when the gap is closed. Constant braking.*
$0 < \dot{\tau}_x < 0.5$	*Decelerated movement*	*Action stops when the gap is closed. Decrease breaking adjust.*

Table 1 Summary Kinematic performance depending on Tau function derivative value

The rate of change of τ_x can be written mathematically as:

$$\dot{\tau}(x) \equiv \dot{\tau}_x = 1 - \frac{X\ddot{X}}{\dot{X}^2}$$

2.3 Tau function derivative

The previous equations were used to control the kinematic performance of the manoeuvre as seen in the TABLE 2.1. For mathematical prove see [1].

In the first case, $\dot{\tau}_x > 1$, the task is guided in an accelerating operation. The speed of the rate of closure is increasing, $\dot{\tau}_x$ increases during the manoeuvre, and the time to close the gap will decrease with time being lower than τ_x for all manoeuvre points. This procedure will end in a collision as not only there is no speed reduction, but the manoeuvre speed is accelerating with time. At the end of the gap closure the rate of change of τ_x drop satisfying that $\dot{\tau}_x = 1$.

The performance of the second case is similar to the previous one but in this one the rate of change is maintained constant instead of increasing during the manoeuvre.

For constant values of the $\dot{\tau}_x$ within the range of 0.5<b<1, the closure of the gap decelerates with time until the end of the action when $\dot{\tau}_x$ increases, $\dot{\tau}_x = 1$. The kinematic performance of the manoeuvre is defined as a collision controlled as the breaking action is increasing with time.

The motion that satisfies $\dot{\tau}_x = 0.5$, is a special type of procedure from the previous example in which the motion stops exactly when the gap is closed. During the manoeuvre the motion is being reduced at a constant rate, the brake procedure is kept constant.

For constant values of the $\dot{\tau}_x$ within the range of 0<b<0.5, the motion also finishes simultaneously with the gap closure. In the previous range of values for $\dot{\tau}_x$, the breaking procedure is being reduced. During the first points of the manoeuvre, the breaking action is more violent, and it will reduce the intensity while the gap is being closed.

Lee has proposed basic principles as baseline for the tau theory [4]. The Tau principles are the following ones: to regulate the rate of closure of a gap is a fundamental activity in guiding a movement, to perceive sensory cues of the gap's dimensional field (haptic, distance, angle…), as flow field information from any sensory mechanism, the closure rate of change of the gap is constantly monitored ,sensed and adjusted, to guide the locomotion motor, the gaps of different linked actions are coupled by keeping constant the ratio between their τ parameters.

2.2.2 Acoustic & Visual Guidance

The importance of Lee's work lies on the fact that his research derived a theory of perceptions guiding actions for different sensory cues [1].

Lee's results set the baseline of a common principles shared, for instance, between optical and acoustic information perceived from the environment as guidance principles.

Lee's experiments include the analysis of breaking procedure of a specific species of bat (Macroderma gigas) when flying through an small size aperture with adjustable size. Experiments were conducted with in two different circumstances. One, Bat's eye was covered, and the other, bat could use its eyes to obtain visual information.[1]

The experiment was designed to test the braking control of the animal under different circumstances, the size of the aperture was adjustable. The change in size of the aperture provide a range of flights for which different demands of sensor flow field is required, the smaller the size of the aperture the higher the demand of sensor motor to obtain a better resolution of the environment spatial mapping. Also, the braking control procedure is an action that demands fast perception and reaction of surrounding object to adjust the flight speed, distance, and angle of approach to the gate. As previously explained, the adjustment of those variables, or gaps to close, is achieved using Tau theory. In this research Lee was interested not in test the

dynamics of the manoeuvre but in dive into the sensory motor guiding the action. Tau theory relies on a sensory variable (S). The S variable is found to be a power function of distance to the gate [1]. The tau function of the variable S is defined as $\tau(s) = \frac{S}{\dot{S}}$. Exactly in the same way that was explained in the previous paragraph, the breaking procedure is controlled by maintaining a constant $\dot{\tau}(s)$.

More detailed description on the connection between the sensory a sensory variable and its tau function and the connection with guidance action is detailed in the paragraph of coupled Tau functions dedicated to sensory function.

Previous experiment of tau theory on visual guided animals has found that humans, birds, and flies follow the same procedure for action planning based on visual cues [13,14,15]. The results suggested that the same cognitive procedure was used by bats and birds even if distinct sensory gazing is used to gather information from the surroundings. Lee's experiment suggested that the acoustic sensory function of echo-delay, echo-intensity or of the angle from which echoes coming from different objects are perceived when approaching a surface could be used for breaking control [1]. The environment information contained acoustic flow filed in the returning echo includes the distance and direction, location, shape, and texture of objects in its surroundings. Moreover, Doppler-shift effect of helps the acoustic sensor motor of bats by emitting narrowband signal of constant frequency for perceiving target motion. As seen in the result of Professor Moss [5,6,7,8] bat's calls are frequency adjusted to compensate for the echo delay. Nevertheless, changes in echo-delay helps the bat to locate and track a target in moving state. The echoes are reflected by its surroundings, but the array of echoes changes constantly due to the movement of the bats. As a result, they conclude that there is an echo flow field providing sufficient information from the environmental state. Gazing visually is similar, but the only difference is that visual information is perceived continuously, whereas echo information is perceived discretely.

The visual flow field provide a structured information field as the light beam is reflected from different surfaces giving differential information about distances, surface materials and change of state, moving, objects. The same is verified by echoes as the sound reflect also in a structured way for all the objects composing the surrounding space. The acoustic flow field can be seen as a differentiable cone,

analogous to the flow field. The auditory flow field is related to the flow field in that it is a differentiable cone. Because the texture of surface elements does not always coincide, the flow field and acoustic field are not isomorphic. [1,2]. Bats employ interaural differences in sound intensity and echo arrival time to compute the sound direction perceived. A range of different sounds can be sensed at the same time, much as it can with visual information, where a variety of images are received at the same time, resulting in a complete mapping of the world. The auditory directional information is obtained from binaural Spectro-temporal information and transformed into spatial information. By analysing echo information and refreshing flow information with each call, the bat has built a spatial model of its surroundings.

Acoustic cues may be split into two categories: direction and distance to objects. The distance to objects is estimated via the Doppler effect since the echo arrival time is directly proportional to the distance to the surface that reflects the sound and produces the echo. Direction is computed from interaural time, call intensity, and spectral differences.

Humans are able to use the binaural difference of echo intensities and delays to derive not only the direction of the sound's source but also to compute qualitatively the direction of movement of that source. Nonetheless, humans have had limited development of the acoustic sensor motor because they have been guided primarily by visual cues [7].

2.2.3 Tau Coupling Guidance

The performance of complex or composed task in a dextrous manner requires the synchronously coupling of two or more actions. To perform in a harmonious way the coupling of those action, the coupling of their times to be finished need to be coupled. This mean that the tau functions are connected in a specific constant way. One of the key concepts examined in Lee's work is the coordination of the movements to link two or more gaps. For instance, when walking in rough terrain a Human need to coordinate the shifting of the eyes to scan possible new surface points to contact in the future step while controlling stability and force to push from one step to the next one.

Therefore, a direct and easier way of control complex actions without diving into the study of the large and complex nervous system architecture. His proposal lies on the continuous examination of the time required to complete an action, or, more specifically, the time required to close a specific gap. Those gaps could include various measurable field such as angles, distances, and forces.

From this concept of linking movements, arise the idea of tau coupling. Two or more gaps being closed jointly is equivalent to keep two tau-functions at a constant ratio. Correlating two tau functions causes the closure of both gaps to occur in a harmonious and controlled manner, synchronising two movements.

Other perception theories seek to comprehend and create a model of the system, from which the movement is derived using Newtonian physics. Other motion theories, link their dynamic model performance to mission planning and generate a control strategy. Nonetheless, apart from its model simplicity, the main advantage of tau theory is the separation of motion planning and control from the model dynamics. Therefore, a control strategy is based on kinematic performance without considering and neither the need of a dynamic model as it is the case of the current project.

Within Lee's work tau coupling is examined only when the movement has started, and his analysis didn't investigate the sensory information perceived that causes the animal to generate the initial movement. Generally, knowing when to start a movement is not fundamental as it only matters not to start at action limit time, for instance start the breaking with enough time to avoid a collision. This limiting time to start will vary with the external conditions, the vehicle dynamics, pilot skill, vehicle performance limitation and is out of the scope of Lee's work and the current research.

Tau is a theory of motion control of future actions. That means control actions need to be taken ahead in time specially to deal with extra time that theoretically doesn't exist but in real moving system like transient responses caused by inertia or system limitations. For that reason, there is a necessity of predictive information coming from the sensory system. As a conclusion, control actions are planned and taken ahead on time or motion action is always delayed with respect of the perception cues from sensors.

2.2.4 Sensory Tau Function

One key concept of tau sensing is that human perception sensors are not designed to assess an angle, a distance in metres, or a force, but rather how those perceived qualities change over time.

In the following paragraphs a review of most common techniques to plan coupled motion using Tau theory are reviewed.

The simpler approach for motion planning using tau theory is to keep the derivative of the tau value constant,

$$\dot{\boldsymbol{\tau}}_{\boldsymbol{y}} = \boldsymbol{k}$$

2.4 Constant derivative of the Tau function

The kinematic results of the previous technique were analysed in previous pages, see

In fact, this turns to be a particular case in which for the coupling of two gaps, $X(t)\ and\ Y(t)$, the gap closure of $X(t)$ is kept constant. Therefore,

$$\dot{\boldsymbol{\tau}}_{\boldsymbol{y}} = \boldsymbol{k}\dot{\boldsymbol{\tau}}_{\boldsymbol{x}} \equiv \boldsymbol{k};\ \dot{\boldsymbol{\tau}}_{\boldsymbol{x}} = \mathbf{1}$$

2.5 Tau coupling between two gaps X and Y

This specific tau-coupling strategy seems to be repeated among different animals as a form to control the velocity of the approach.

Previously it has been explained the basic principles of tau theory and how the sensor motor guide the locomotion action, how complex tasks are coupled and that action lags sensor perception as motion is planned based on the environment cues. In this section a detailed explanation on how this sensor action connection is done, based on tau coupling, idea is developed. For the following description it is important to differentiate between sensory tau function, τ_s, and motion tau function, τ_M.

The link between the motion tau function into sensory tau function occurred if and only if a sensory gap, S, within a sensory flow field is a power function of a motion gap, M (so that $s = CM^{\sigma}$, for constant C and M) then:

$$\boldsymbol{\tau_M = \sigma \tau_S}$$

2.6 Relation between Tau function of Motion and Sensory Tau

This way motion-tau is coupled into the sensory-tau and its value is specified by the value of the sensory tau by a constant scale factor [4].

The animal couple motion-taus as well as couple sensory-taus. This coupling is done under different circumstance depending on the animal and their sensor motor development. Lee Has provided an indicative approach on which motion fields could be sensed and therefore, coupled with each perceptual system from [4]

Row	Perceptual System	Sensory Gap	Dimension	Motion Gap	Dimension	Power Law	Tau-Coupling
1	Vision echolocation	w_0	distance	Z	distance	$w_0 = CZ^{-1}$	$\tau_Z = -\tau_{w_0}$
2	Vision echolocation	w	distance	Z	distance	$w = CZ^{-1}$	$\tau_Z = -\tau_w$
3	Vision echolocation	w	distance	W	distance	$w = CW$	$\tau_W = \tau_w$
4	Vision echolocation	θ	angle	Θ	angle	$\theta = \Theta$	$\tau_\Theta = \tau_\theta$
5	Vision echolocation	ϕ	angle	Φ	angle	$\phi = \Phi$	$\tau_\Phi = \tau_\phi$
6	Vision	β	angle	R	distance	$\beta = CR^{-1}$	$\tau_R = -\tau_\beta$
7	Echolocation	d	time	R	distance	$d = CR$	$\tau_R = \tau_d$
8	Echolocation	i	sound intensity	R	distance	$i = CR^{-\mu}$	$\tau_R = -\mu\tau_i$
9	Electrolocation	v	voltage	D	distance	$v = CD^{-1.7}$	$\tau_D = -1.7\tau_v$
10	Electrolocation	p	voltage	R	distance	$p = CR^{-2}$	$\tau_R = -2\tau_p$
11	Infrared vision	h	infrared intensity	R	distance	$h = CR^{-2}$	$\tau_R = -2\tau_h$

Figure 3 Relation Between Sensory and Motion Tau Function [4]

The first case to study is and steering example. This is the case aalysed later in the research analyst.

The steering manoeuvre has the objective of changing the flight path to a motion line goal. The angle between the direction of motion OM and the goal direction OG is denoted as θ_{MOG}, while the angle between a reference line OR and the goal line of motion OG is denoted as θ_{ROG}. The steering manoeuvre objective is to close the angular gap by making $\theta_{MOG} = 0$. Thus, the motion is guided mainly by τ_{MOG}, that is the motor angle tau or tau function of motion of the gap angle θ_{MOG}. One simple approach is keeping the value of tau to infinite the value of the angle will be kept constant. Other strategy is to keep the value of $\dot{\tau}_{MOG} = k$, (0<k<1) then result in a turning straight until meeting the goal point [4].

To successfully perform this strategy, the animal must first move its sensory flow field to the goal point. The motion produced must then reduce the angle to close the

motion angle. Once the motion has started and the angle is reducing, the motion functions must keep a constant value before 0.5, $\dot{\tau}_{MOG} = k$, k<0.5, and the path followed will reduce the angle at a constant deceleration until the motion direction (OM) coincide with the motion-goal direction OG that is equivalent to an angle zero. $\theta_{MOG} = 0$. This kinematic performance is explained before and summarized in table 1.

David Lee had found that for the values in the procedure to get to the goal point the tau gaps of τ_{MOG} and τ_{ROG} are coupled.[4]

The values of ROM angle are usually small as the perception cues comes from a small angle ahead in time. The animal is gazing in the motion of the path that close the gap. Basically, the animal is gazing in the direction of the goal to perceive cues to derive the next step in the motion. The point of refence that guides the motion also change periodically to upgrade each time the gazing, or cue perception more generally speaking.

Both he θ_{ROG} and the θ_{MOG} are critical in developing a guiding strategy to complete this manoeuvre process. Thus, the tau function of those two motion angles is coupled.

In fact, only the set of point that compose the circular path to the goal satisfied the following relation:

$$\boldsymbol{\tau_{MOG} = -\tau_{ROG}}$$

2.7 Example of a synchronously closure of two gaps

The previous formula is a mathematical representation that could be read as 'the time to close the gap of the angle θ_{MOG} need to be equal and negative to the time to close the gap of the angle θ_{ROG}. When this relationship is satisfies and finished the reference, motion and goal line are pointing in the same direction. As stablished in the basic principles of Tau theory, τ_{ROG} is negative as its gap is being closed. In the same way, all the other points that are not in the path to the goal direction verify that

$$\boldsymbol{\tau_{MOG} \neq -\tau_{ROG}}$$

2.8 Tau function that satisfied a successful Tau closure of two gaps

The tau information could also use to control the braking procedure as the τ_{MOG} is the time to arrival to the goal from point O at the current closure ratio. So, breaking could be controlled by keeping $\dot{\tau}_{MOG}$ constant.

For a manoeuvre composed by steering and breaking there is a condition of tau-coupling between the gaps. If the tau function of distance to a goal gap is τ_{DG} and the tau motion function of the angle to the goal is τ_{MOG}. The gaps are coupled when a specific ratio is kept constant. The model will follow the mathematically expression:

$$\boldsymbol{\tau_{DG} = k\tau_{MOG}}$$

2.9 Tau function of linear gap closure of two gaps with different dimensions

The range of the k conditioned to $0 < \mathrm{k} < 1$, ensures the function gap tend to zero, or the gap is closed. So, the angle θ_{MOG} tend to zero and simultaneously the gap of the distance to the goal, D_G, would tend to zero. Therefore, both gaps are closed together at the same time. Specifically, for a $\mathrm{k} > 0.5$, the closure ratio of the distance gap, D_G, leaves some residuals in the rate of closure once the goal point is reached. Lee termed this manoeuvre as energized Approach [4]. Whether for a $\mathrm{k} < 0.5$ the clousure rate tendo to zero as the goal is approached.

Negotiating Obstacles is another manoeuvre of interested based on tau guidance. In this review it sonly explained the process of rounding the obstacles but for further guidance strategy sees [4].

The obstacle voidance by rounding it is straightforward derived from the previous explanation for steering manoeuvre. To steer around an obstacle, the motion tau function guiding the movement is the τ_{MOG}. A simple example that visualizing is to imagine a car moving inside a roundabout. The motion line of the car looks to meet the tangent line of the roundabout as a goal line. Thus, the gap to be closed is the one created by approaching the roundabout and the motion that leads to a path straight to the circle's tangent line.

For a perfect circular pattern, if the motion kept the tau function to infinite the angle will be kept constant, if the velocity is kept constant the automobile will drive in circles while staying within a constant distance of both road boundaries.

Lee's hypothesis offered a method for developing a navigation system that manoeuvres in such a manner that the distance to the environment's limiting points is chosen. Those limitations are the safety limits imposed by the performance of the vehicle itself, as determined by vehicle dynamics [4].

The final approach technique is the last strategy to be discussed. Consider the previously mentioned steering case but as seen from the air. The same procedure of steering around a surface lead to the idea of steer into a surface. In a lateral movement, this is equivalent to keep the wheel parallel to a surface. This method is extensively used in landing and take-off manoeuvres. Similarly, to the path followed after leaving a roundabout and correcting the motion line to keep vehicle motion line between lanes.

David Lee has investigated the manoeuvre from two approaches, whether the goal point, contact point in case of vertical motion, is specified or not. If the point of ground touch is defined in advance, while the closure of distance gap, $\tau_G \equiv the\ \tau\ function\ of\ D_G$, the angle gap is simultaneously getting closed, $\tau_{OGS} \equiv the\ \tau\ of\ \theta_{OGS}$. Both, τ_{OGS} and τ_G are implicitly linked in this manoeuvre. However, Lee´s research has found that is not necessary to sense the angle gap closure (τ_{OGS}) but only to connect the reference and the goal motion line. Both, as Lee argued, are felt by separate sensory systems. (See table of sensory connections 2.1).

David Lee has experimented with the same species of bat as professor Moss, E. Fuscus, and within his research there was an experiment based on the coupling between the speed and an angle [17]. The experiment has proved that bats coordinate the angle of approach and speed of flight for landing manoeuvres. As the bat reached a perch, where it hanged invertedly, the velocity is virtually zero. To arrive at the destination, point with zero velocity the bat kept the $\dot{\tau}_x$ constant, being τ_x the time to close the distance to the goal point. In fact, the bat coupled the time to close the angle gap from the current motion line to the desired goal line direction, τ_A , with the τ_x. As previously stated, this ensures that both gaps are close concurrently, and that once both, the speed and distance to the goal, are almost zero, the bat heading angle is aligned with the point of arrival.

2.2.5 Intrinsic & Extrinsic Tau Guidance.

The coupling extrinsically of two or more tau function led to synchronous movement. Nevertheless, it is well known that the coupling of those tau functions is achieved intrinsically by the animal. The motor system is guided by the mission planner of the animal, extrinsic movement, but the mission planner worked autonomously by survival impulses, intrinsic movements, developed through evolution.

An external source could be the source of motivation leading the movement as for example if a human is asked to push a button in moving state. The human need to coordinate the movement of the finger to reach the button in the desired place at the desired angle while coupling the force that will apply on it. Distance, angle, and haptic variables are therefore the dimension fields coordinated in the motion.

The movement of the button imposed the path to follow. A comparable scenario would be when a bat catches a prey. The hunter's movement is guided by the prey path. Avoiding an obstacle is an example in which the obstacle specifies the way not to follow, avoid, whether it is static or moving, as opposed to the preceding example. Constraints in action would originate from a variety of variable fields, depending on the environment and the state of the activity. For example, a constraint might be temporal, such as following a pattern at a certain frequency, or spatial, such as avoiding an obstacle or following a predetermined route.

Instrument playing is a topic of study as the coupling of the taus is coordinate with the frequency of playing, or tempo. The animal extrapolates the present knowledge of state based on prior perceived events to close the gap.

As the previous topic is more related to nervous system and brain activity, experiments focused on the activity of the motor cortex appear to explain the movement direction. [18], the topic is not covered in the current research. The only thing to mention about this topic is that the animal nervous system generates intrinsic tau to be coupled with locomotion. The same procedure is used as with extrinsic tau coupling. The difference between intrinsic and extrinsic tau-guidance is that the former comes from the nervous system, whereas the latter comes from environmental cues sensed by the animal.

3 Methodology

3.1 Data Collection

The data used in the current research that allows to do the analysis of the flight behaviour of the Bat, E. Fuscus, come from the Johns Hopkins Laboratory. The data was provided according to a research collaboration made between Dr L. Lu and Dr C. Moss. Moss and her colleague sent the data pack in MATLAB format to Dr Lu.

The work of professor Moss is described in full in the literature review section. Her research is focused on animal behaviour and adaptative interaction with its environment, primarily cluttered and open environments. Moss investigated the mechanism of bat flight as a whole manoeuvre. That is, she examined the bat's flight path from start to finish. That is, her research is centred on the bat's whole flight path, with the goal of validating hypothesis such as stereotypy flight, and the possible role of memory on the flight pattern, and to connect the extensive work done of visual cues guiding the animal locomotion for a non-visual cue's guidance strategy, in this case stereo cues.

The main goal of the Johns Hopkins University Bat Lab's study is auditory perception in animals and how this sensory information leads the animal in varied navigation situations and conditions such as obstacle avoidance and target tracking.

The data provided is the result of a series of experiments with trained bat from the species, E. Fuscus. Nine bats were trained in open environment to catch preys and once its ability to catch the mealworm is sharped the bats were tested in an artificial forest. The artificial forest is composed by 12 artificially manufactured trees. Also, a wall was situated in a particular way that obstacle the bat in case it tried to flight in circles rounding the forest. This way the bat is motivated to flight within the interior artificial forest [8].

The experiments were conducted in a Laboratory Flight room of 7.3x6.4x2 m3. The illumination material provided an obscure red light ambient with a wavelength lower than 650nm. This way the bat's visual guidance is nullified.

The audio recording of the data was done using a square array of twenty microphones surrounding the room. To avoid reverberation both the ceiling and the walls were covered with sound absorbent material.

The video recording of the flight path was conducted using two high-speed infrared video cameras with an operating frequency of 240 frames per second [7]. For further information about the lab and the experiment please read [7],[8].

For the data analysis different bats and flight experiments were provided. The research was focused on a particular Bat mentioned as B57 in the research of C. Moss. The data used for the analysis come from the pack of artificial forest as the objective is to validate the hypothesis of tau guidance when flying in a cluttered environment.

A data analysis tool was developed to automate the research process in the future. Hence, even only one bat was studied the same tool could be used to quicker obtain critical parameter of other bat's flight cases. The scalability of the tool for the analysis was done with the aim of continue the research with most detail in the future.

The data packs provided was arranged into two main structures. One, containing the data from the camera recording, or 3-D spatial trajectory data, and sound data, or vocalization signal emitted by the animal when flying. The former division is a simplification because the data structure for video and sound contained more information than the preceding section. For the previous reason, a preliminary data selection and cleaning was carried out in order to combine the relevant data and make it easier to manage for algorithm implementation.

3.2 Data Analysis

3.2.1 Video Data

First, a general overview of the animal trajectory was conducted. In this study, the animal's trajectory was plotted in both three and two dimensions including the artificial forest, twelve trees, and prey position. It was critical to include those two parameters to understand the flight, since the bat's flying changed depending on whether prey capture and/or obstacle avoidance were involved in the process [5,6,7,8].

Then, the flight path altitude was avoided as the analysis results were based on the flight heading angle, that is constrained in a two-dimensional space.

The position information data points that make up the whole trajectory route discretize the animal's continuous flight path into a data set based on video frame frequency.

The heading angle, θ_{flight}, was calculated from the trajectory frames using a simple two-point differentiation. At each instant, the heading angle is tangent to the flight path. The heading angle was one of the most critical parameters in the analysis. This angle was obtained using the positive X-axis as zero degrees and kept the range between 0º to 360º.

The turn rate was calculated simply by subtracting the heading angle between two successive points. The direct units for the turn rate were degrees per frame, [deg º/frame], which was then multiplied by the frame frequency to get degrees per second, [deg º/second].

3.2.2 Sound Data

The data recorded by the microphones array were included in the sound data for each case. Moss has already corrected the data for spherical effects and air conditions. The data information that is important for the analysis was the frame corresponding to video frame, and the sound intensity perceive by each microphone for each frame.

To compare both data information two approaches were conducted. First, it was filtered the already analyses video data to made it correlate with the sound data frames. Second, the sound data were interpolated to fit the video data. The following image included a comparison between both fram frequencies using as example the sixth case studied:

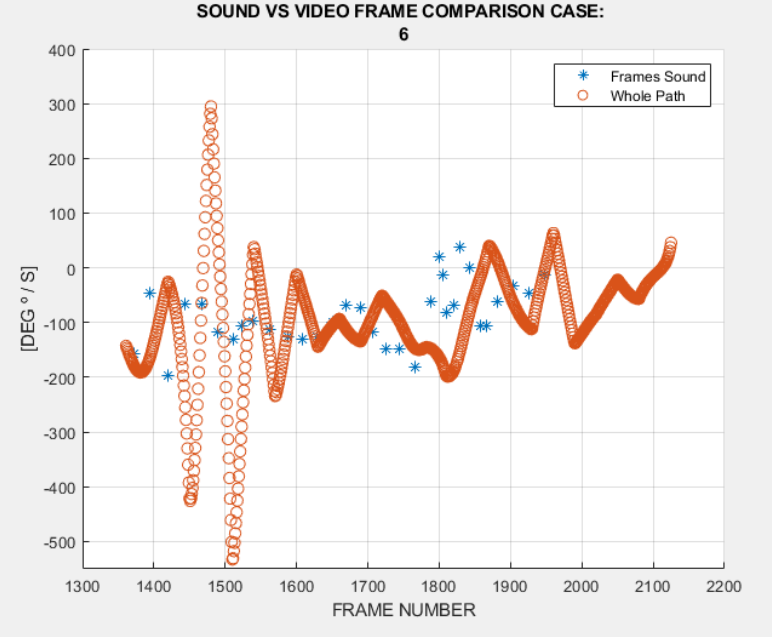

Figure 4 Data density comparison between Sound and Video data

The latter was chosen as the final option for two key reasons. First, there were cumulative errors in the analysis, as evidenced by the graph included. Second, the density of the data using only the sound frames was insufficient to accomplish effective optimization and data fitting for the proposed model.

To begin the analysis, the microphone array position from the paper schematic figures was implemented in the 2-D plots. Because the precise position of the microphones was never received, there was a small error in the bat's vocalisation direction value.

A direct difference between each microphone and the current bat location in space was conducted from the fixed position of the microphones array to construct a vector of directions pointing each microphone while the bat was flying.

To create a final weighted vector array, the previously computed 20-direction vector flow field was weighted using the intensity perceived by each microphone for each frame. This weighted vector flow field modelled the vocalization call produced by the bat, as proposed by Moss' work [5,7]. The previous algorithm produced a flow field of twenty vectors. Based on Moss' knowledge of the biological mechanics of bat vocalisation motors, only one, the biggest value, was selected as the primary direction component of the composed vocalization. [5,6,7,8]. In the result section a

plot of the vocalization vector produced in each frame of the flight is included. The previous selection could be expressed mathematically as:

$$\vec{\boldsymbol{H}} = \sum_{\boldsymbol{n}} \vec{\boldsymbol{I}}_{\boldsymbol{i}}$$

3.1 Sound flow field

Being:

$\vec{H} = Resultan\ Sound\ Vector.$

$\vec{I_i} = Weighted\ Intensity\ Vector\ from\ the\ Bat\ to\ microphone\ .$

In our case $n = 20$ and $i =$ corrected weighted magnitude for each microphone.

Using the same approach as with the flight path angle, the gazing angle, was determined from the emitted vocalisation direction. For later comparison, this gazing angle was again restricted to the same range of angles as the flight path. That range is [0º, 360º].

It was critical to emphasise that the vocalisation vector was created using only one vector from the vocalisation vector field, the vector with the highest intensity. As shown in the figure 1, the highest intensity corresponds to microphone number 2, and the bat's vocalisation vector has been simplified such that it points directly and specifically to this microphone. Thus, an error would have been accumulated if the bat vocalisation was recorded between two successive microphones with similar intensity.

3.3 Data Comparison

From the linear model proposed by Moss [7],

$$\dot{\boldsymbol{\theta}}_{\boldsymbol{flight}}(\boldsymbol{t} + \boldsymbol{delay}) = \boldsymbol{k}\boldsymbol{\theta}_{\boldsymbol{gaze}}(\boldsymbol{t})$$

3.2 Moss´s Linear delayed model between Turn rate and Gazing angle

To create the model, the previously computed turn rate, $\dot{\theta}_{flight}$, and gazing angle, θ_{gaze}, must be compared linearly fit and obtain the linear parameter or k value. The scatter plot produced from the selected points was fitted linearly using first-order

polynomial curve fitting based on the least-squared error approach. The linear polynomial parameters, namely the slope of the linear correlation or k value, are the objective outcomes. the linear correlation parameter provided the necessary information to derive the guidance strategy as it is described in the Tau theory dynamic performance section.

3.3.1 Choosing The Manoeuvre

A variety of specific manoeuvres points from various flight scenarios were chosen for the current study. The selection of the manoeuvre was done by trial and error as there is no particular formula to follow. After the analysis was performed in some manoeuvres a part of the set of point were cut or the set were split in two or more cases to analyses separated.

So, the first step of the process is to choose the manoeuvre to derive the linear correlation. In professor Moss work this was accomplished using the whole flight. From the tau- theory basis the bat is closing gaps as it flight through the environment, therefore, in a whole flight the bat close not only close a single gap but a group of gaps. Those gaps could be coupled between them.

For that reason, to derive a linear relationship is better to use a constrained set of points composing a manoeuvre. This set of points are chosen based on visual inspection of the flight paths. the reason to choose a manoeuvre are the following:

I. Isolate obstacles: When dealing with multiple obstacles the bat most probably coupled the motion round them. This could lead to misunderstood of the behaviour. Also, is more difficult to constrains the beginning point and end point when dealing with more than one obstacle.

II. Understand the environment: As seen in the review of literature, Moss work, is verified that the animal modifies its behaviour not only in terms of vocalization emission patterns, both emitted in groups and modulated in frequency, but the speed, slow down even at a cost of energy consumption, and even the activation of other sensory systems if possible, as limited view or memory to flight in stereotype patterns. It is clear the bat will flight different avoiding obstacles than hunting a worm.

The following graphs demonstrated the importance of dividing the whole flight path into specific manoeuvres.

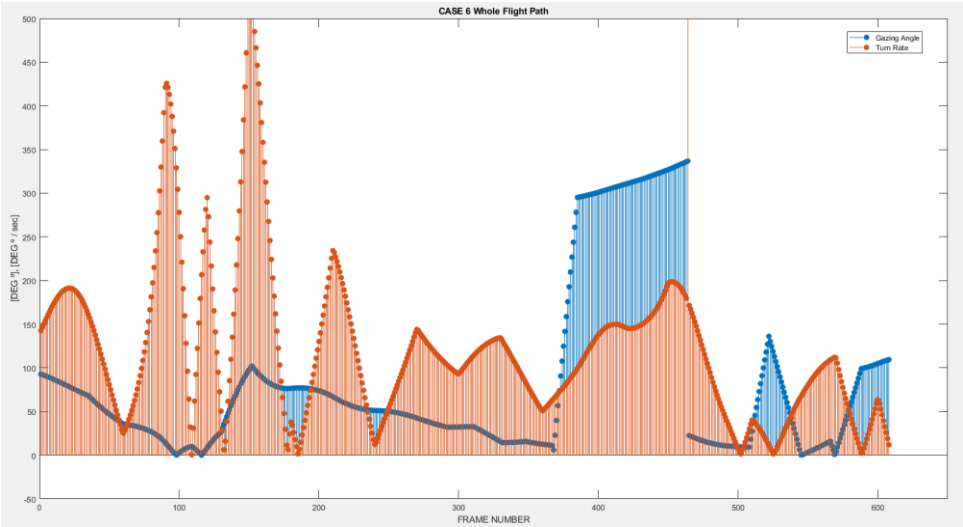

Figure 5 Gazing Angle and Turn Rate Comparison for the Whole Flight Path

Some ranges of points were spotted to follow a similar pattern with a small delay in the discrete frame. Moreover, there were a point with a really big value that were avoided for the analysis. For the previous reason, a data cleaner for this particular error was included.

The output as seen in the table of manoeuvres, see results section. lead to a set of around 10 points. To do a linear fit first an interpolation was done. The idea was to get at least 100 points before obtaining linear fit parameters. The command from MATLAB Interp was used to achieve the desired set of points. This command has several algorithms to use, there were studied and plotted to choose between them. Moreover, once the plot was obtained it was decided to cut the range of manoeuvre points to fit the last sound emission recorder. After the last sound frame recorder, the data points of vocalization had to be extrapolated instead of interpolated and thus, the value diverge. If those values were used a bigger error would have been accumulated. The next image summarized the interpolation analysis, the case six was used for the example:

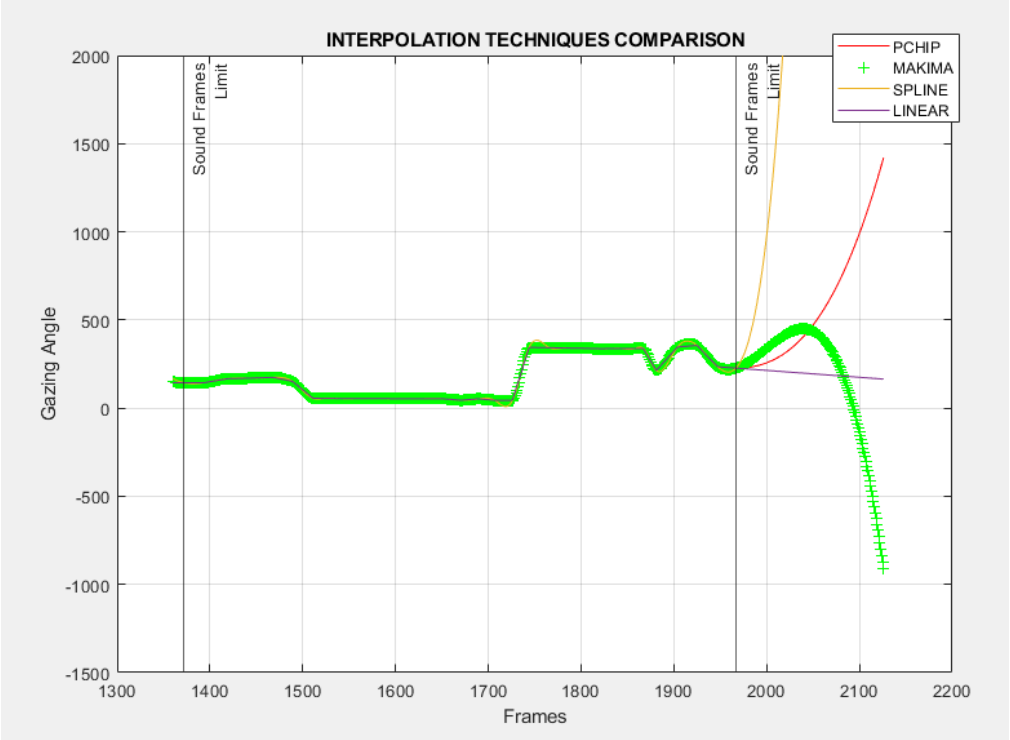

Figure 6 Figure 6 Interpolation Techniques Comparison

3.3.2 Optimisation Process & Parameter Identification

Discrete plots, comparing gazing angle and turn rate, were used to perform the initial approximations to get values to use as first guesses in the optimization procedure. Both sets of points were compared on a graph to see whether there was any pattern similitude between the gaze angle data and the turn rate data ‘ahead on time. That is, the turn rate set of points, from a particular manoeuvre, was fixed and the gazing angle values were chosen to be prior to the start of the fixed turn rate range of points.

Once an approximation value was obtained, the optimization was done using AMTLAB optimization algorithms ‘fminsearch’ and ‘fmincon’. Fminsearch is a simpler and faster algorithm but have less parameter to tune, thus, depending on the optimization problem to solve one or the other need to be chosen. In the current optimization problem the fminsearch algorithm was used as it is faster the current optimization problem did not required the fmincon algorithm.

The objective function, or cost function was created to find the minimum values, k value and $delay$, that optimize the least-squared error between the gazing angle and the turn rate at a optimal $delay$. This methodology helped tunning simultaneously both the ka parameter and the lag parameter for the maximum correlation parameter

between the two set of points. As the data point fixed in the manoeuvre were the turn rate instead of the equation:

$$\dot{\boldsymbol{\theta}}_{\boldsymbol{flight}}(\boldsymbol{t}+\boldsymbol{delay}) = \boldsymbol{k}\boldsymbol{\theta}_{\boldsymbol{gaze}}(\boldsymbol{t})$$

3.3 Moss´s Linear delayed model between Turn rate and Gazing angle

An equivalent equation was used:

$$\dot{\boldsymbol{\theta}}_{\boldsymbol{flight}}(\boldsymbol{t}) = \boldsymbol{k}\boldsymbol{\theta}_{\boldsymbol{gaze}}(\boldsymbol{t}-\boldsymbol{delay})$$

3.4 Equivalent equation adapted for the optimization algorithm

Thus, the function to optimize is:

$$\boldsymbol{F}_{\boldsymbol{opt}}(\boldsymbol{X},\boldsymbol{Y},\boldsymbol{delay},\boldsymbol{t},\boldsymbol{k}) = \boldsymbol{X}(\boldsymbol{t}) - \boldsymbol{k} * \boldsymbol{Y}(\boldsymbol{t}-\boldsymbol{delay})$$

3.5 Simplified Cost function

Where:

- $X(t) \equiv \dot{\theta}_{flight}$
- $Y(t-delay) \equiv \theta_{gazing}$
- $k \equiv Linear\ fit\ parameter$
- $Delay \equiv Time\ lag\ between\ turn\ rate\ and\ gazing\ angle$

In Moss's work this delay or lag is denoted as τ but in the current study the Greek letter τ denotes the tau function of a gap, or the time to close the gap associated to the function.

The cost function optimizing the function is the least square error between those values.

$$\boldsymbol{J}(\boldsymbol{X},\boldsymbol{Y},\boldsymbol{t},\boldsymbol{Delay},\boldsymbol{k}) = \frac{\boldsymbol{1}}{\boldsymbol{2m}}\sum_{\boldsymbol{i=1}}^{\boldsymbol{m}}[\boldsymbol{X}(\boldsymbol{t}) - \boldsymbol{k} * \boldsymbol{Y}(\boldsymbol{t}-\boldsymbol{delay})]\,[\boldsymbol{X}(\boldsymbol{t}) - \boldsymbol{k} * \boldsymbol{Y}(\boldsymbol{t}-\boldsymbol{delay})]' + \boldsymbol{v}(\boldsymbol{t})$$

3.6 Cost function

$v(t) = biased\ error$

4 Results

In the following section the results from the current research from the previously explained data analysis is shown. The data analyse tool created to derive the following results is included in the Appendix, for further detail or use please contact the author or supervisor of the research.

The results are summarized in a table at the end of the chapter. The cases that have been studied are detailed in the methodology chapter, manoeuvre chosen section.

The Bat's flight path was included in the analysis to visualise the manoeuvre followed and easier connect it with the results obtained for each case. Using the data as discretized path by splitting the entire flight into a sequence of movements was done on purpose, resulting in different outcomes from the same flying experiment of the same Bat.

To ease the understanding of the reader instead of the technical name provided by Professor Moss the case were named using the natural number case from the folder. In the following images containing the whole flight path the technical code and the case number are included.

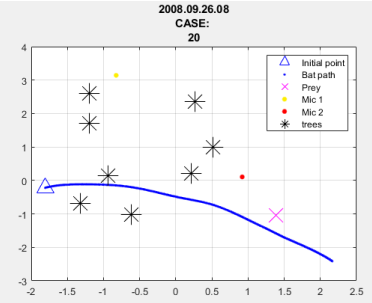

Figure 7 Flight Path Experiment Case 20

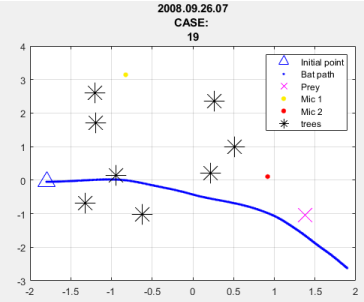

Figure 8 Flight Path Experiment Case 19

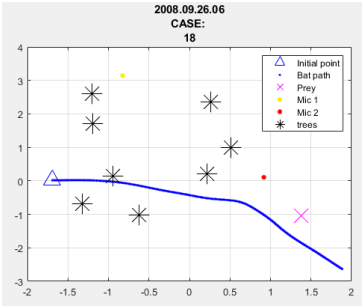

Figure 9 Flight Path Experiment Case 18

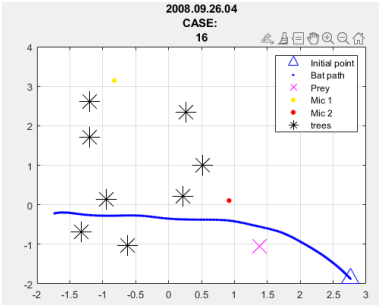

Figure 10 Flight Path Experiment Case 17

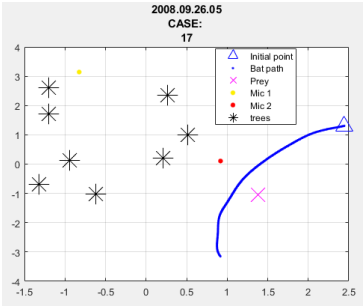

Figure 11 Flight Path Experiment Case 16

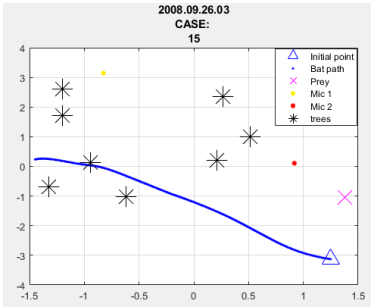

Figure 12 Flight Path Experiment Case 15

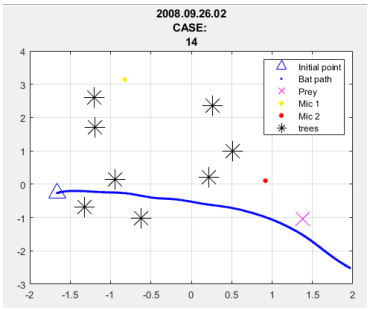

Figure 13 Flight Path Experiment Case 14

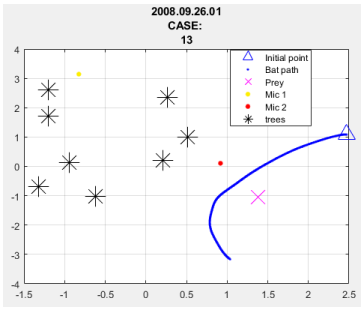

Figure 14 Flight Path Experiment Case 13

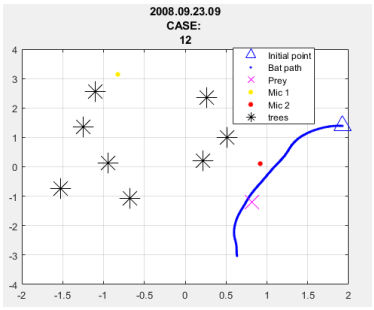

Figure 15 Flight Path Experiment Case 12

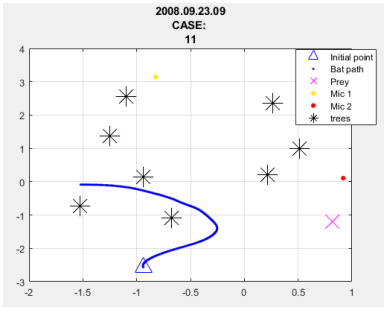

Figure 16 Flight Path Experiment Case 11

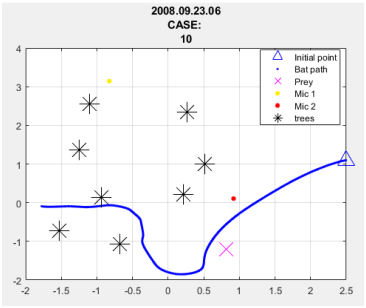

Figure 17 Flight Path Experiment Case 10

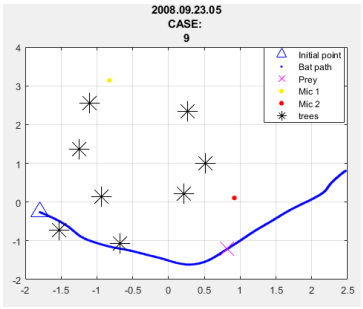

Figure 18 Flight Path Experiment Case 9

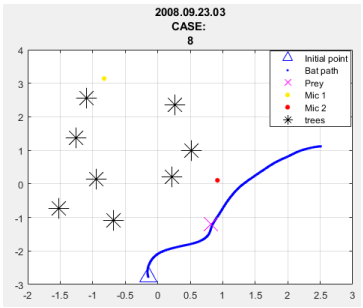

Figure 19 Flight Path Experiment Case 8

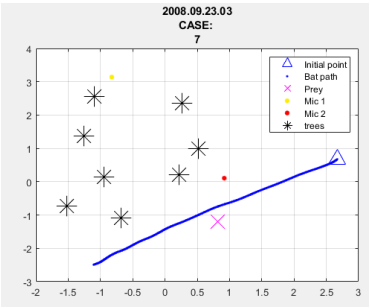

Figure 20 Flight Path Experiment Case 7

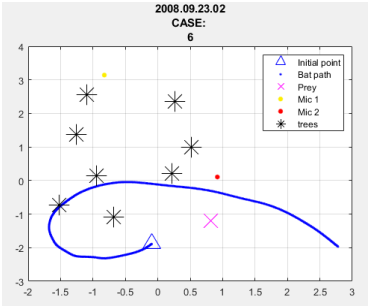

Figure 21 Flight Path Experiment Case 6

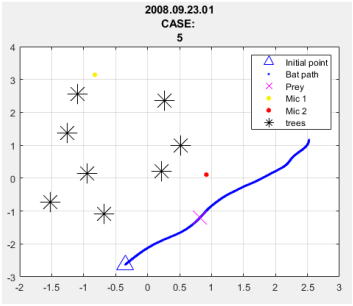

Figure 22 Flight Path Experiment Case 5

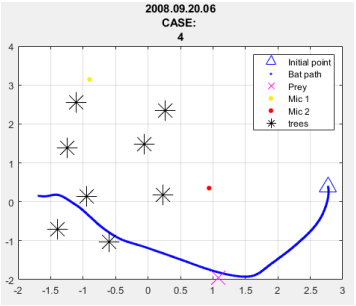

Figure 23 Flight Path Experiment Case 4

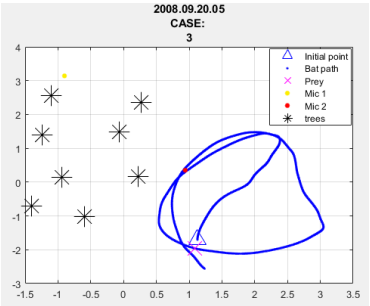

Figure 24 Flight Path Experiment Case 3

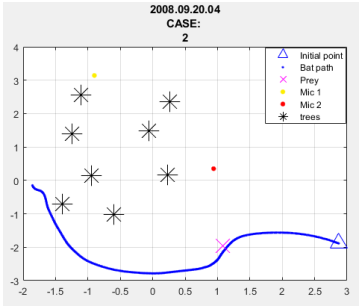

Figure 25 Flight Path Experiment Case 2

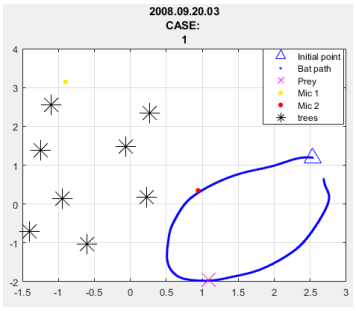

Figure 26 Flight Path Experiment Case 1

A plot including both, the Maximum vocalization vector and fight path direction vector, or heading Vector, were include in this section. Noted that just a few points, in fact, the sound recording frames, were included to avoid saturation of the plot and ease on the visualization. Vector were escalated in a way to avoid overlay; thus, scalar magnitude should not be taken as reference. Dashed Blue line correspond to heading vector and solid black line to the maximum vocalization vector.

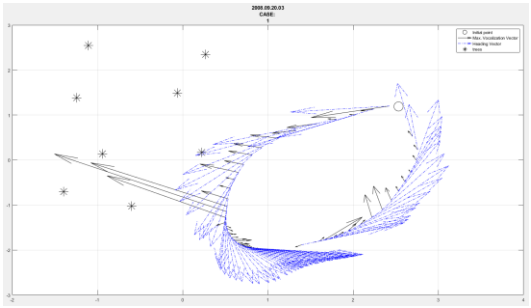

Figure 27 Heading Angle VS Gazing Angle Case 1

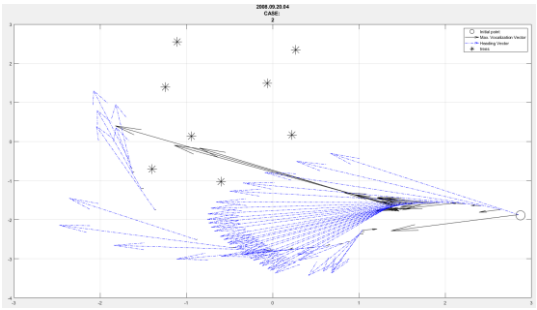

Figure 28 Heading Angle VS Gazing Angle Case 2

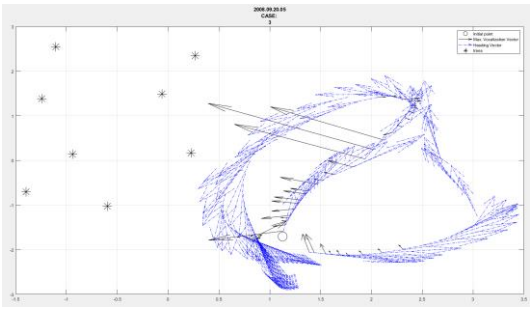

Figure 29 Heading Angle VS Gazing Angle Case 3

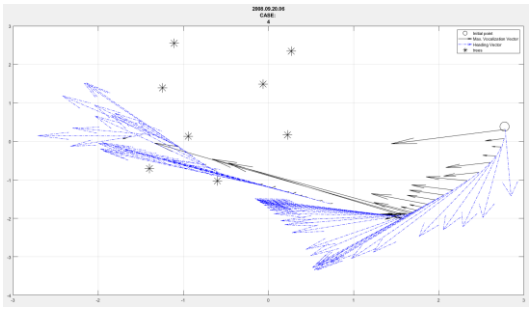

Figure 30 Heading Angle VS Gazing Angle Case 4

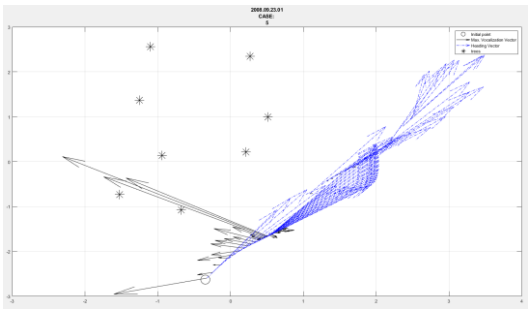

Figure 31 Heading Angle VS Gazing Angle Case 5

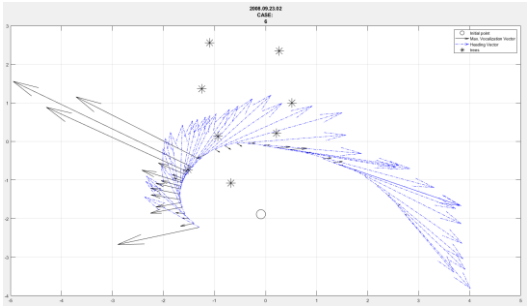

Figure 32 Heading Angle VS Gazing Angle Case 6

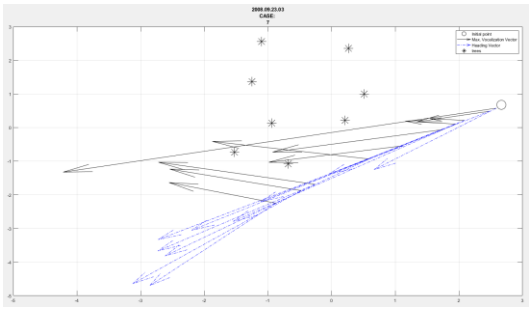

Figure 33 Heading Angle VS Gazing Angle Case 7

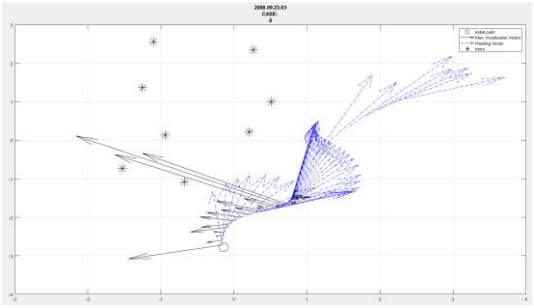

Figure 34 Heading Angle VS Gazing Angle Case 8

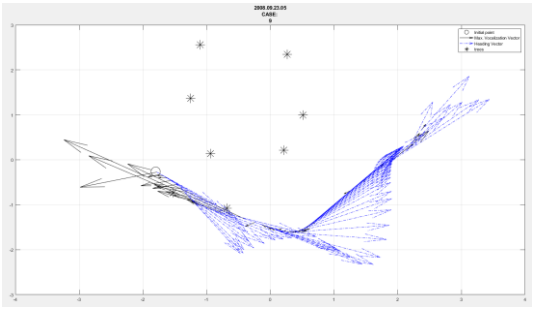

Figure 35 Heading Angle VS Gazing Angle Case 9

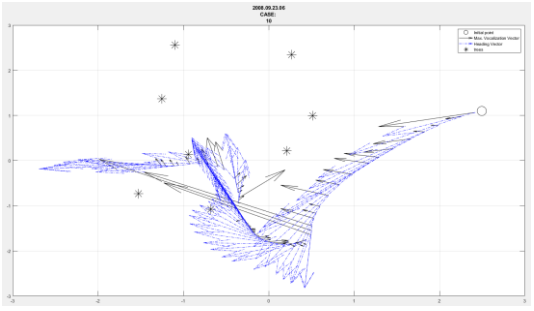

Figure 36 Heading Angle VS Gazing Angle Case 10

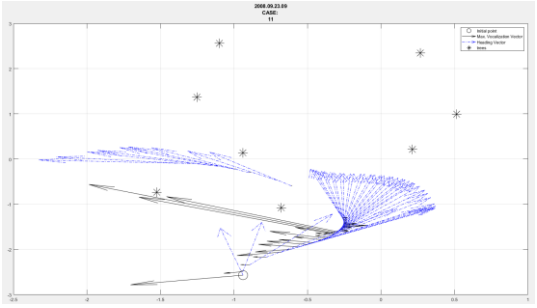

Figure 37 Heading Angle VS Gazing Angle Case 11

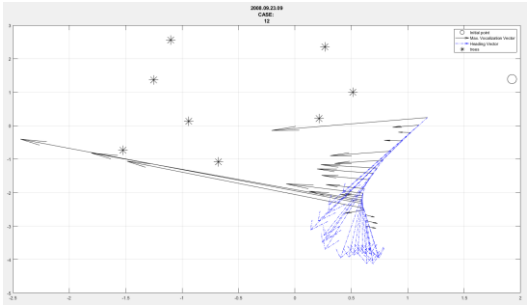

Figure 38 Heading Angle VS Gazing Angle Case 12

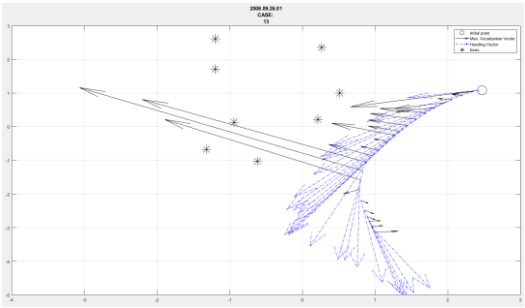

Figure 39 Heading Angle VS Gazing Angle Case 13

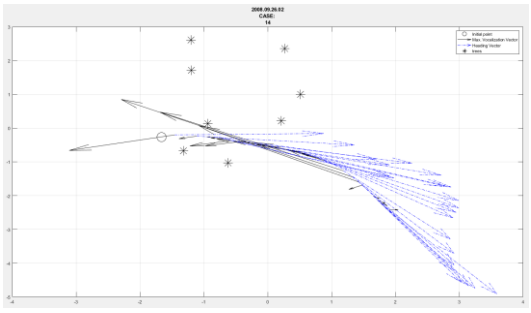

Figure 40 Heading Angle VS Gazing Angle Case 14

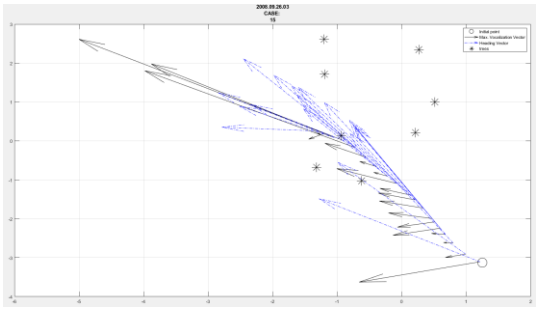

Figure 41 Heading Angle VS Gazing Angle Case 15

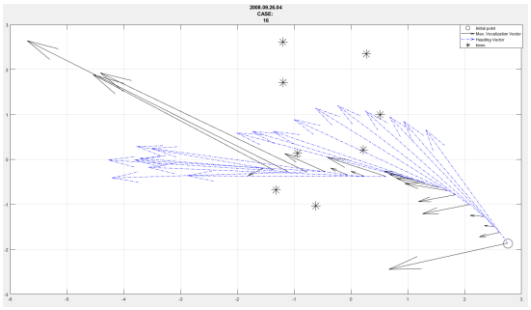

Figure 42 Heading Angle VS Gazing Angle Case 16

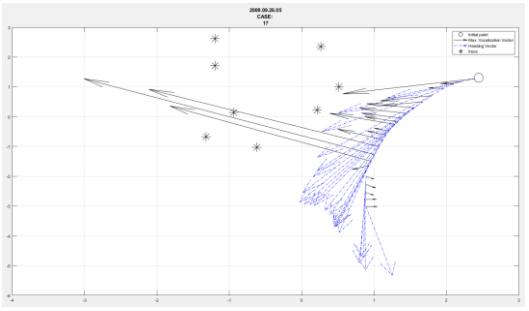

Figure 43 Heading Angle VS Gazing Angle Case 17

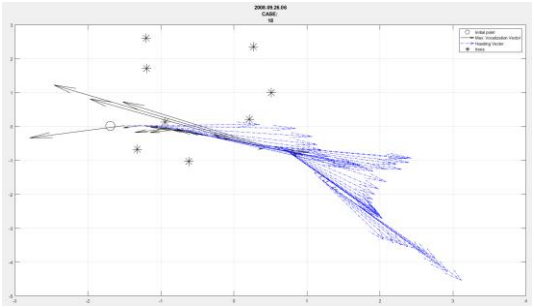

Figure 44 Heading Angle VS Gazing Angle Case 18

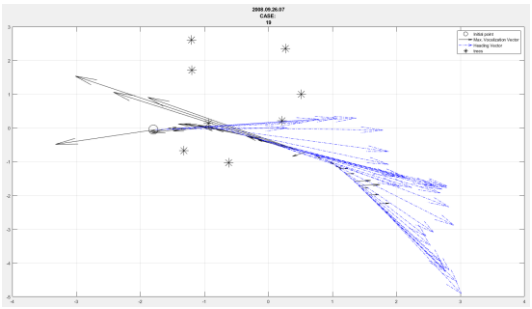

Figure 45 Heading Angle VS Gazing Angle Case 19

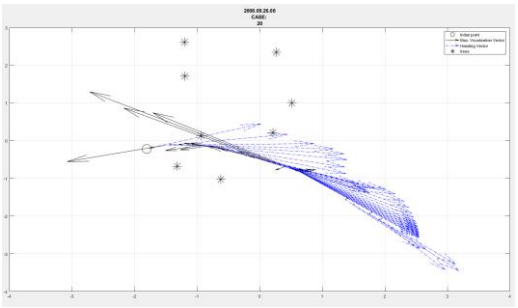

Figure 46 Heading Angle VS Gazing Angle Case 20

CASE 1

The path's interested manoeuvre was the one containing the points number 270 to 430 from the flight path data of the bat. After the analyse was carried out the author decide to shorten the set of points to the 325 to 425 ones.

270 to 430.

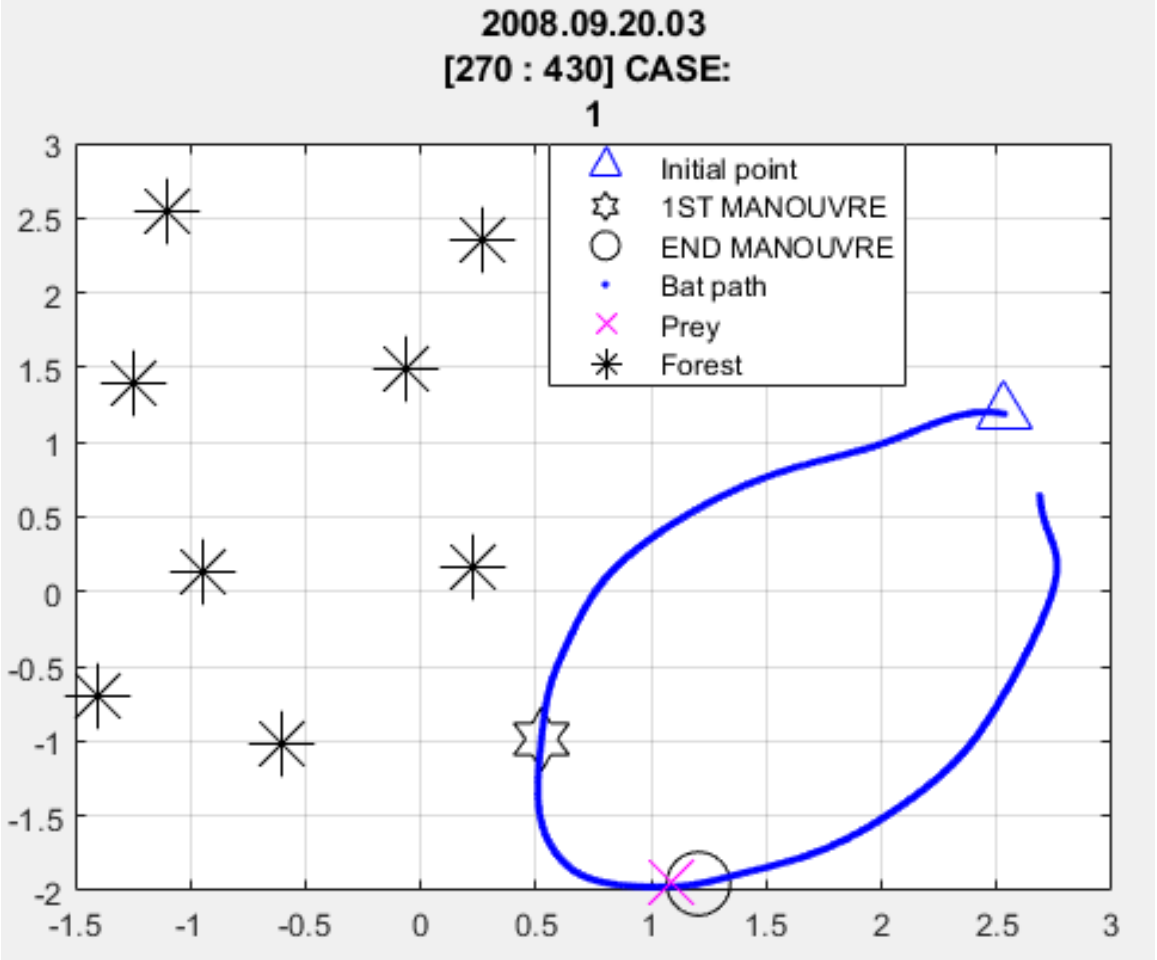

Figure 47 Case 1 [270 430] Analysis path

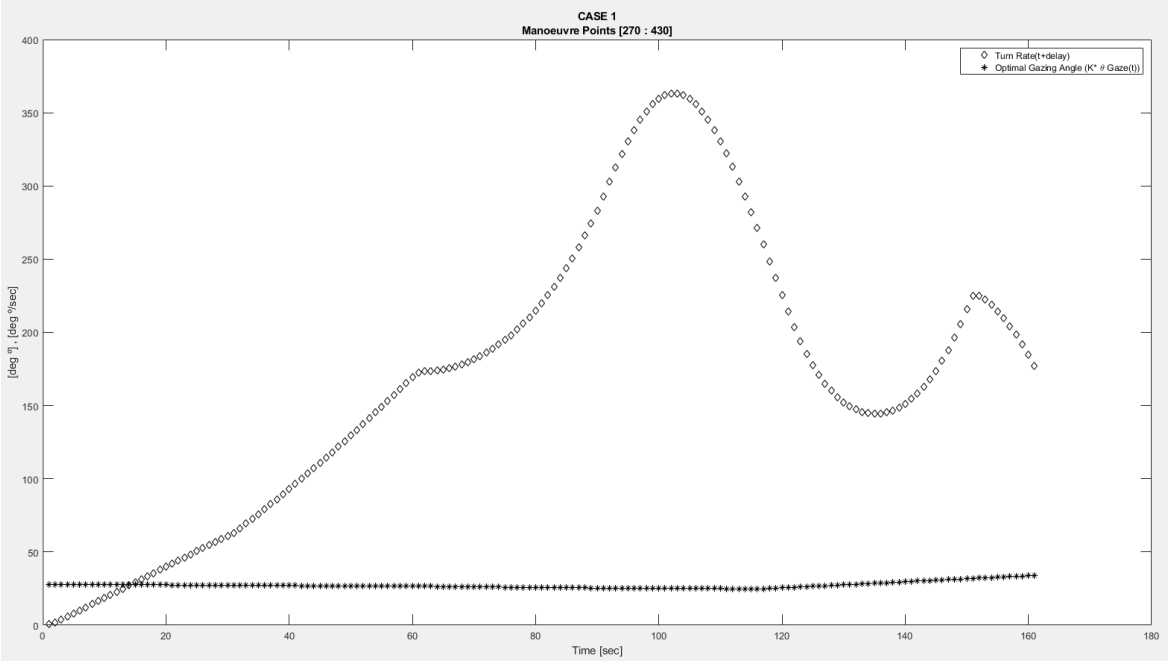

Figure 48 Case 1 [270 430] Turn rate VS gazing Angle

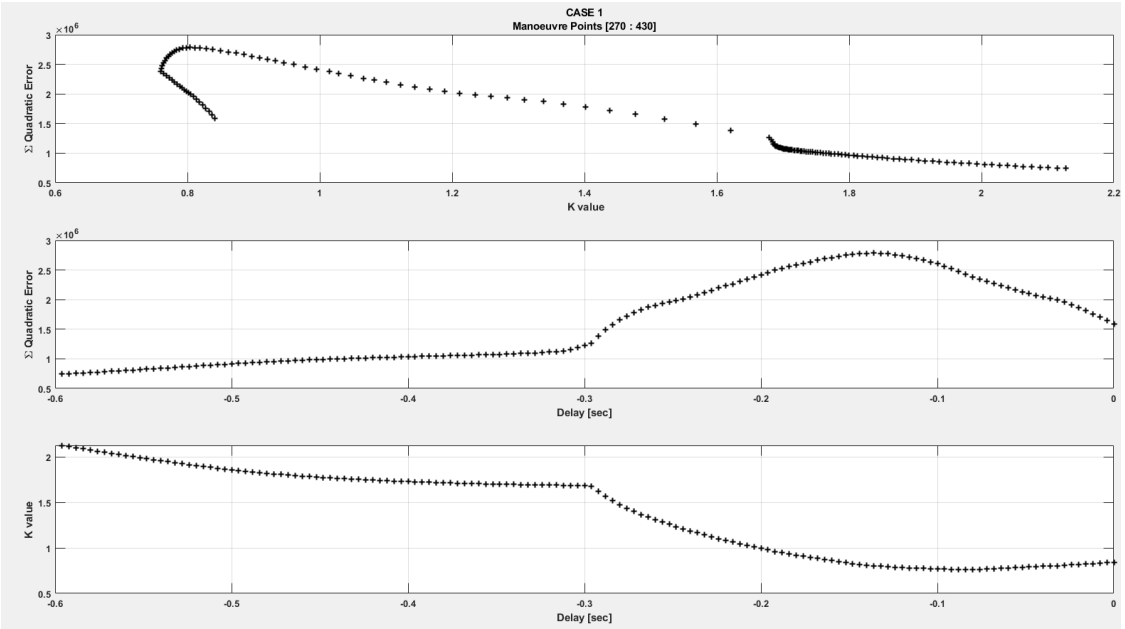

Figure 49 Case 1 [270 430] Quadratic Error, Delay and K value

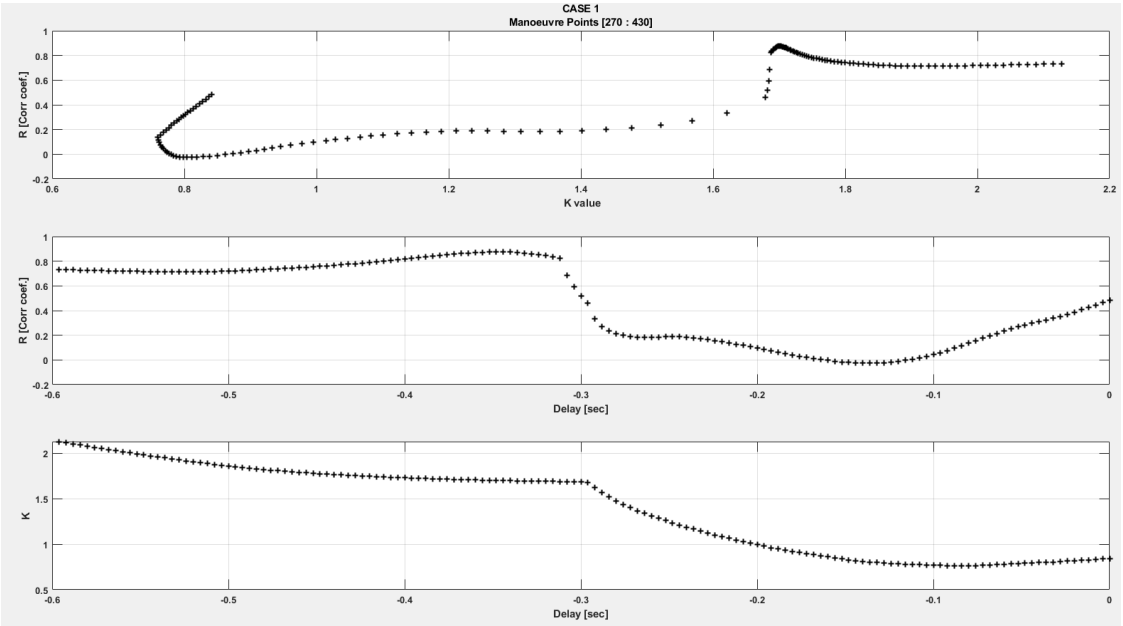

Figure 50 Case 1 [270 430] R, Delay and K value

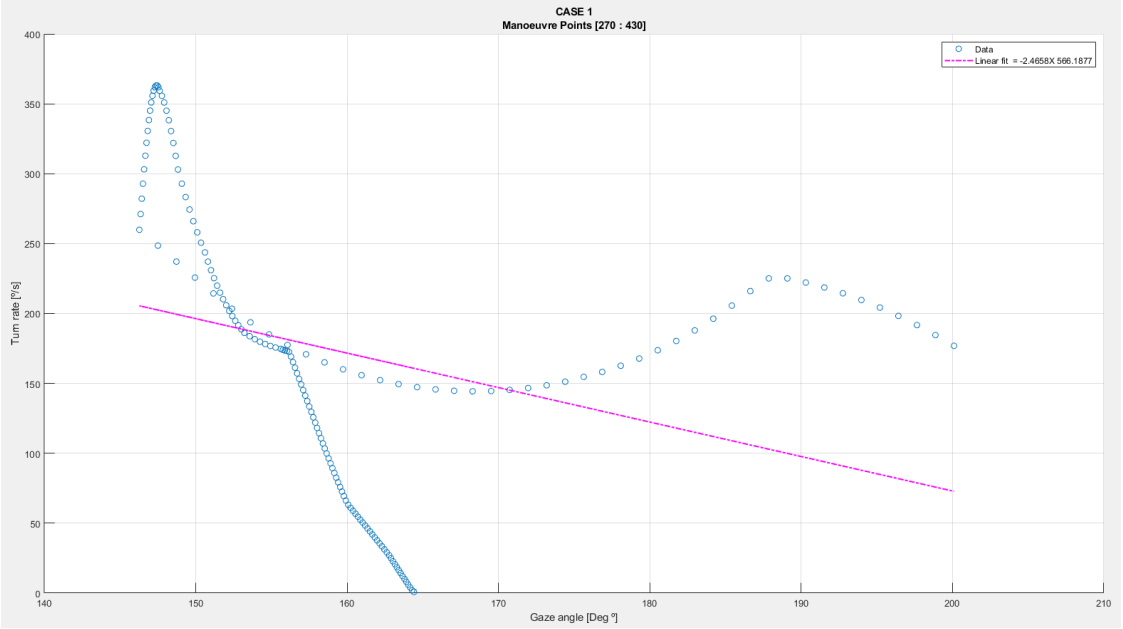

Figure 51Case 1 [270 430] Linear Regression

350 to 425

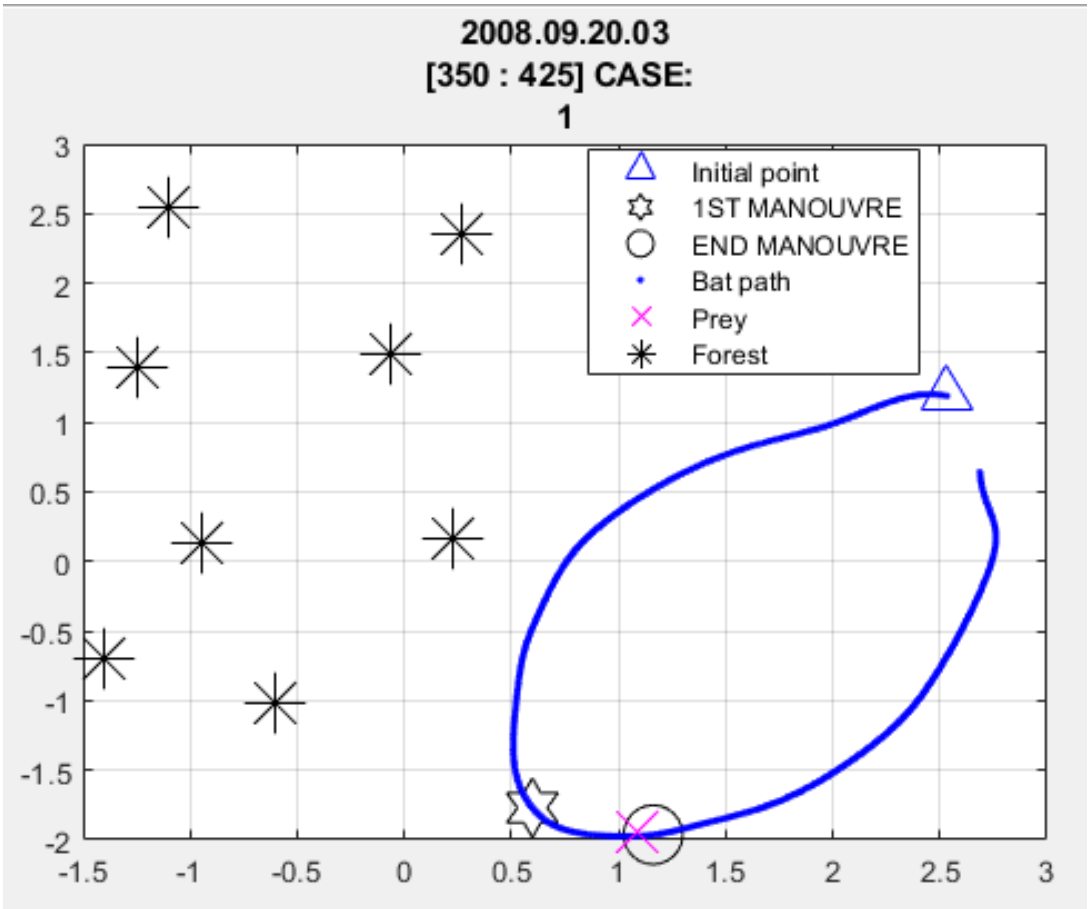

Figure 52 Case 1 [350 425] Analysis path

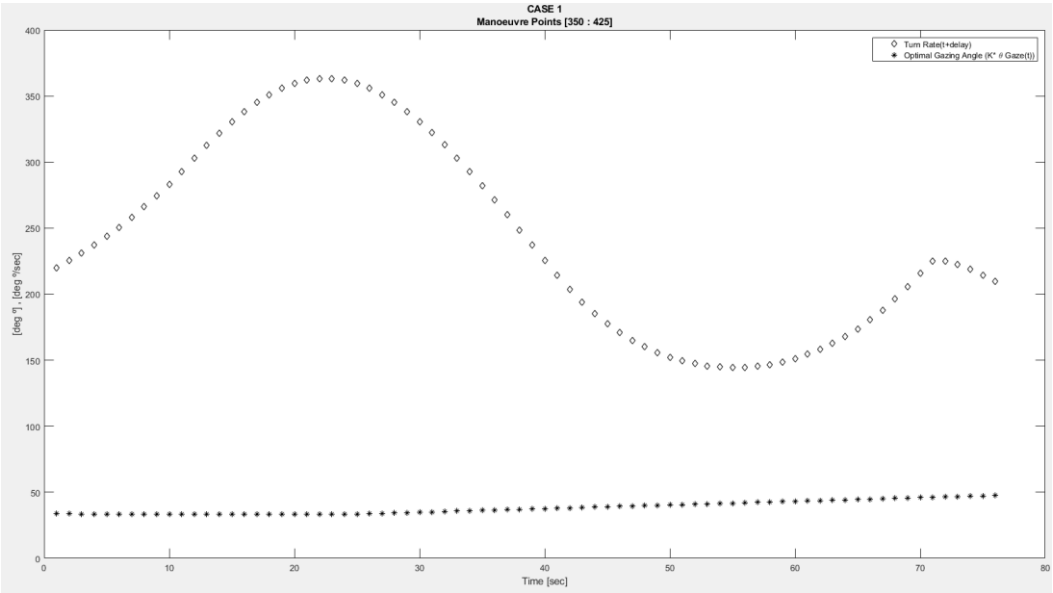

Figure 53 Case 1 [350 425] Turn Rate and Gazing Angle Comparison

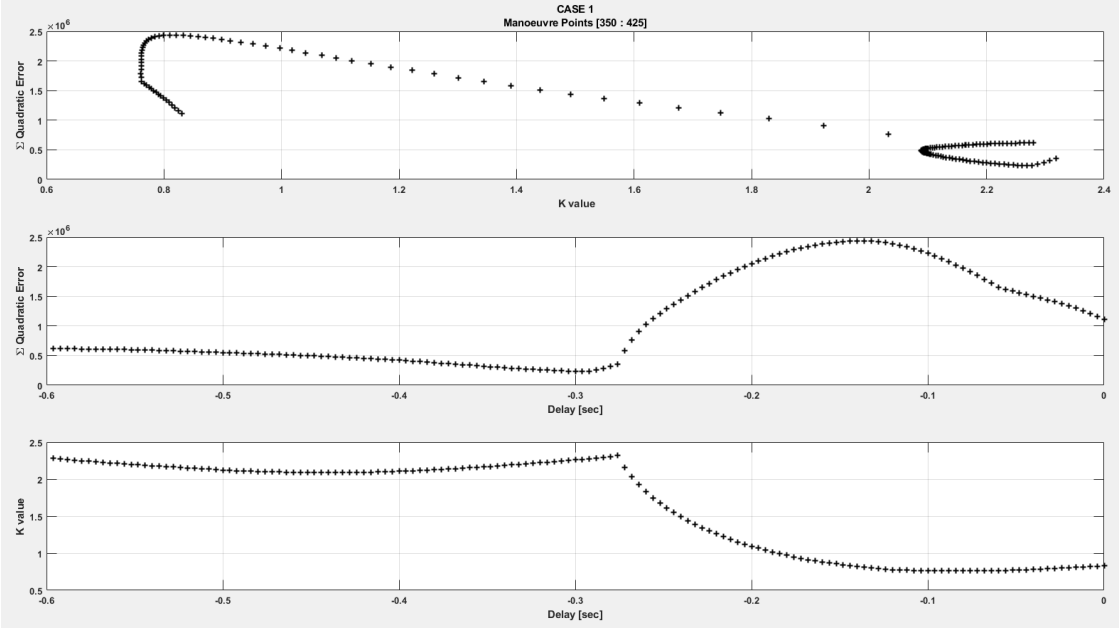

Figure 54 Case 1 [350 425] Quadratic Error, Delay, and k value

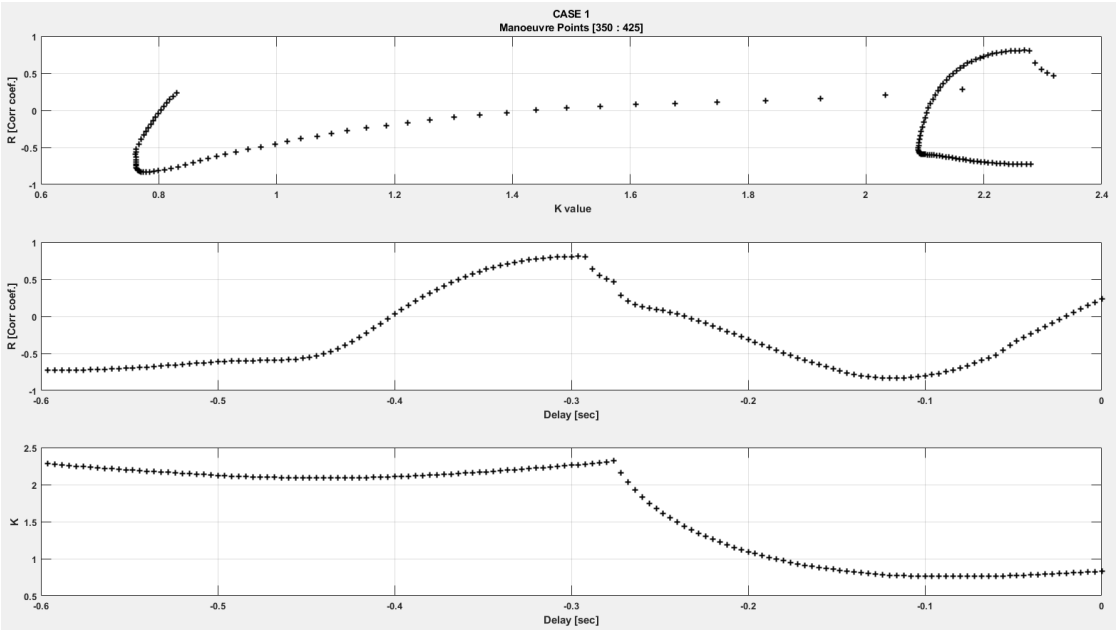

Figure 55 Case 1 [350 425] R, Delay and K value

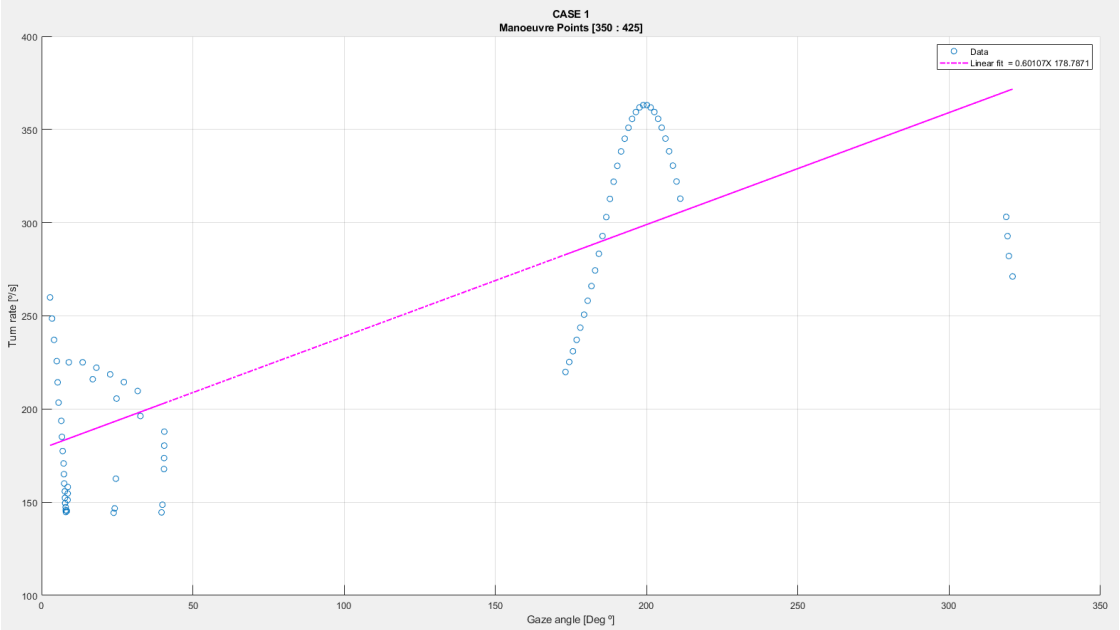

Figure 56 Case 1 [350 425] Linear Regression

CASE 2

80 to 170

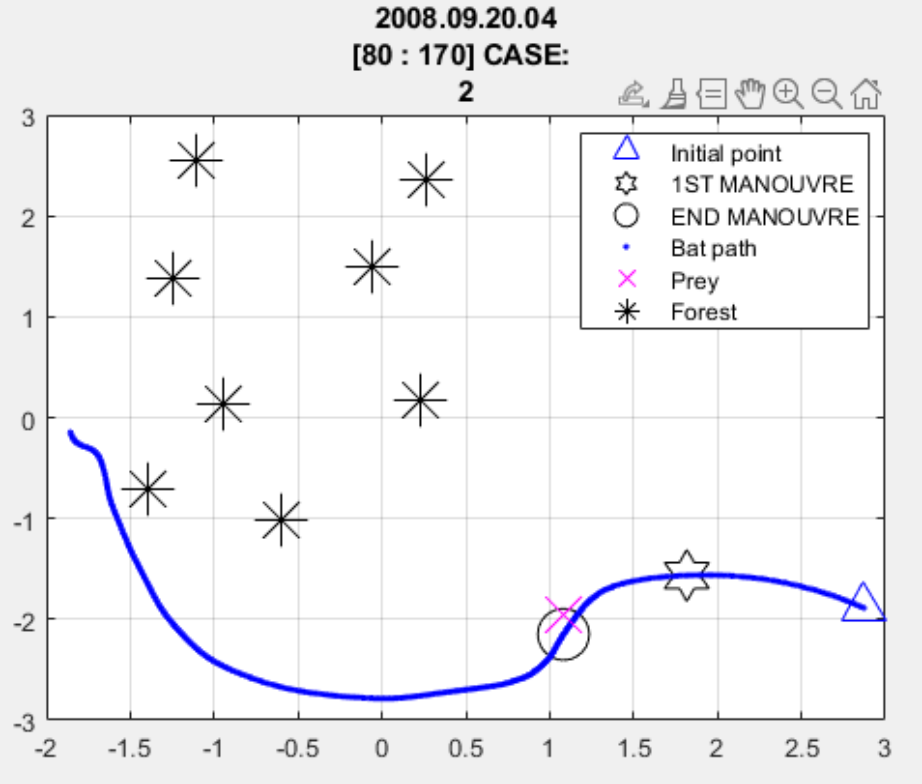

Figure 57 Case 2 [80 170] Fight Path

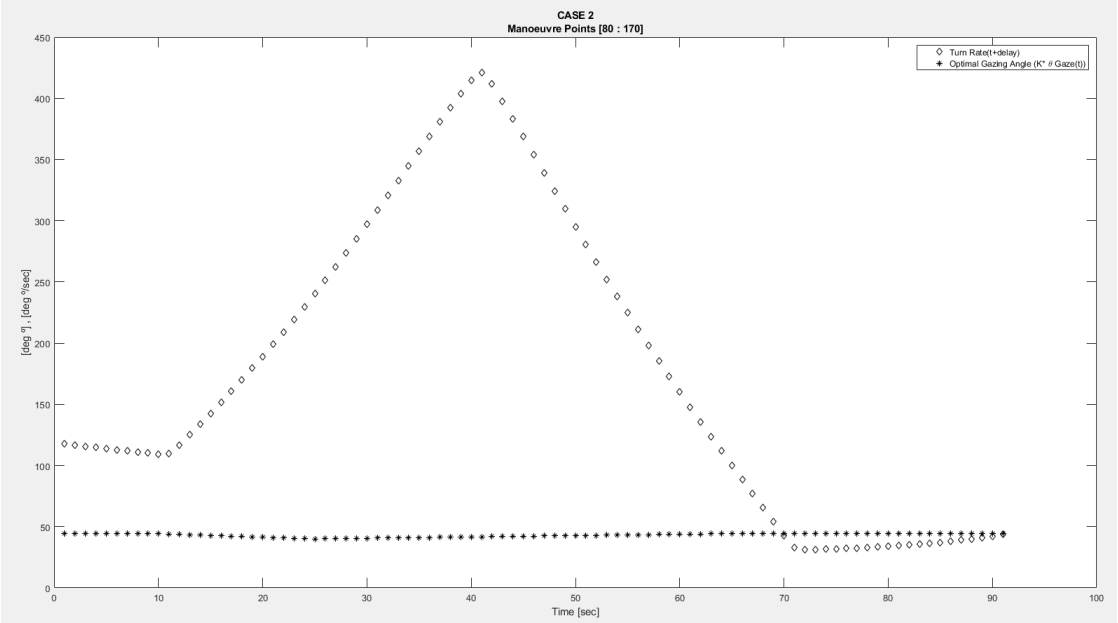

Figure 58 Case 2 [80 170] Turn Rate and Gazing Angle Comparison

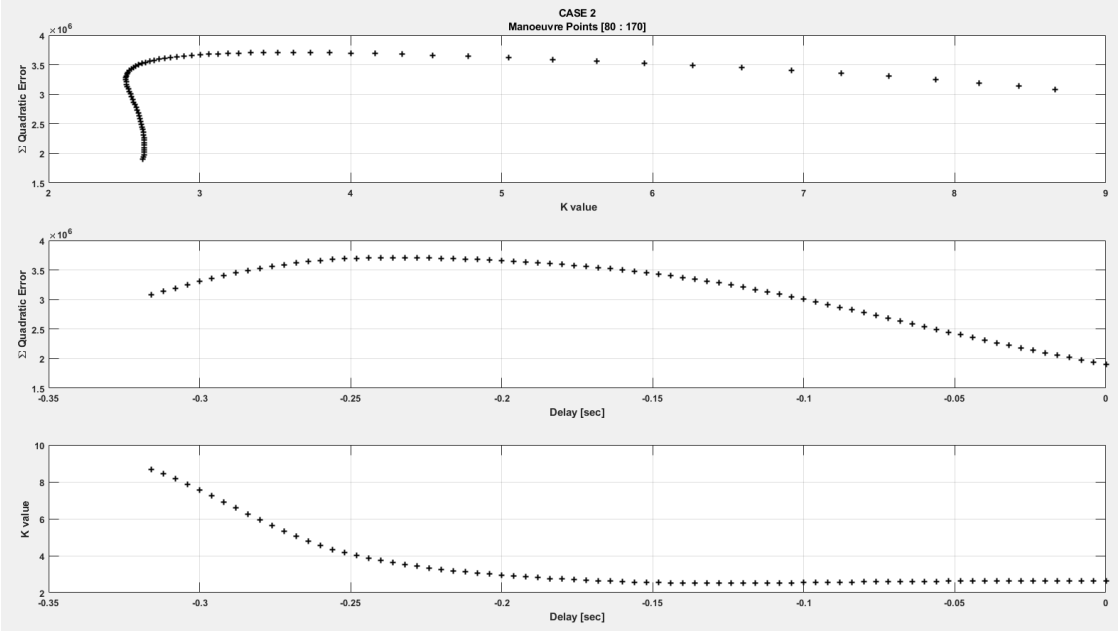

Figure 59 Case 2 [80 170] Quadratic Error, Delay, and k value

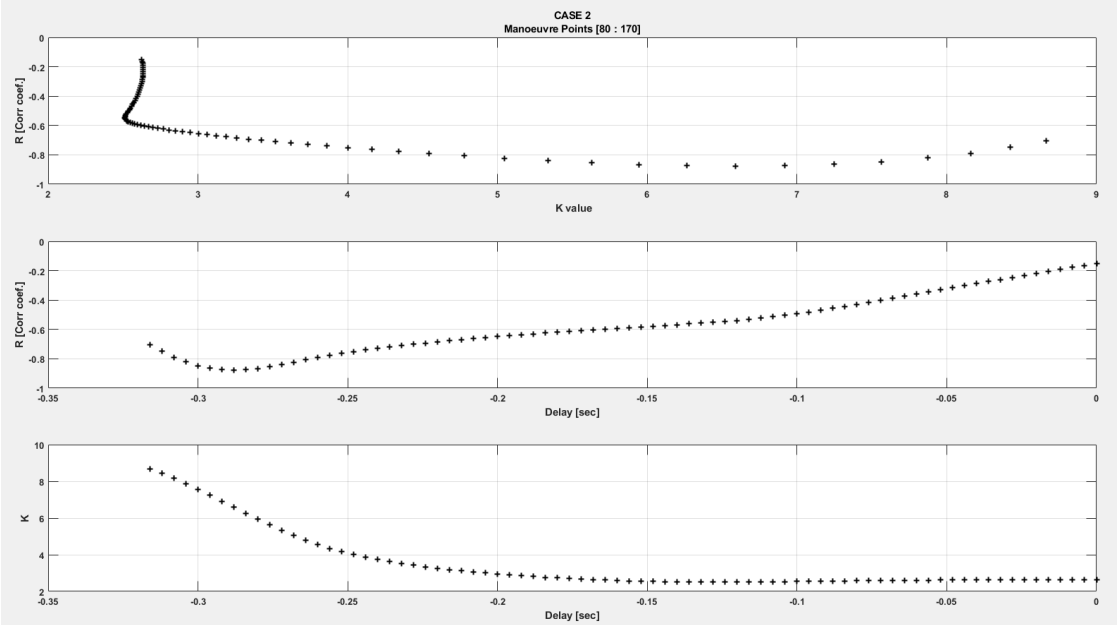

Figure 60 Case 2 [80 170] R, Delay and K value

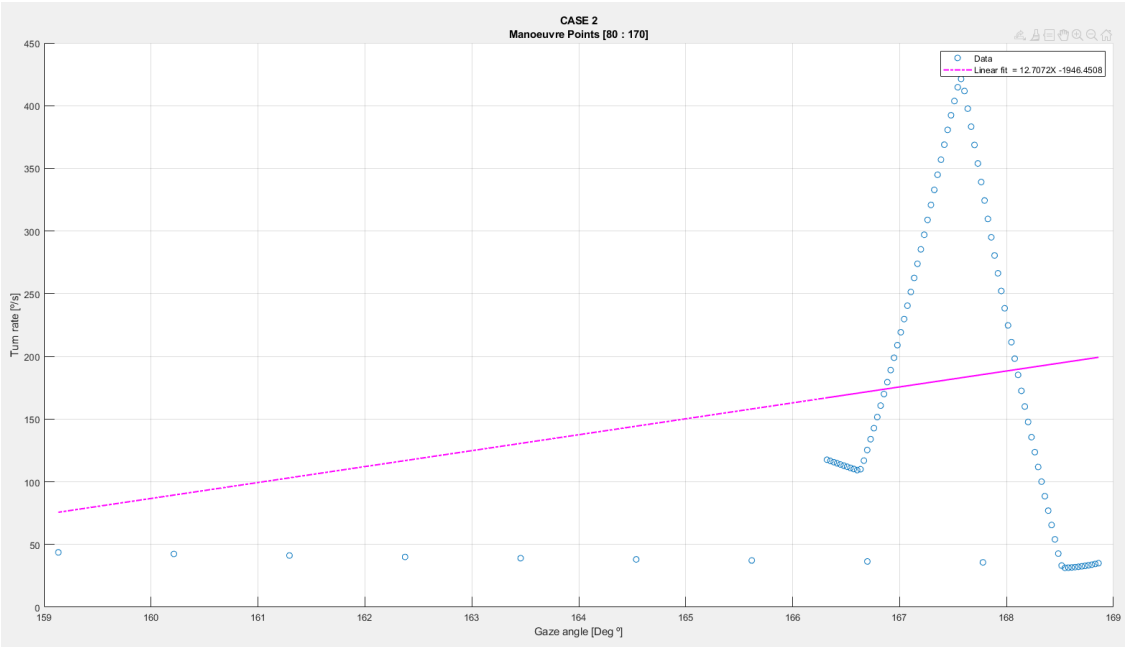

Figure 61 Case 2 [80 170] Linear Regression

Case 3

1620 1709

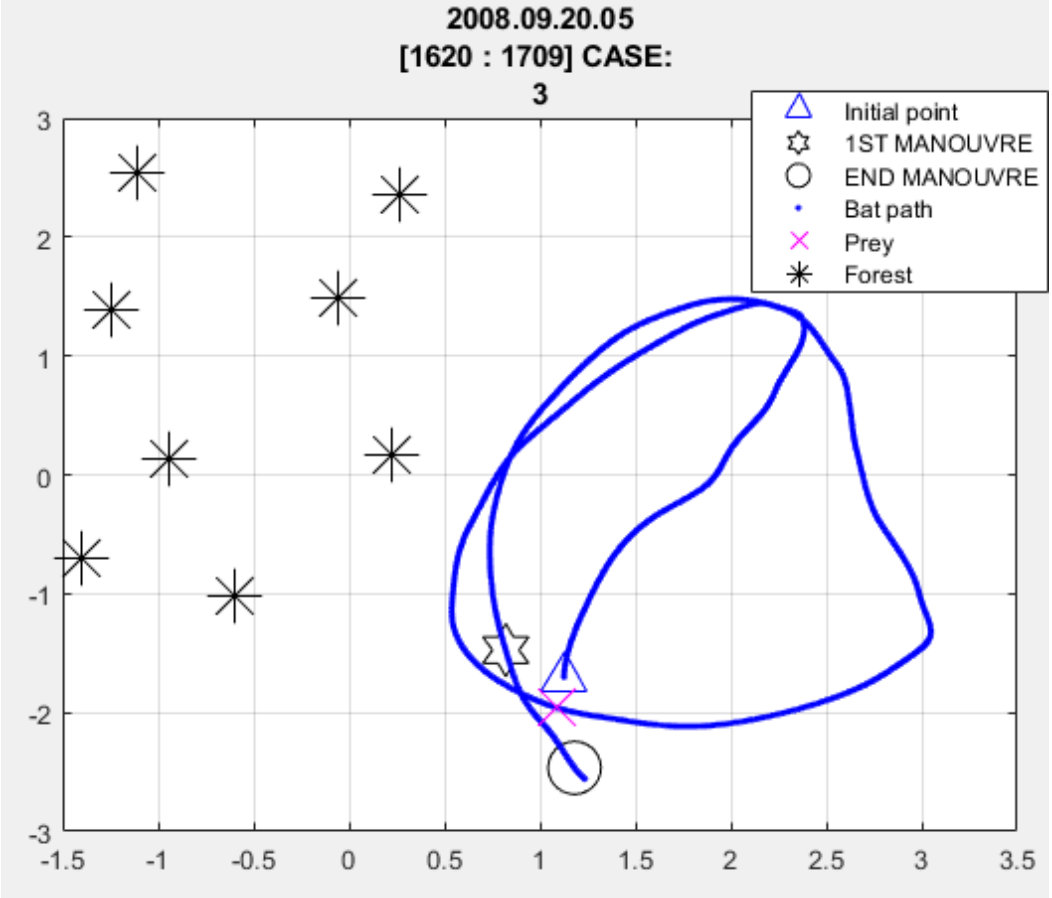

Figure 62 Case 3 [1620 1709] Fight Path

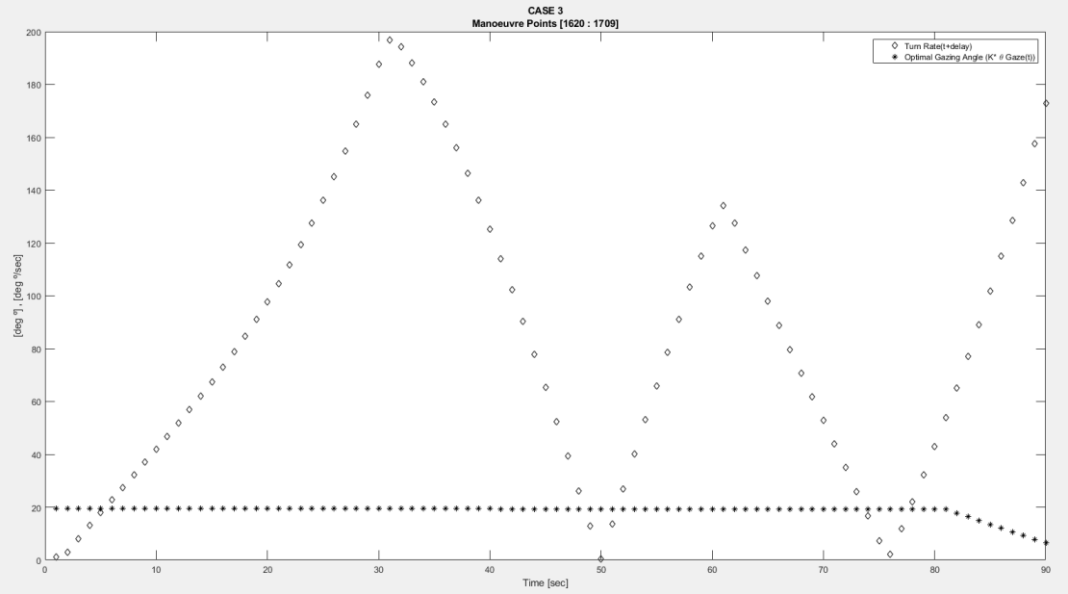

Figure 63 Case 3 [1620 1709] Turn Rate and Gazing Angle Comparison

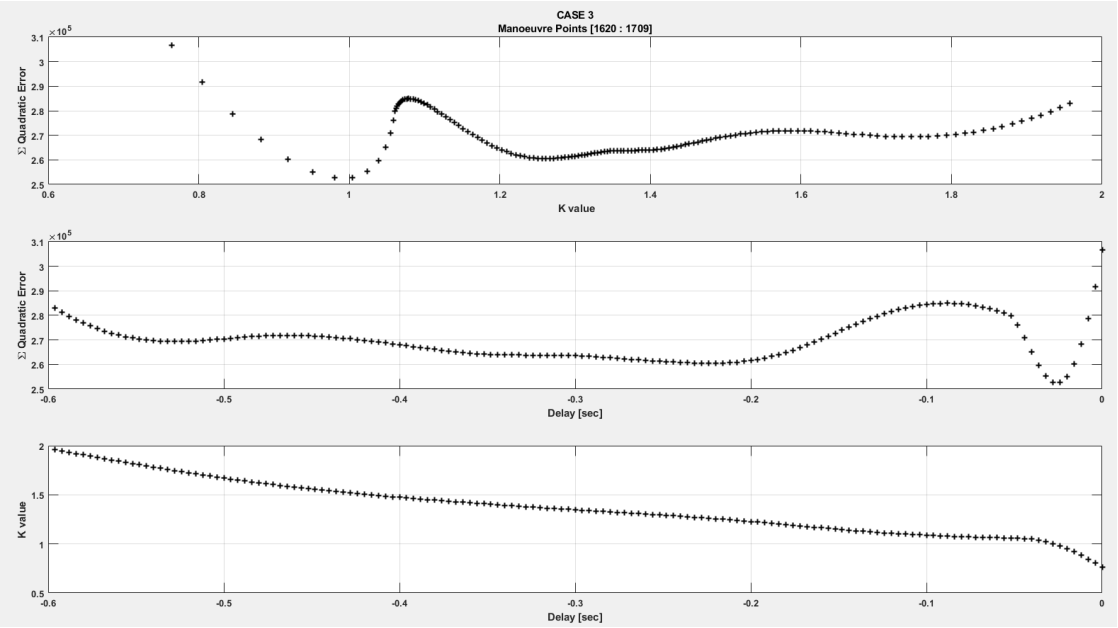

Figure 64 Case 3 [1620 1709] Quadratic Error, Delay and K value

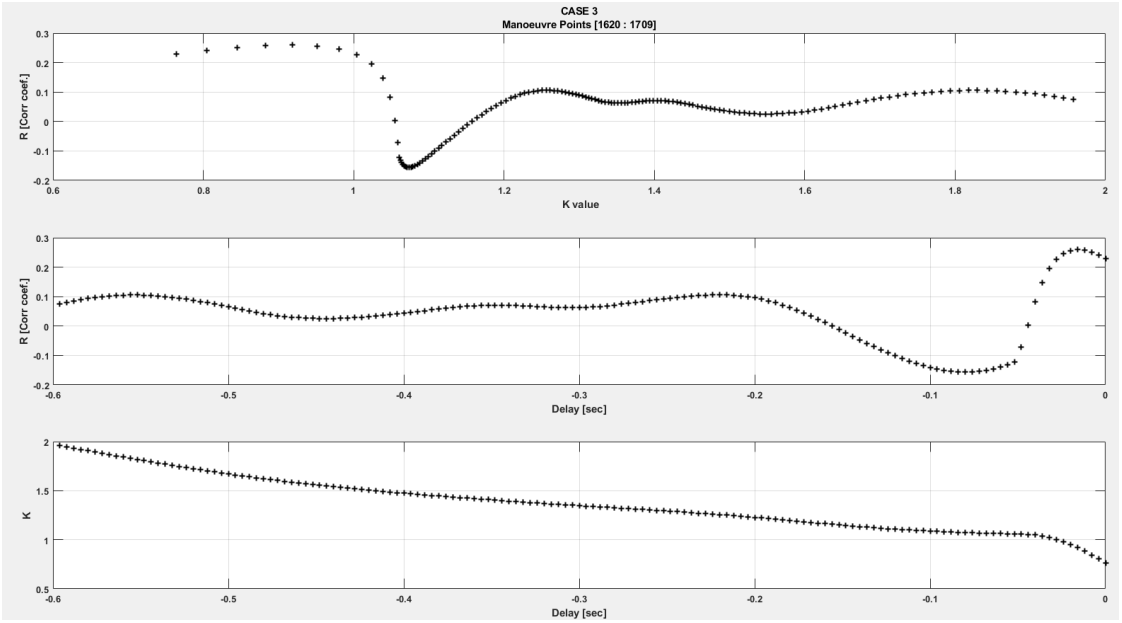

Figure 65 Case 3 [1620 1709] R, Delay and K value

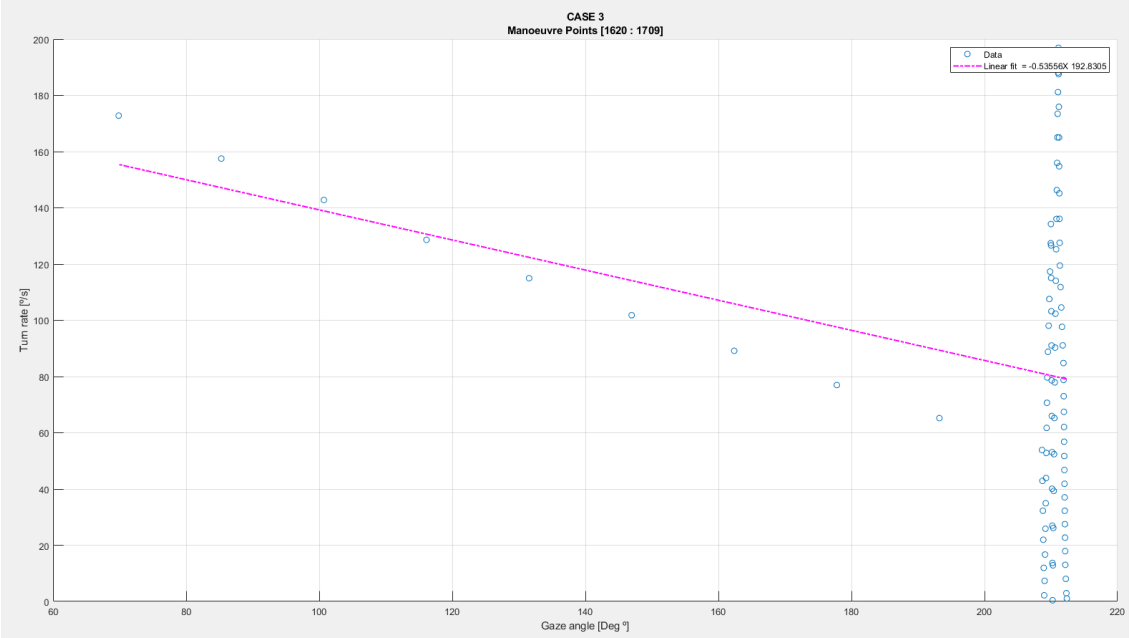

Figure 66 Case 3 [1620 1709] Linear Regression

1500 1620

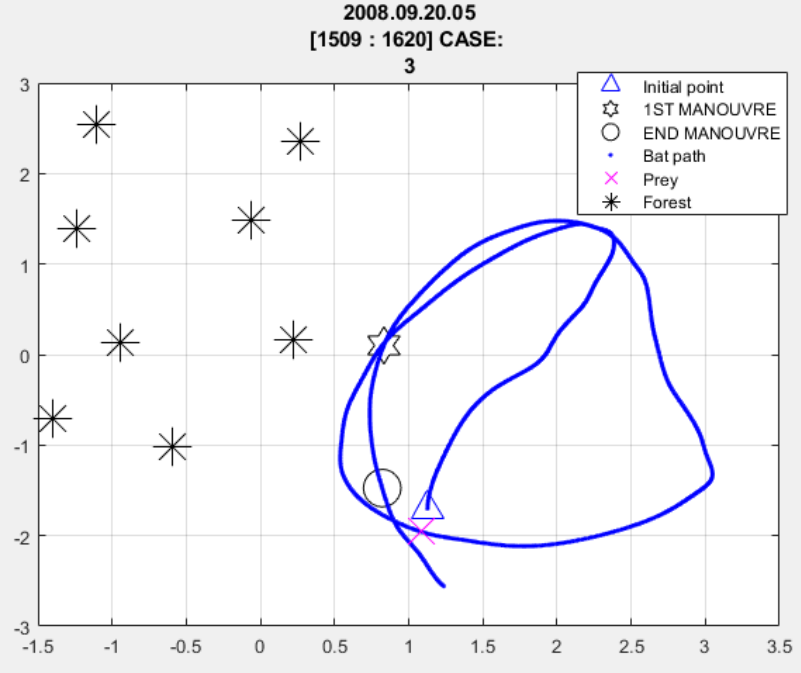

Figure 67 Case 3 [1500 1620] Fight Path

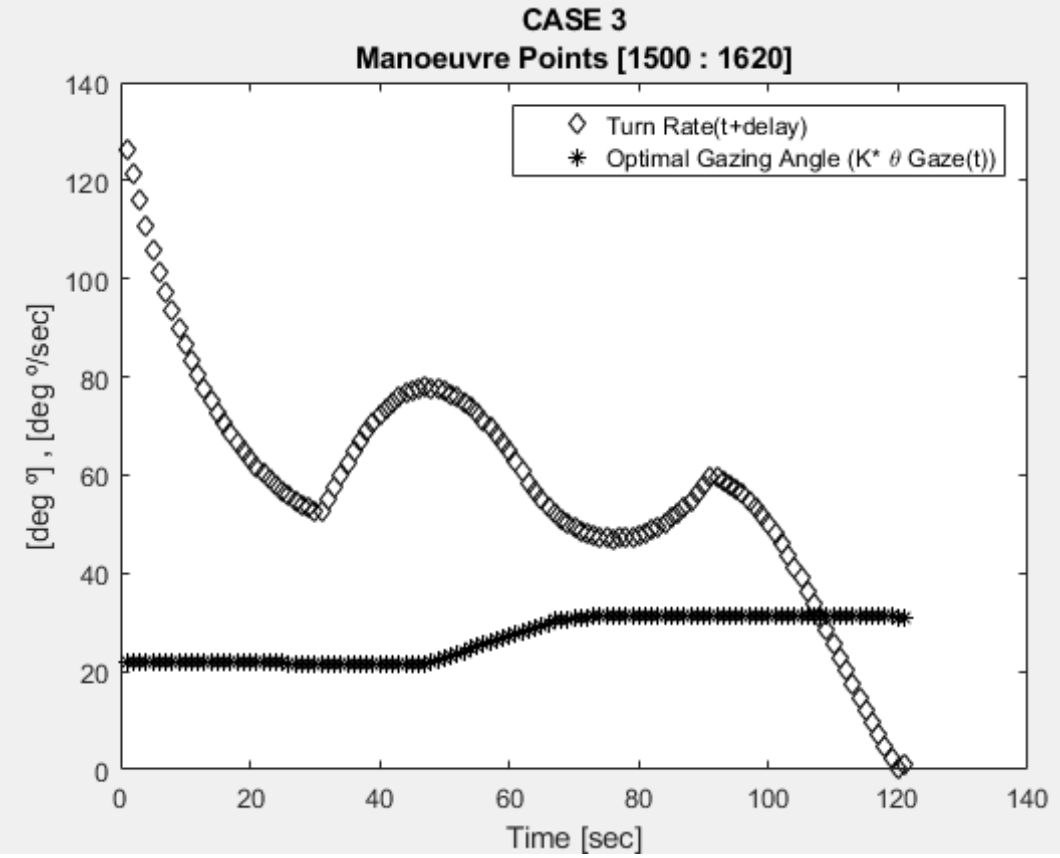

Figure 68 Case 3 [1500 1620] Turn Rate and Gazing Angle Comparison

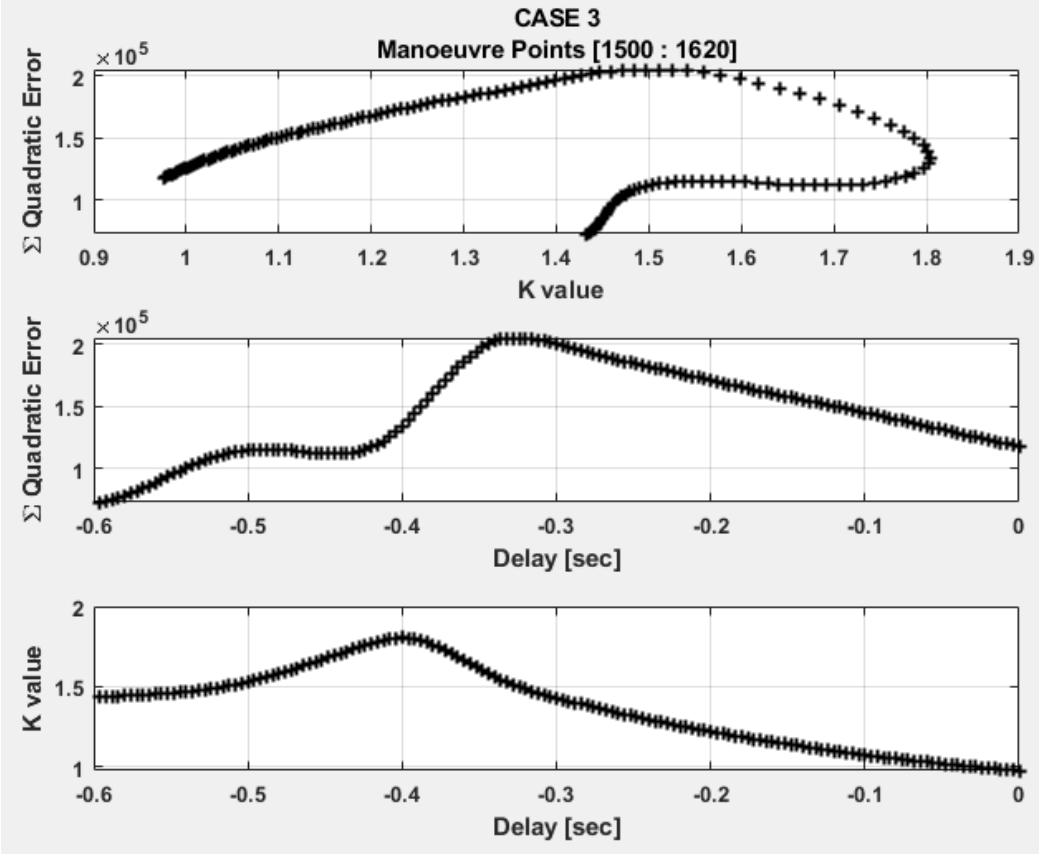

Figure 69 Case 3 [1500 1620] Quadratic Error, Delay and K value

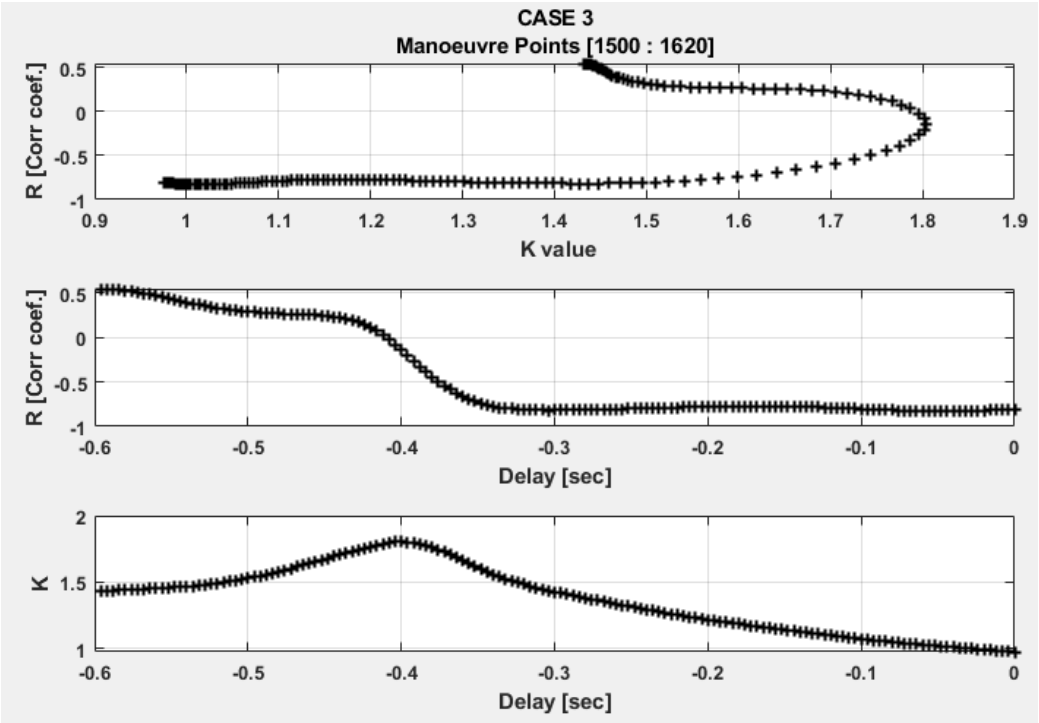

Figure 70 Case 3 [1500 1620] R, Delay and K value

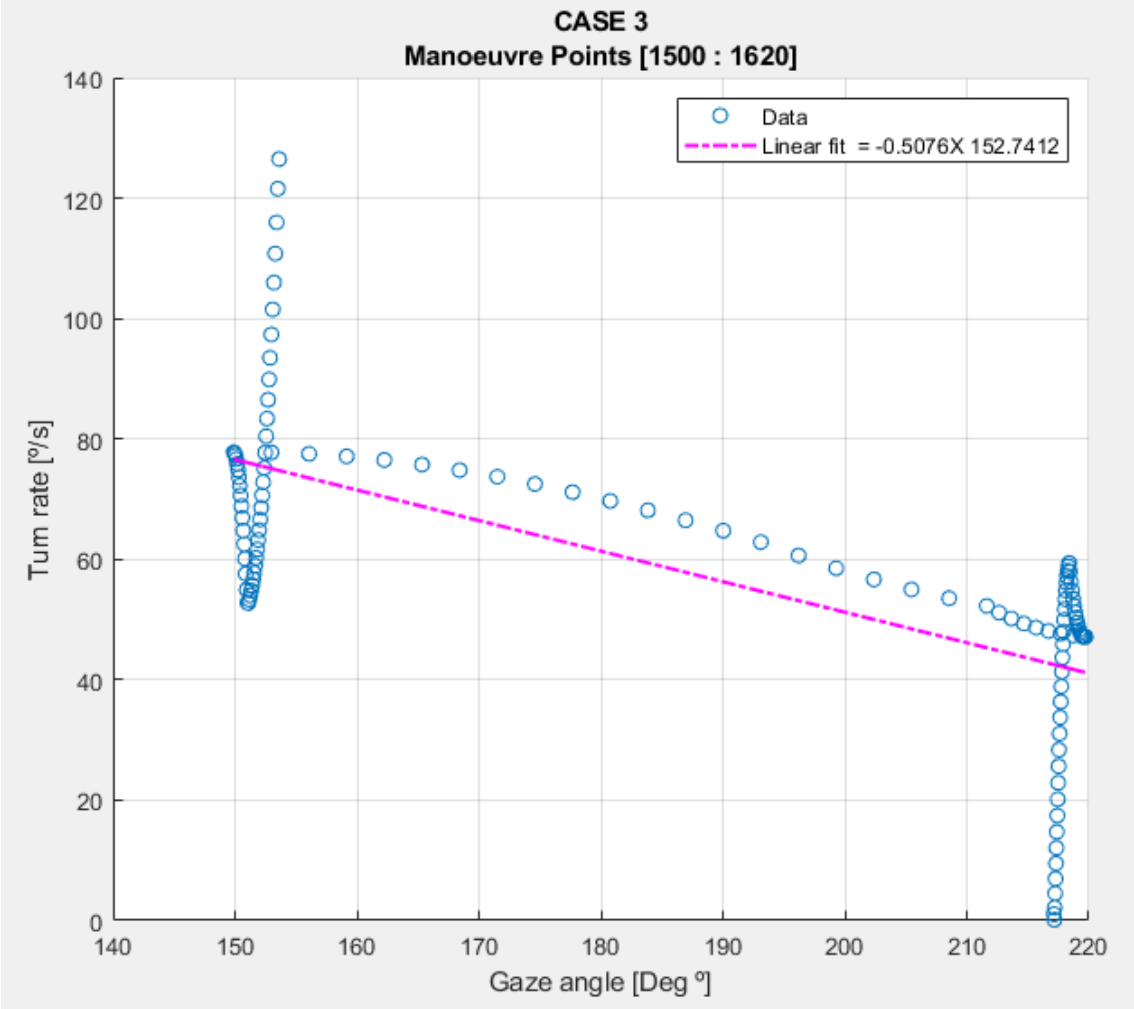

Figure 71 Figure 68 Case 3 [1500 1620] Linear Regression

1500 1709

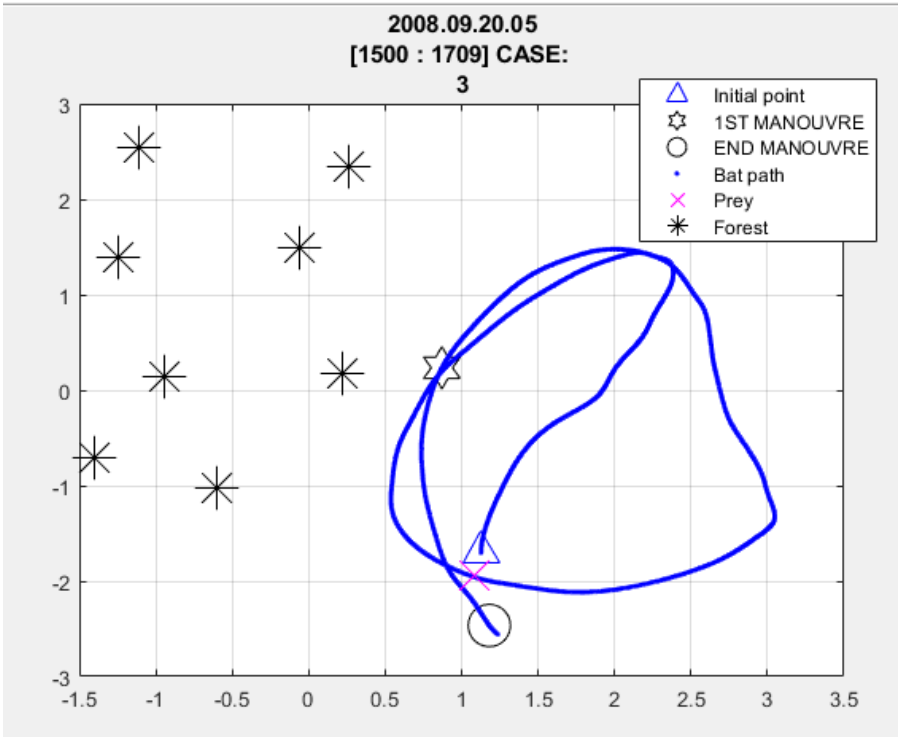

Figure 72 Case 3 [1500 1709] Flight Path

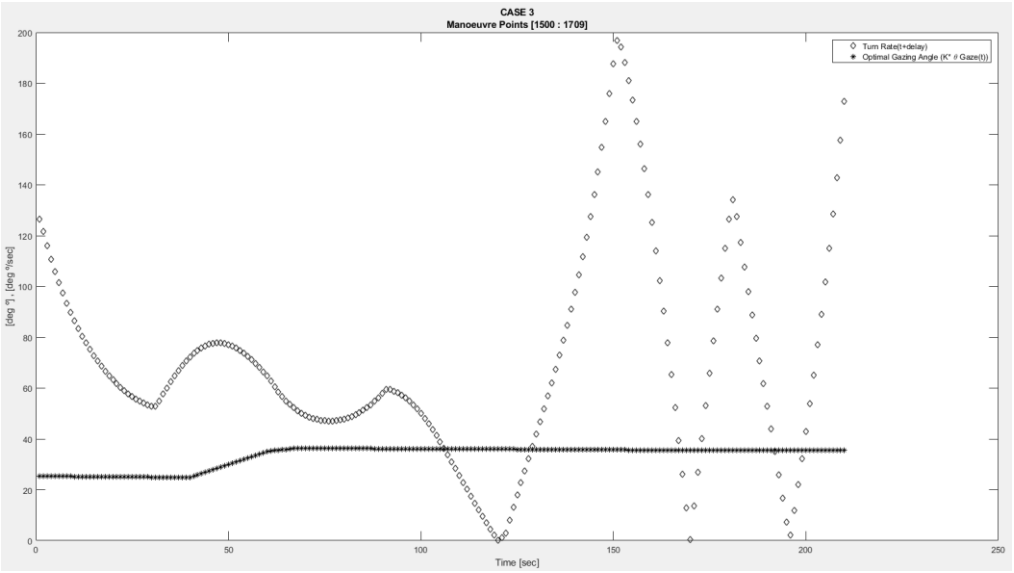

Figure 73 Case 3 [1500 1709] Turn Rate and Gazing Angle Comparison

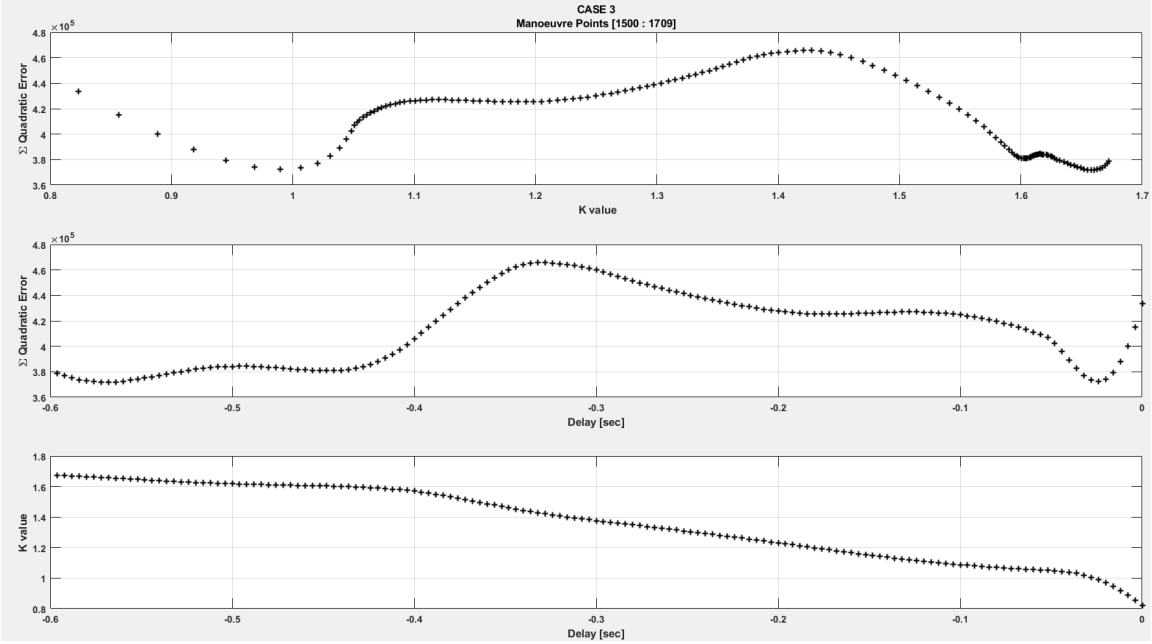

Figure 74 Case 3 [1500 1709] Quadratic Error, Delay and K value

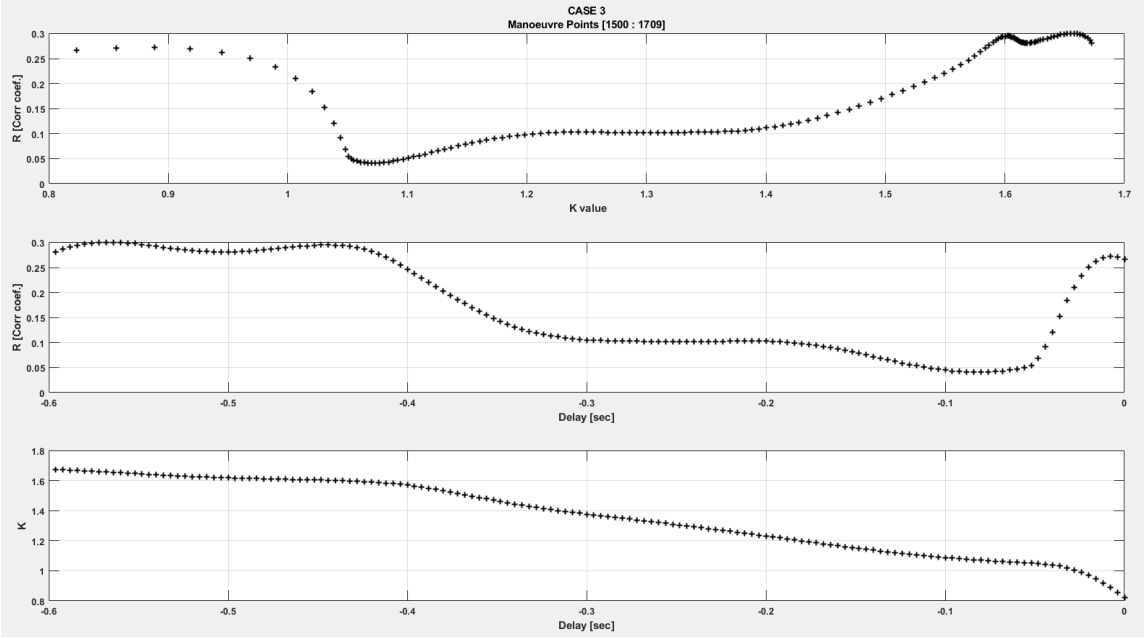

Figure 75 Case 3 [1500 1709] R, Delay and K value

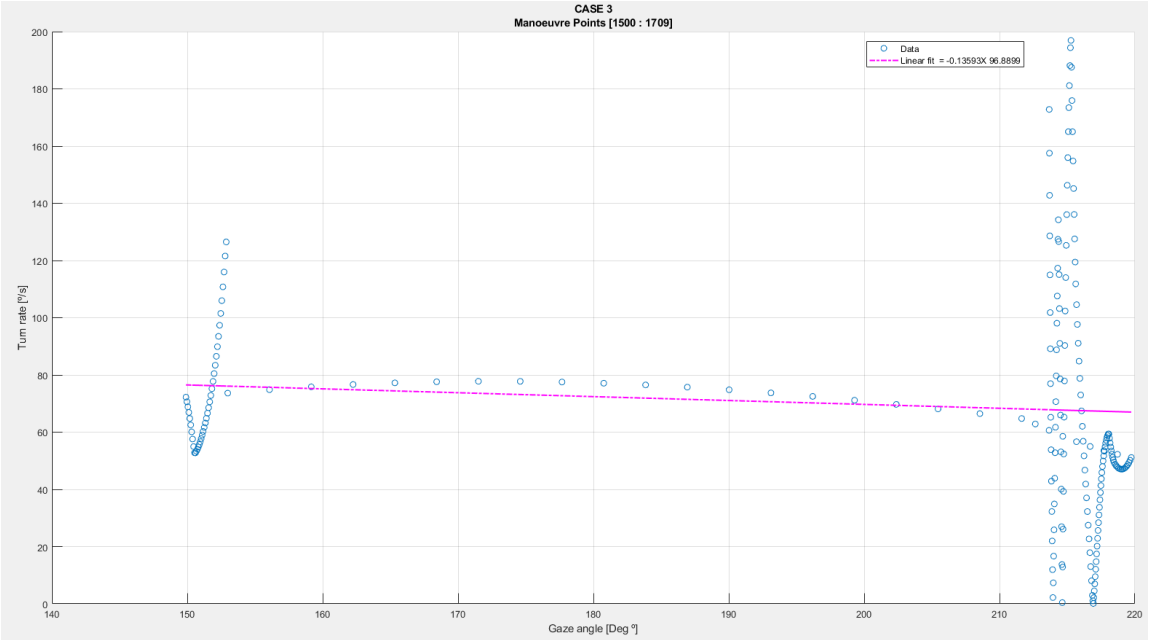

Figure 76 Case 3 [1500 1709] Linear Regression

950 1050

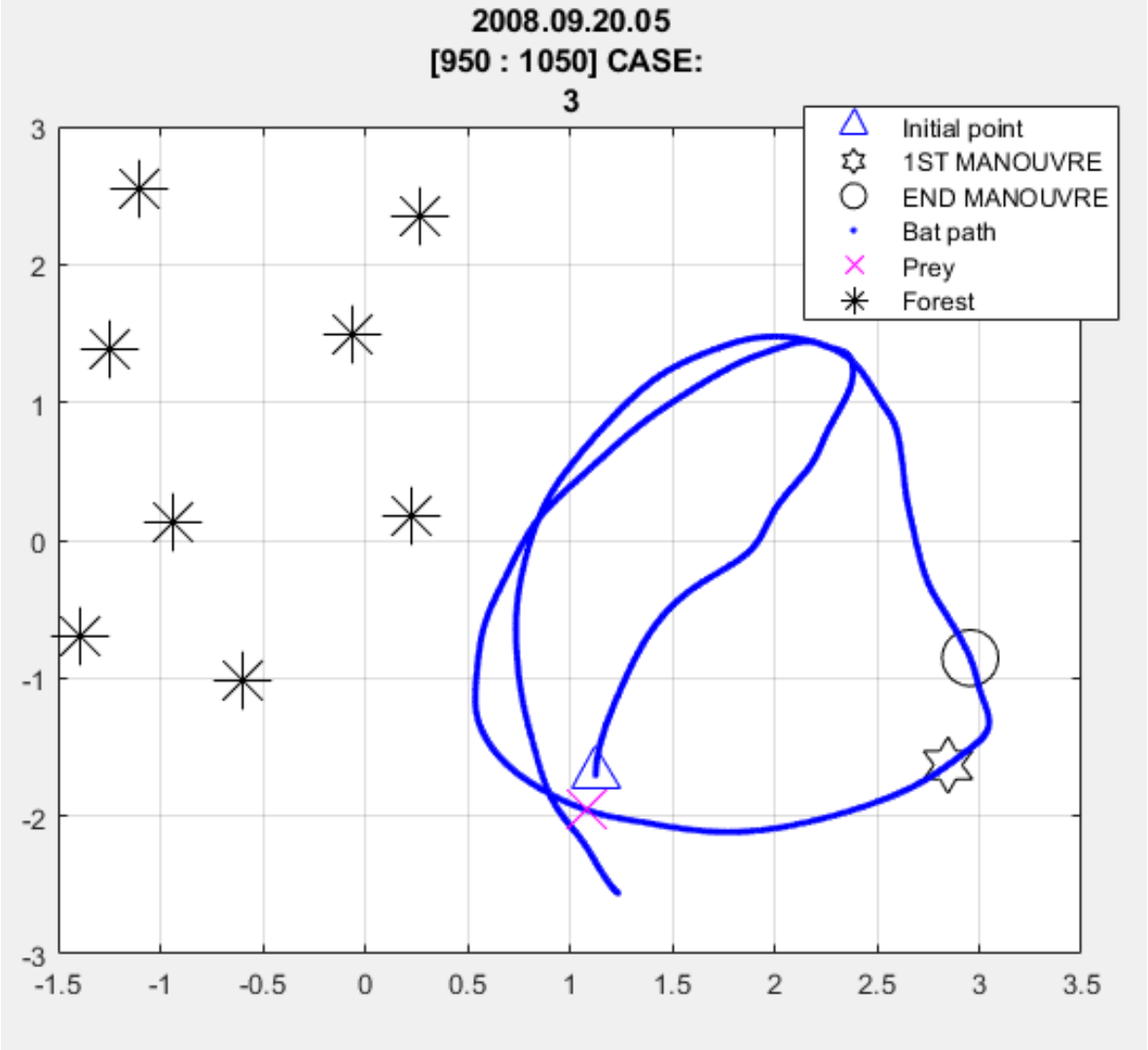

Figure 77 Case 3 [950 1050] Flight Path

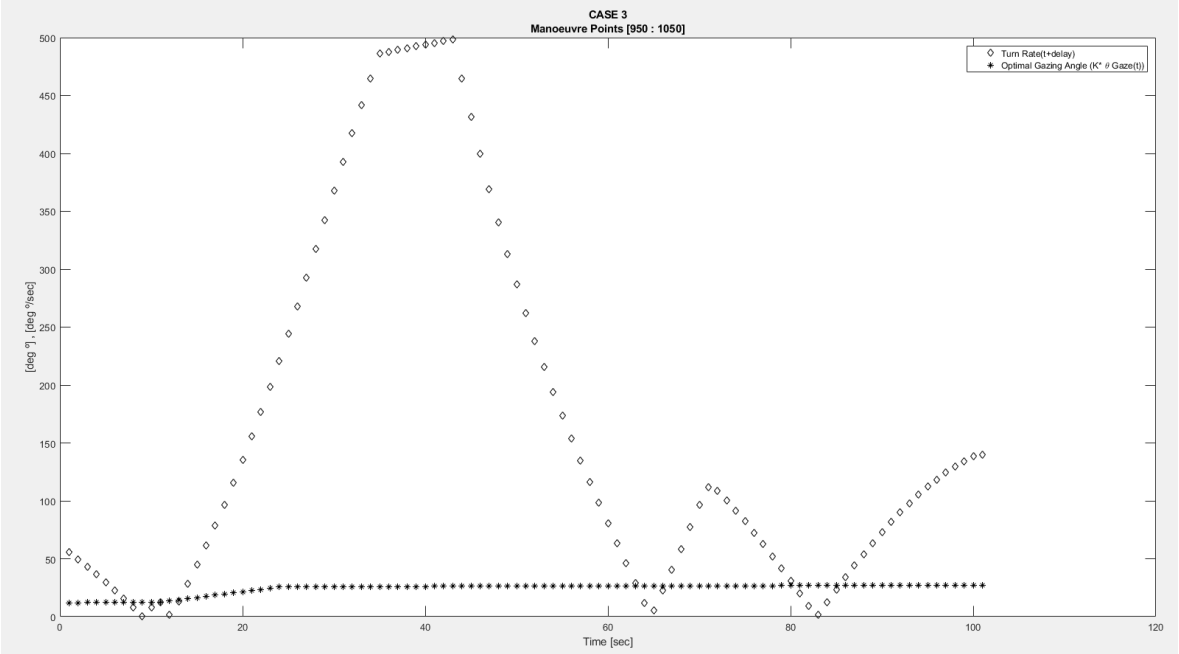

Figure 78 Case 3 [950 1050] Turn Rate and Gazing Angle Comparison

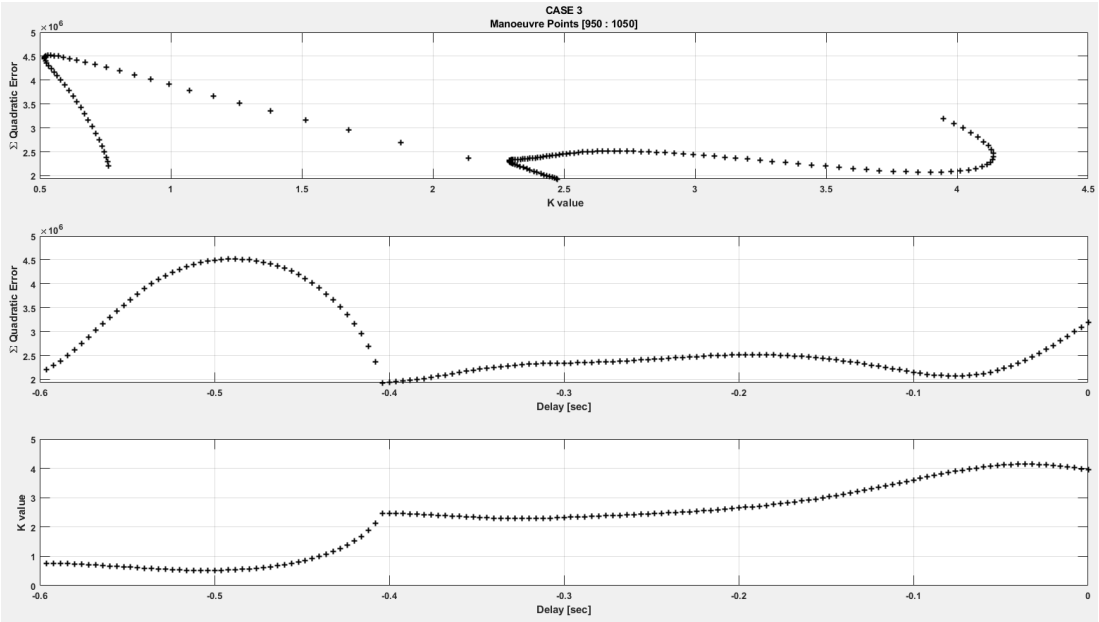

Figure 79 Case 3 [950 1050] Quadratic Error, Delay and K value

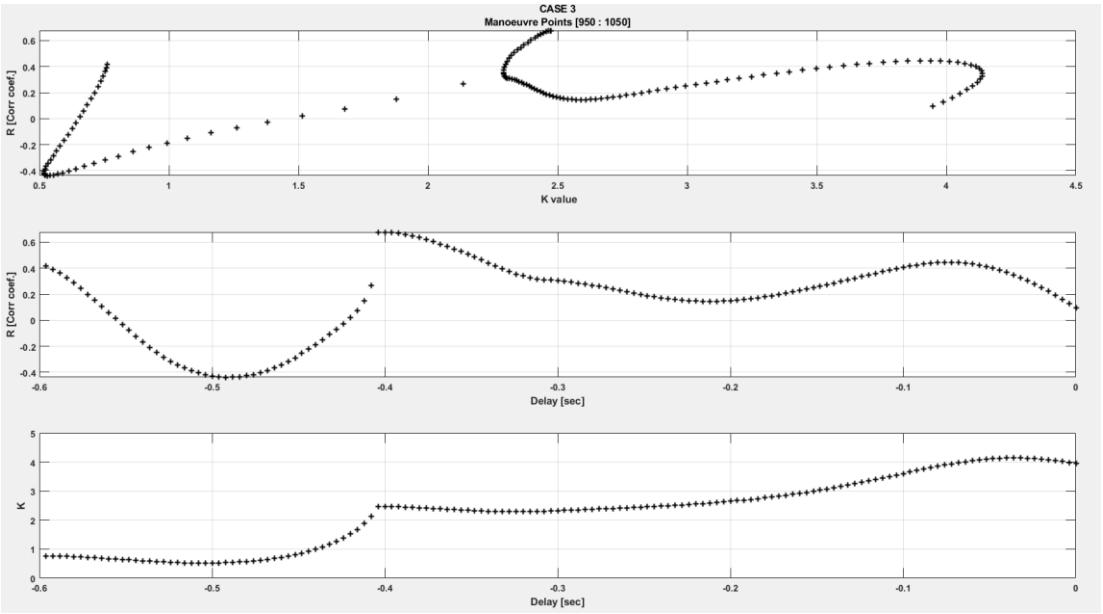

Figure 80 Case 3 [950 1050] R, Delay and K value

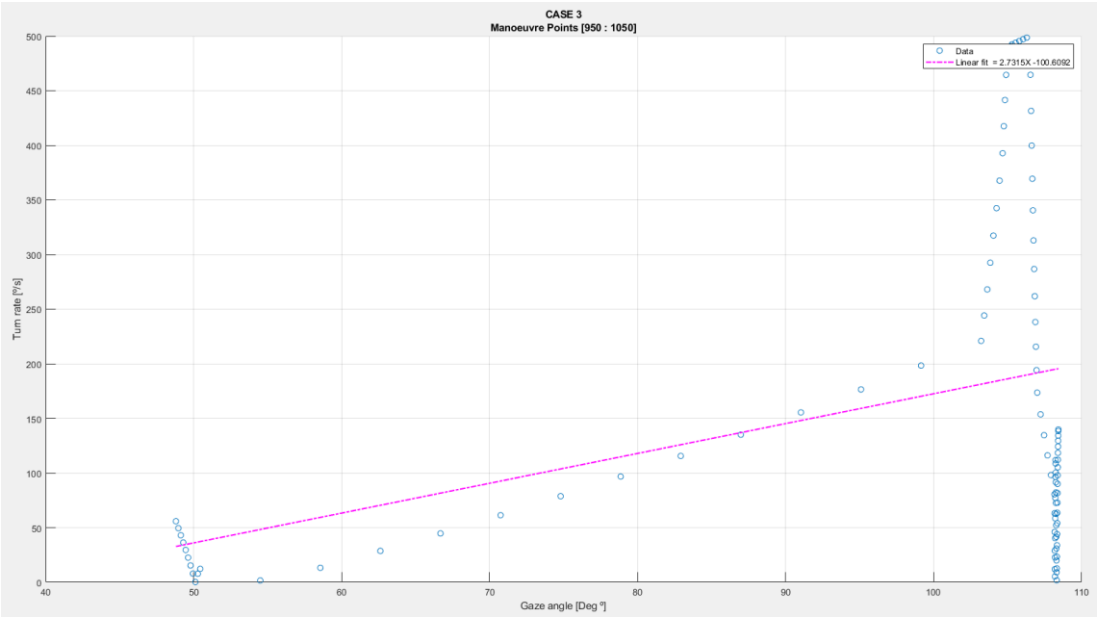

Figure 81 Case 3 [950 1050] Linear Regression

600 780

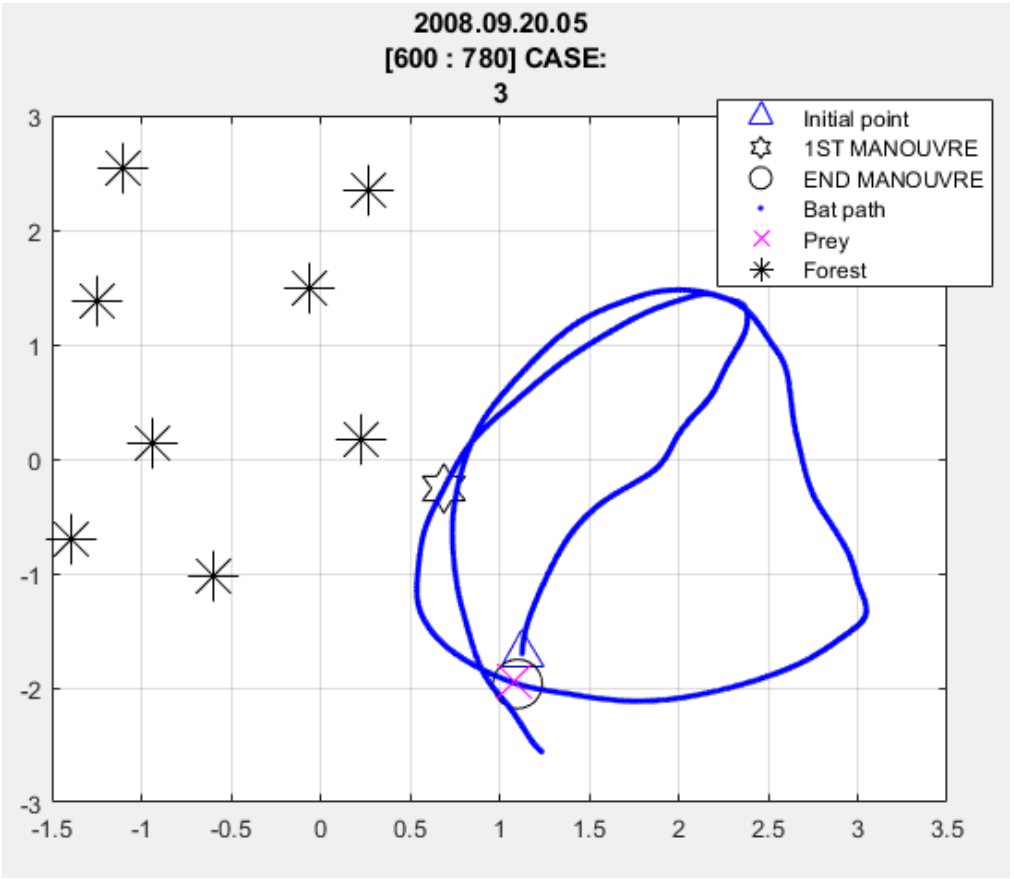

Figure 82 Case 3 [600 780] Flight Path

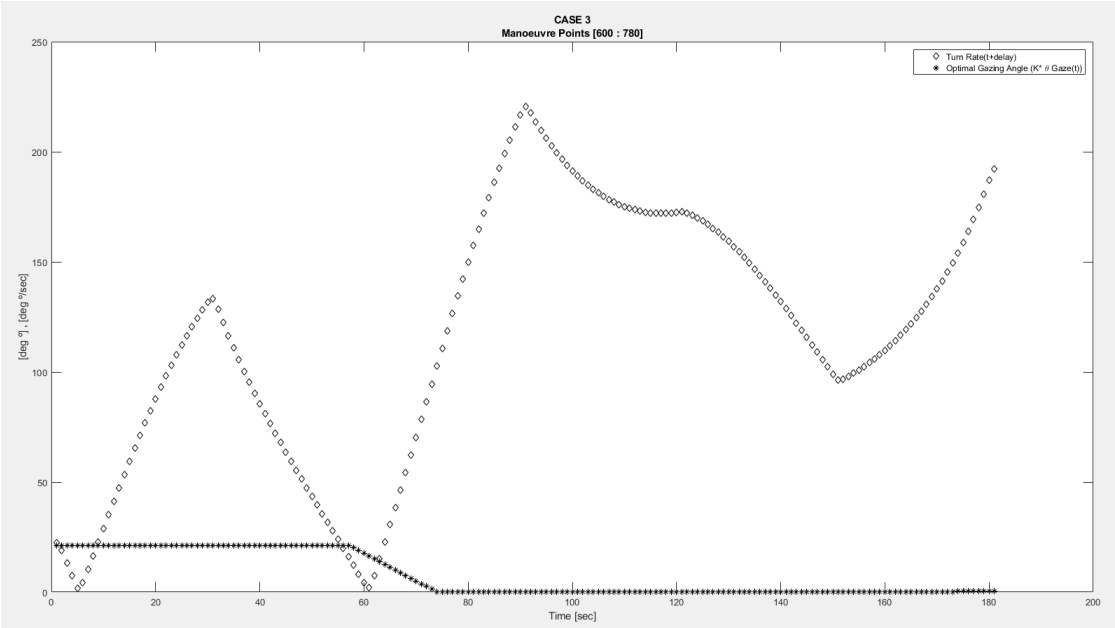

Figure 83 Case 3 [600 780] Turn Rate and Gazing Angle Comparison

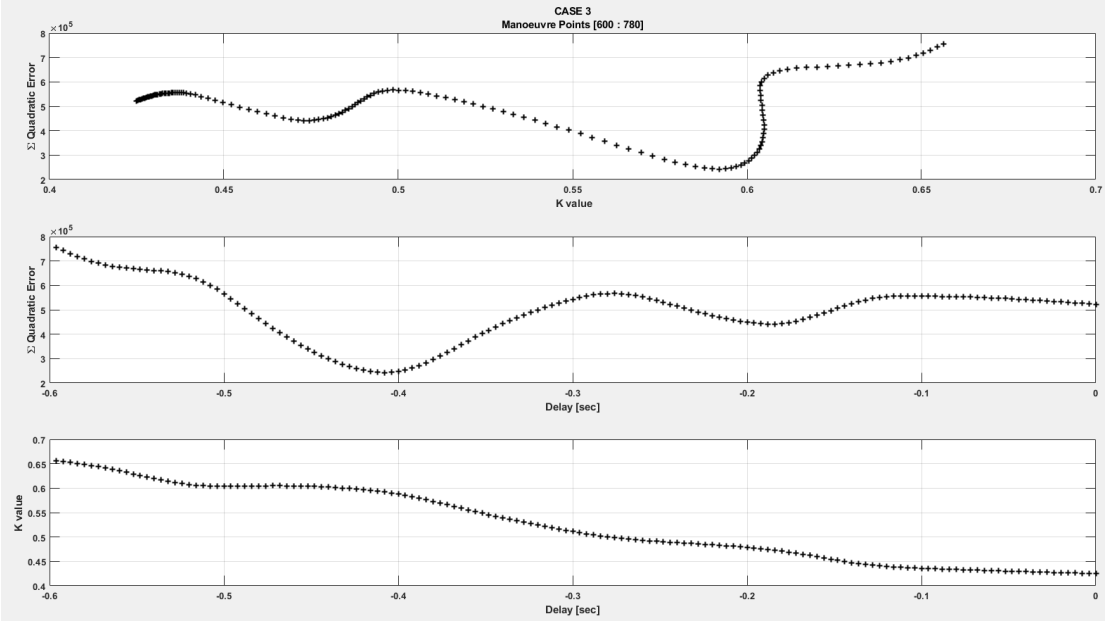

Figure 84 Case 3 [600 780] Quadratic Error, Delay and K value

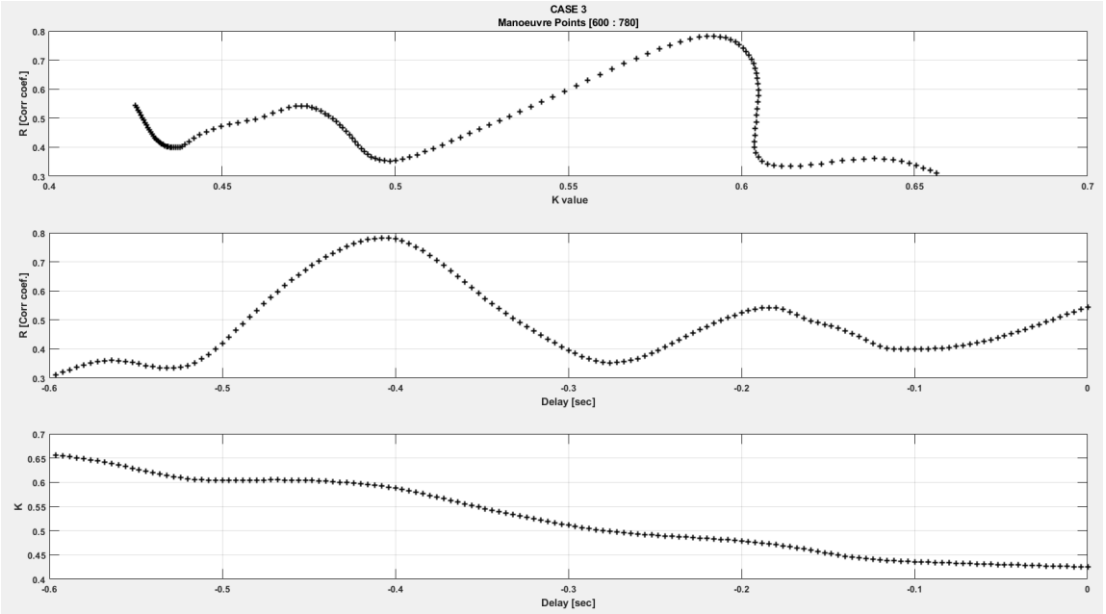

Figure 85 Case 3 [600 780] R, Delay and K value

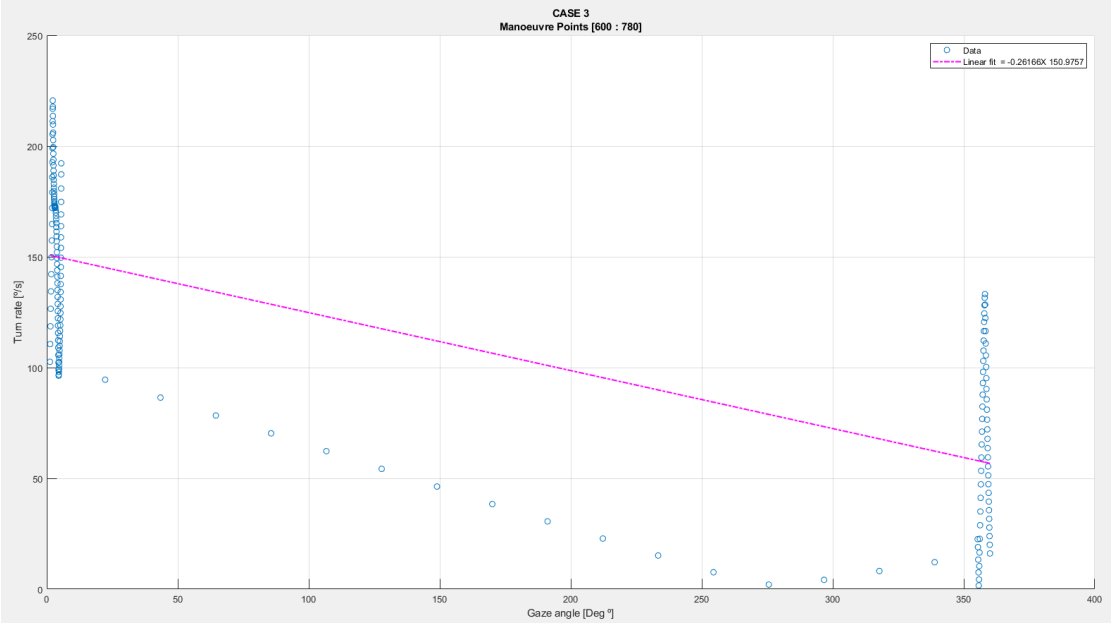

Figure 86 Case 3 [600 780] Linear Regression

220 300

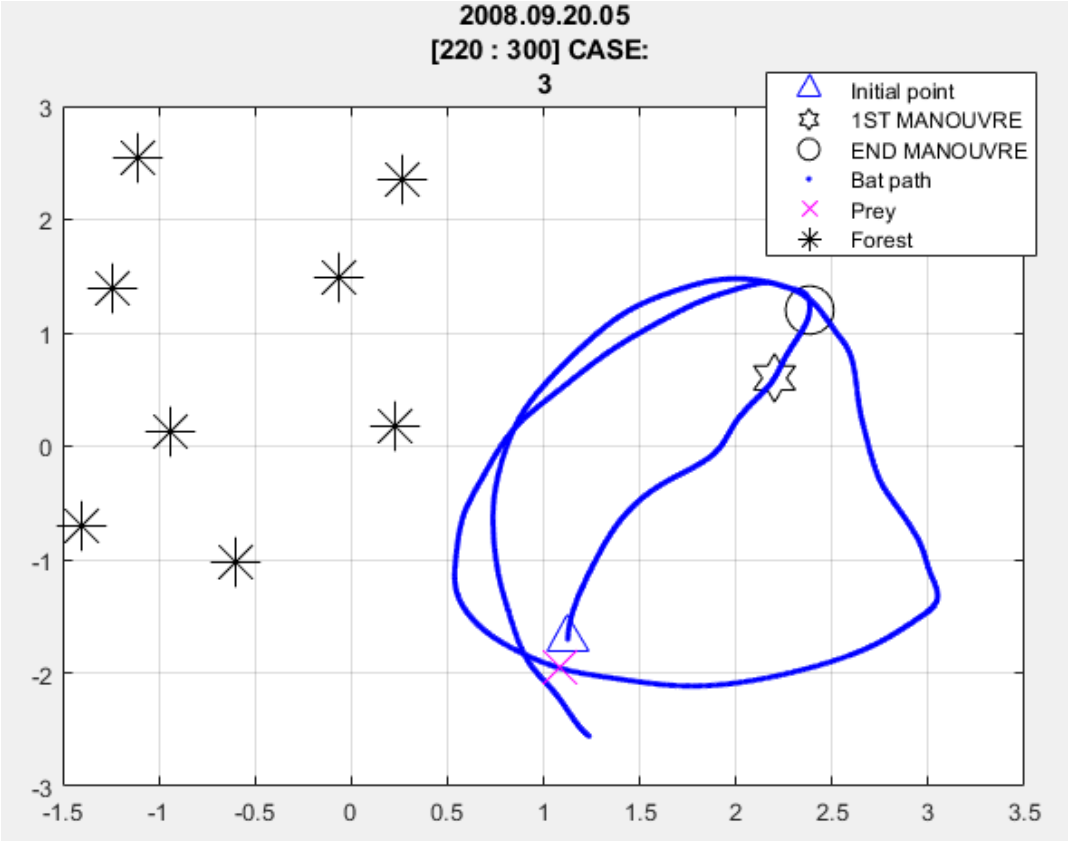

Figure 87 Case 3 [220 300] Flight Path

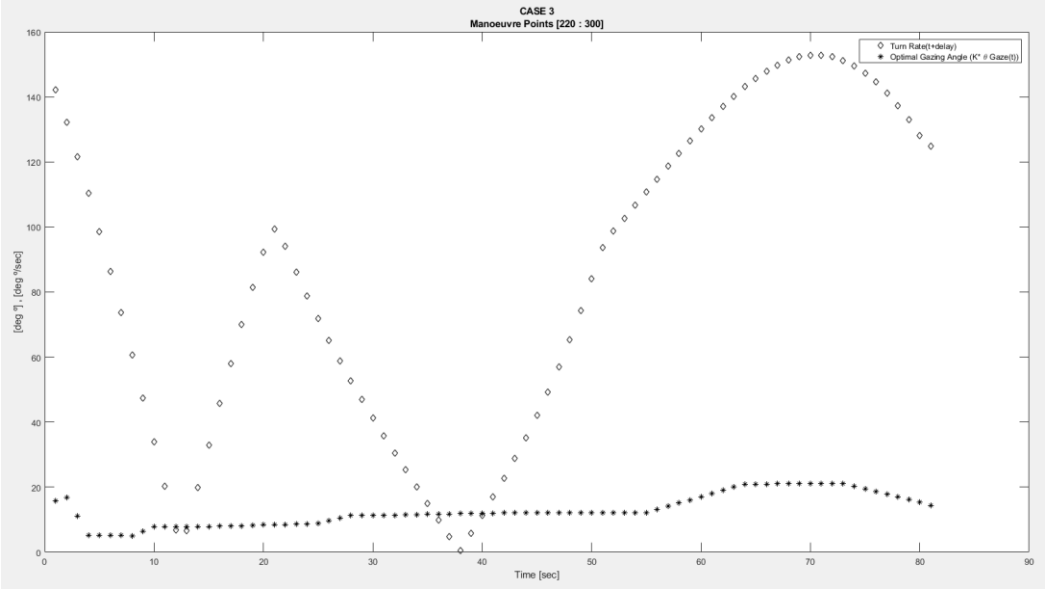

Figure 88 Case 3 [220 300] Turn Rate and Gazing Angle Comparison

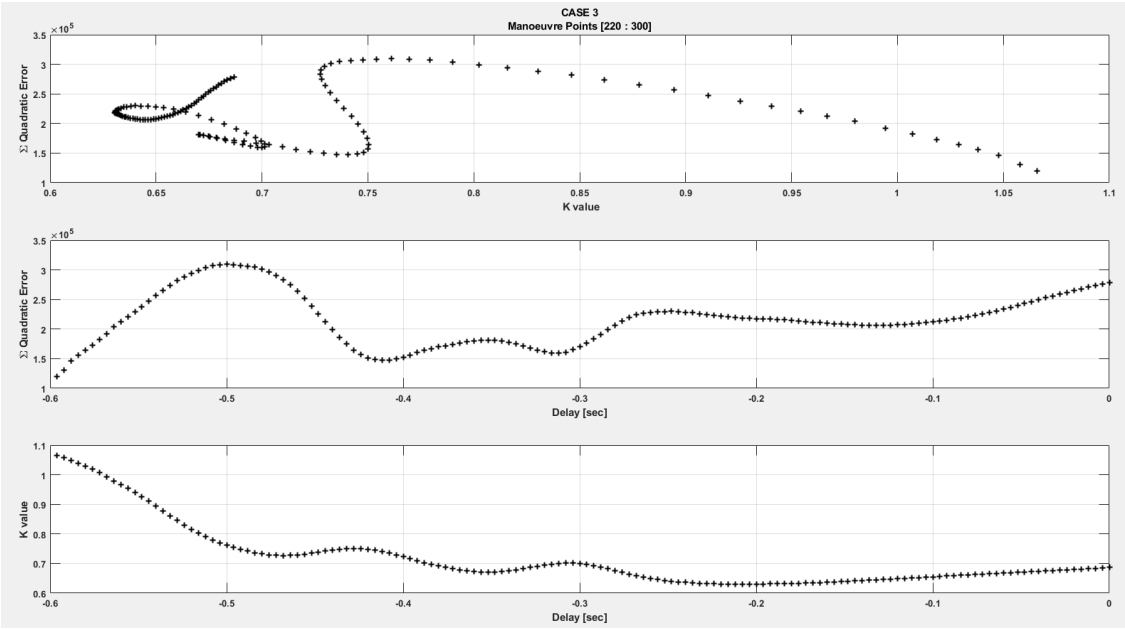

Figure 89 Case 3 [220 300] Quadratic Error, Delay and K value

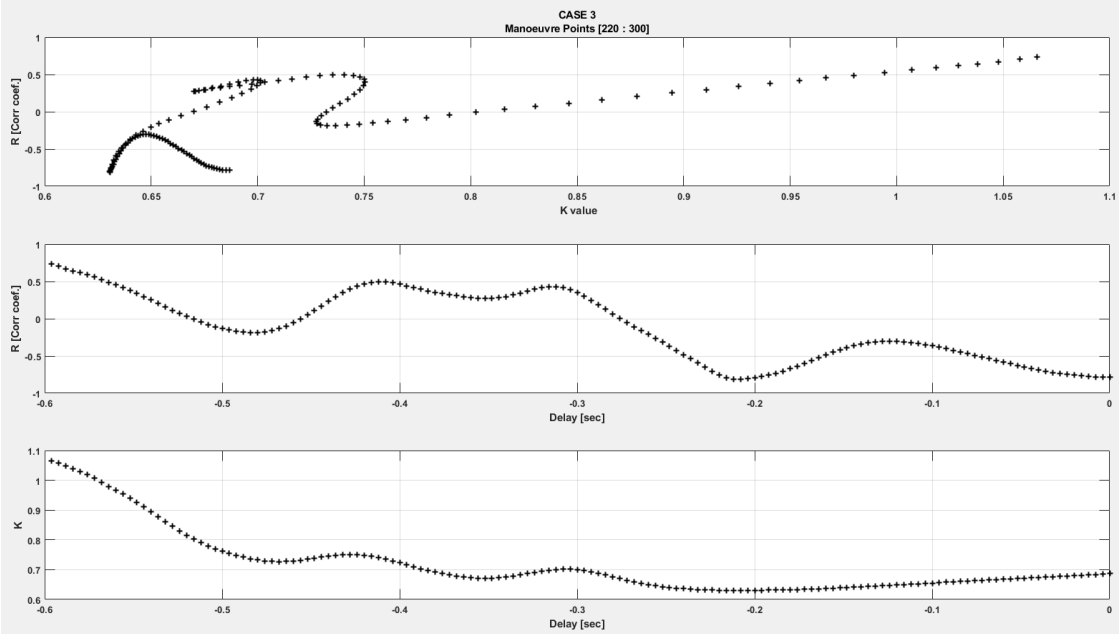

Figure 90 Case 3 [220 300] R, Delay and K value

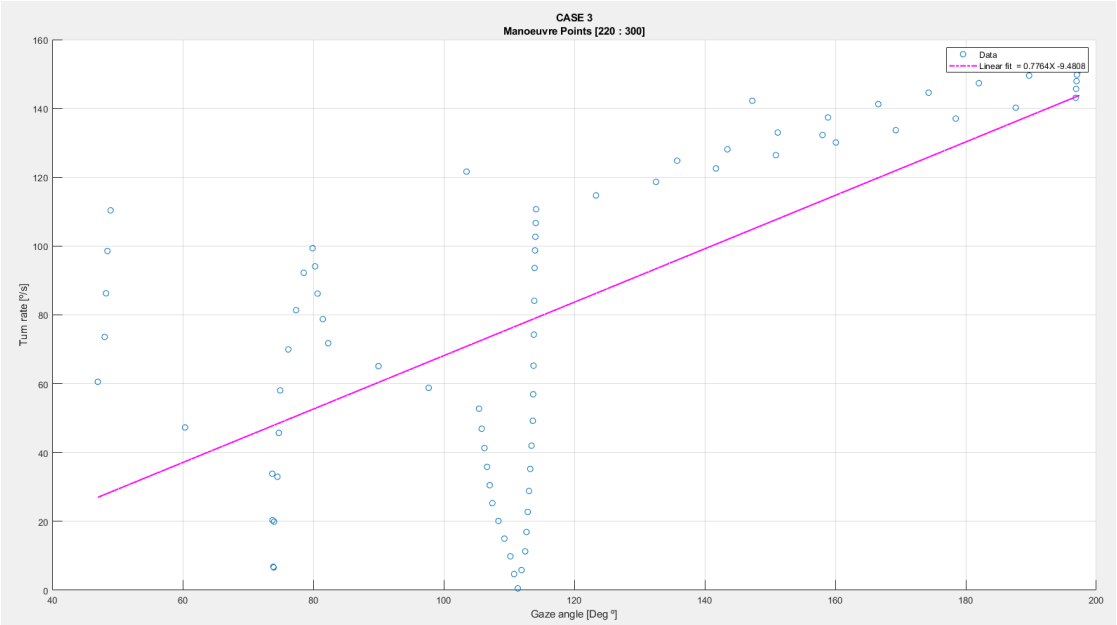

Figure 91 Case 3 [220 300] Linear Regression

220 350

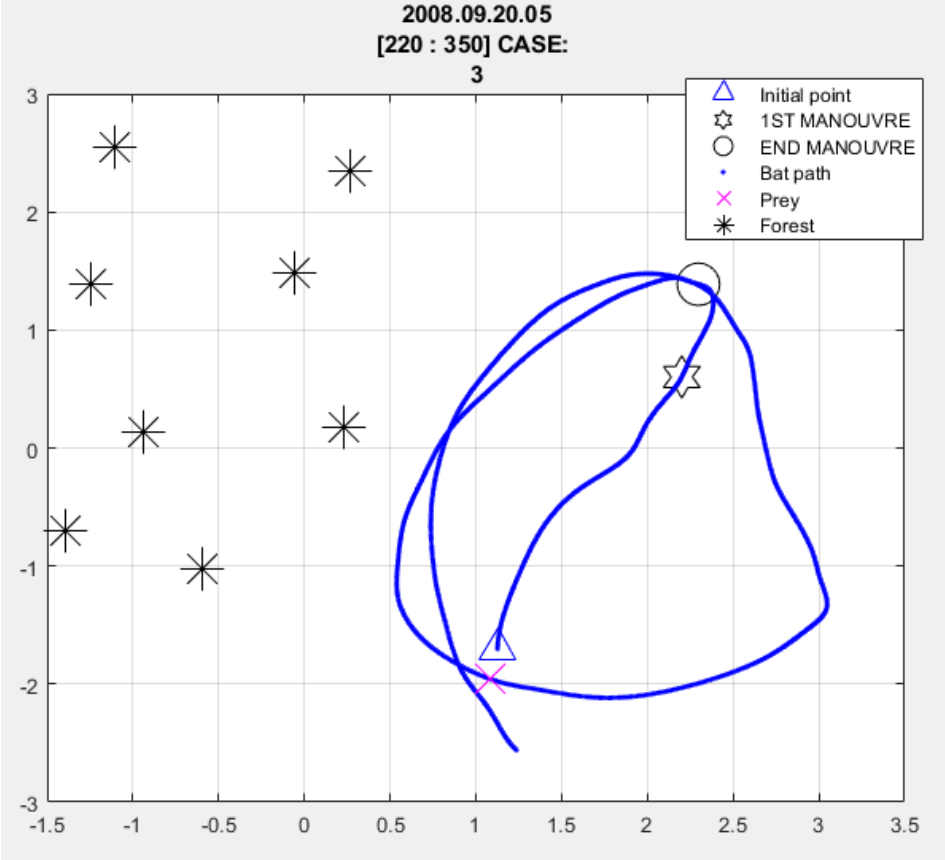

Figure 92 Case 3 [220 350] Flight Path

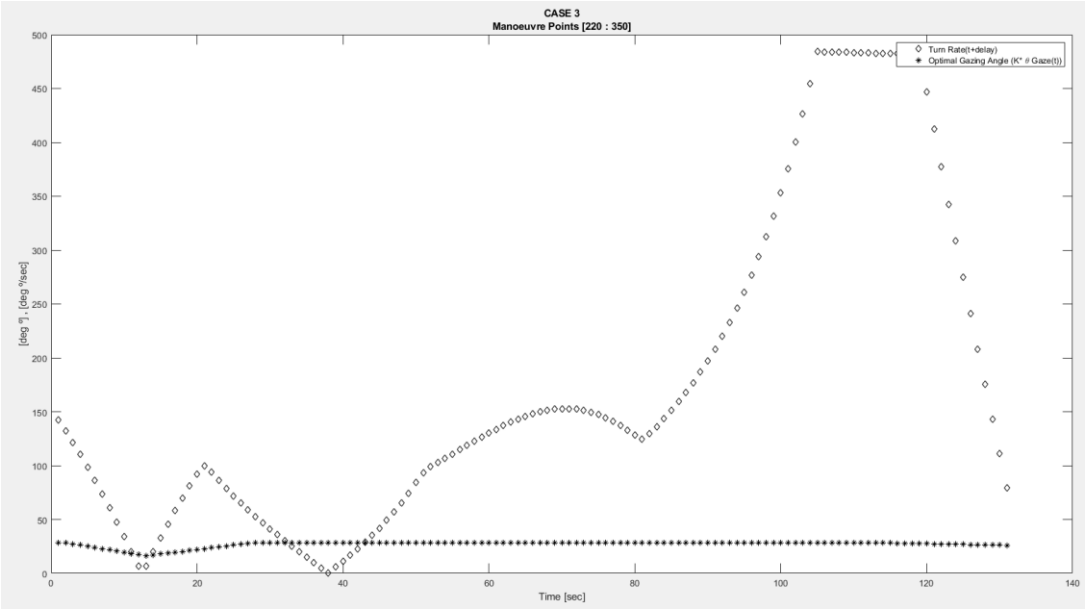

Figure 93 Case 3 [220 350] Turn Rate and Gazing Angle Comparison

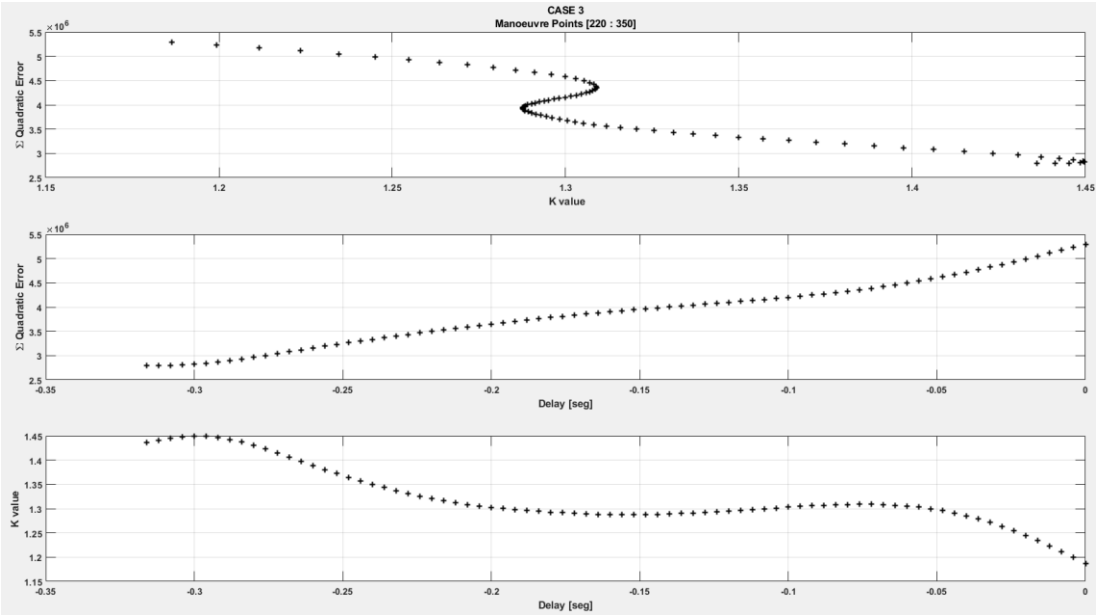

Figure 94 Case 3 [220 350] Quadratic Error, Delay and K value

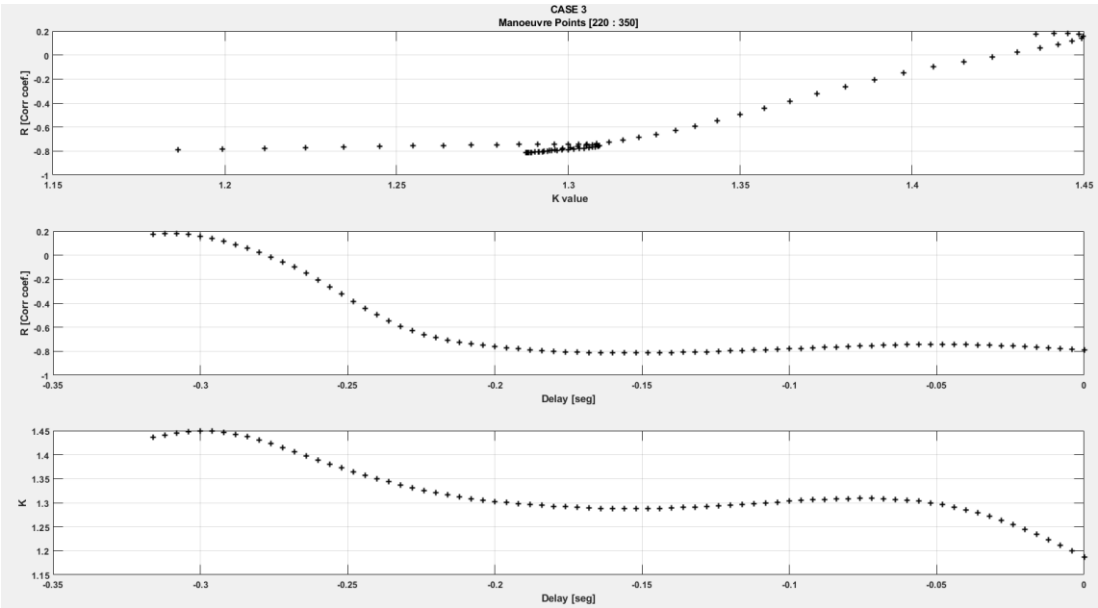

Figure 95 Case 3 [220 350] R, Delay and K value

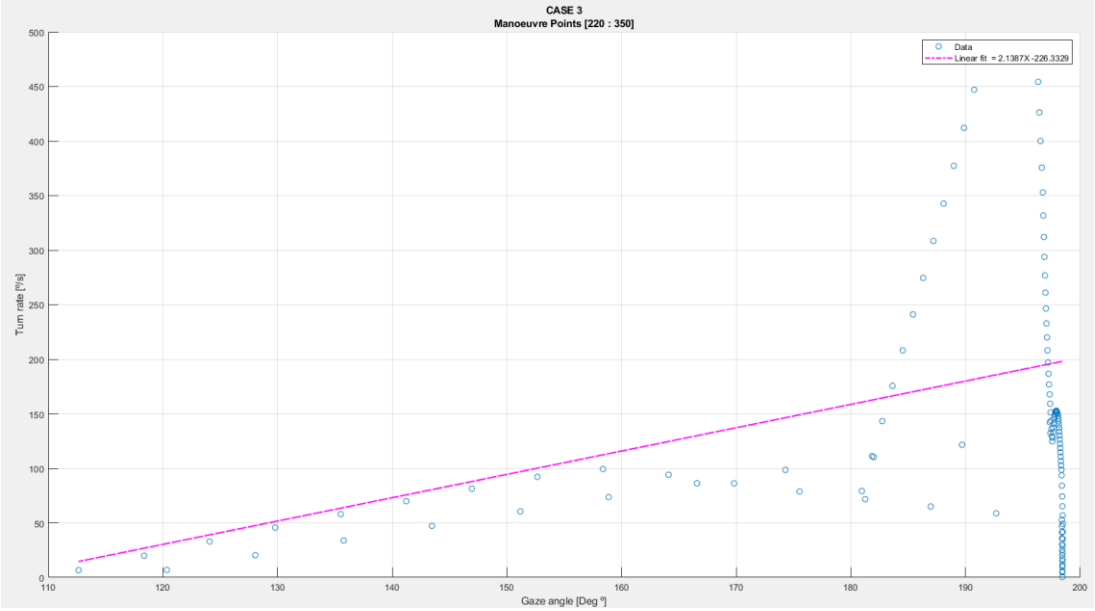

Figure 96 Case 3 [220 350] Linear Regression

CASE 4

570 623

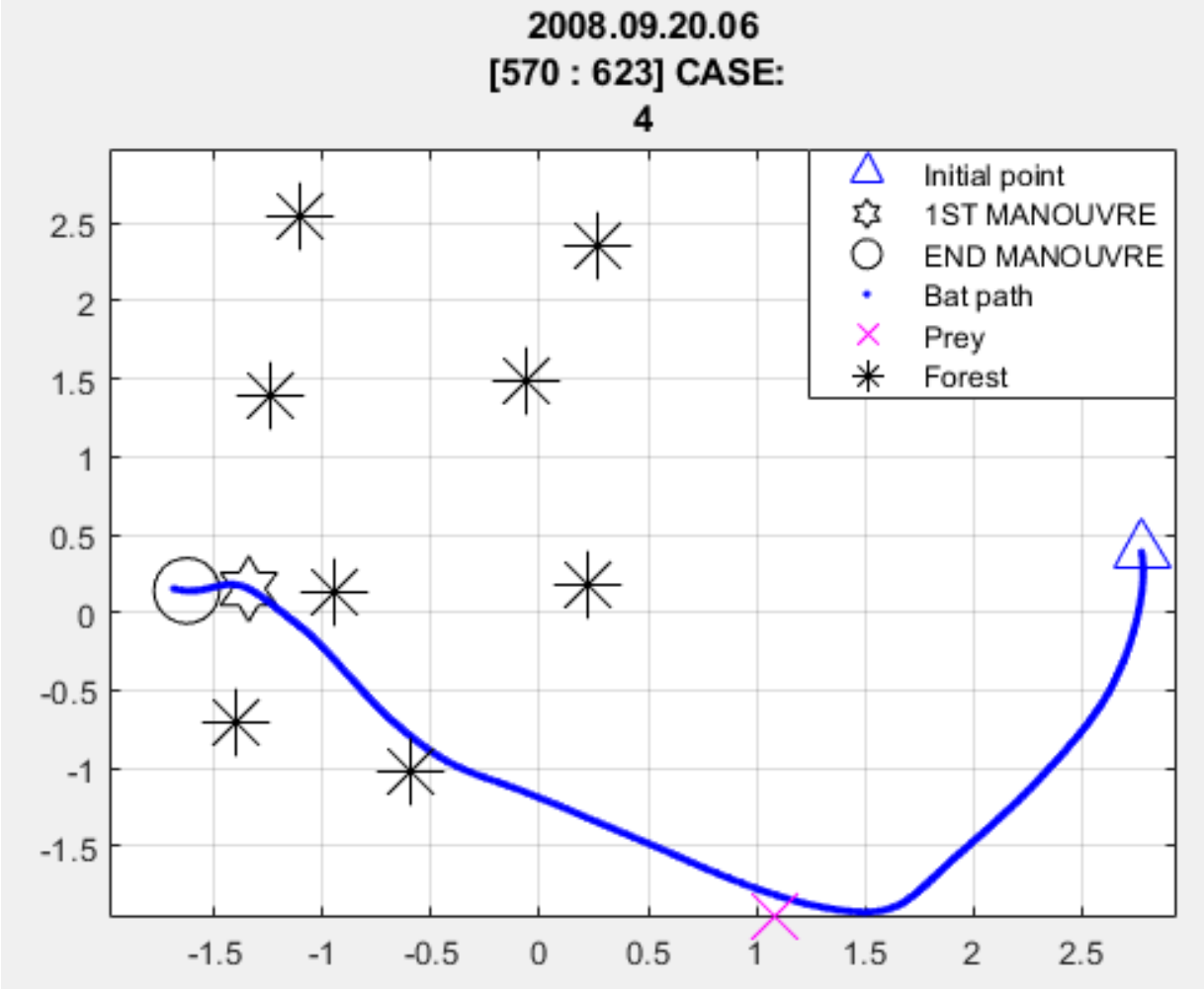

Figure 97 Case 4 [570 623] Flight Path

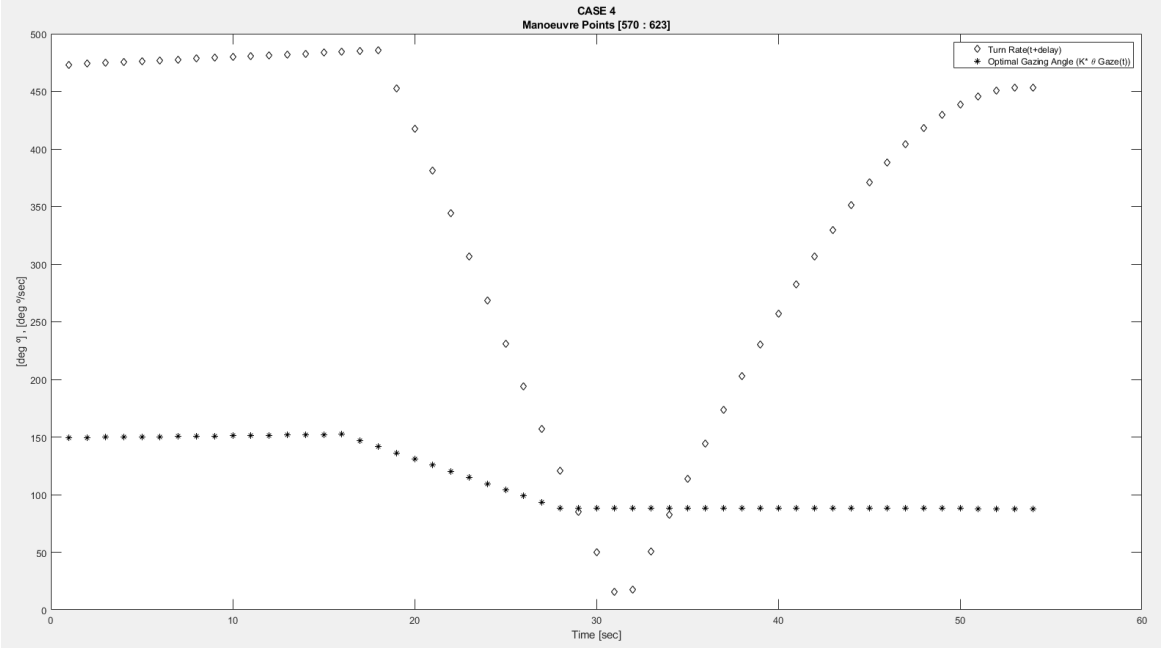

Figure 98 Case 4 [570 623] Turn Rate and Gazing Angle Comparison

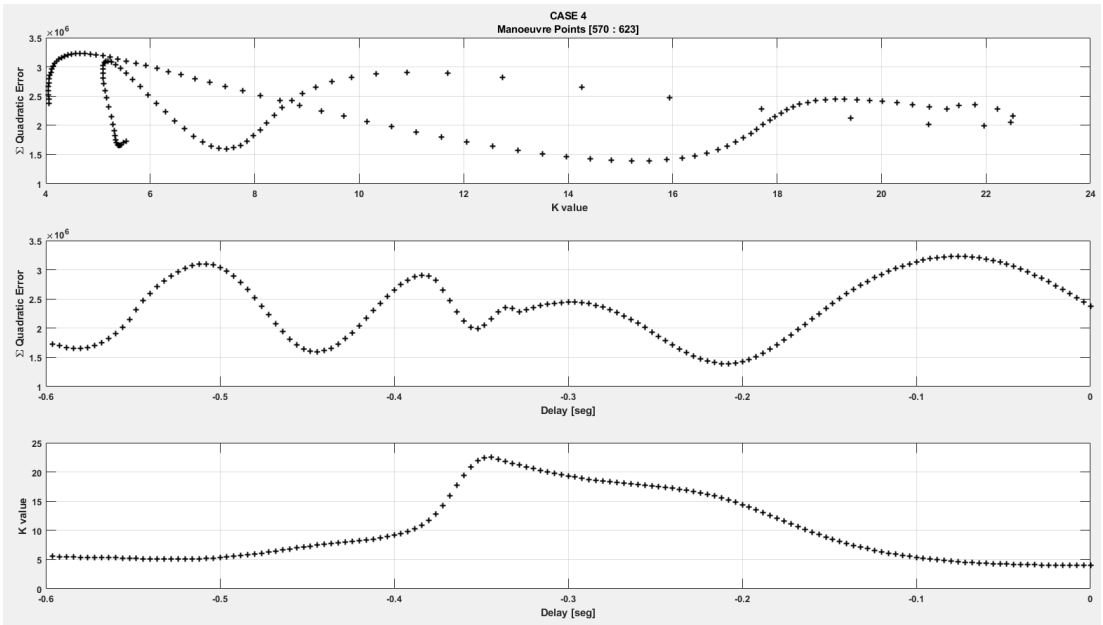

Figure 99 Case 4 [570 623] Quadratic Error, Delay and K value

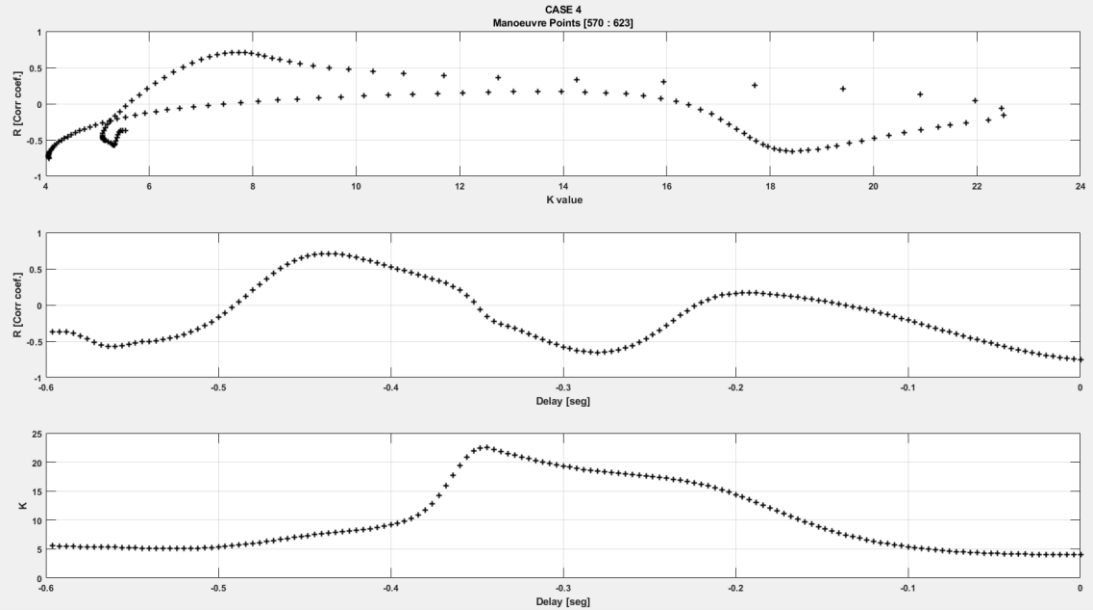

Figure 100 Case 4 [570 623] R, Delay and K value

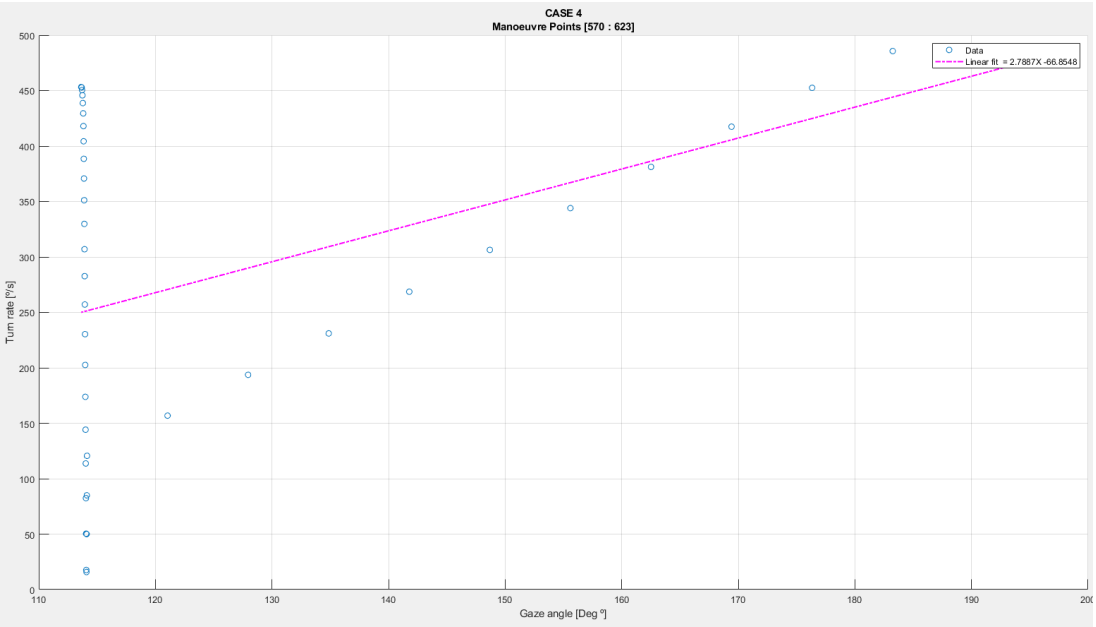

Figure 101 Case 4 [570 623] Linear Regression

450 553

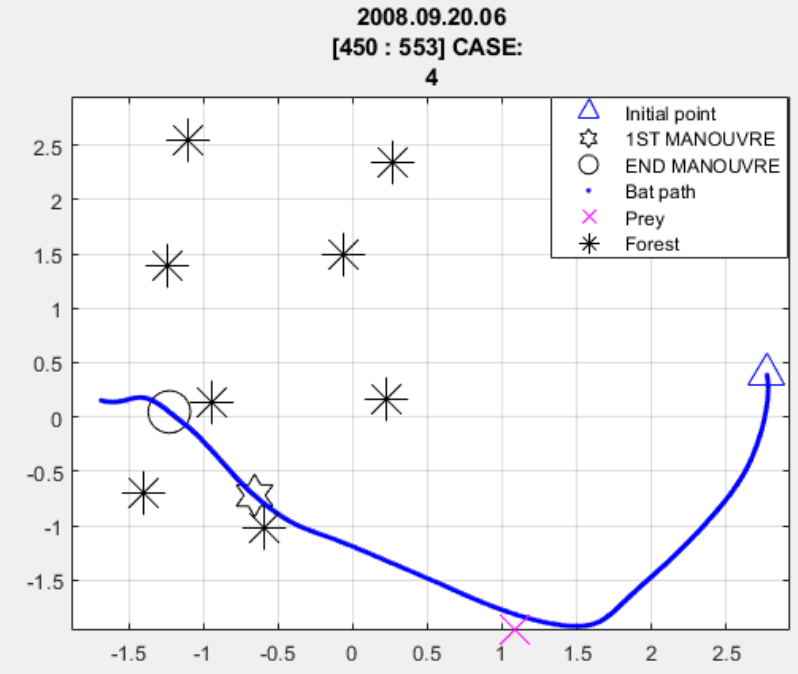

Figure 102 Case 4 [450 553] Flight Path

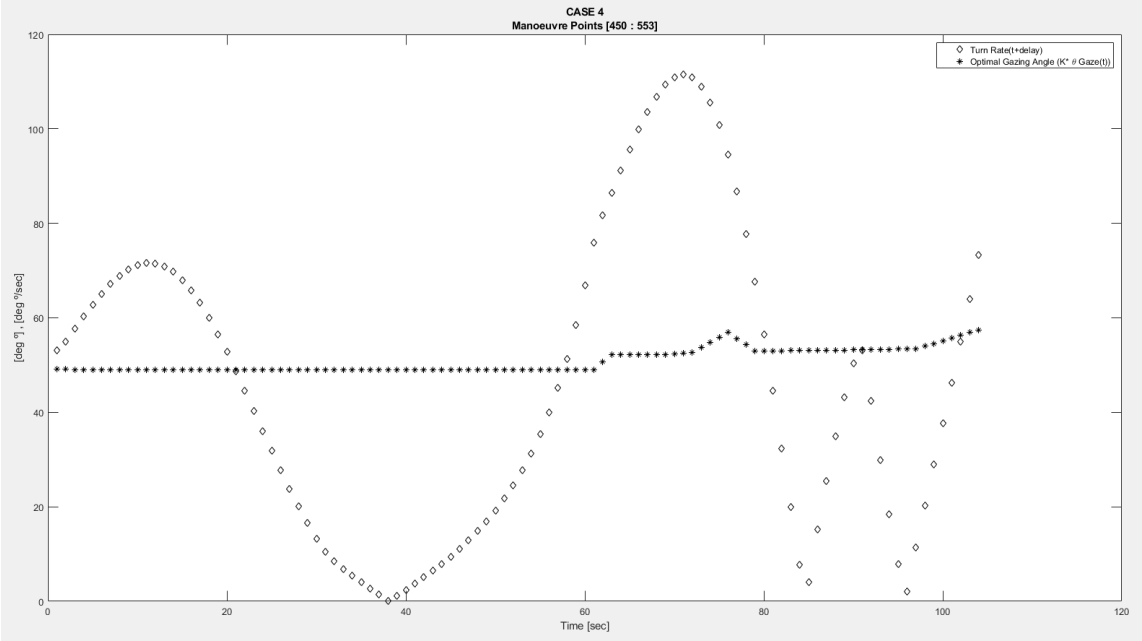

Figure 103 Case 4 [450 553] Turn Rate and Gazing Angle Comparison

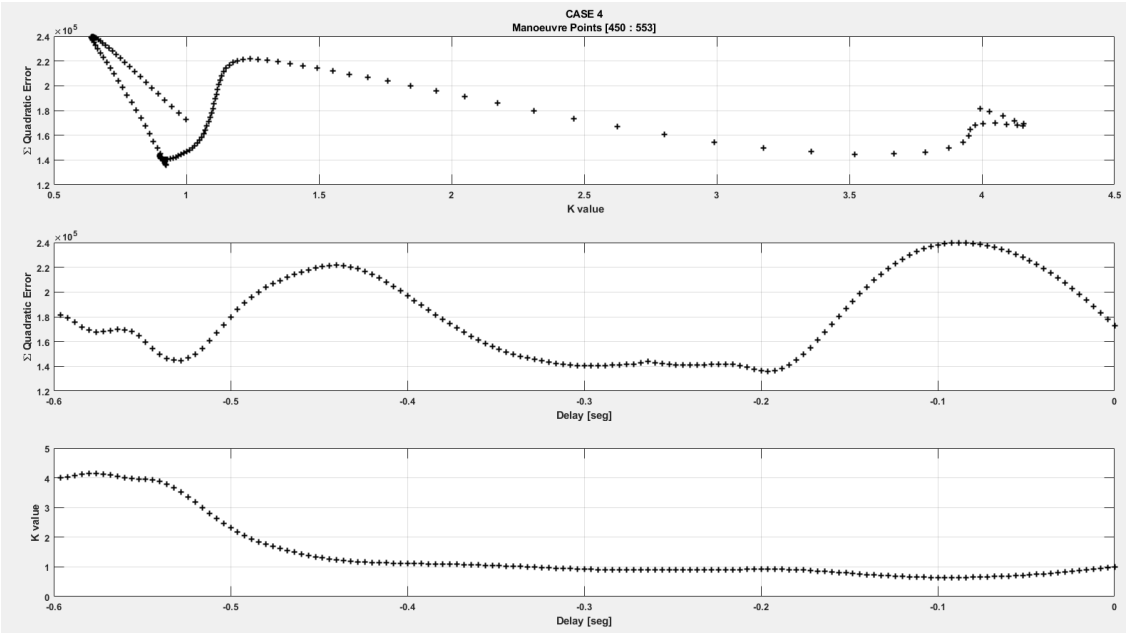

Figure 104 Case 4 [450 553] Quadratic Error, Delay and K value

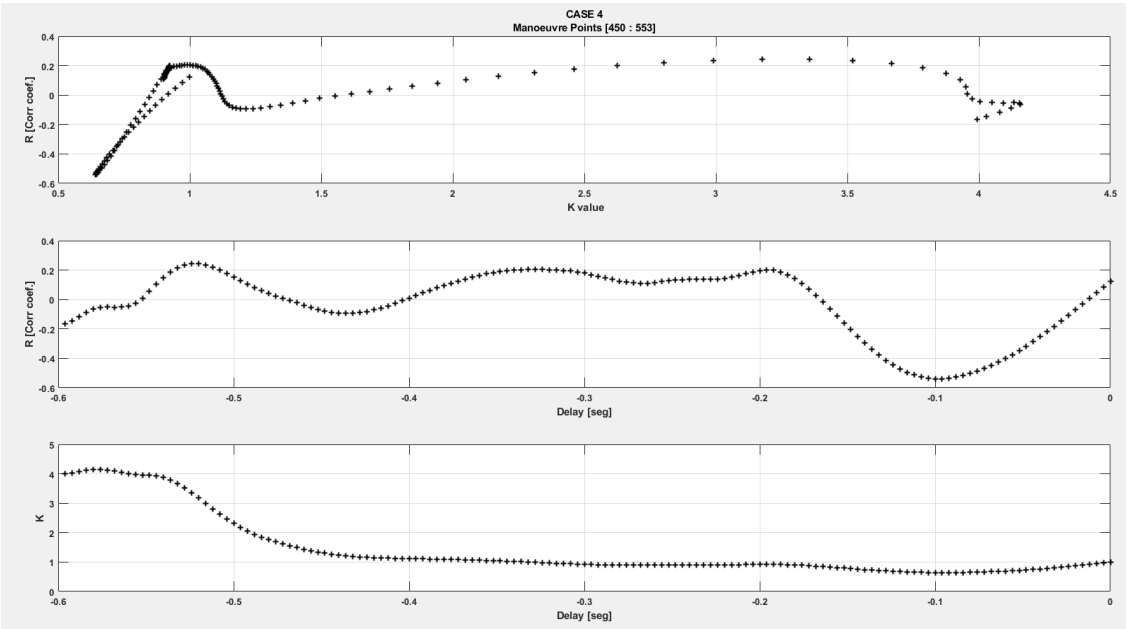

Figure 105 Case 4 [450 553] R, Delay and K value

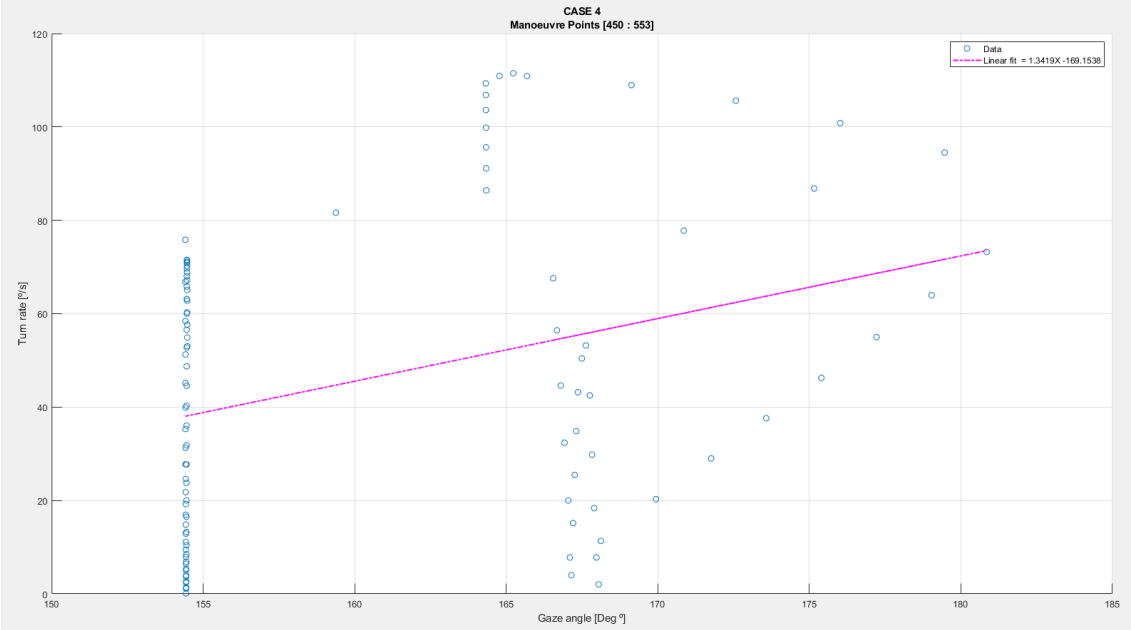

Figure 106 Case 4 [450 553] Linear Regression

450 623

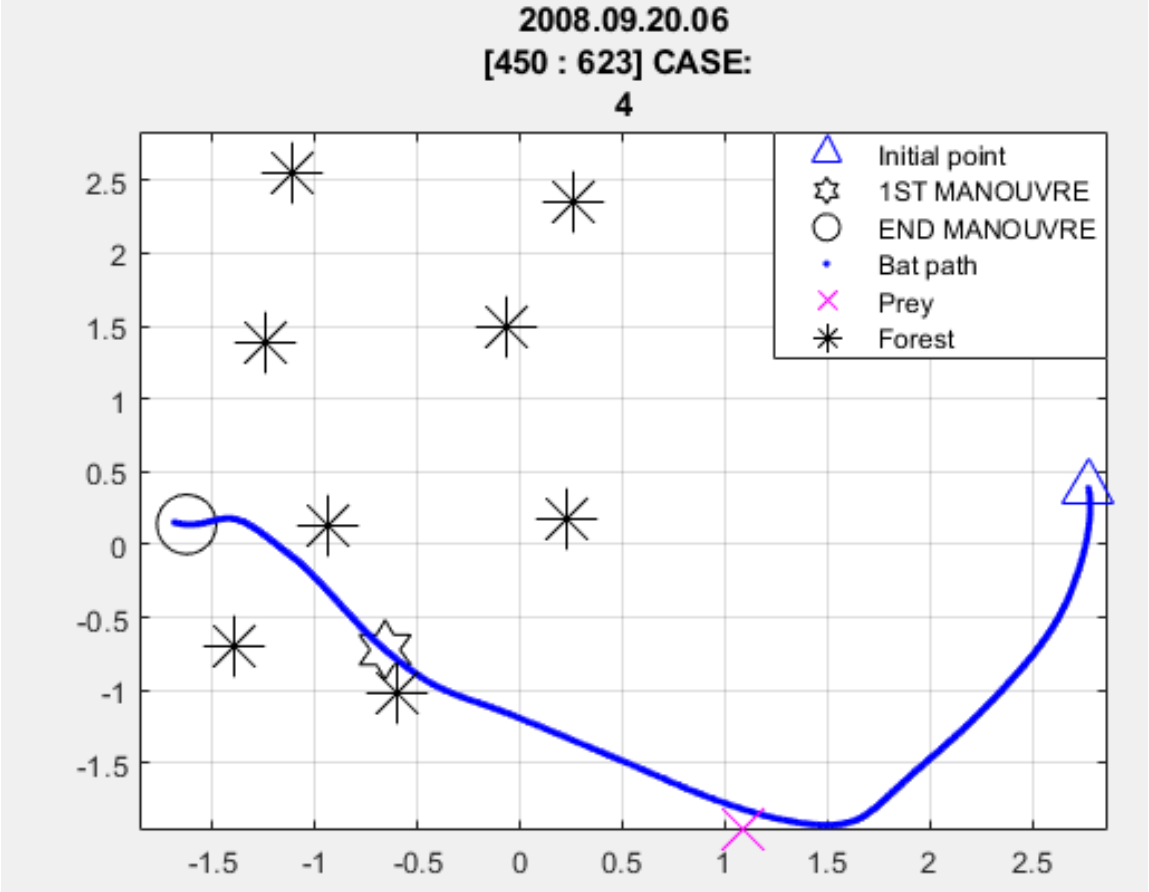

Figure 107 Case 4 [450 623] Flight Path

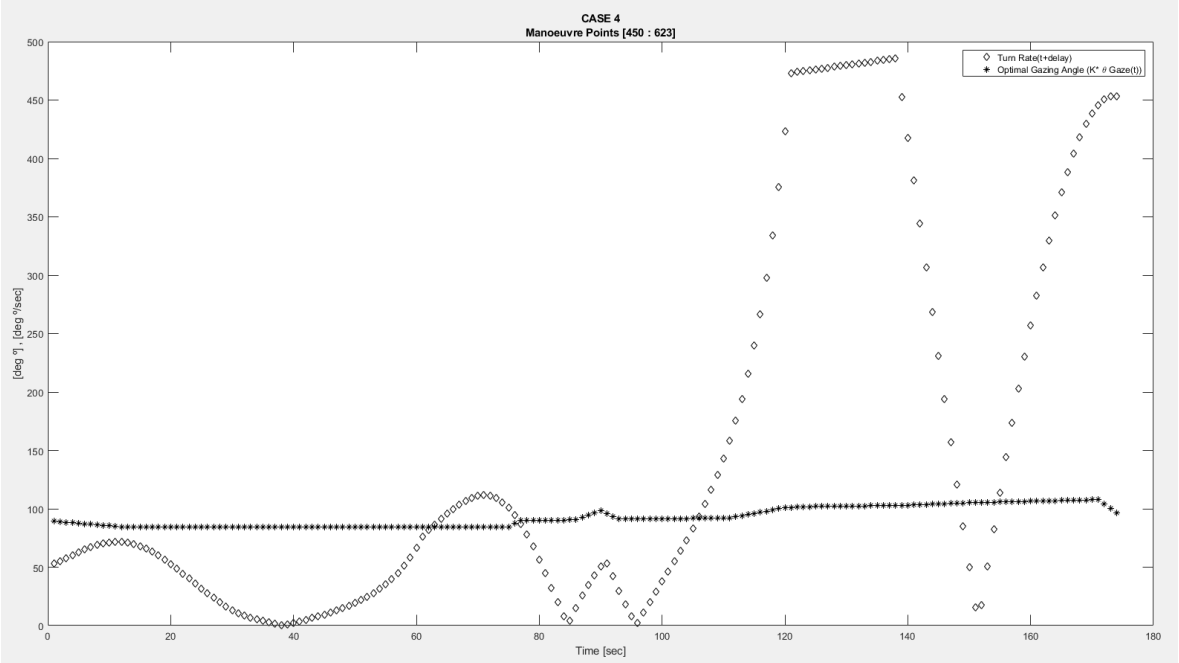

Figure 108 Case 4 [450 623] Turn Rate and Gazing Angle Comparison

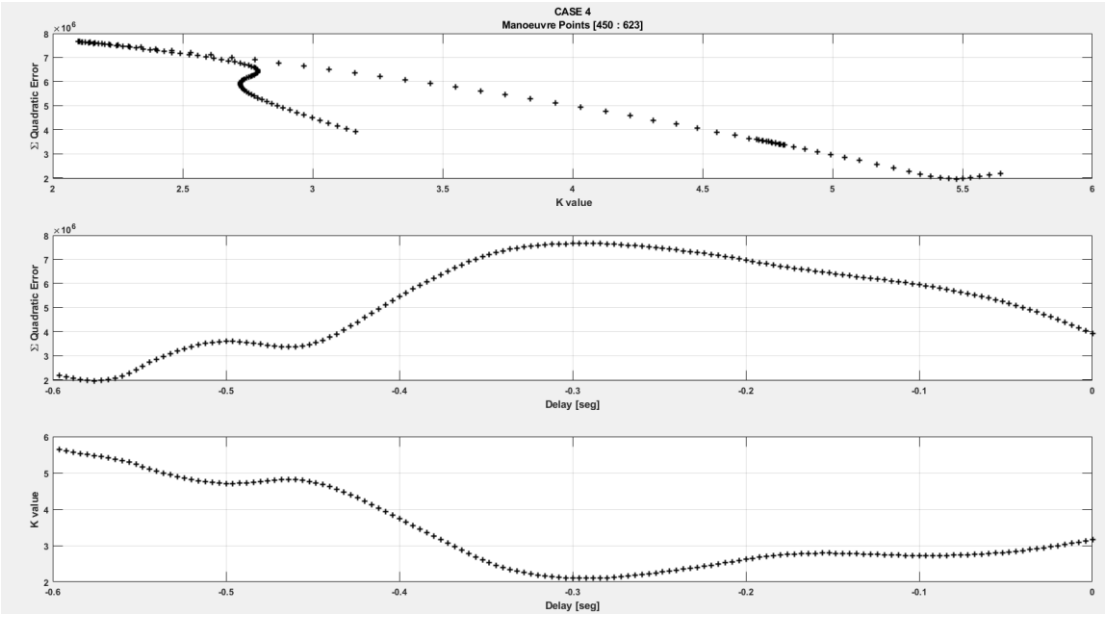

Figure 109 Case 4 [450 623] Quadratic Error, Delay and K value

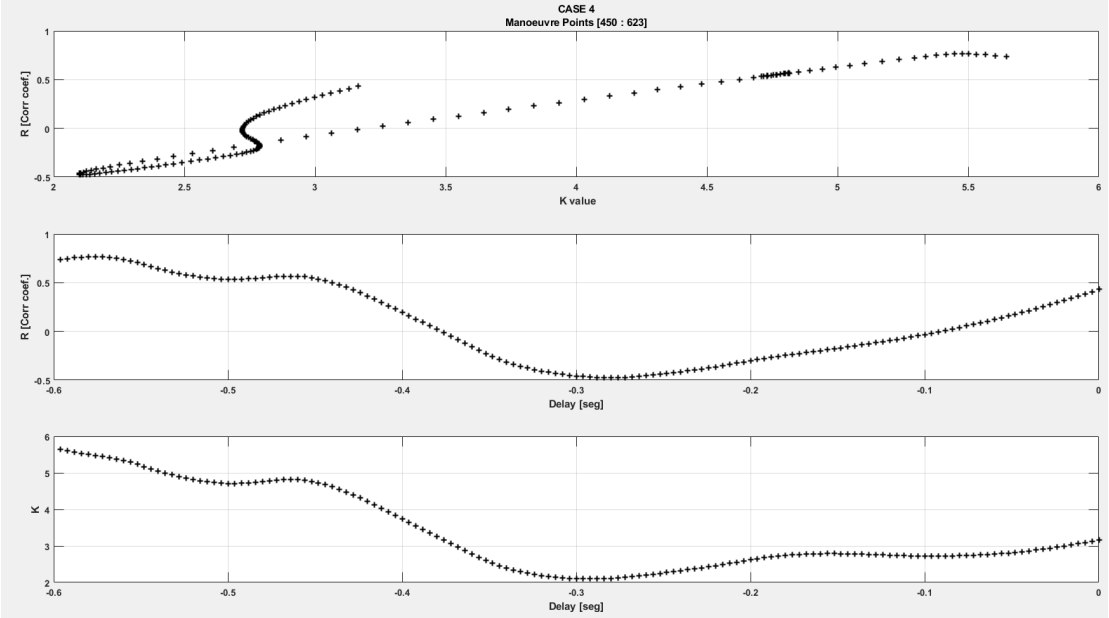

Figure 110 Case 4 [450 623] R, Delay and K value

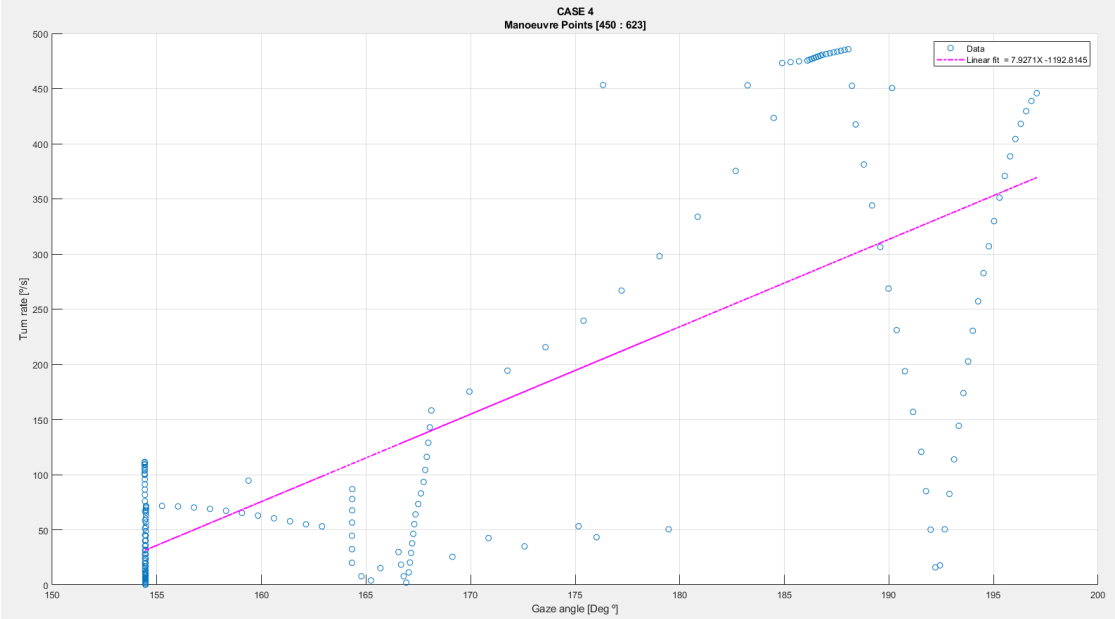

Figure 111 Case 4 [450 623] Linear Regression

350 435

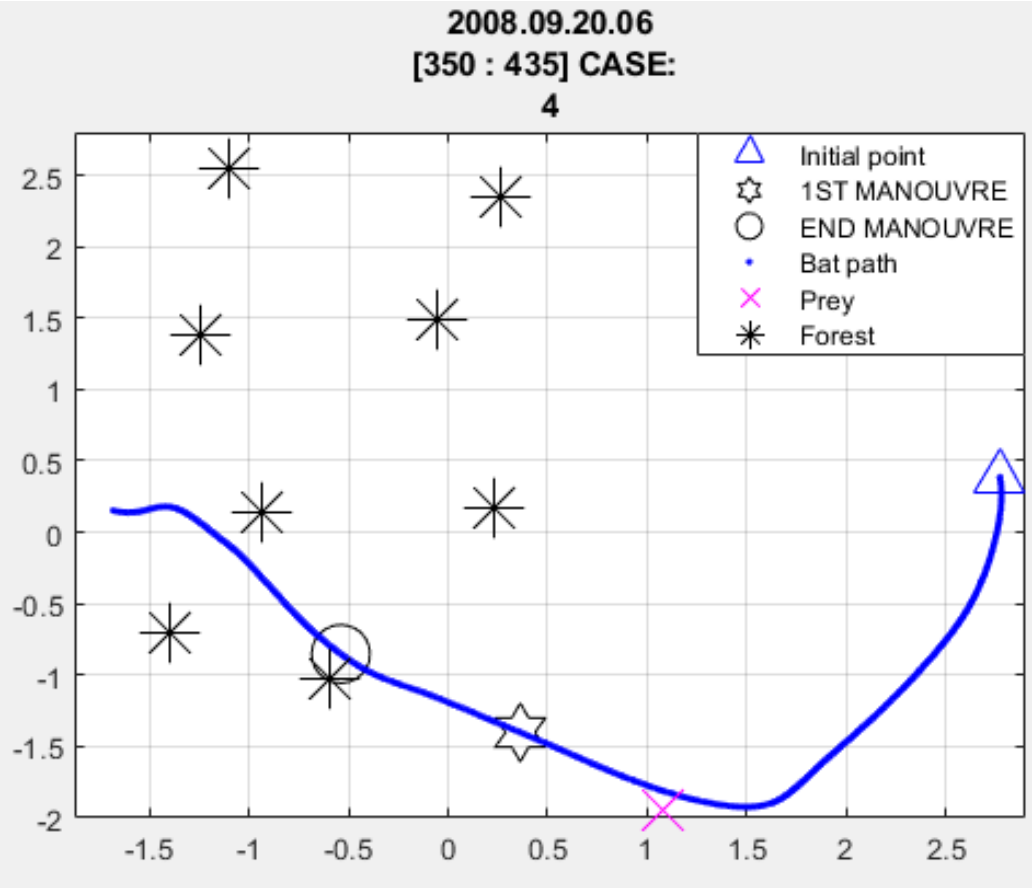

Figure 112 Case 4 [350 435] Flight Path

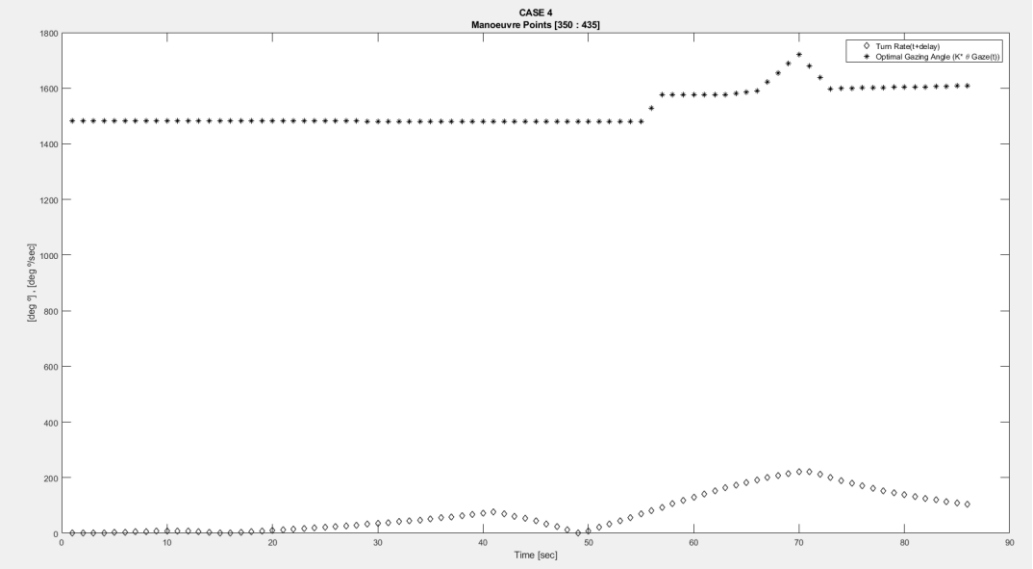

Figure 113Case 4 [350 435] Turn Rate and Gazing Angle Comparison

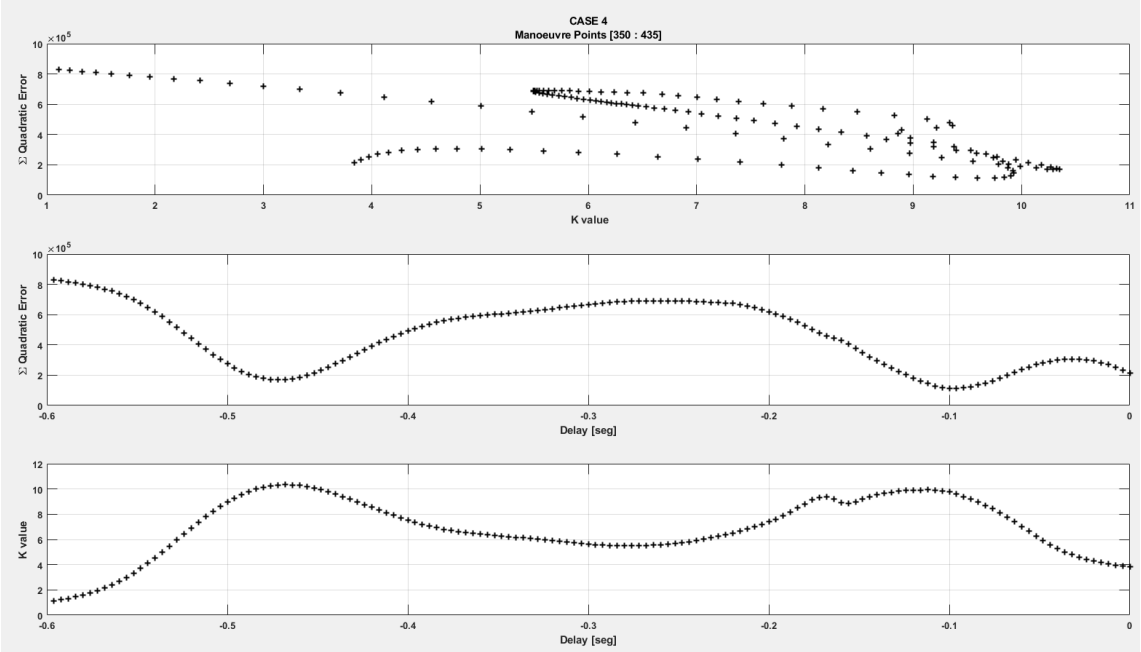

Figure 114 Case 4 [350 435] Quadratic Error, Delay and K value

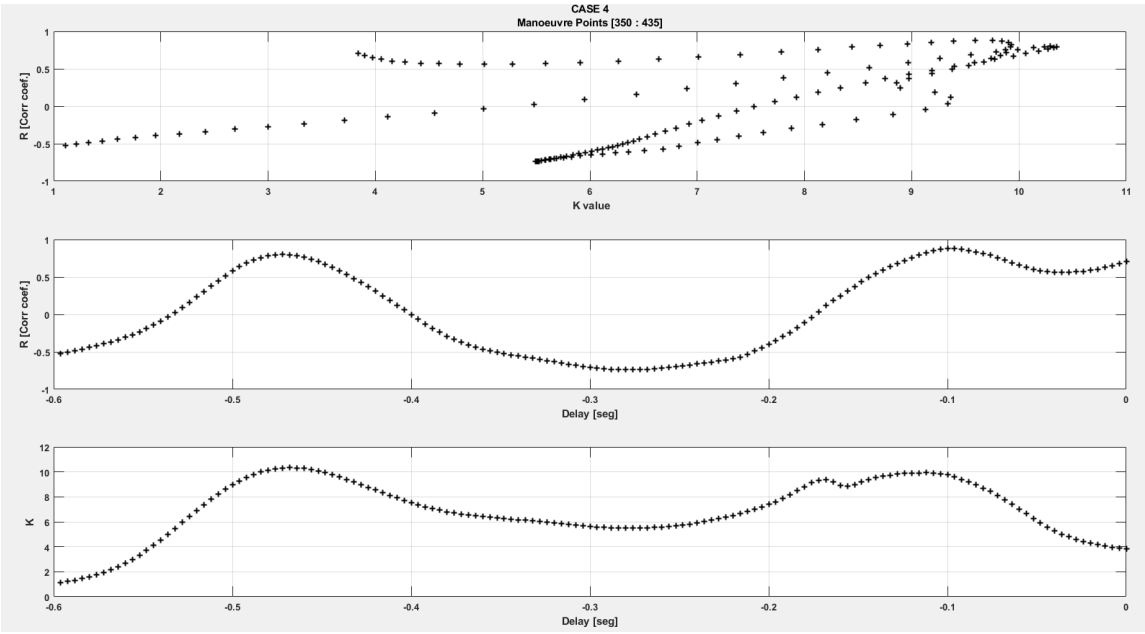

Figure 115 Case 4 [350 435] R, Delay and K value

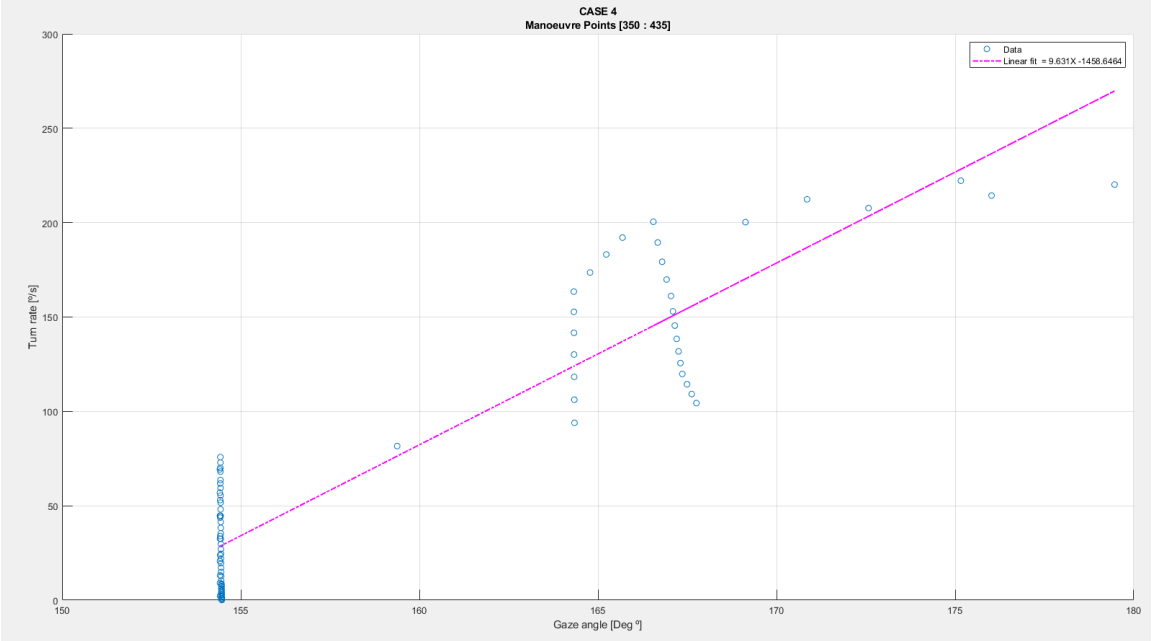

Figure 116 Case 4 [350 435] Linear Regression

220 280

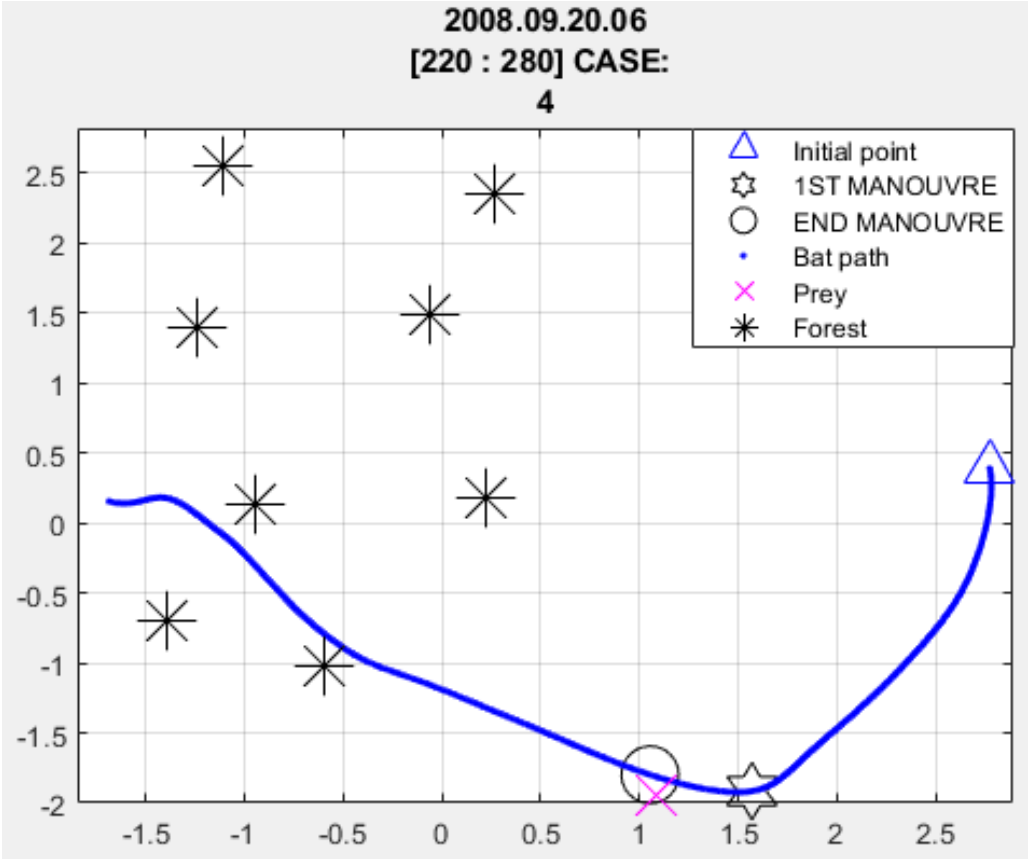

Figure 117Case 4 [220 280] Flight Path

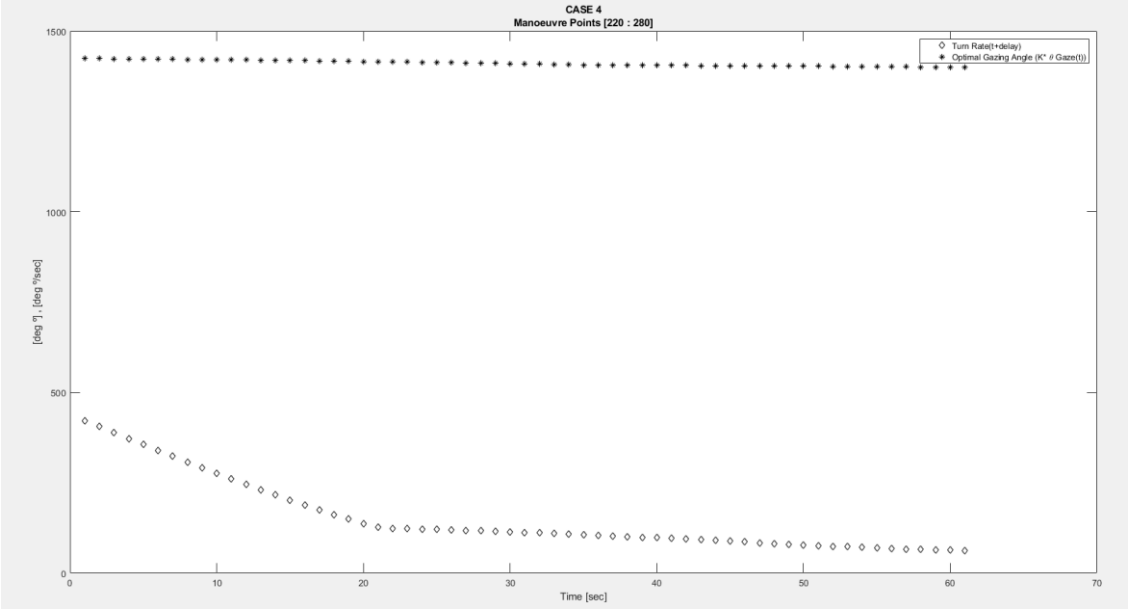

Figure 118 Case 4 [220 280] Turn Rate and Gazing Angle Comparison

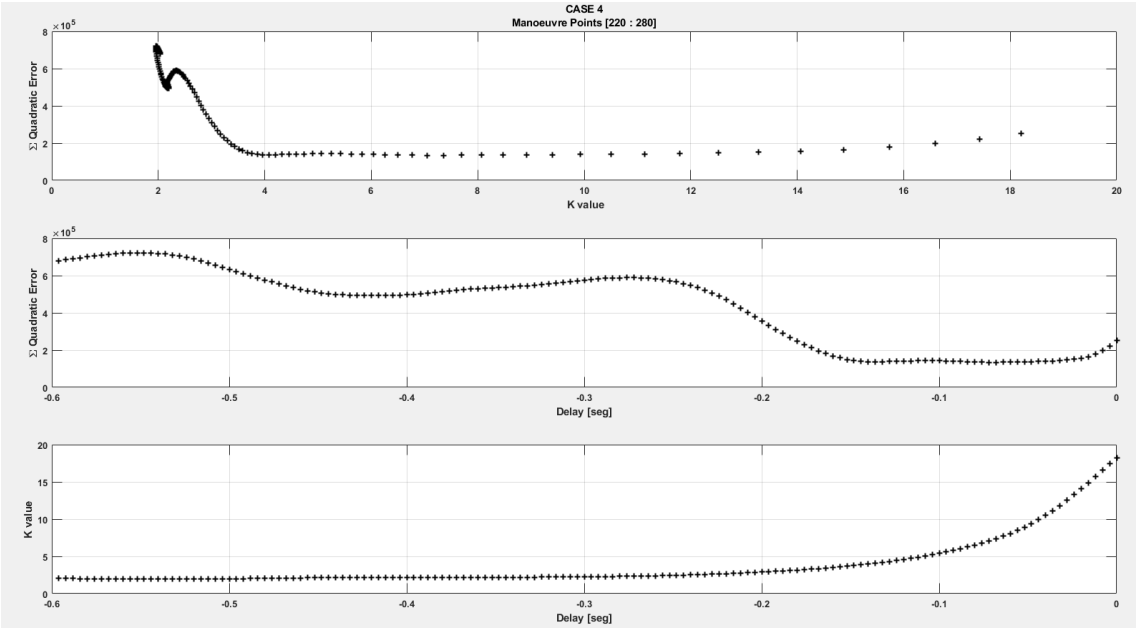

Figure 119 Case 4 [220 280] Quadratic Error, Delay and K value

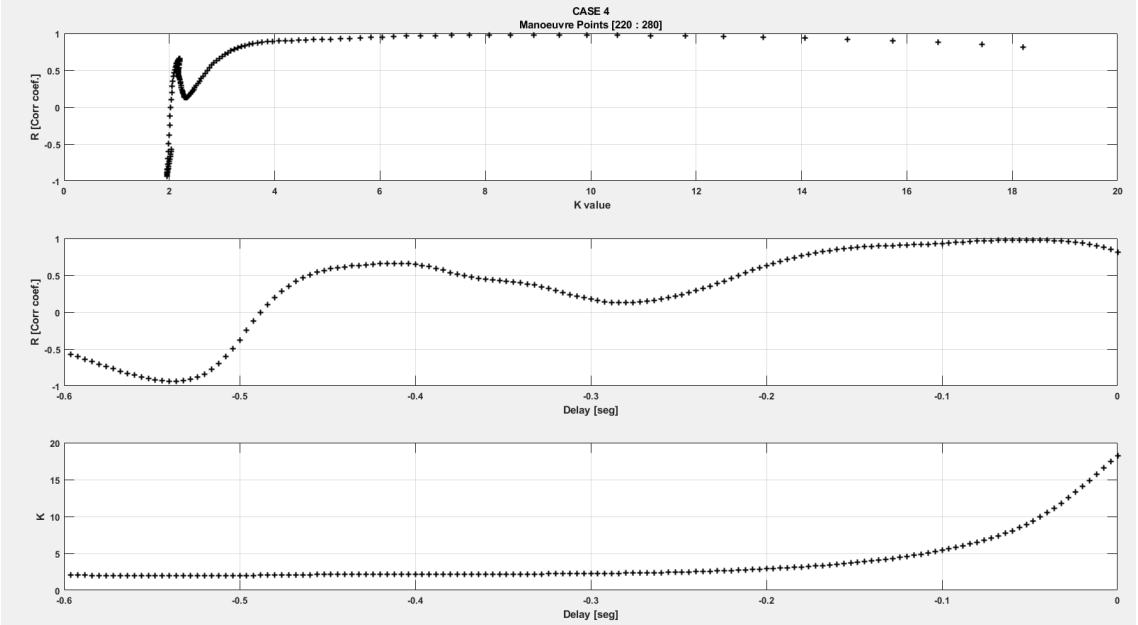

Figure 120 Case 4 [220 280] R, Delay and K value

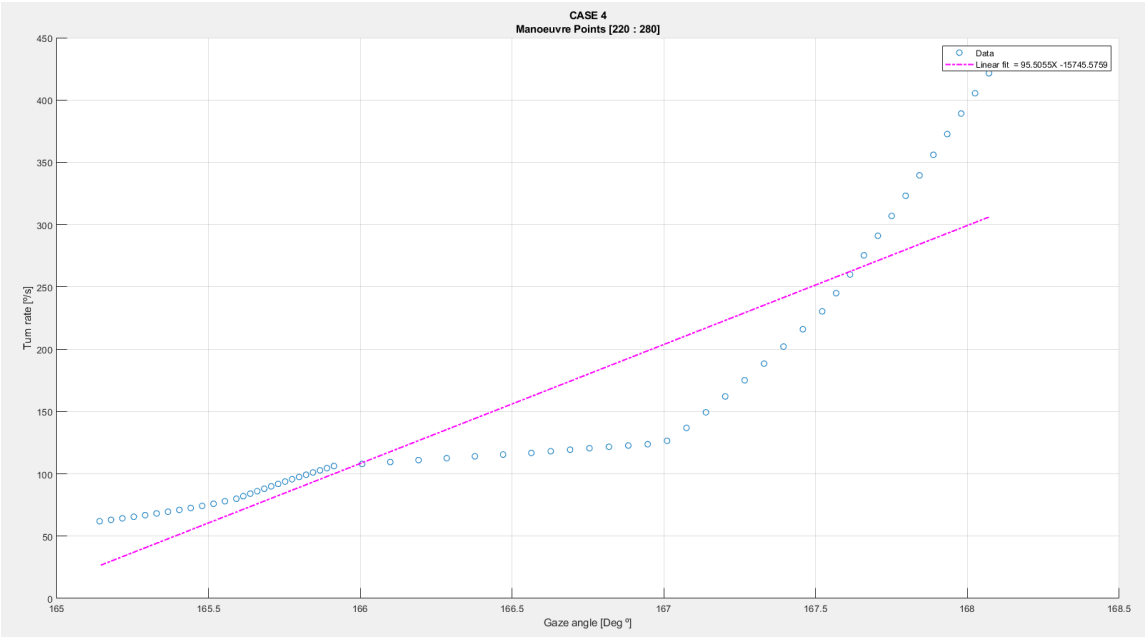

Figure 121Case 4 [220 280] Linear Regression

150 280

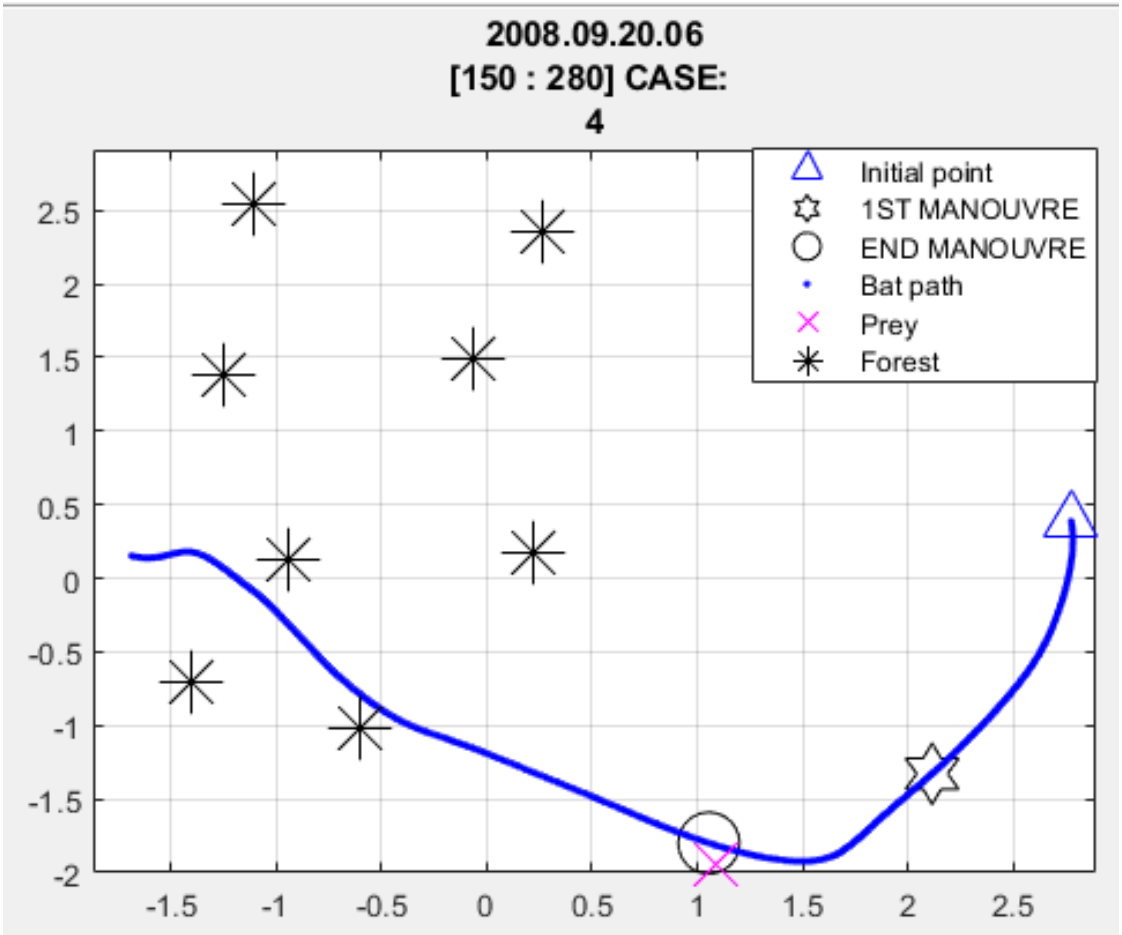

Figure 122 Case 4 [150 280] Flight Path

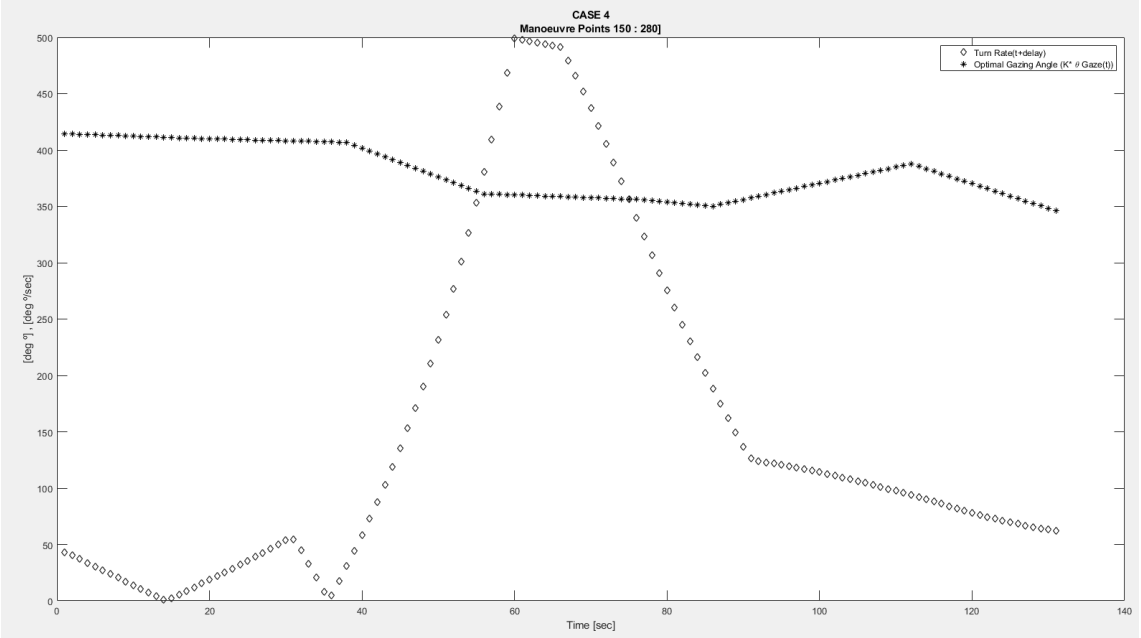

Figure 123 Case 4 [150 280] Turn Rate and Gazing Angle Comparison

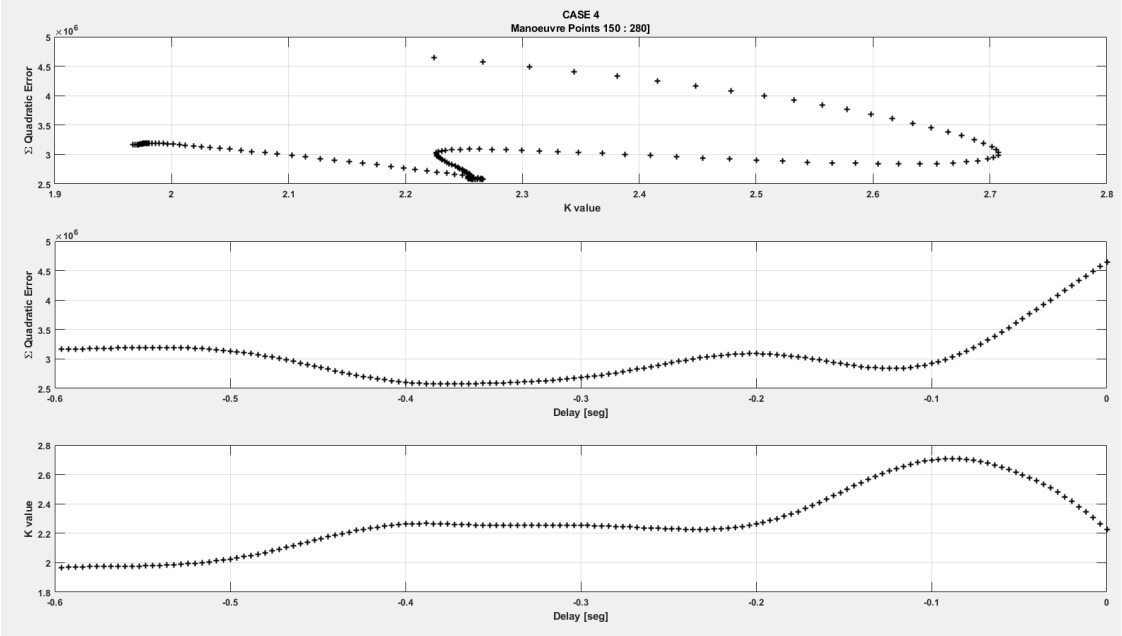

Figure 124 Case 4 [150 280] Quadratic Error, Delay and K value

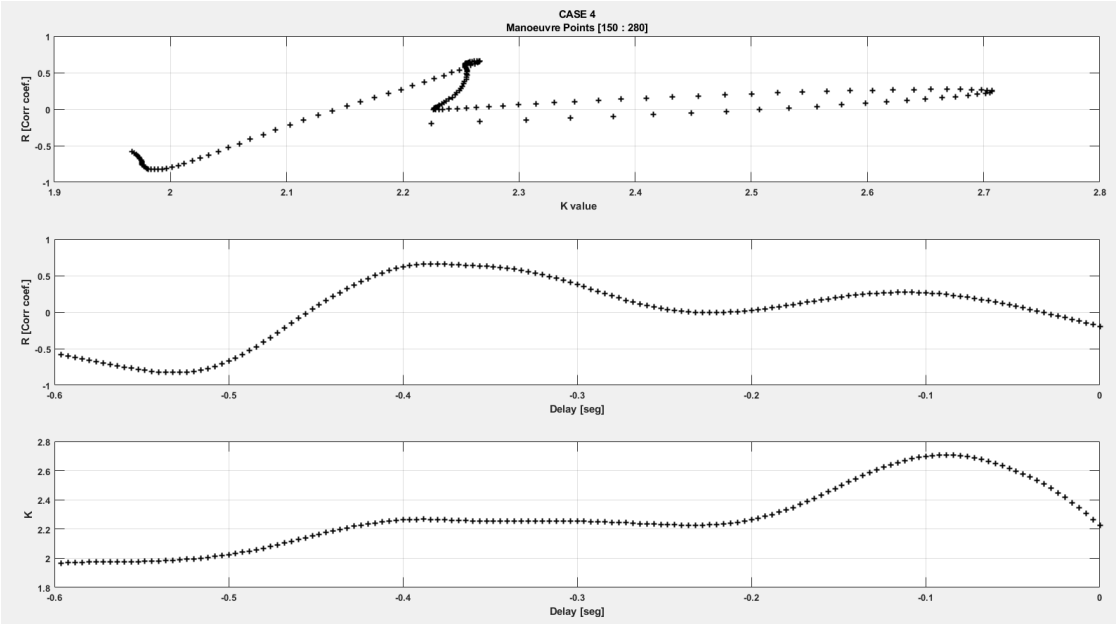

Figure 125 Case 4 [150 280] R, Delay and K value

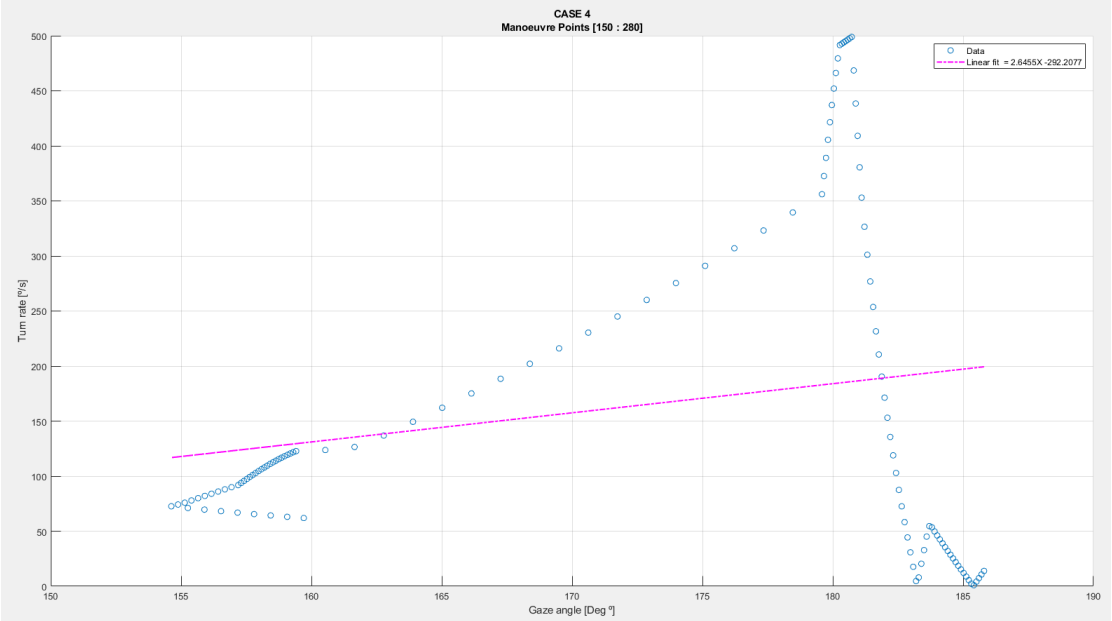

Figure 126 Case 4 [150 280] Linear Regression

50 170

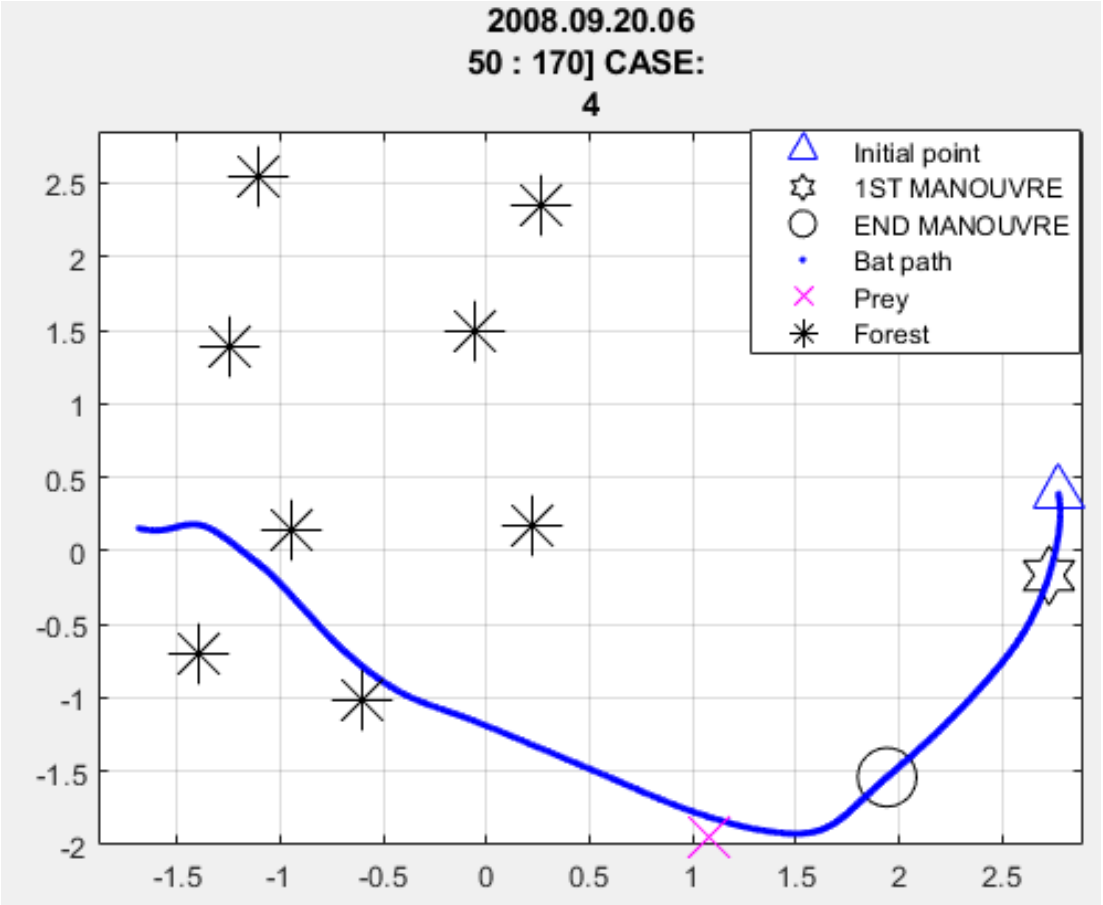

Figure 127 Case 4 [150 170] Flight Path

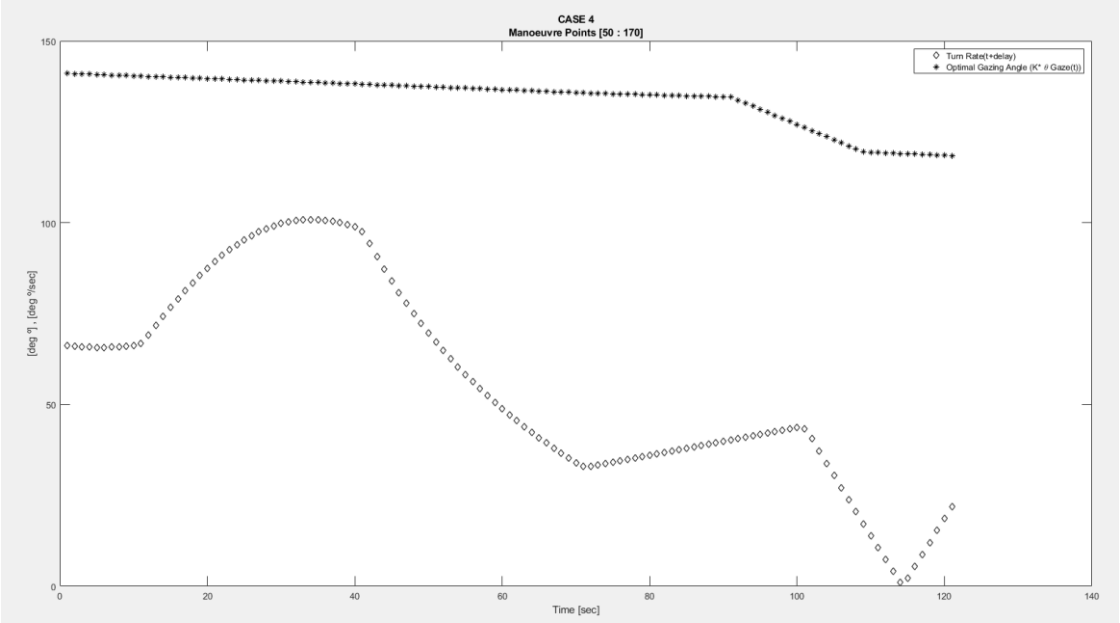

Figure 128 Case 4 [150 170] Turn Rate and Gazing Angle Comparison

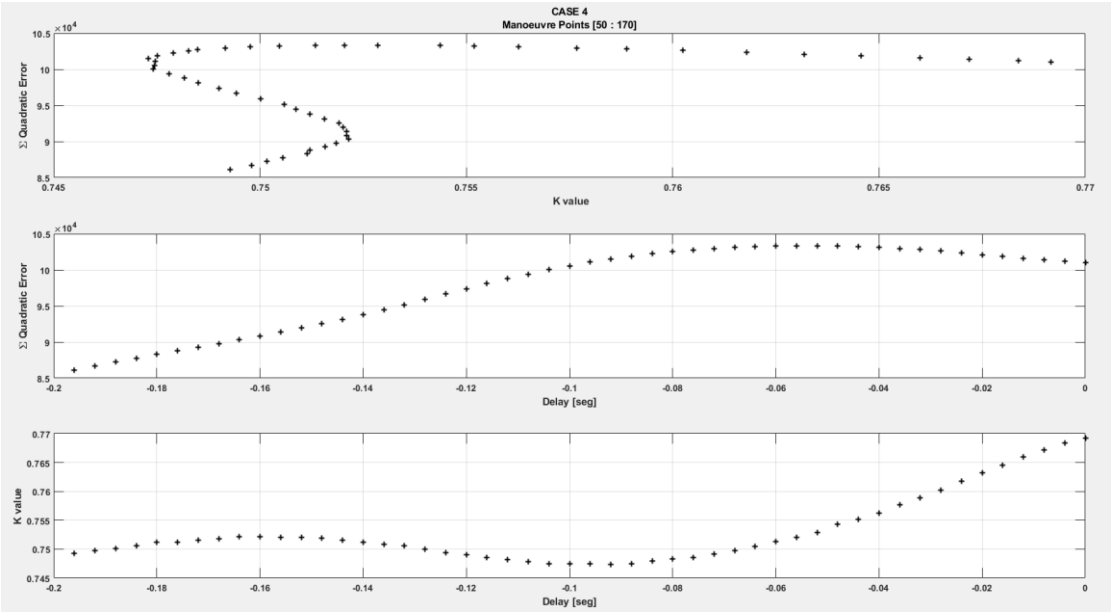

Figure 129 Case 4 [150 170] Quadratic Error, Delay, and k value

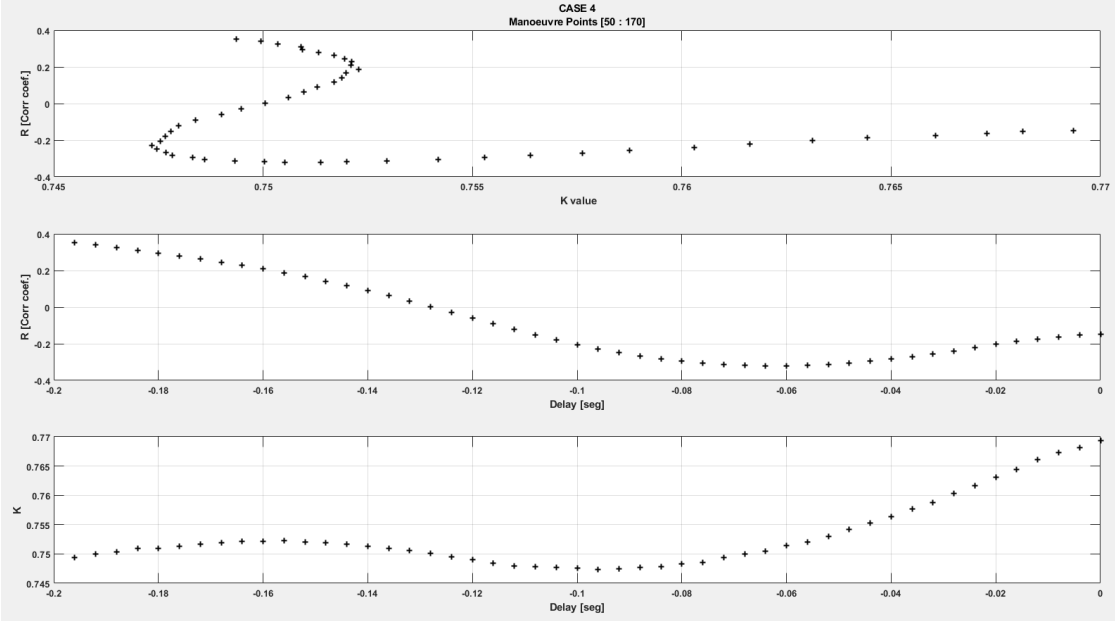

Figure 130 Case 4 [150 170] R, Delay and K value

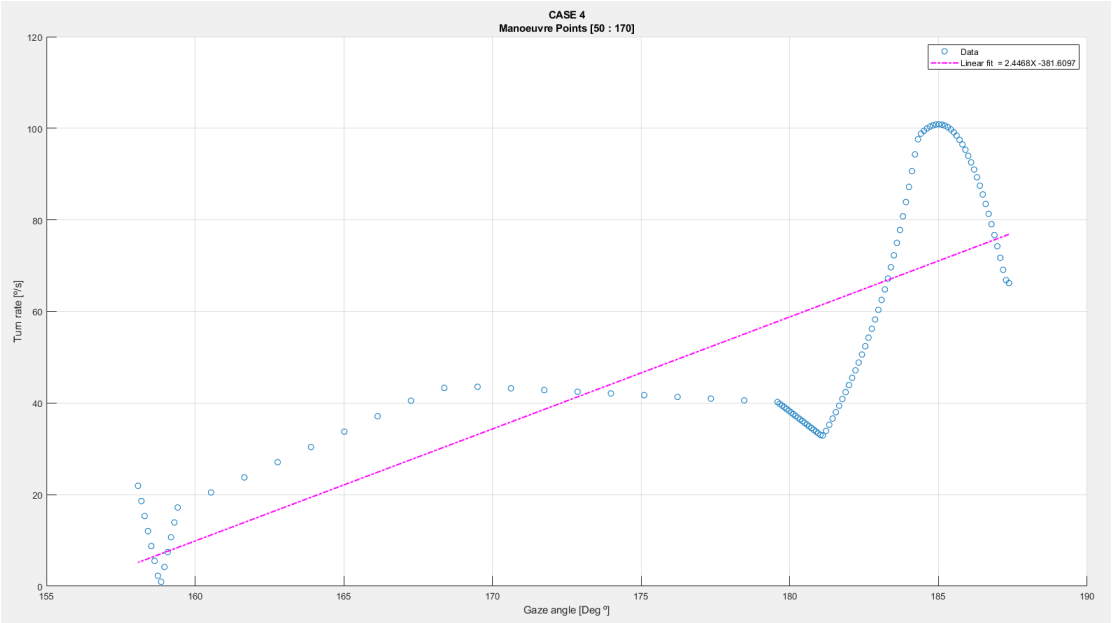

Figure 131 Case 4 [150 170] Linear Regression

Case 5

70 180

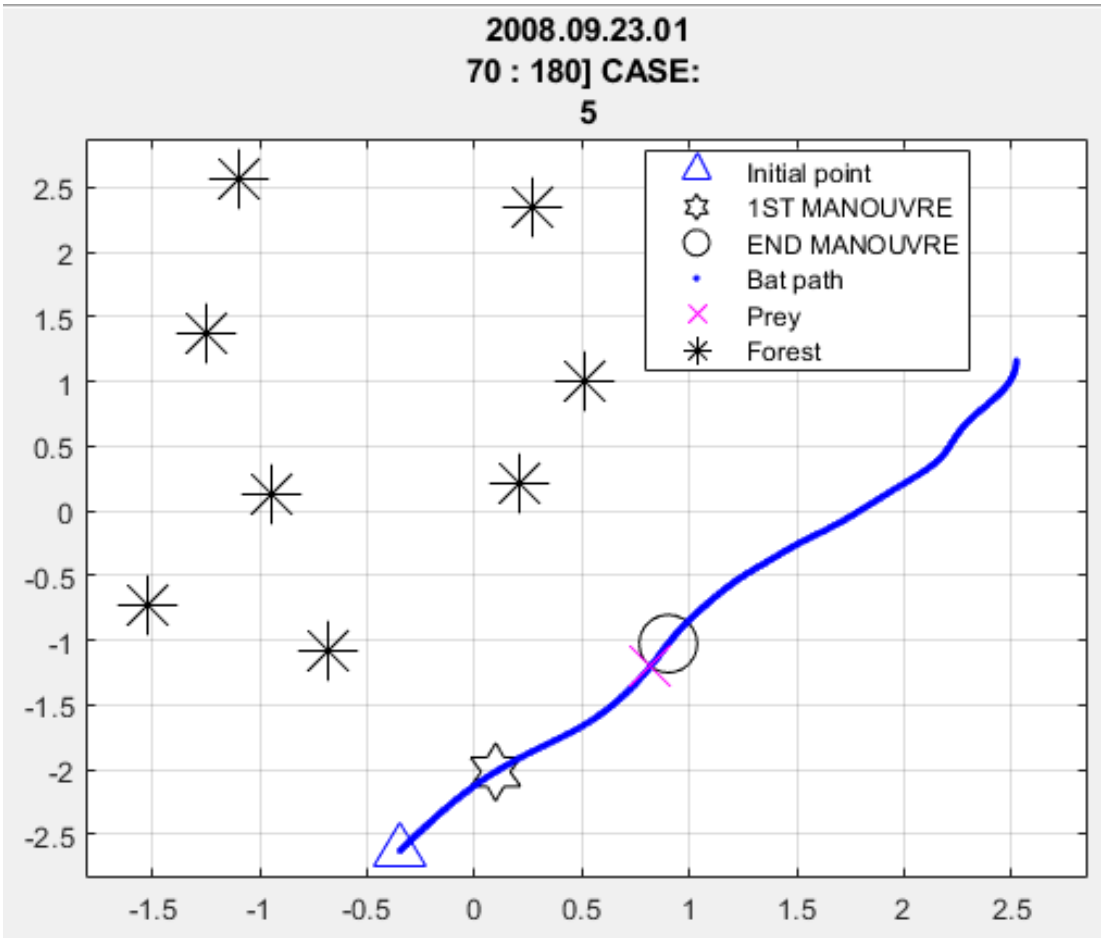

Figure 132 Case 5 [70 180] Flight Path

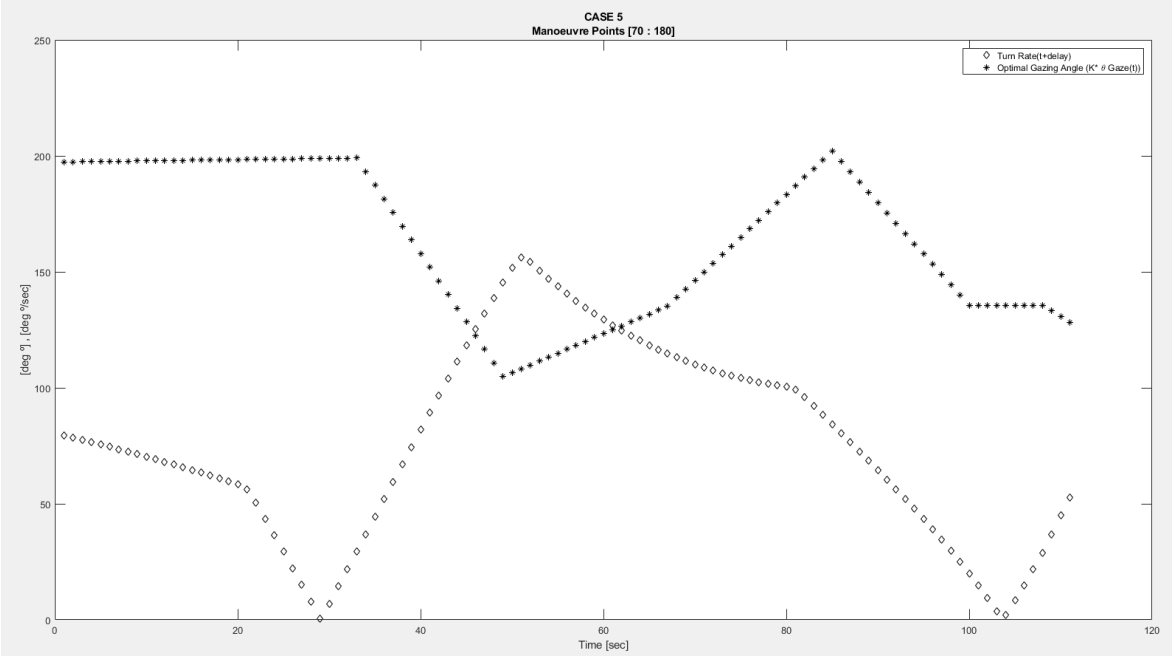

Figure 133 Case 5 [70 180] Turn Rate and Gazing Angle Comparison

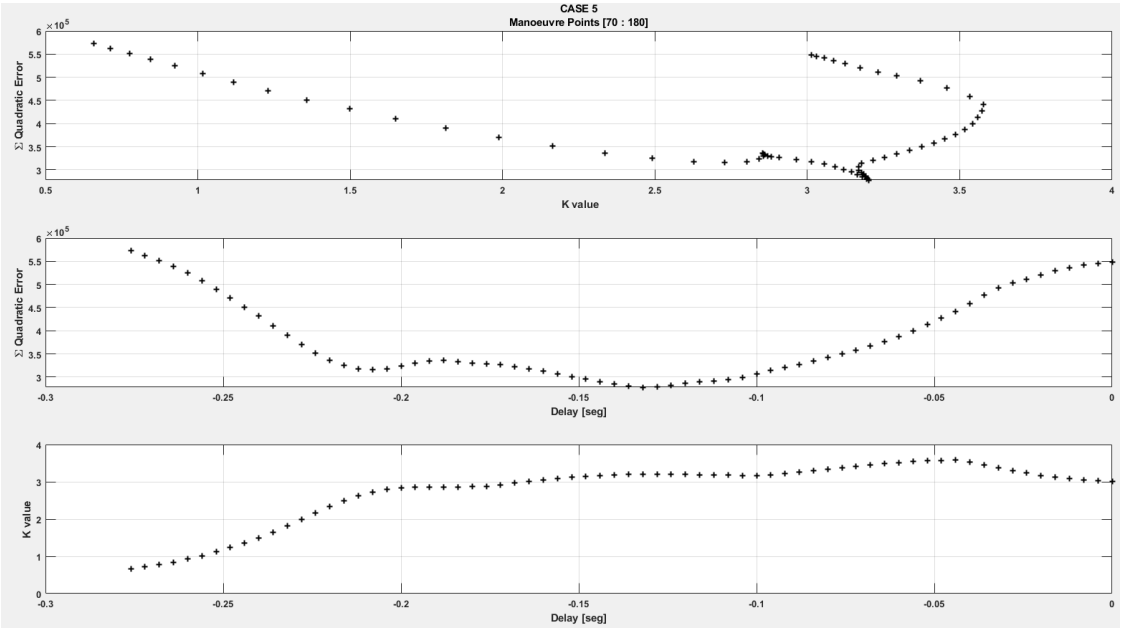

Figure 134 Case 5 [70 180] Quadratic Error, Delay and K value

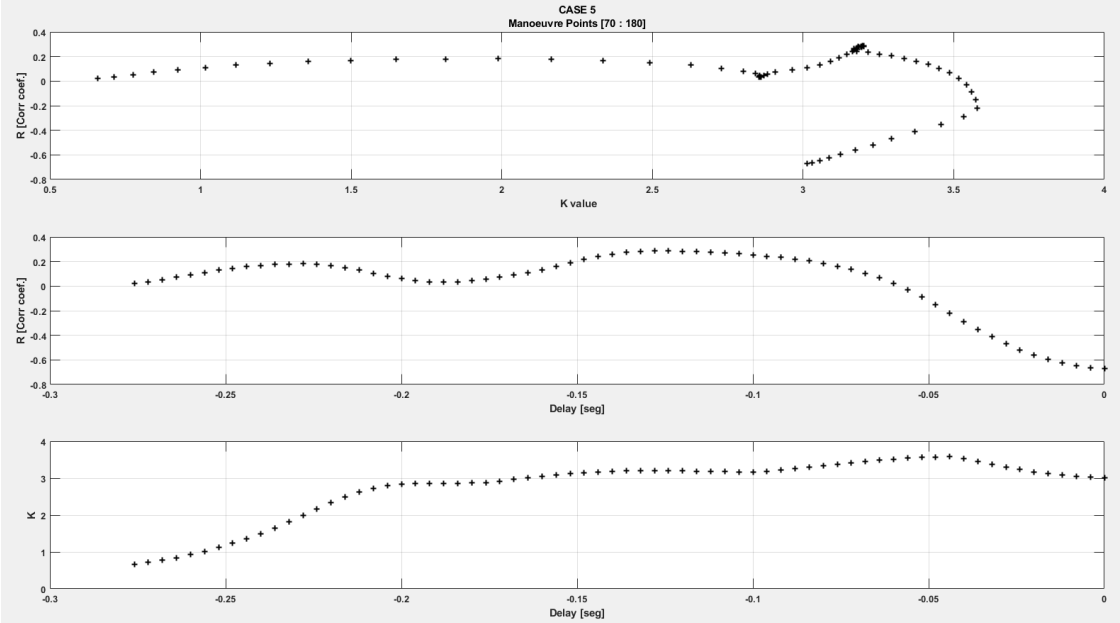

Figure 135 Case 5 [70 180] R, Delay and K value

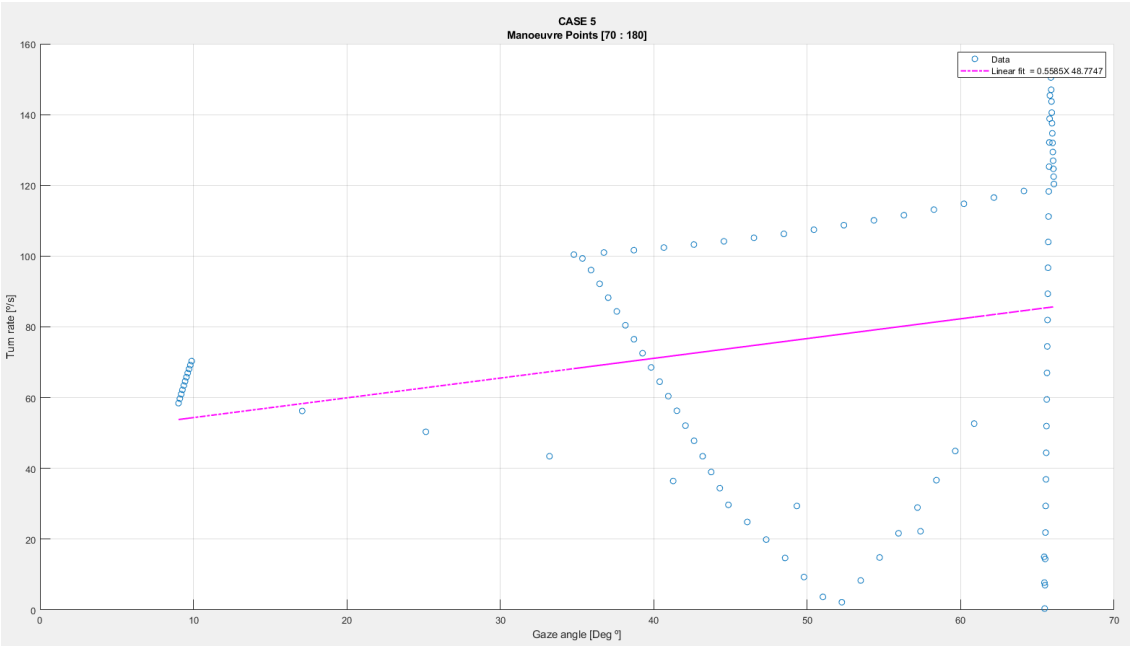

Figure 136 Case 5 [70 180] Linear Regression

CASE 6

520 to 608

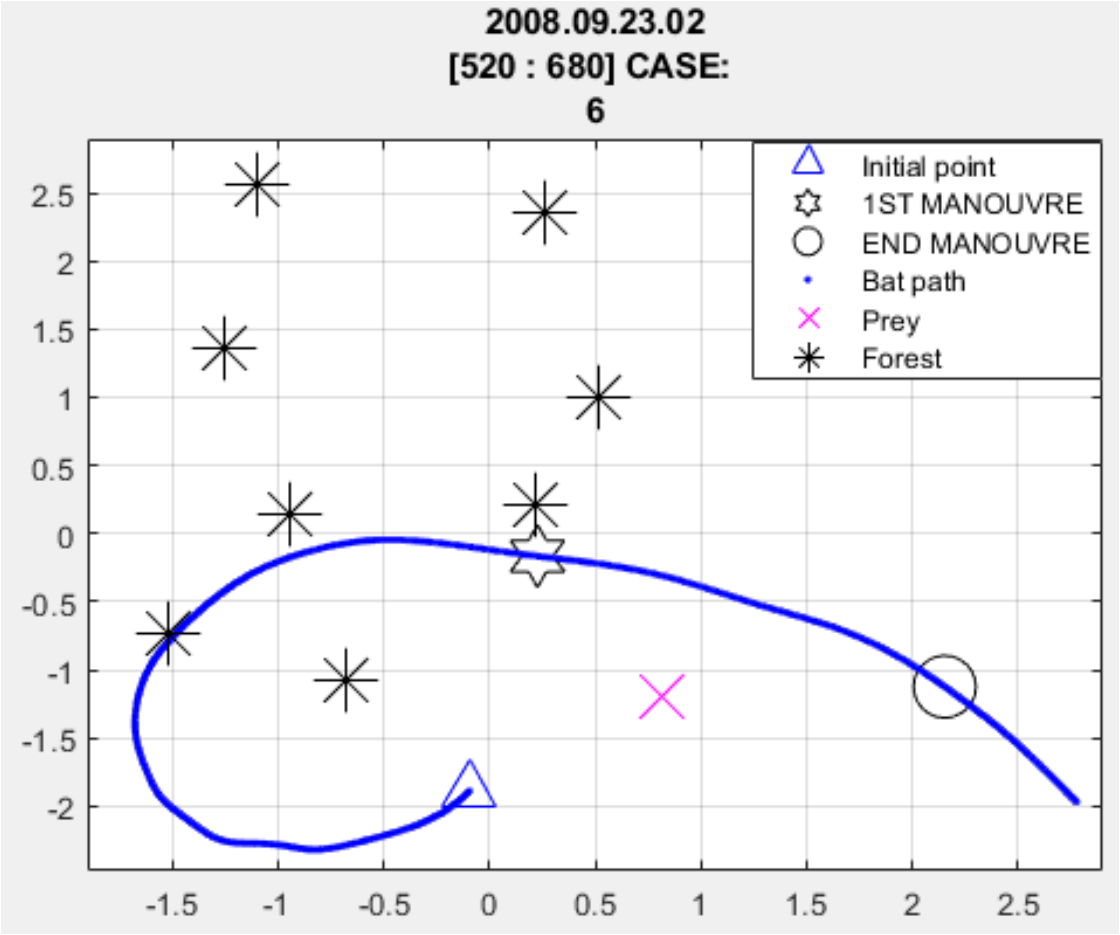

Figure 137 Case 6 [520 608] Flight Path

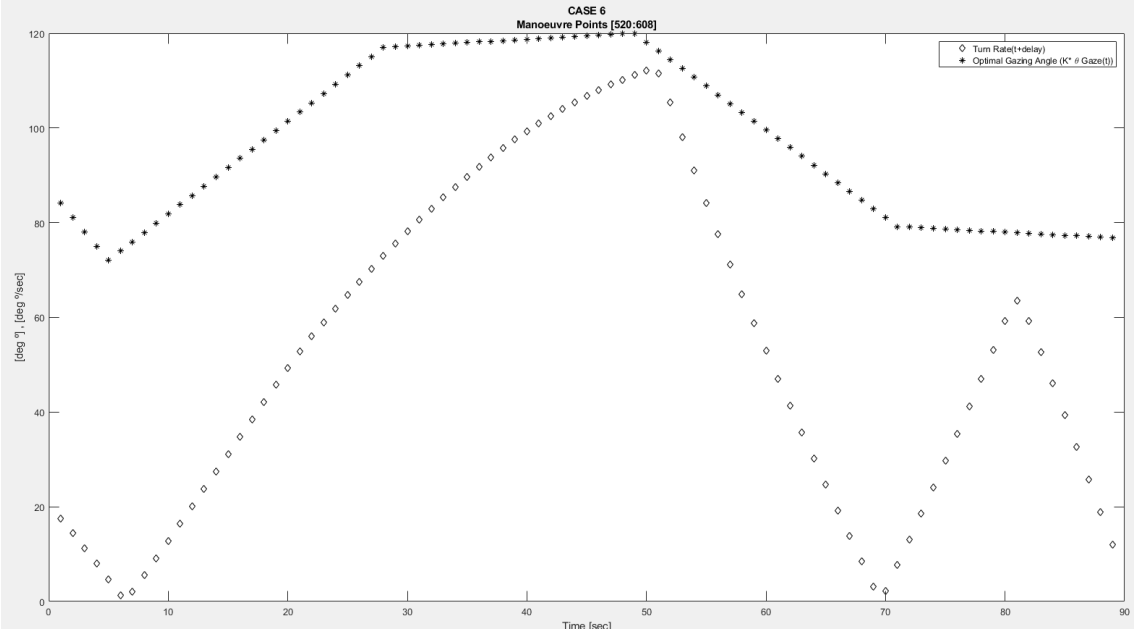

Figure 138 Case 6 [520 608] Turn Rate and Gazing Angle Comparison

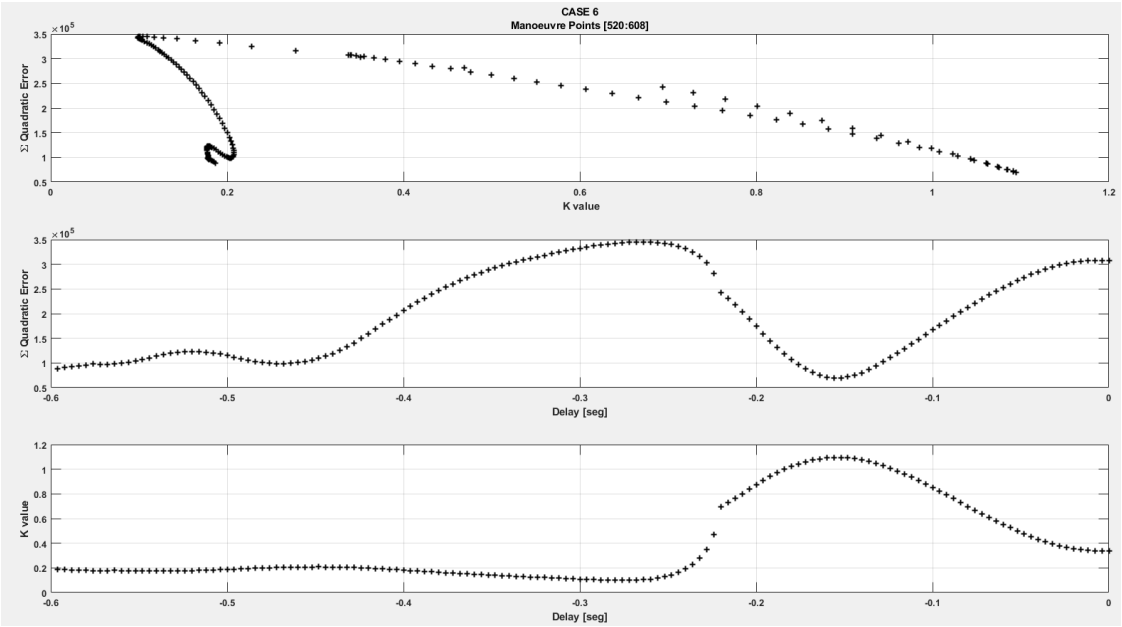

Figure 139 Case 6 [520 608] Quadratic Error, Delay and K value

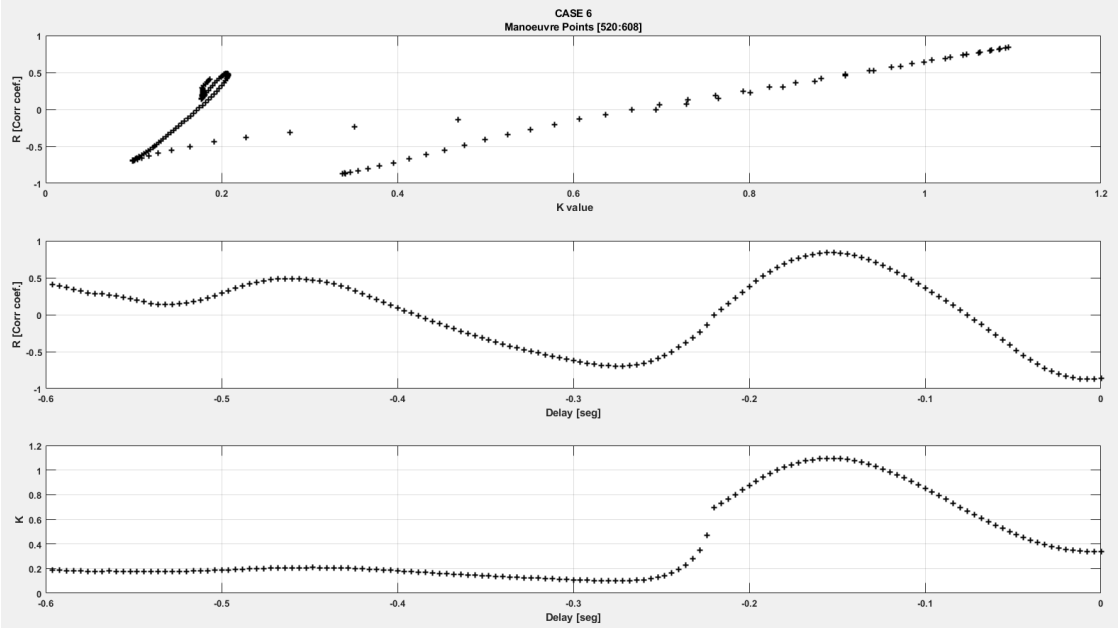

Figure 140 Case 6 [520 608] R, Delay and K value

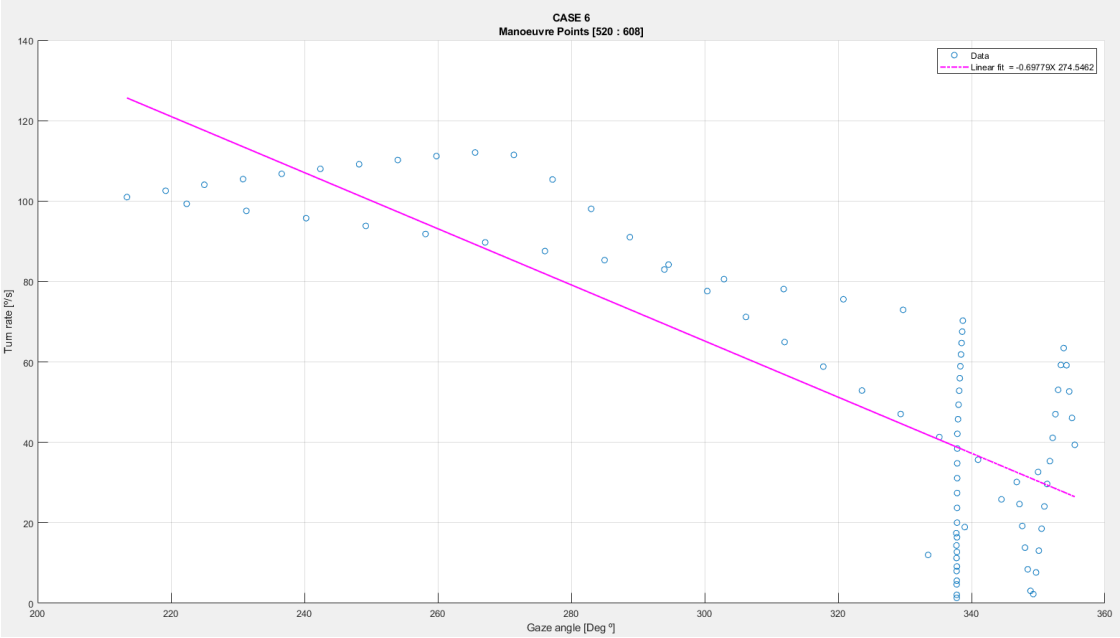

Figure 141 Case 6 [520 608] Linear Regression

360 510

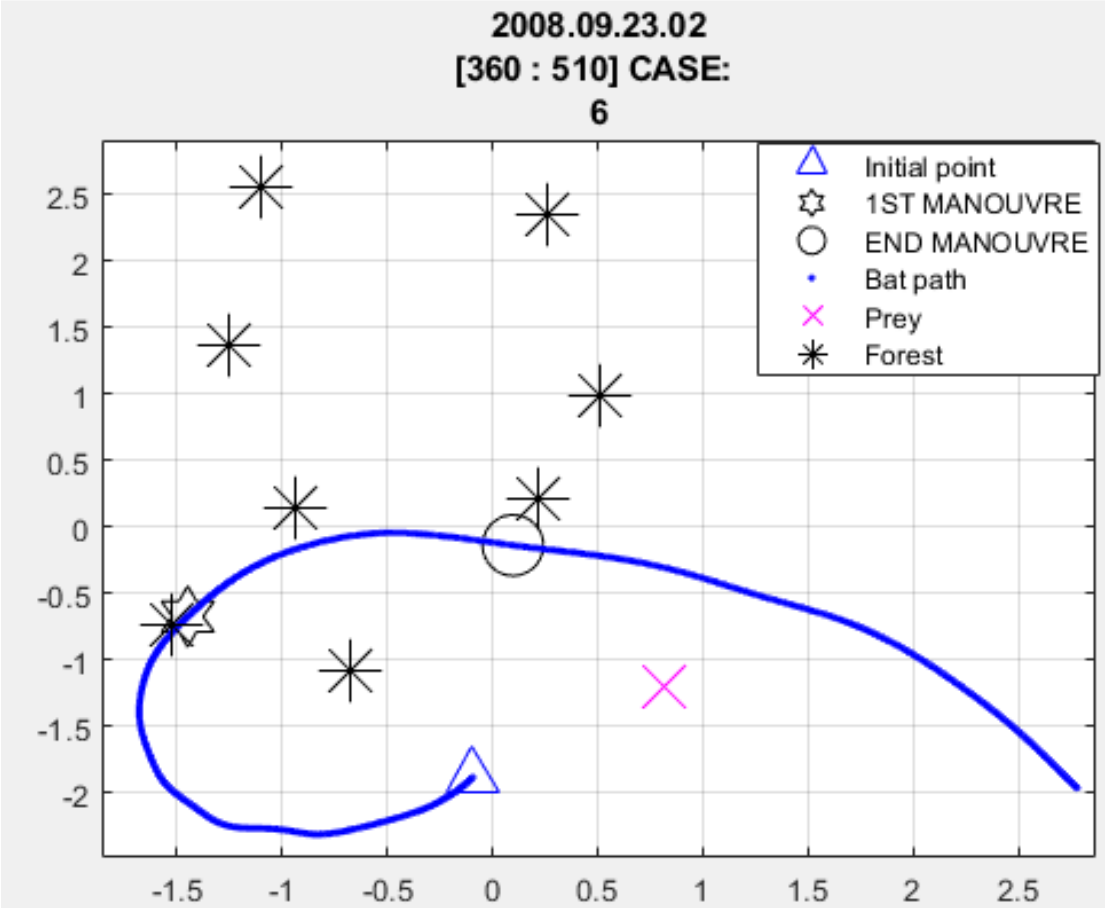

Figure 142 Case 6 [3690 510] Flight Path

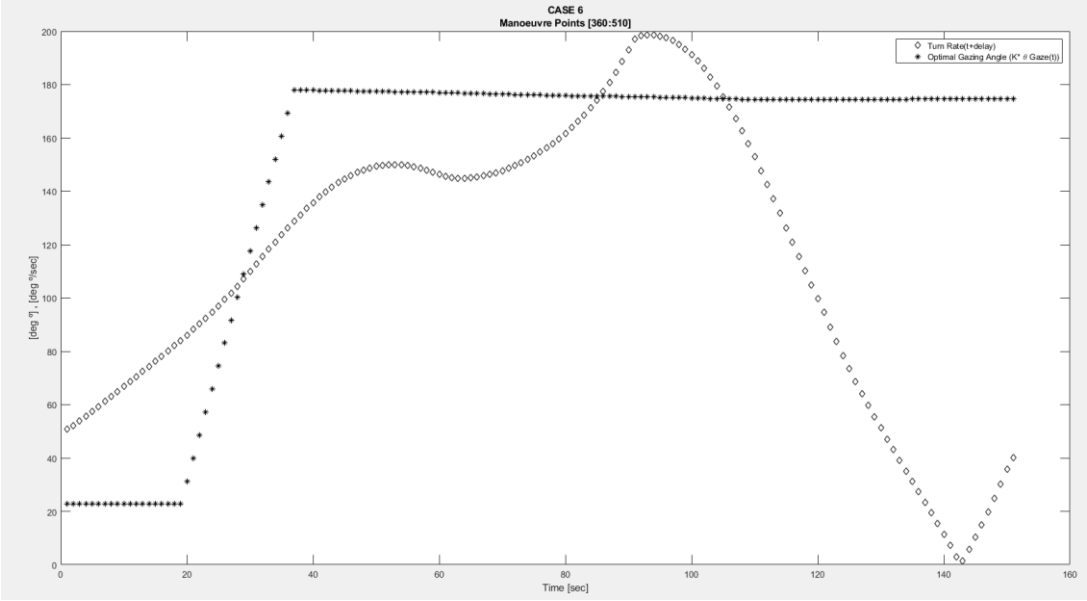

Figure 143 Case 6 [3690 510] Turn Rate and Gazing Angle comparison

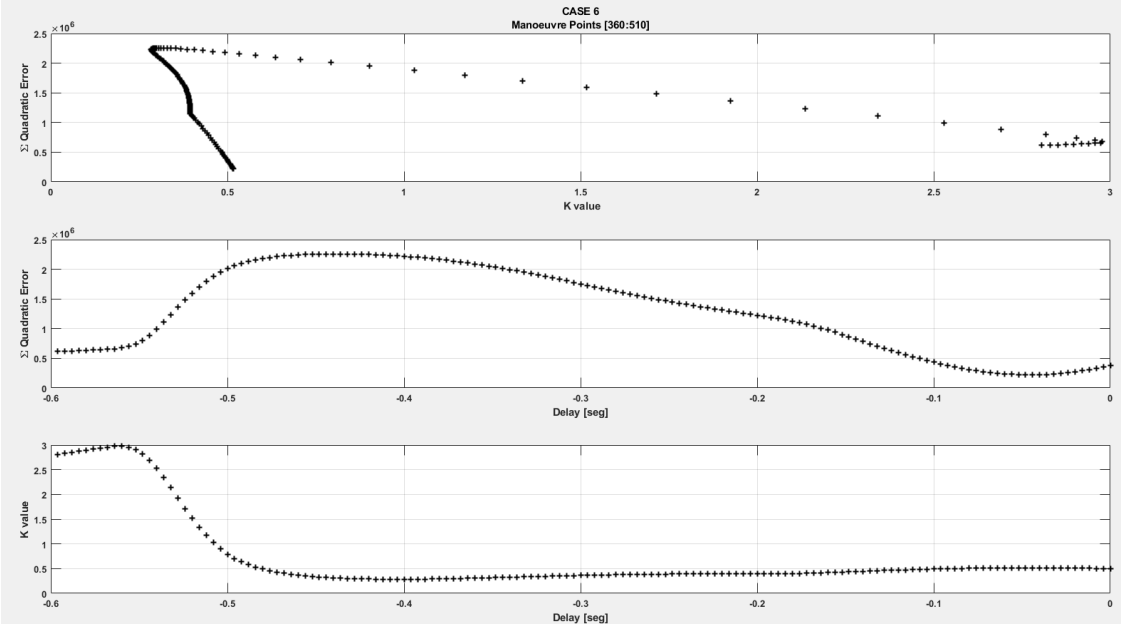

Figure 144 Case 6 [3690 510] Quadratic Error, Delay and K value

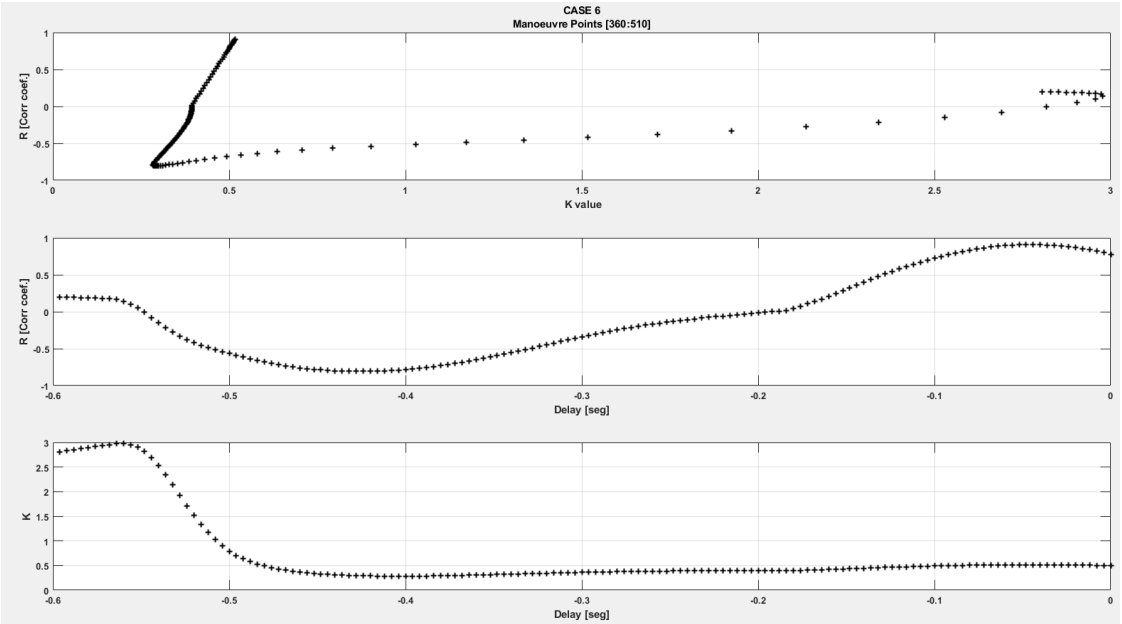

Figure 145 Case 6 [3690 510] R, Delay and K value

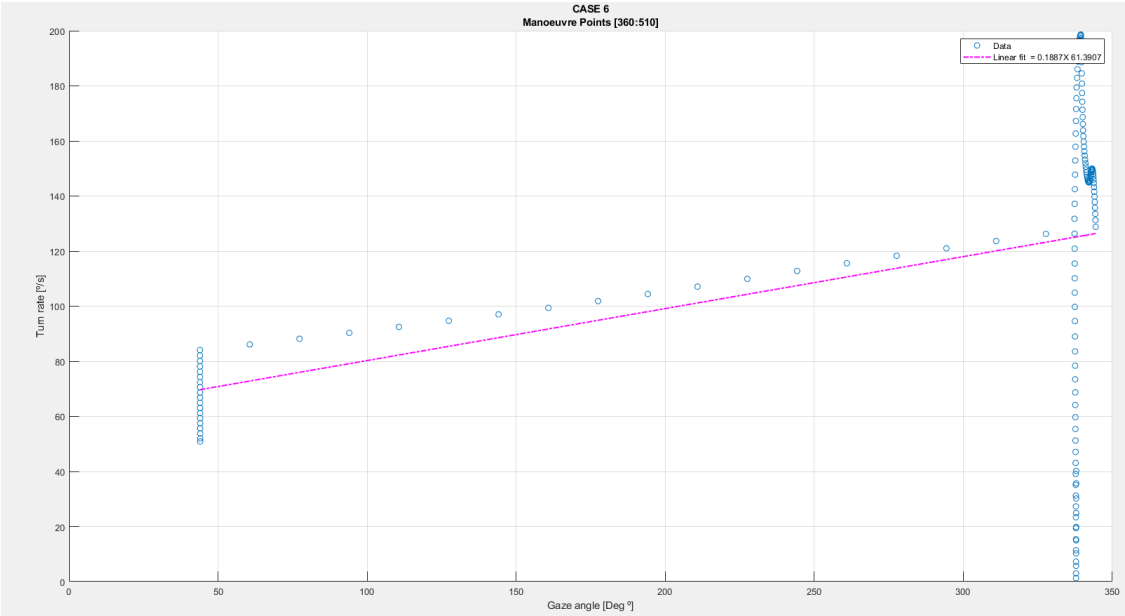

Figure 146 Case 6 [3690 510] Linear Regression

200 360

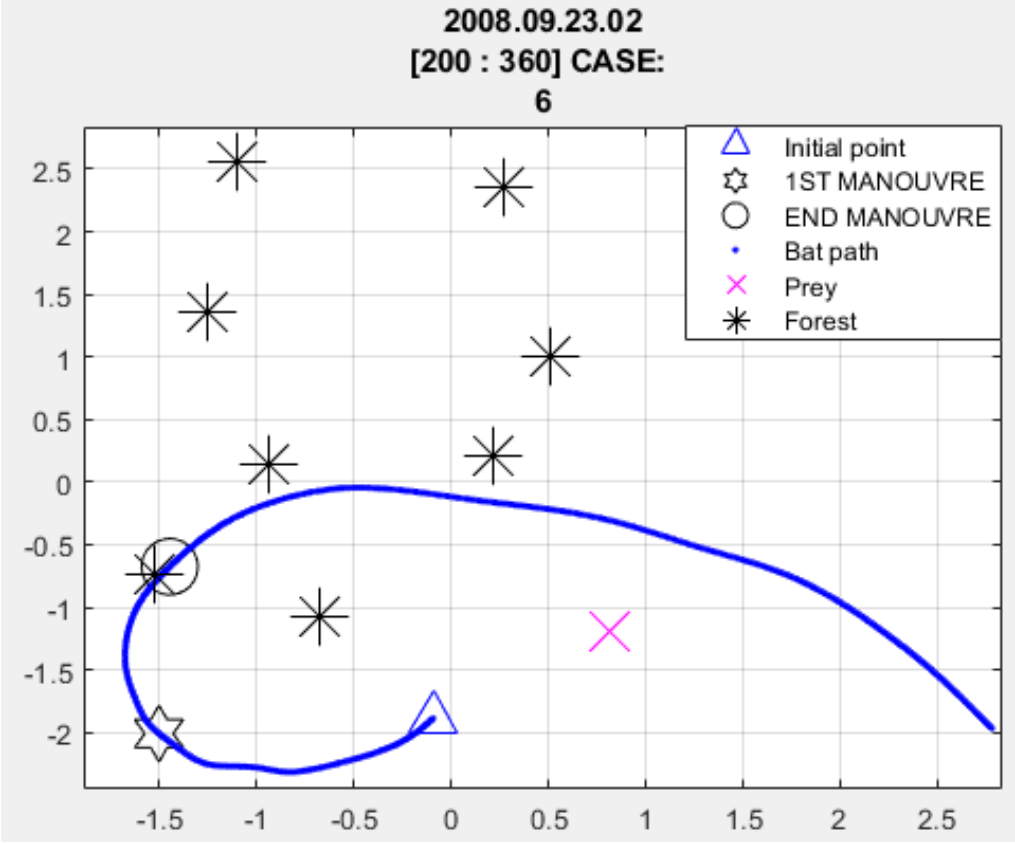

Figure 147 Case 6 [200 360] Flight path

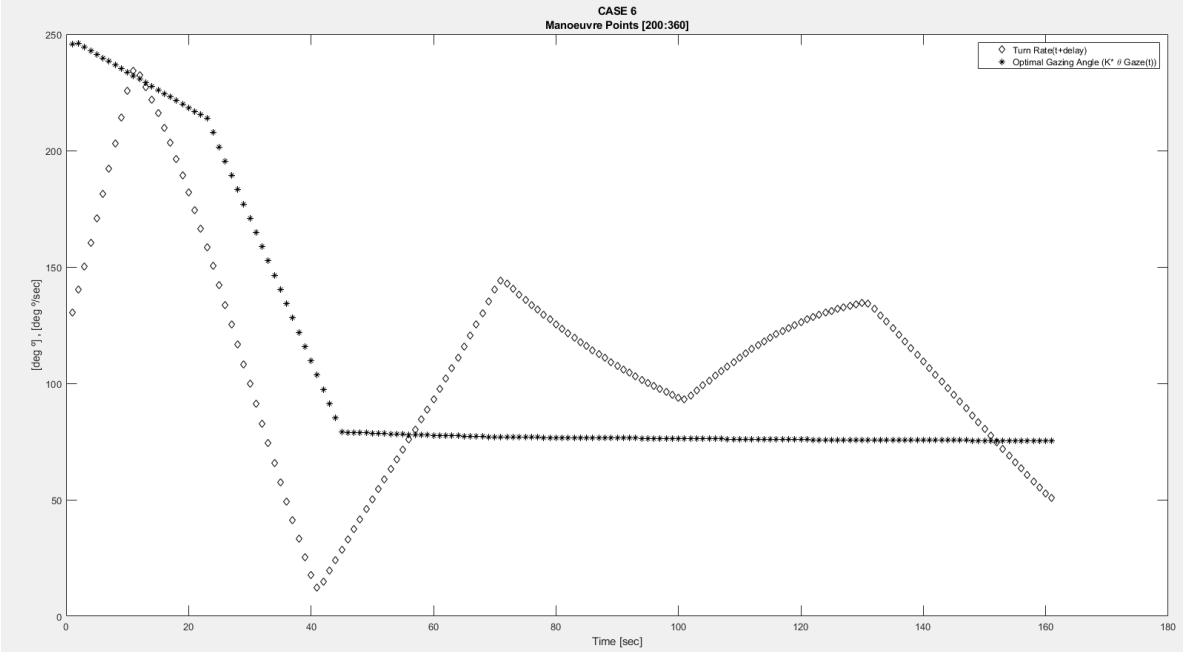

Figure 148 Case 6 [200 360] Turn Rate and Gazing Angle comparison

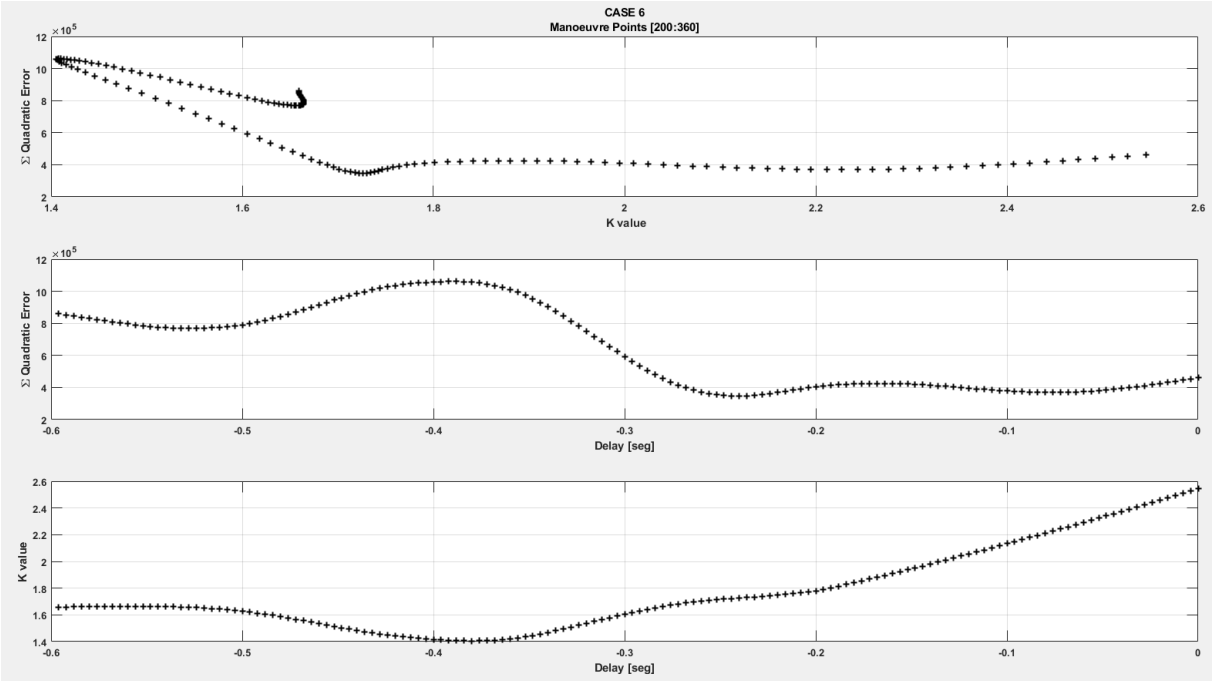

Figure 149 Case 6 [200 360] Quadratic Error, Delay and K values

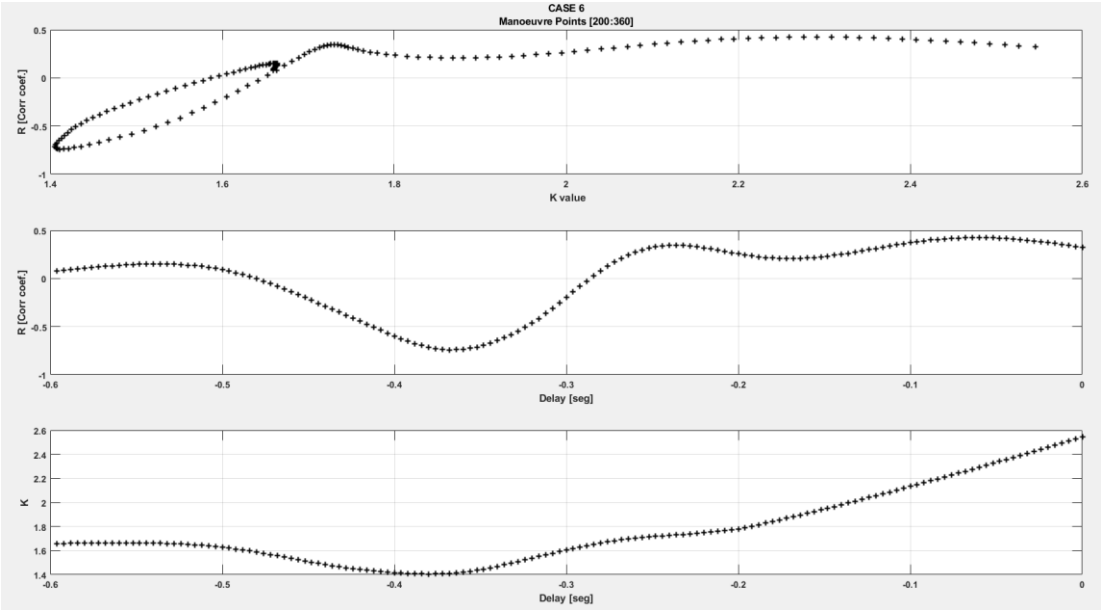

Figure 150 Case 6 [200 360] R, Delay and K values

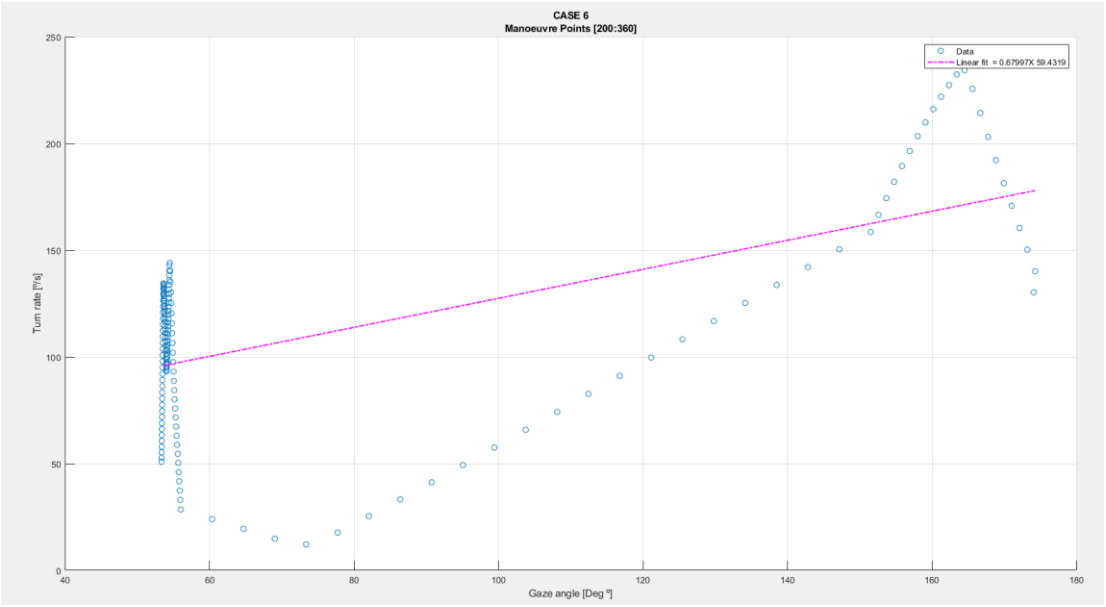

Figure 151 Case 6 [200 360] Linear Regression

150 190

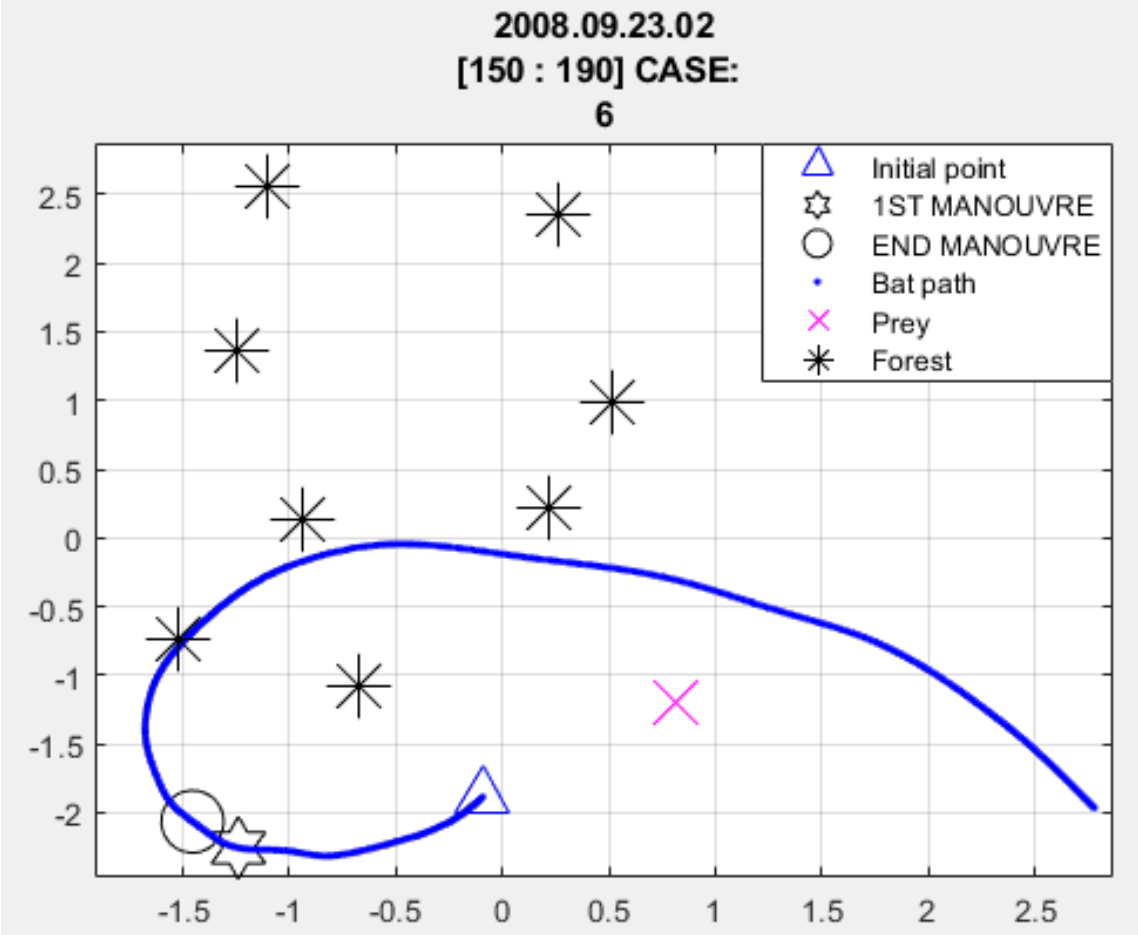

Figure 152 Case 6 [150 190] Flight Path

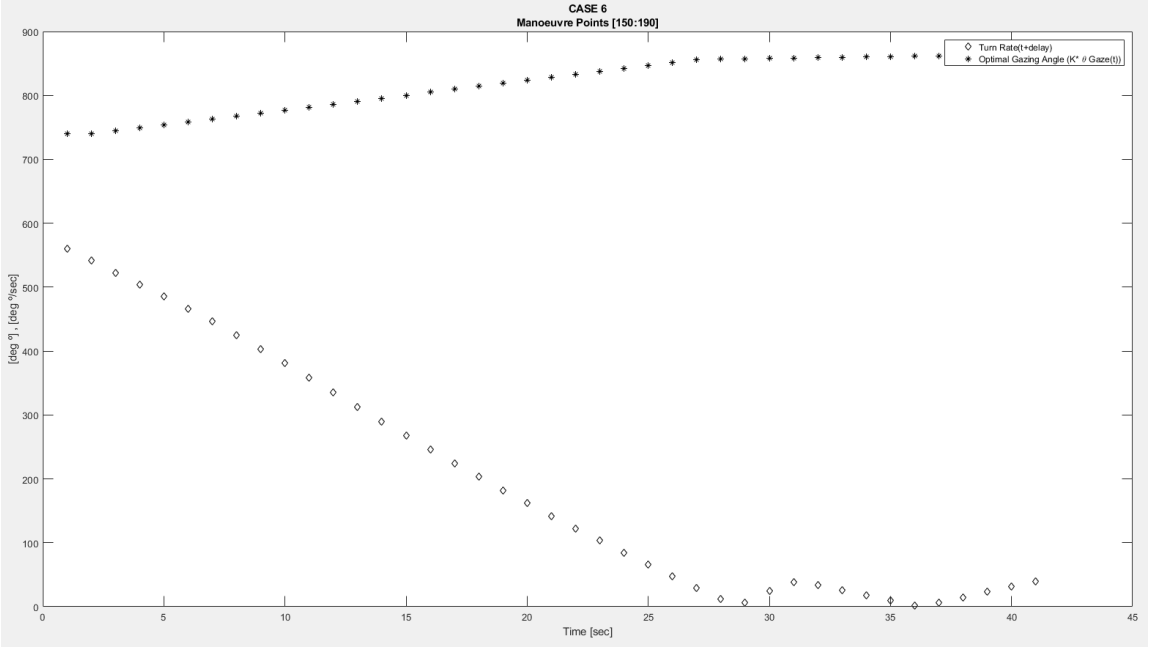

Figure 153 Case 6 [150 190] Turn Rate and Gazing Angle comparison

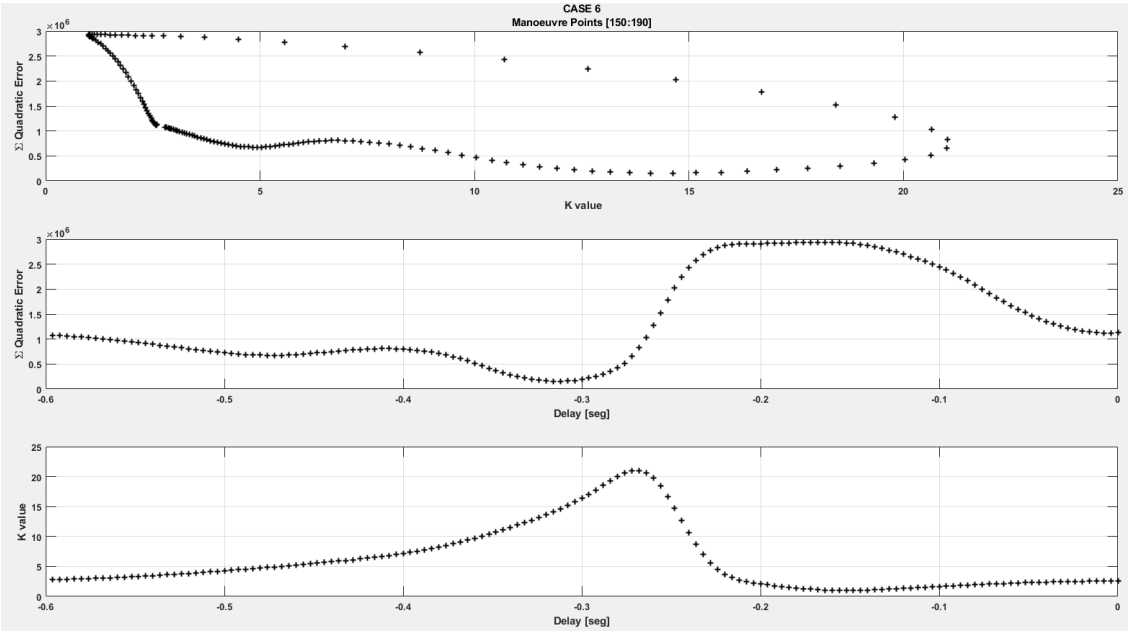

Figure 154 Case 6 [150 190]Quadratic Error, Delay and K values

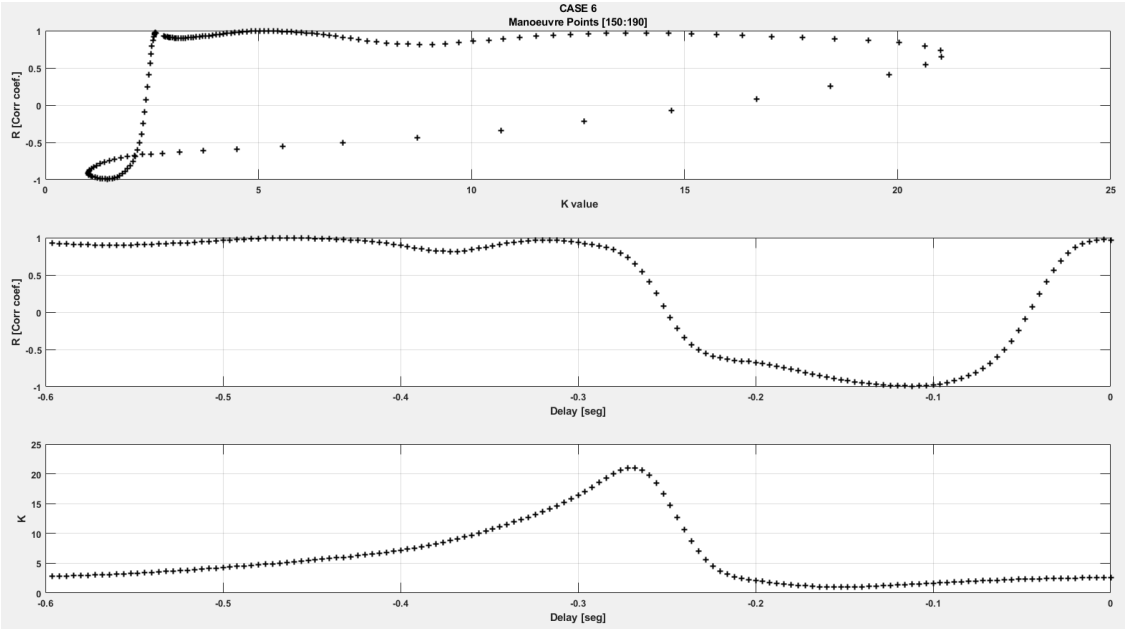

Figure 155 Case 6 [150 190]R, Delay and K values

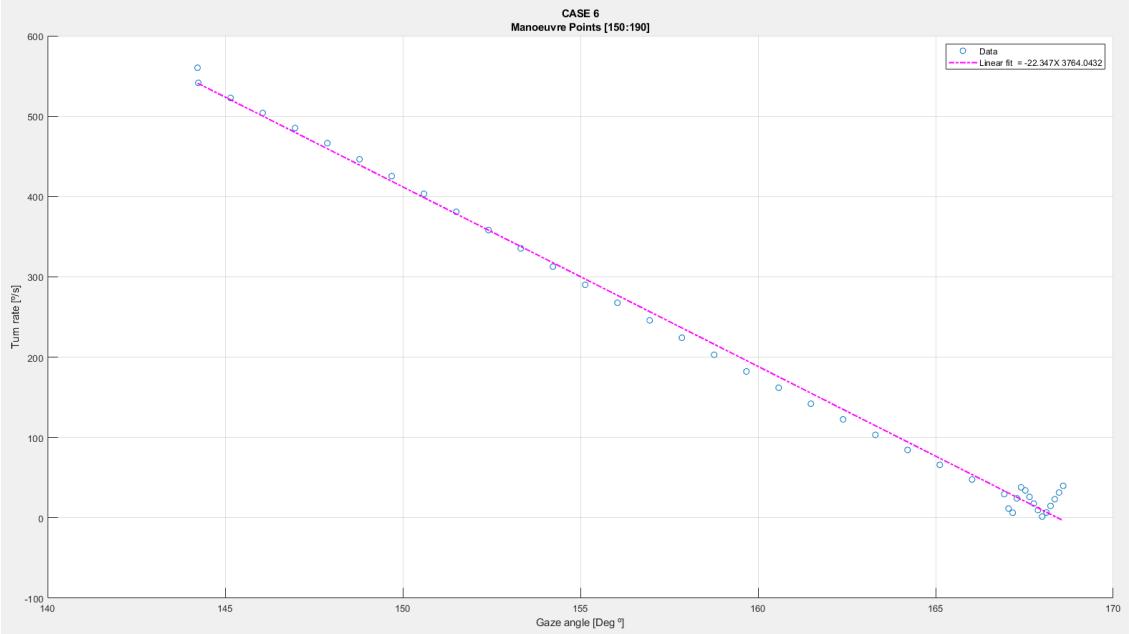

Figure 156Case 6 [150 190] Linear Regression

150 360

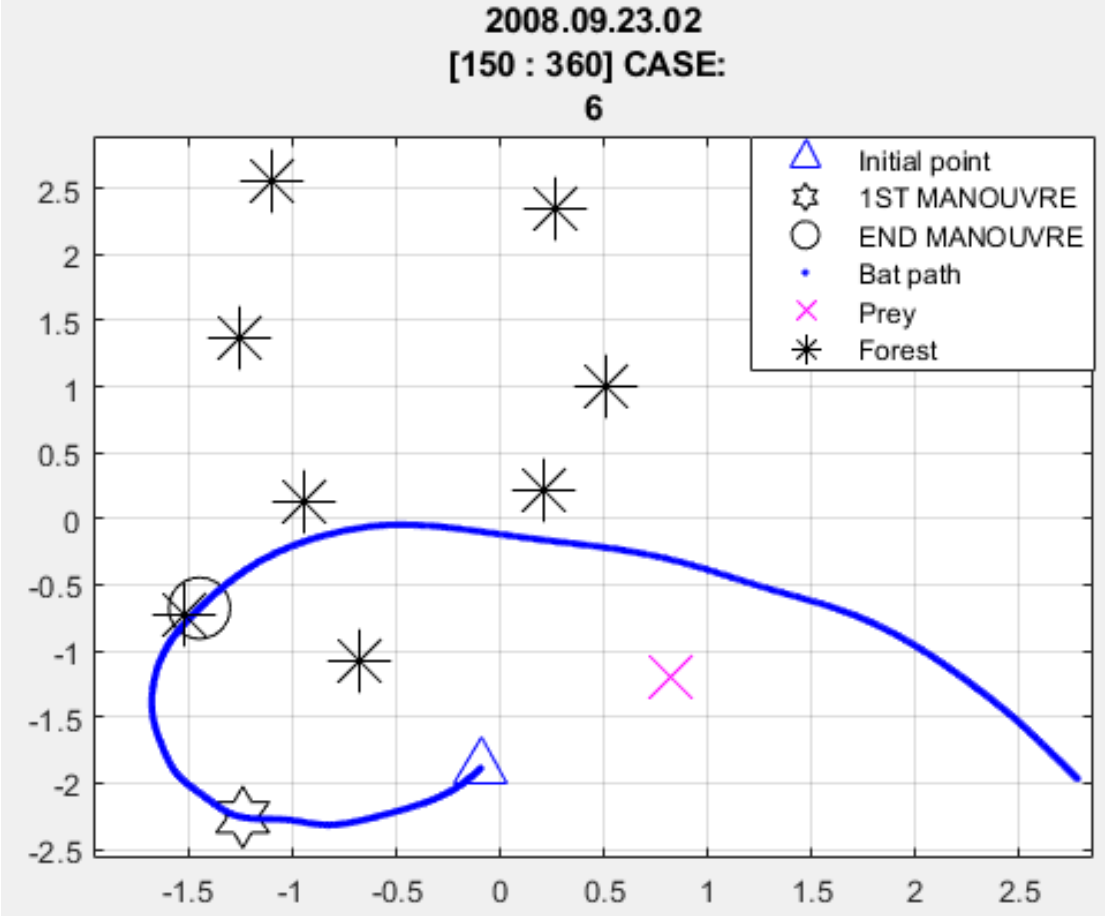

Figure 157Case 6 [150 360] Flight Path

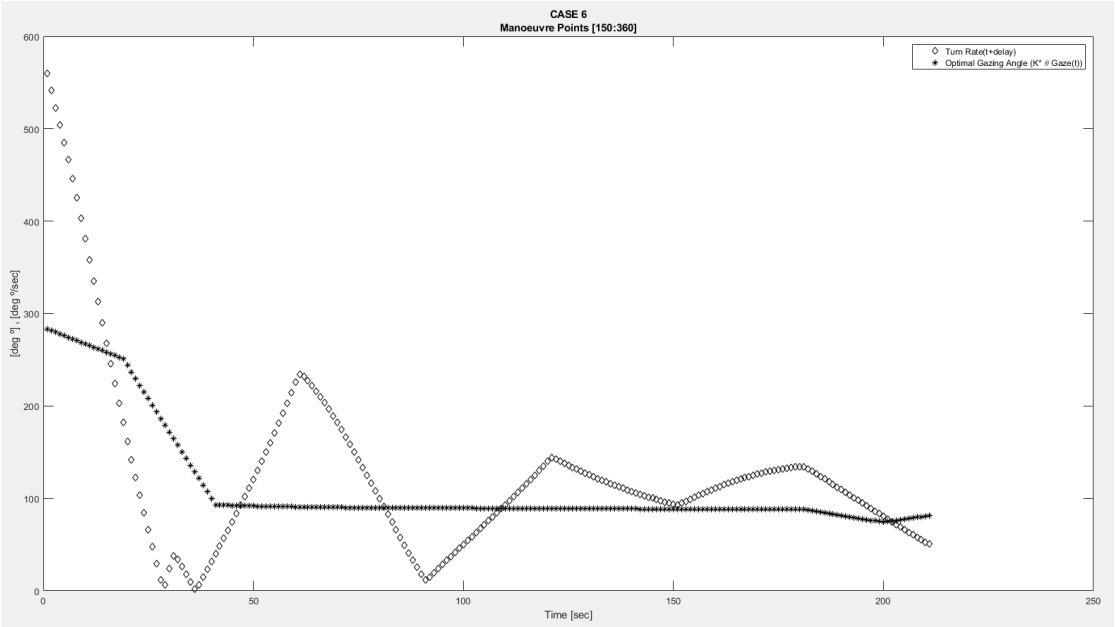

Figure 158 Case 6 [150 360] Turn Rate and Gazing Angle Comparison

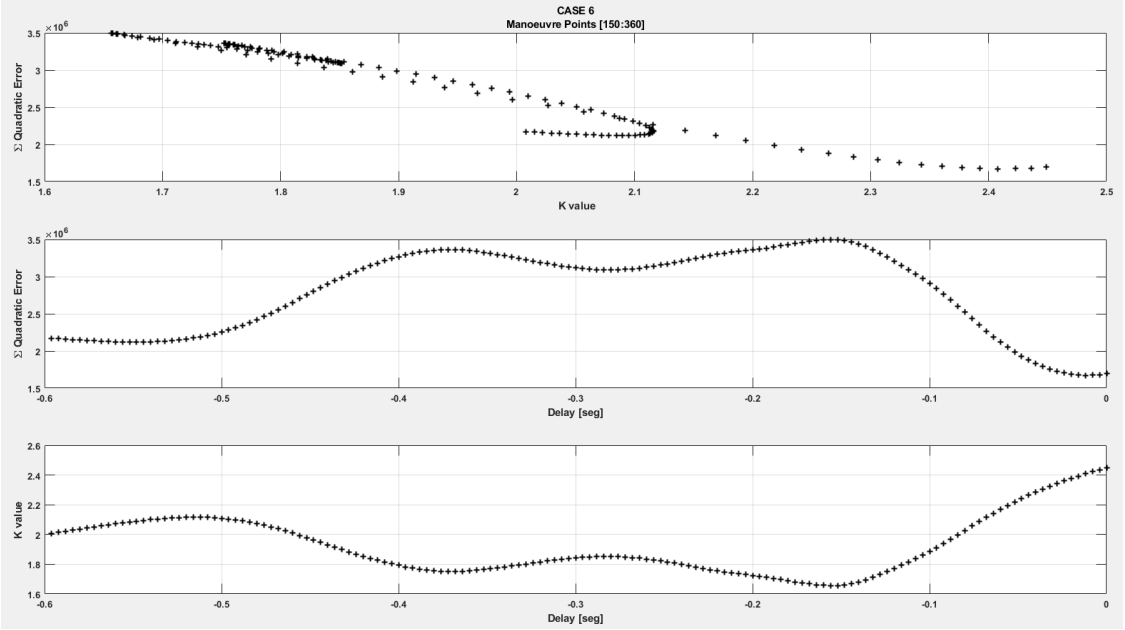

Figure 159 Case 6 [150 360] Quadratic Error, Delay and K values

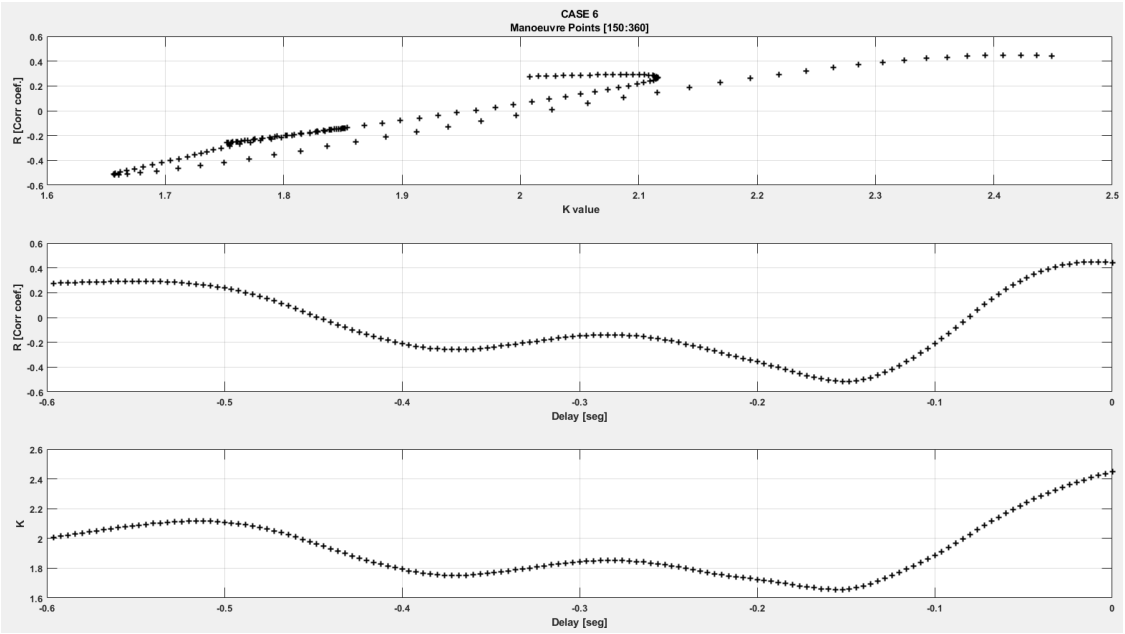

Figure 160 Case 6 [150 360] R, Delay, and K values

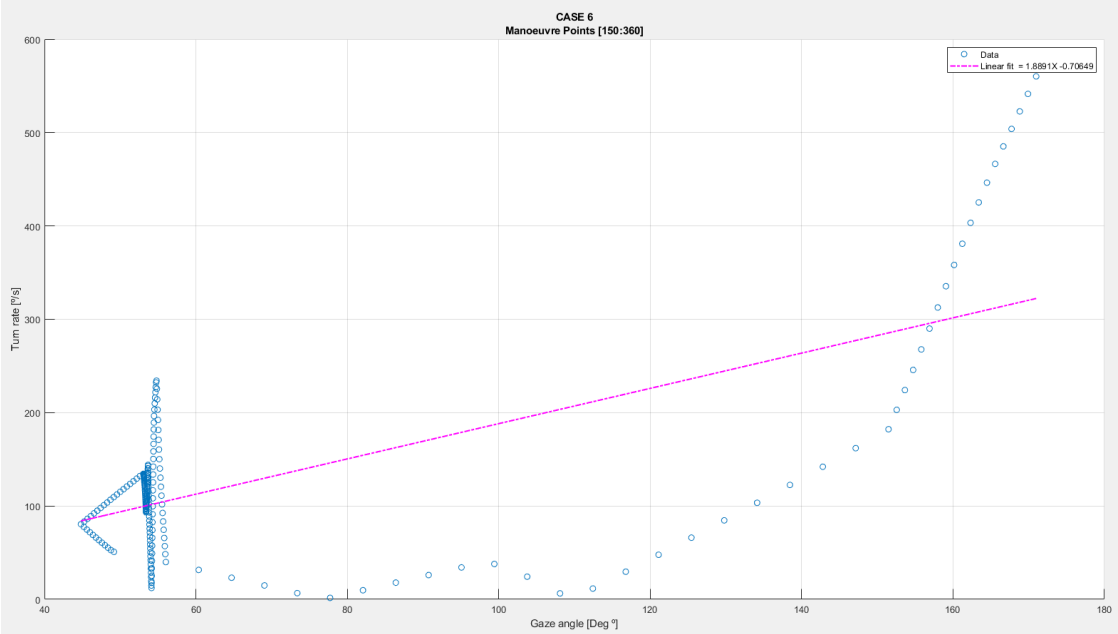

Figure 161Case 6 [150 360] Linear Regression

CASE 11

190 359

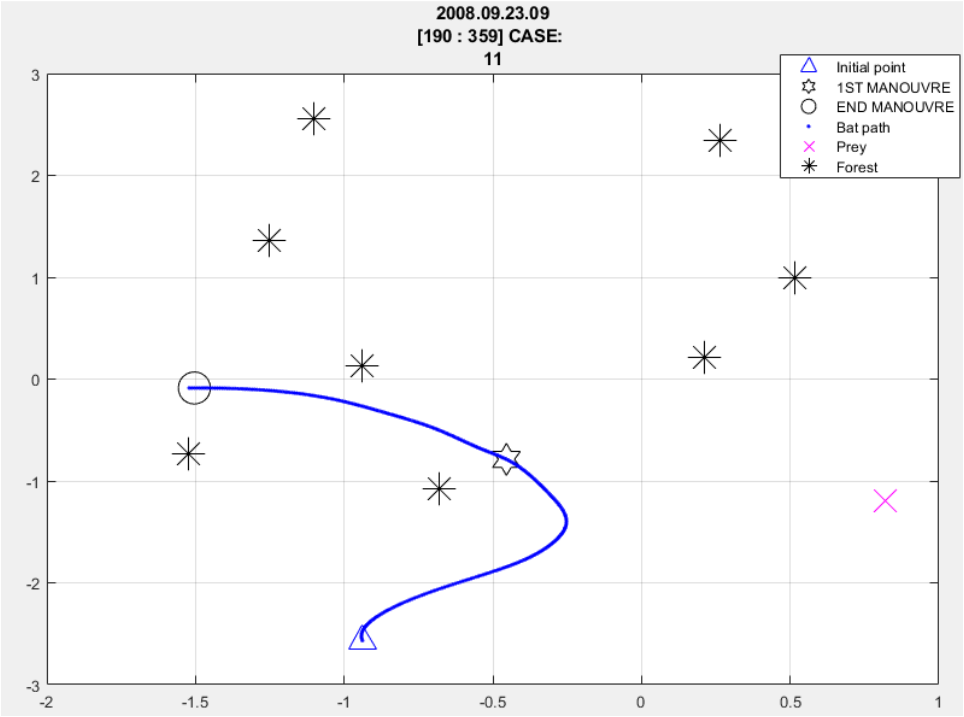

Figure 162 Case 11 [190 359] Flight path

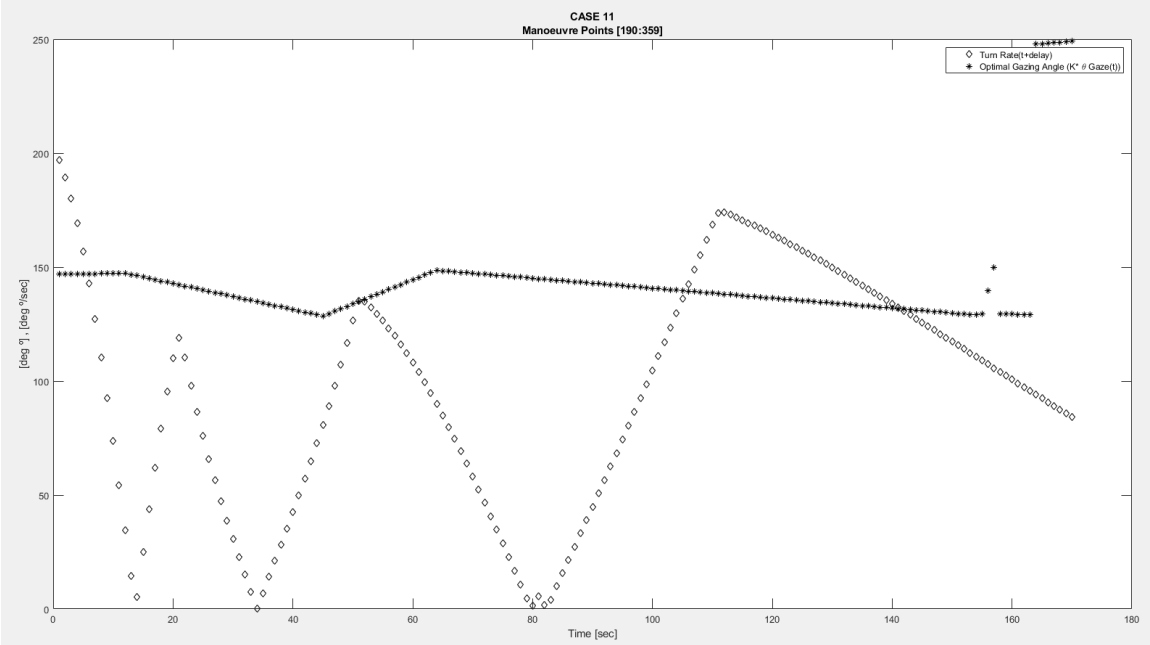

Figure 163 Case 11 [190 359] Turn Rate and Gazing Angle Comparison

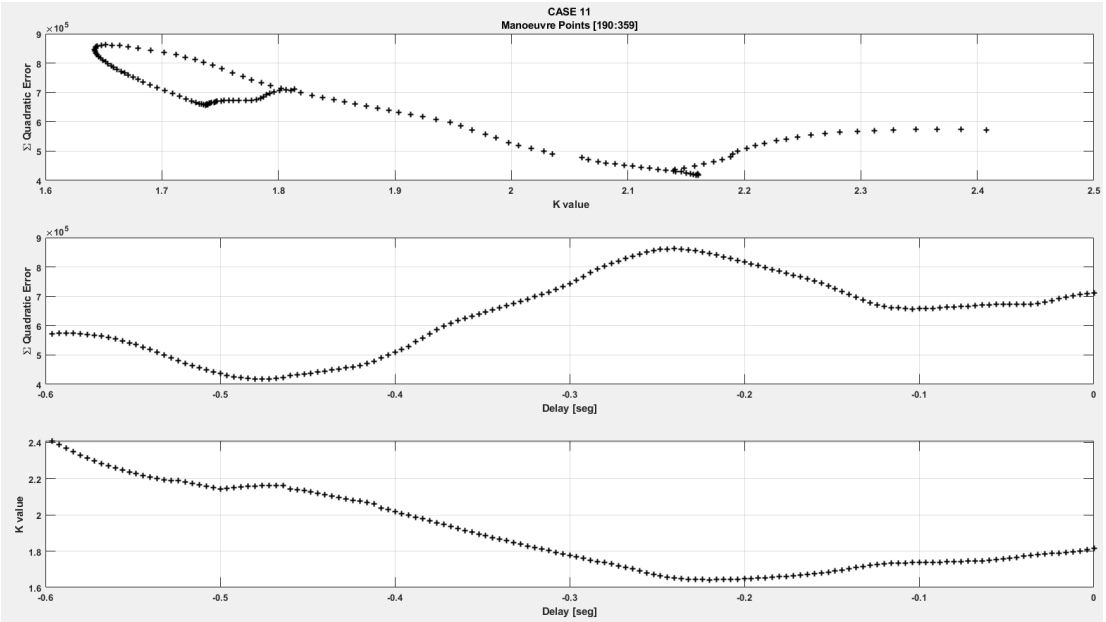

Figure 164 Case 11 [190 359] Quadratic Error, Delay and K values

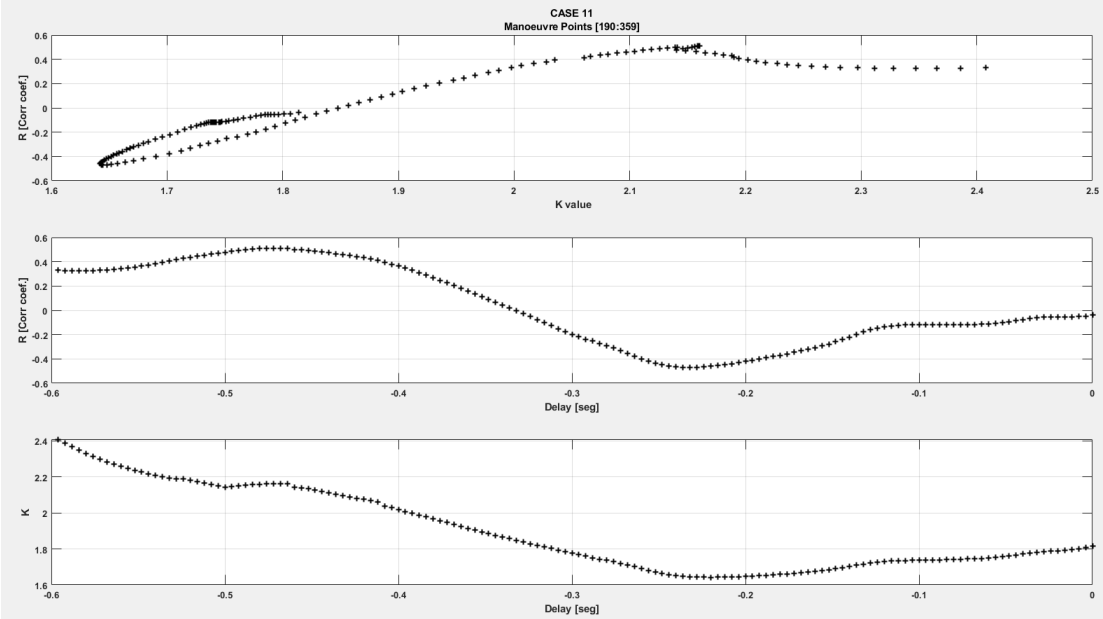

Figure 165 Case 11 [190 359] R, Delay and K values

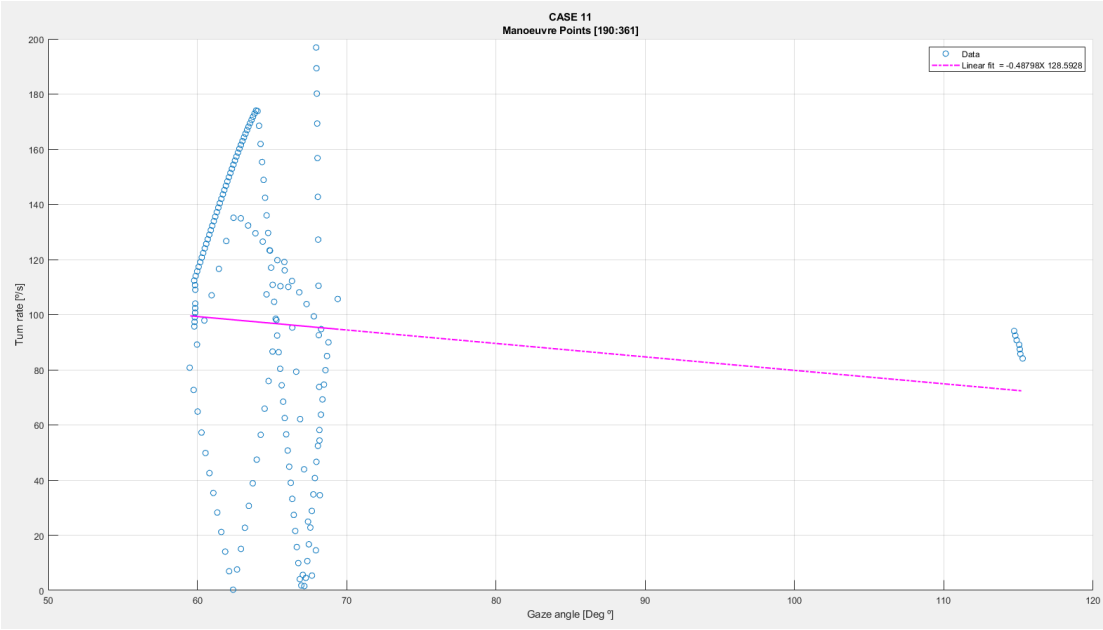

Figure 166 Case 11 [190 359] Linear Regression

50 170

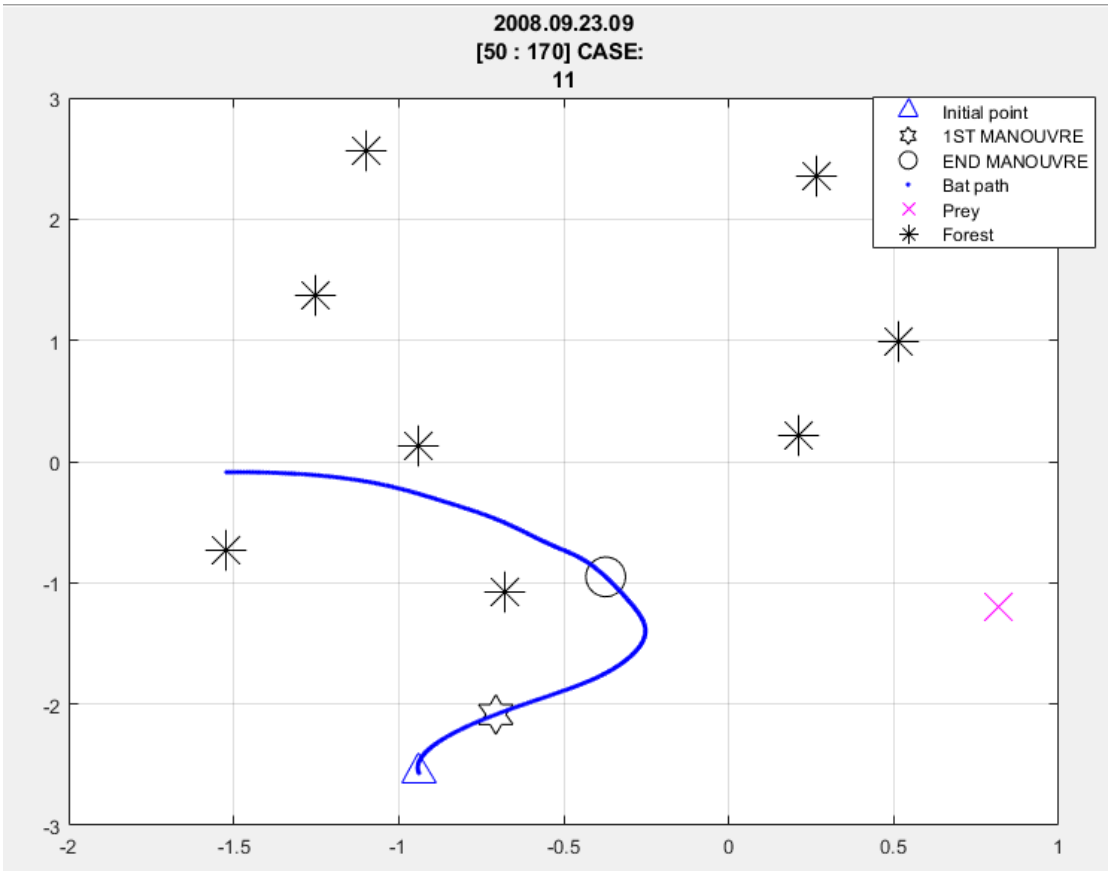

Figure 167Case 11 [50 70] Flight Path

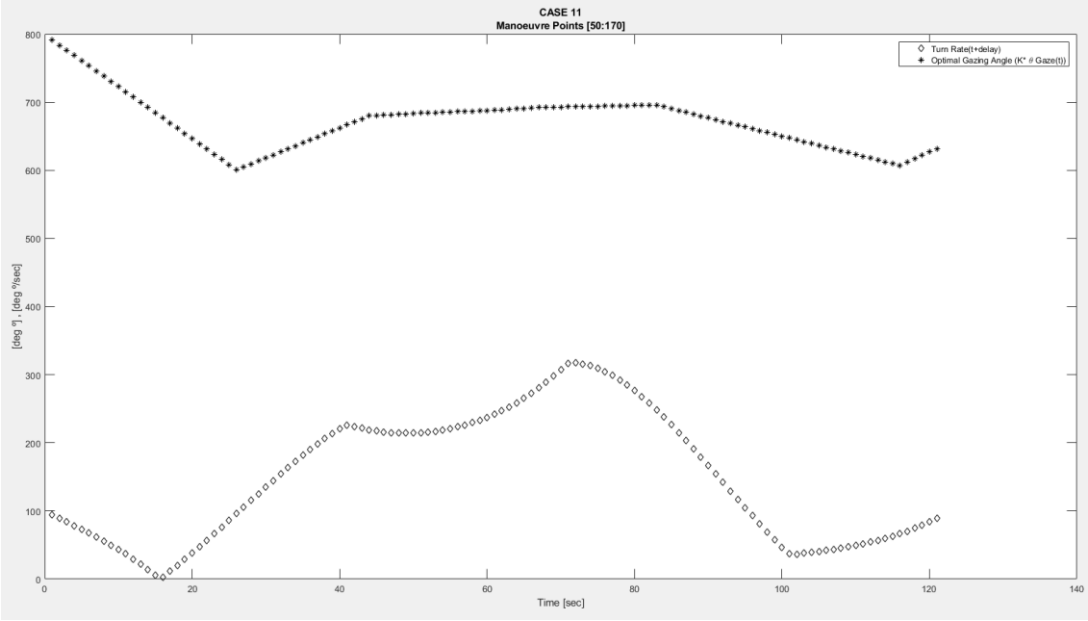

Figure 168Case 11 [50 70] Turn Rate and Gazing Angle Comparison

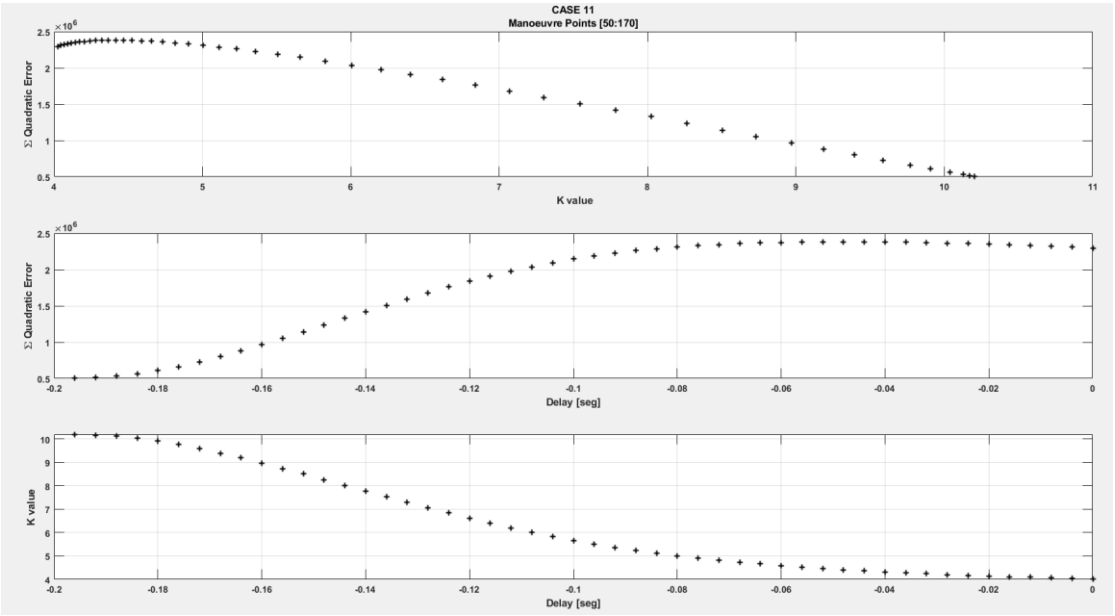

Figure 169Case 11 [50 70] Quadratic Error, Delay and K values

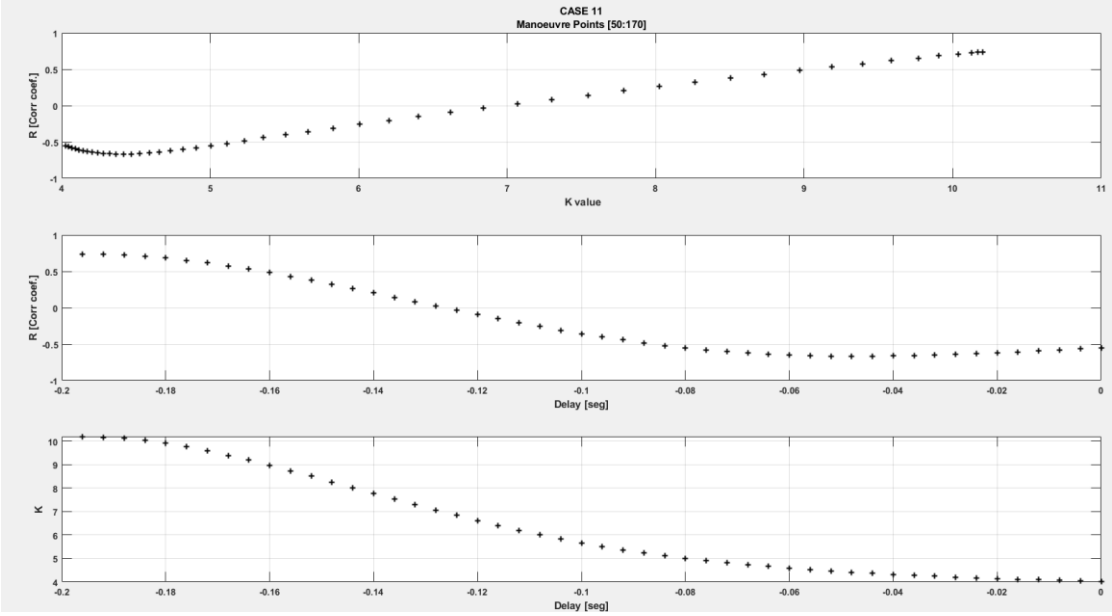

Figure 170 Case 11 [50 70] R, Delay and K values

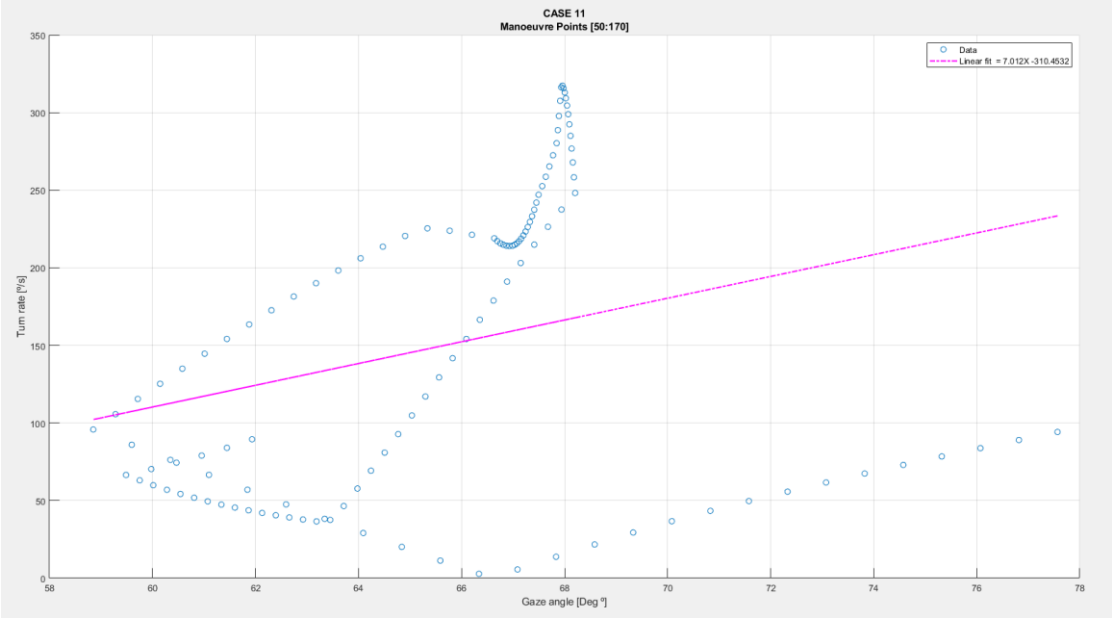

Figure 171Case 11 [50 70] Linear Regression

CASE 13

240 330

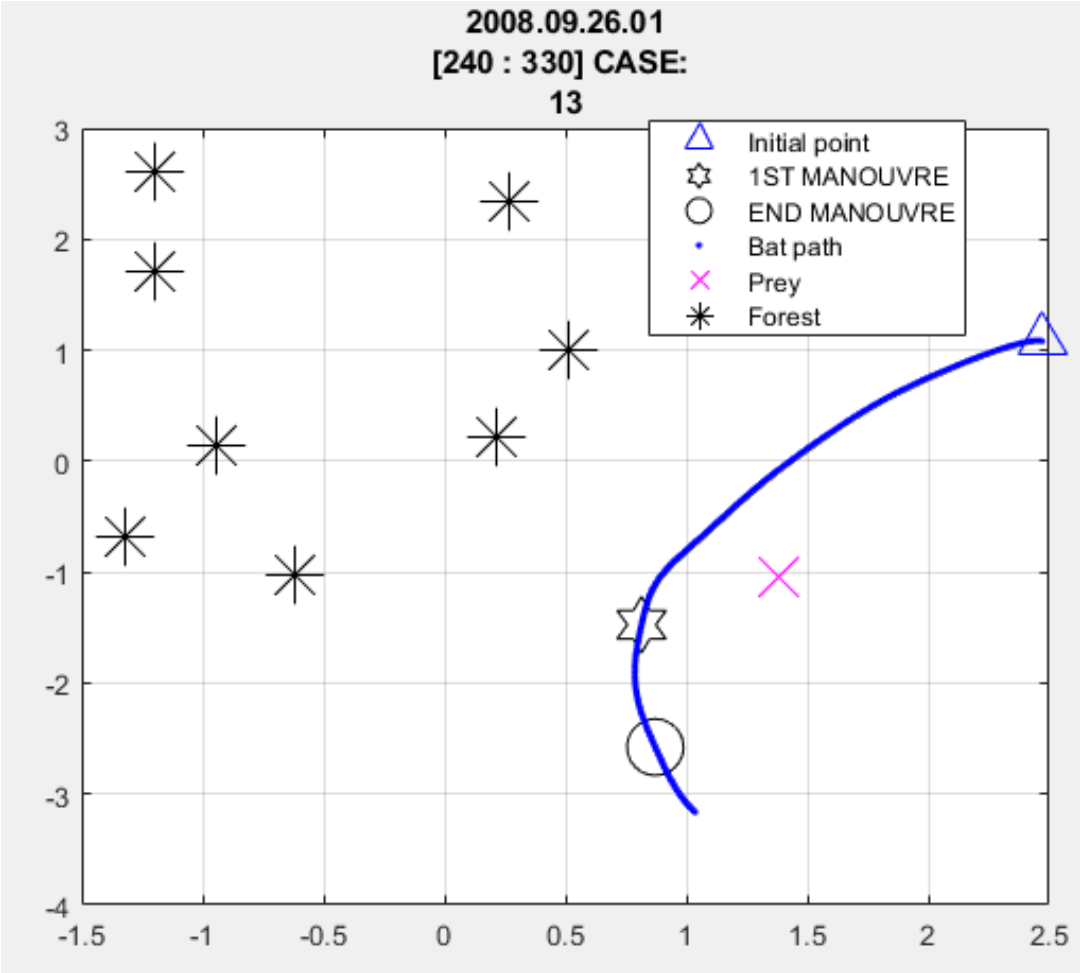

Figure 172Case 13 [240 330] Flight Path

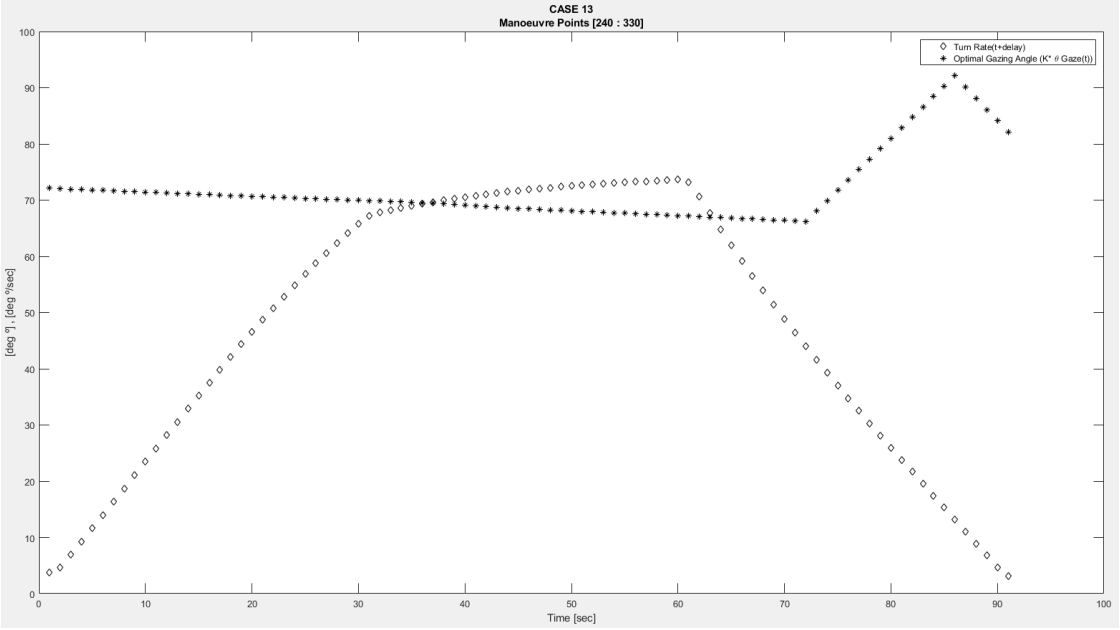

Figure 173Case 13 [240 330] Turn Rate Vs Gazing Angle

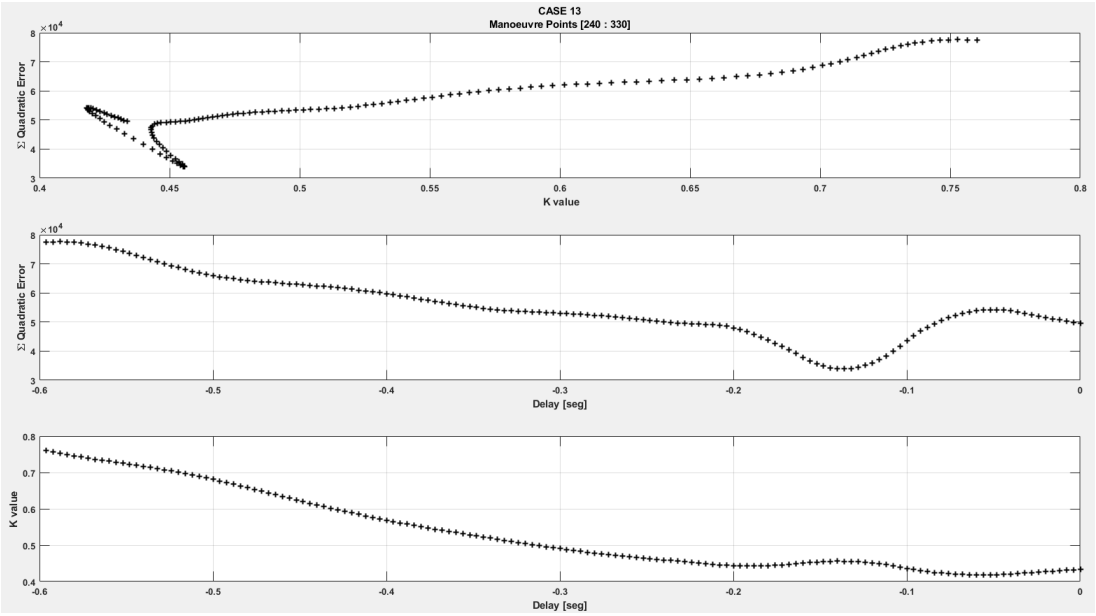

Figure 174Case 13 [240 330] Quadratic Error, Delay and K values

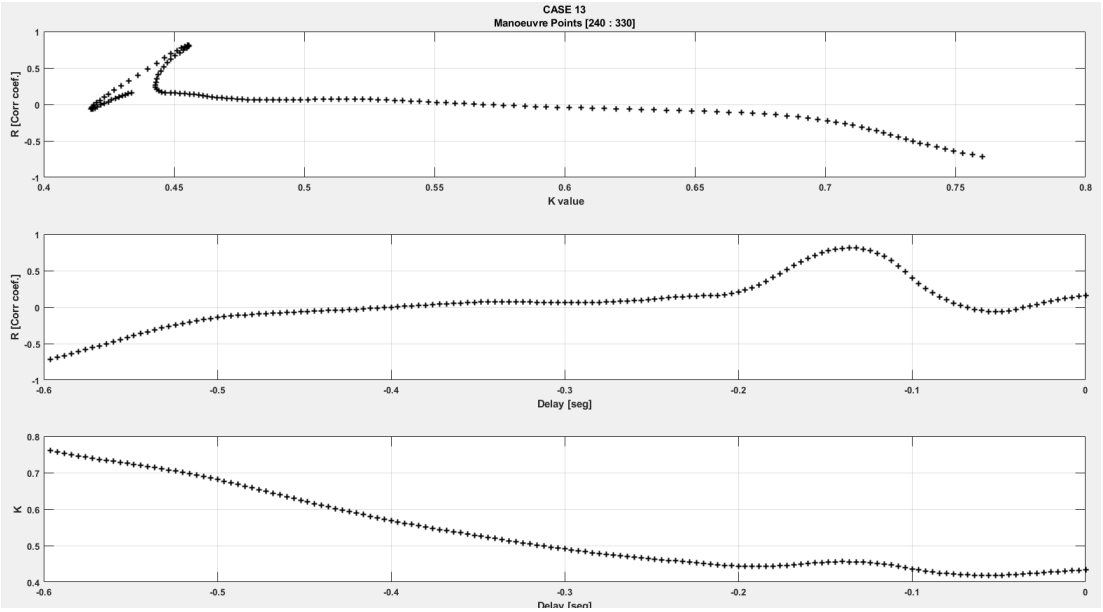

Figure 175Case 13 [240 330] R, Delay and K values

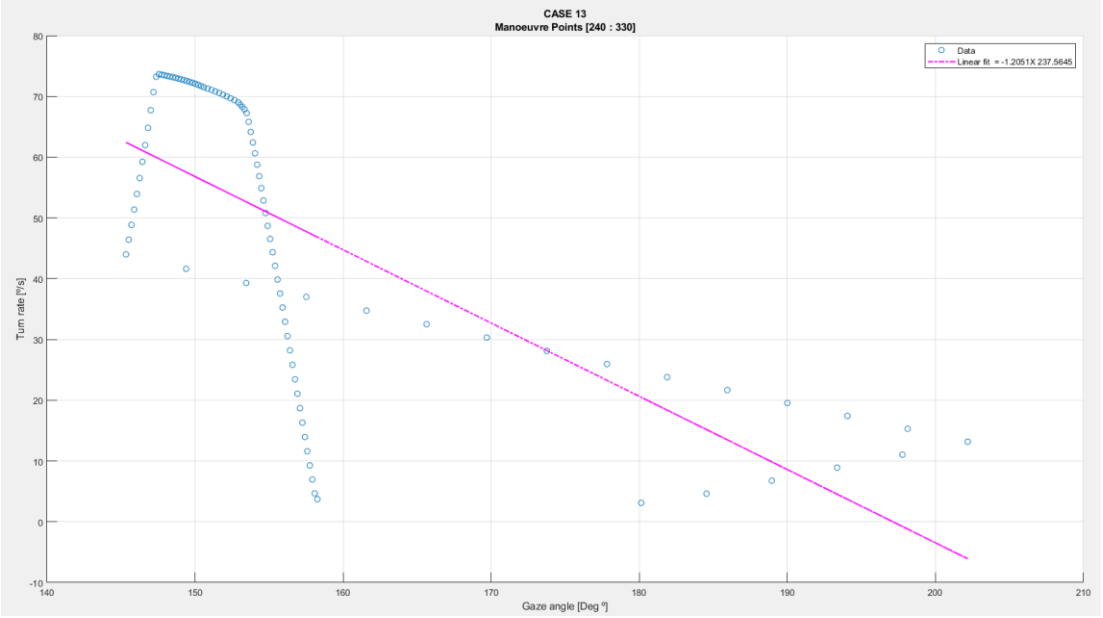

Figure 176Case 13 [240 330] Linear Regression

200 378

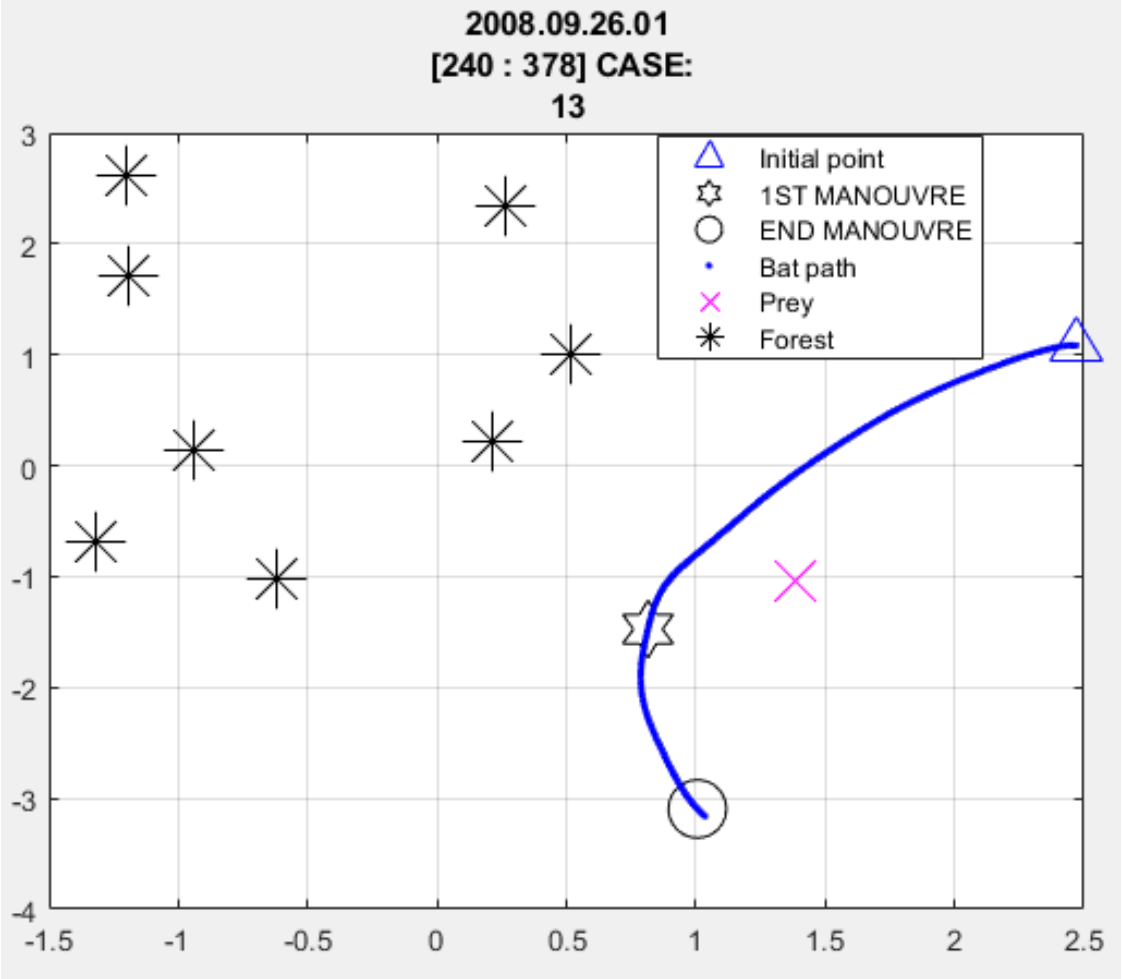

Figure 177Case 13 [240 378] Flight Path

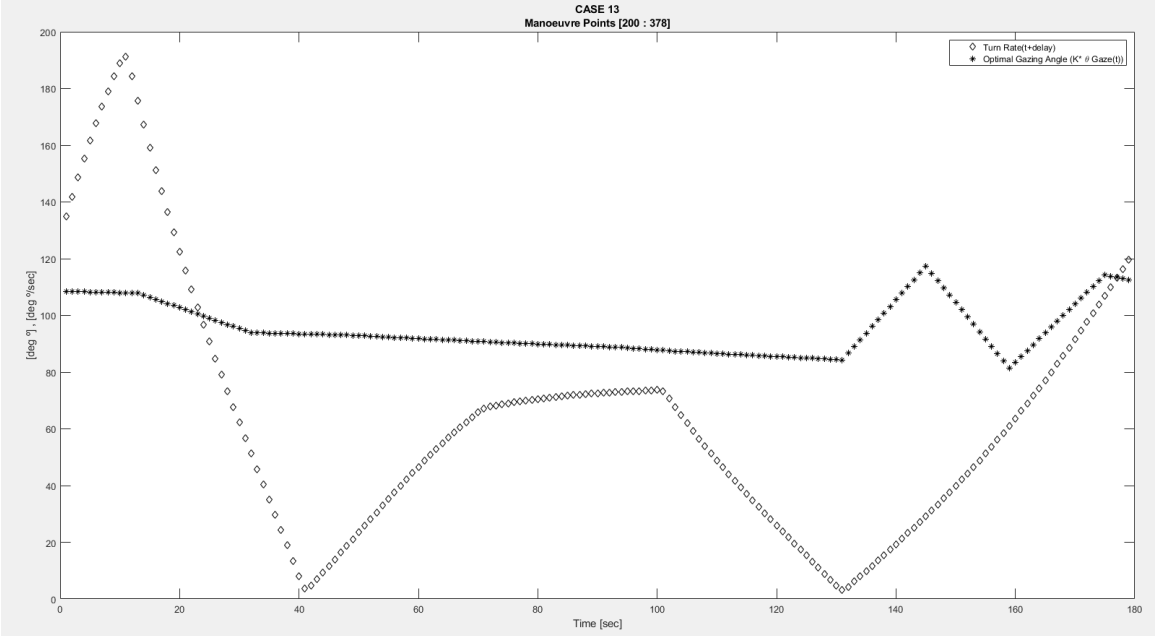

Figure 178Case 13 [240 378] Turn Rate vs Gazing Angle

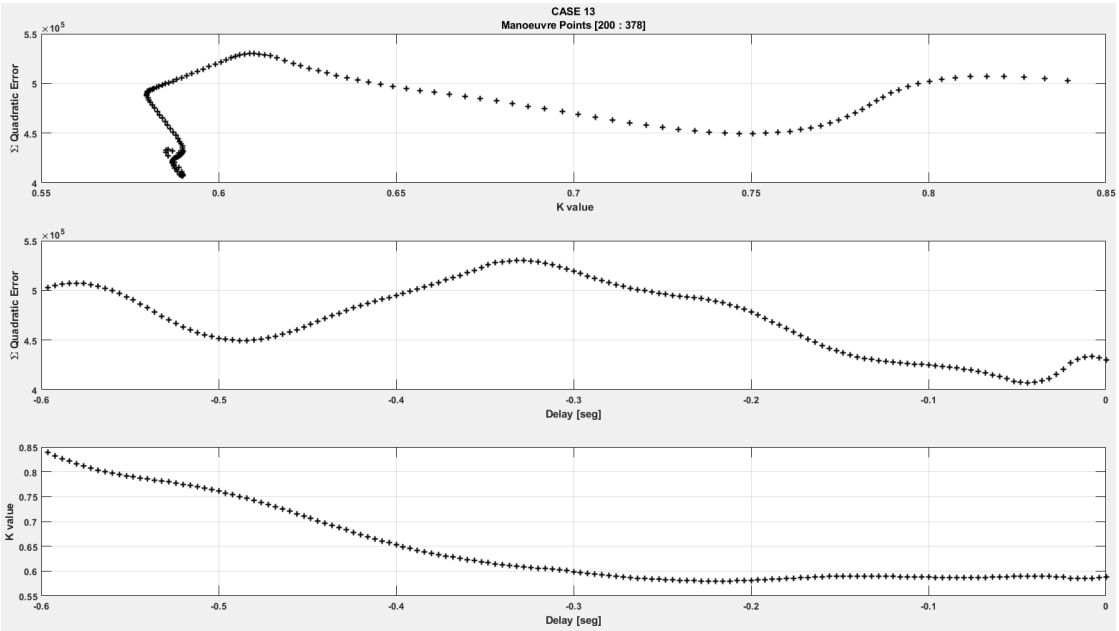

Figure 179Case 13 [240 378] Quadratic Error, Delay and K values

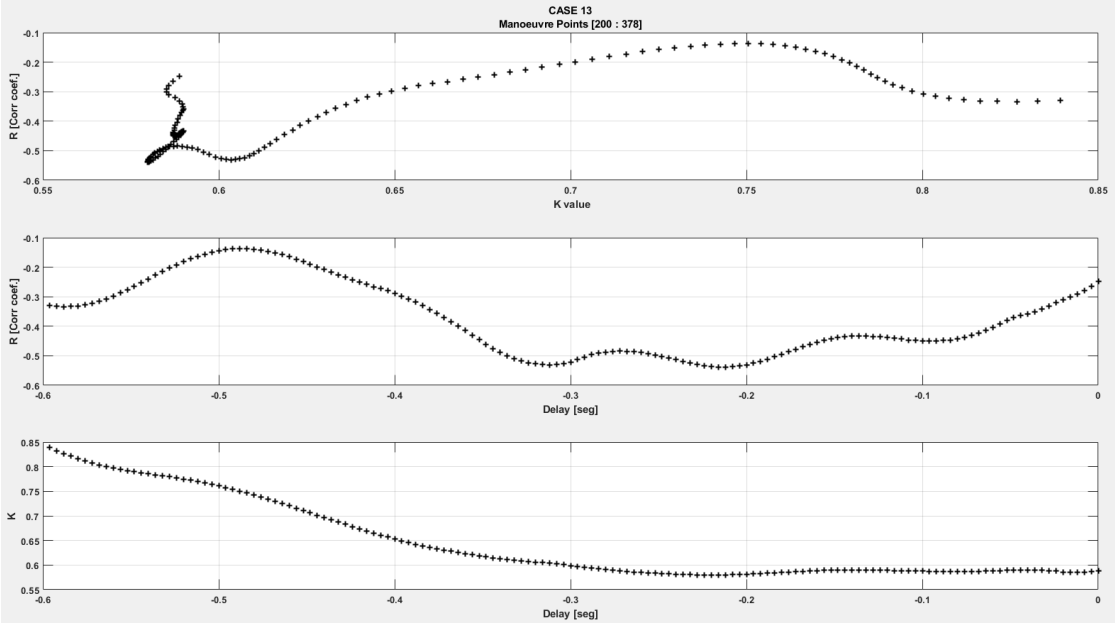

Figure 180Case 13 [240 378] R, Delay, and k values

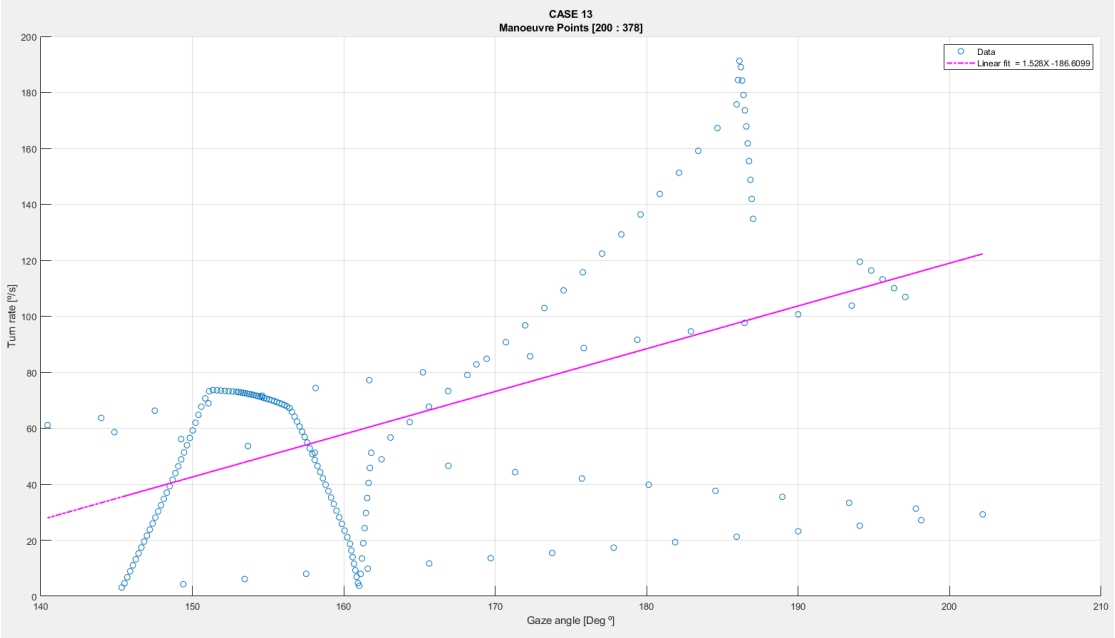

Figure 181Case 13 [240 378] Linear Regression

100 378

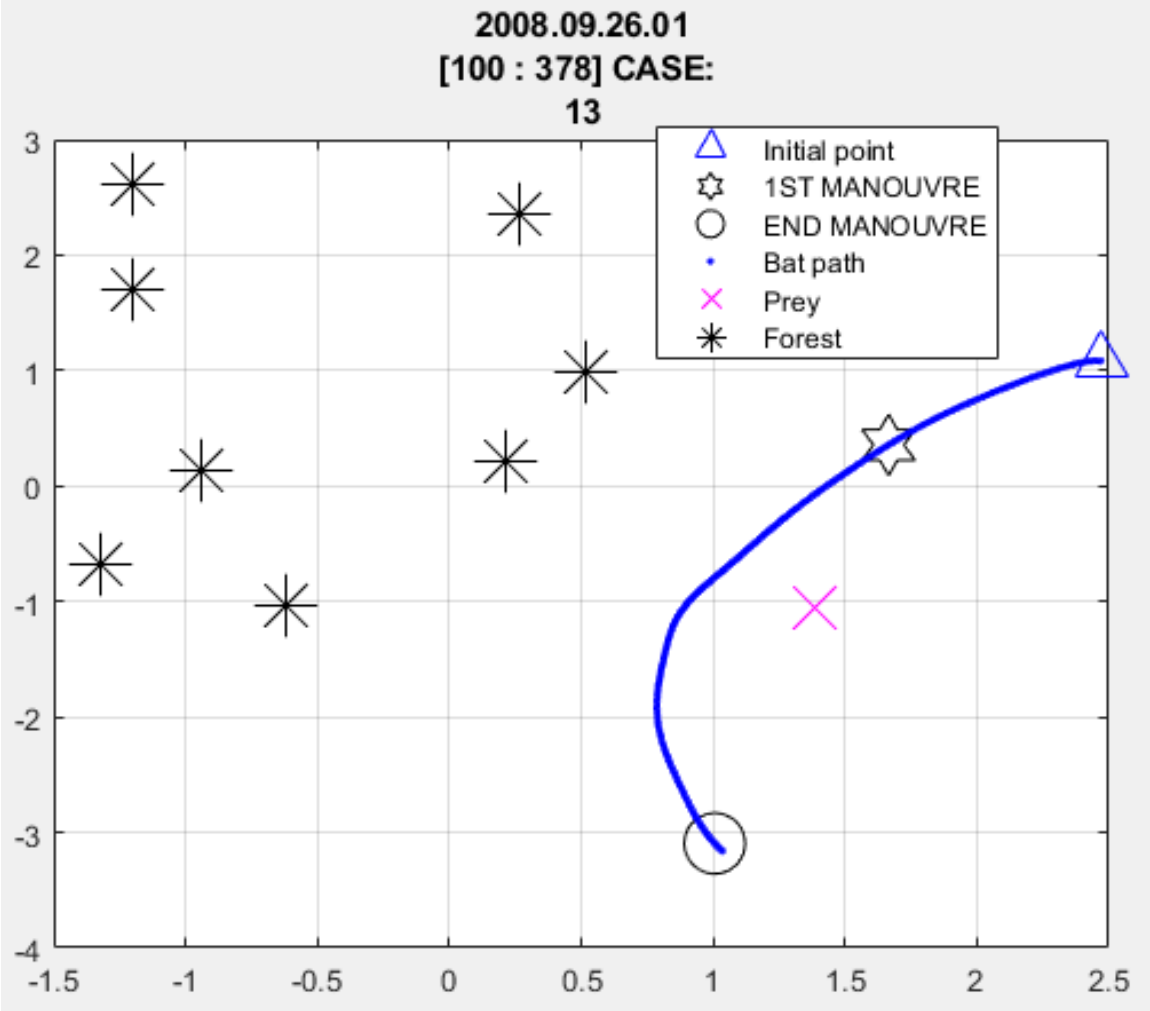

Figure 182Case 13 [100 378] Flight Path

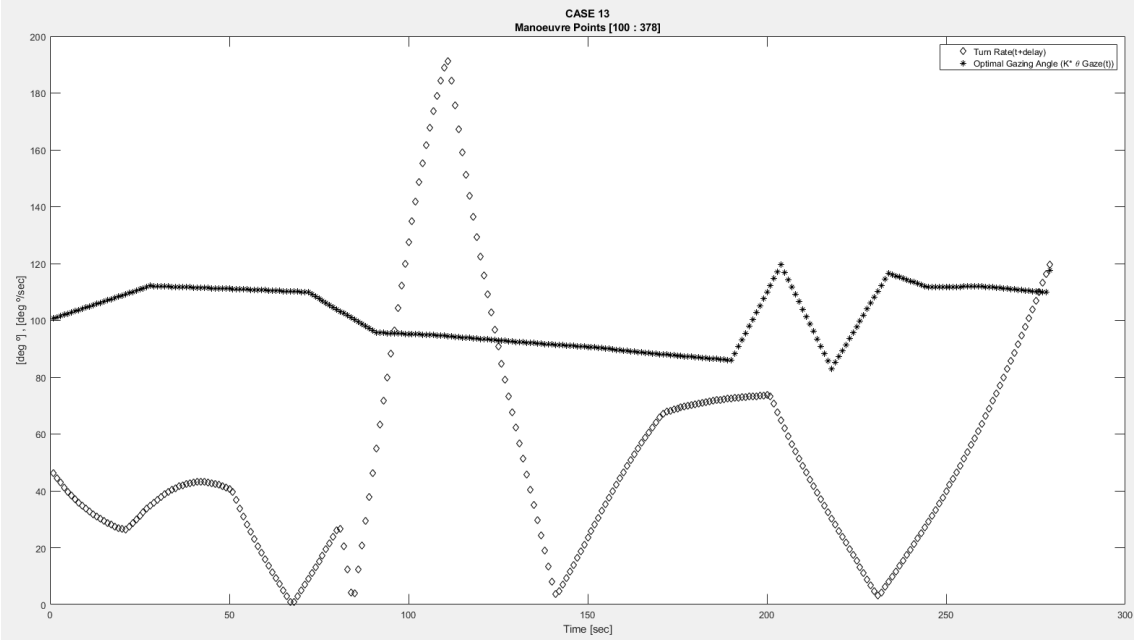

Figure 183Case 13 [100 378] Turn Rate vs Gazing Angle

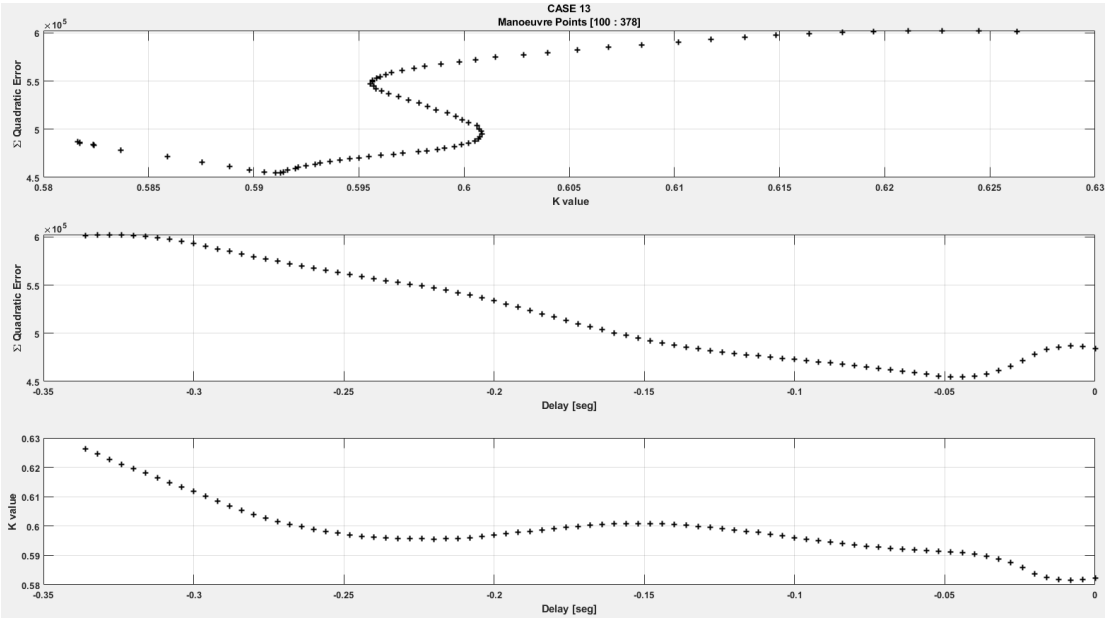

Figure 184Case 13 [100 378] Quadratic Error, Delay, and k values

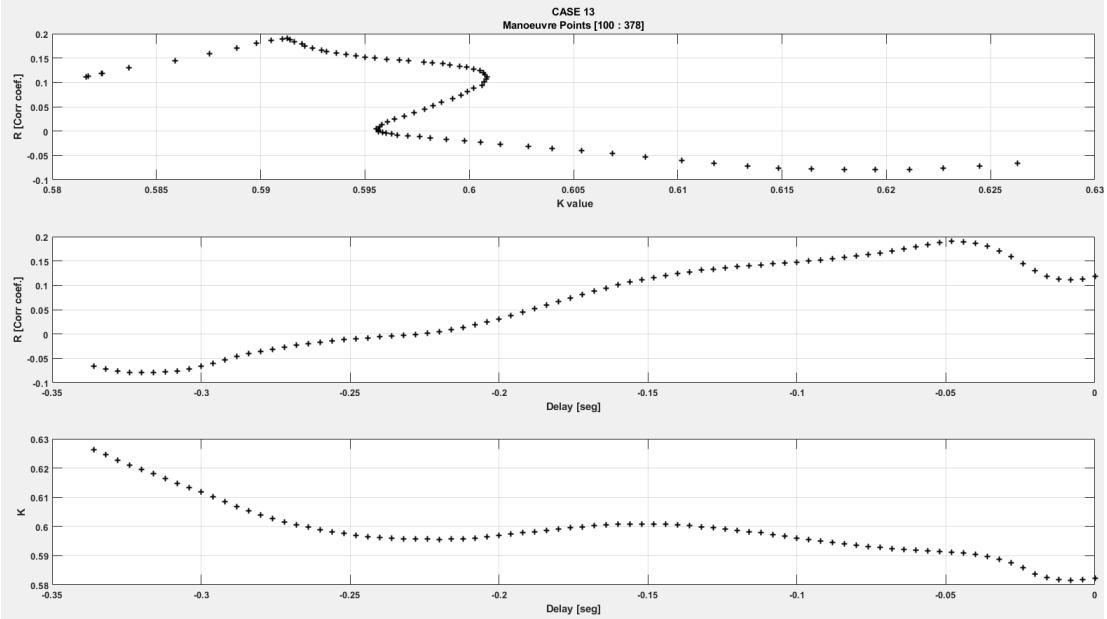

Figure 185Case 13 [100 378] R, Delay and K values

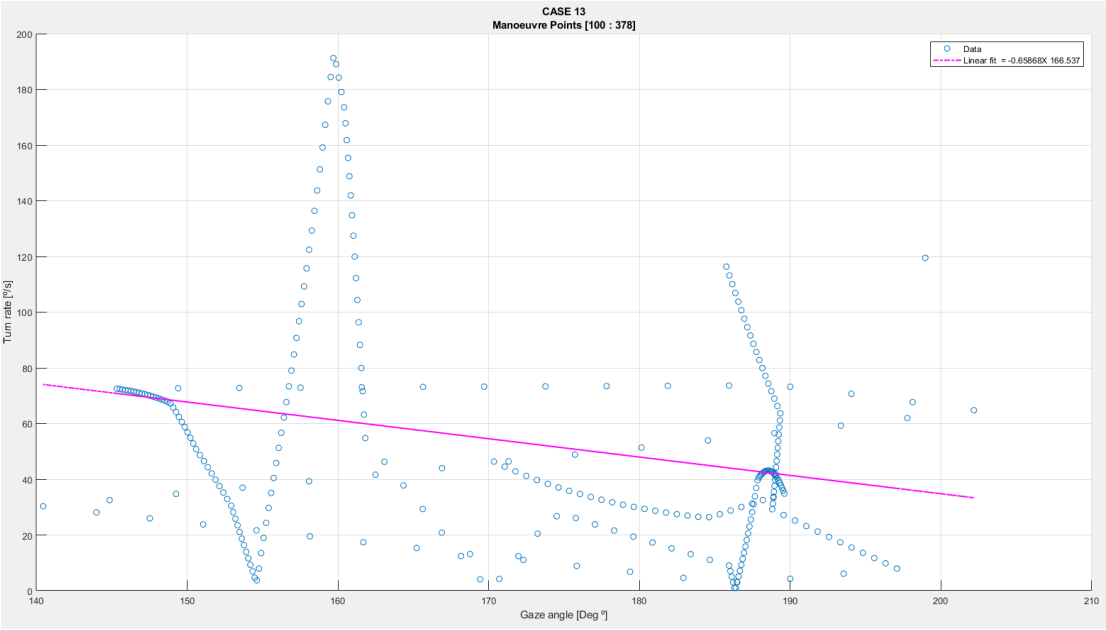

Figure 186Case 13 [100 378] Linear Regression

Case 20

30 90

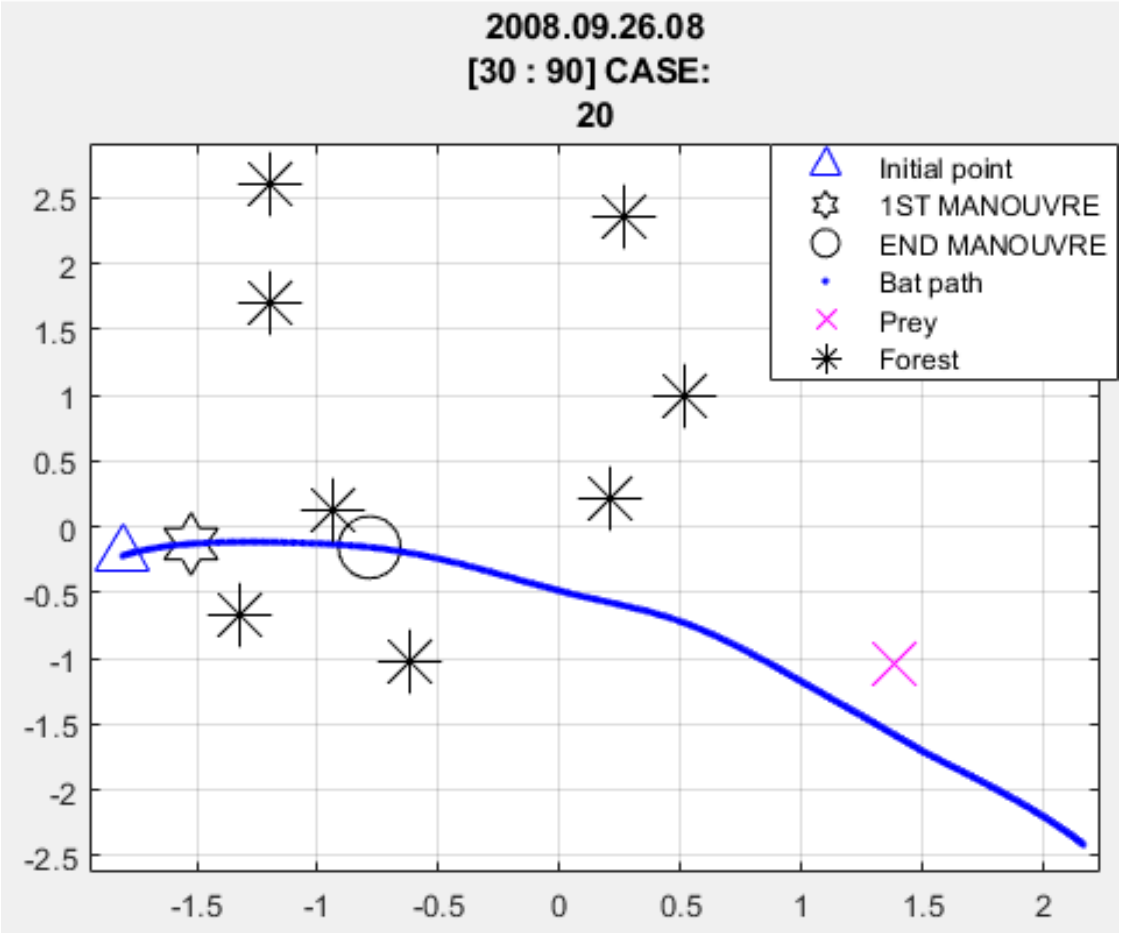

Figure 187Case 20 [90 90] Flight Path

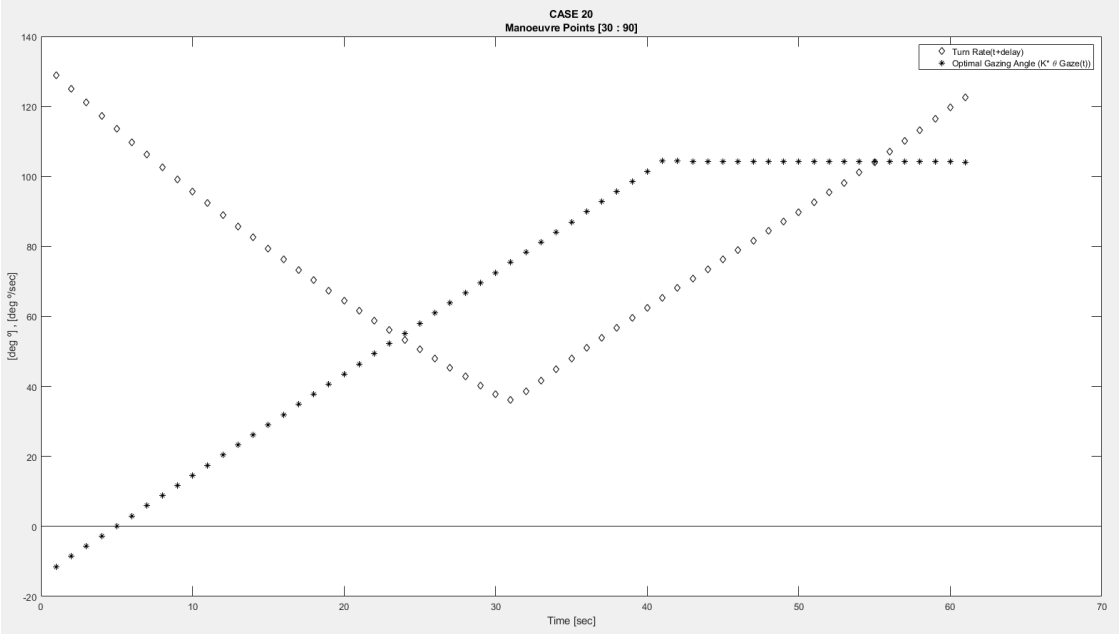

Figure 188Case 20 [90 90] Turn Rate VS Gazing Angle

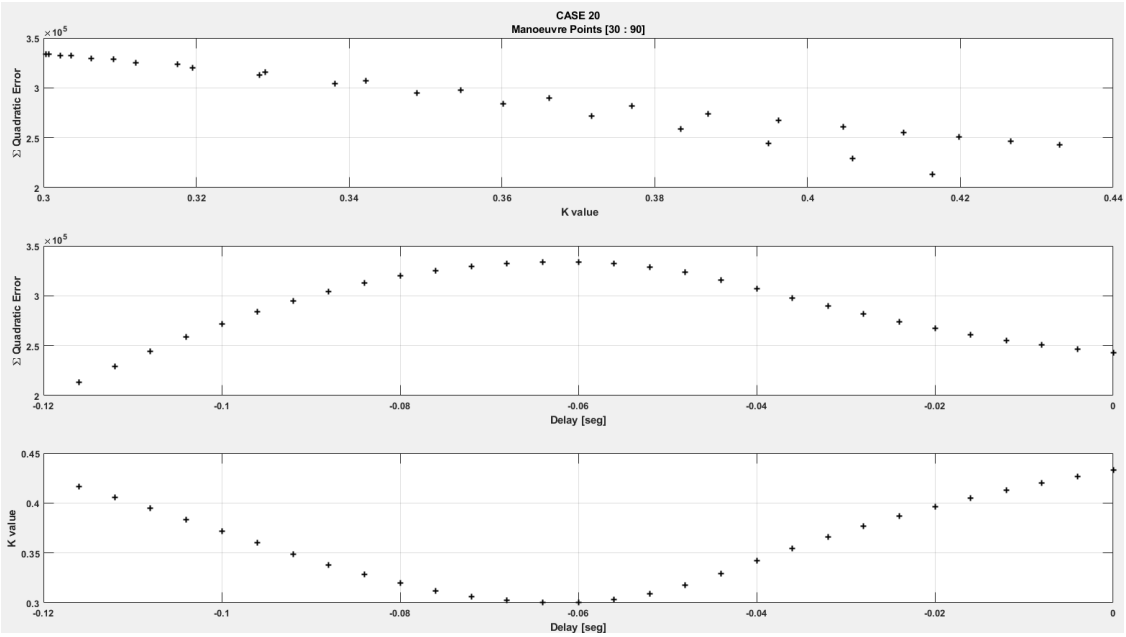

Figure 189Case 20 [90 90] Quadratic Error, Delay and K values

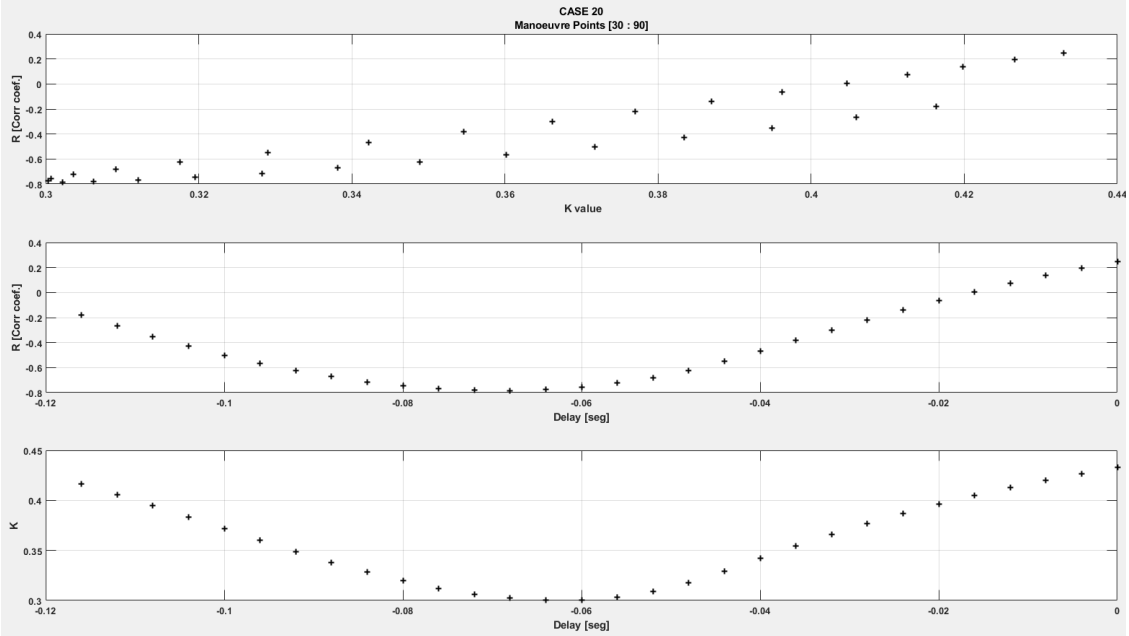

Figure 190Case 20 [90 90] R, Delay and K values

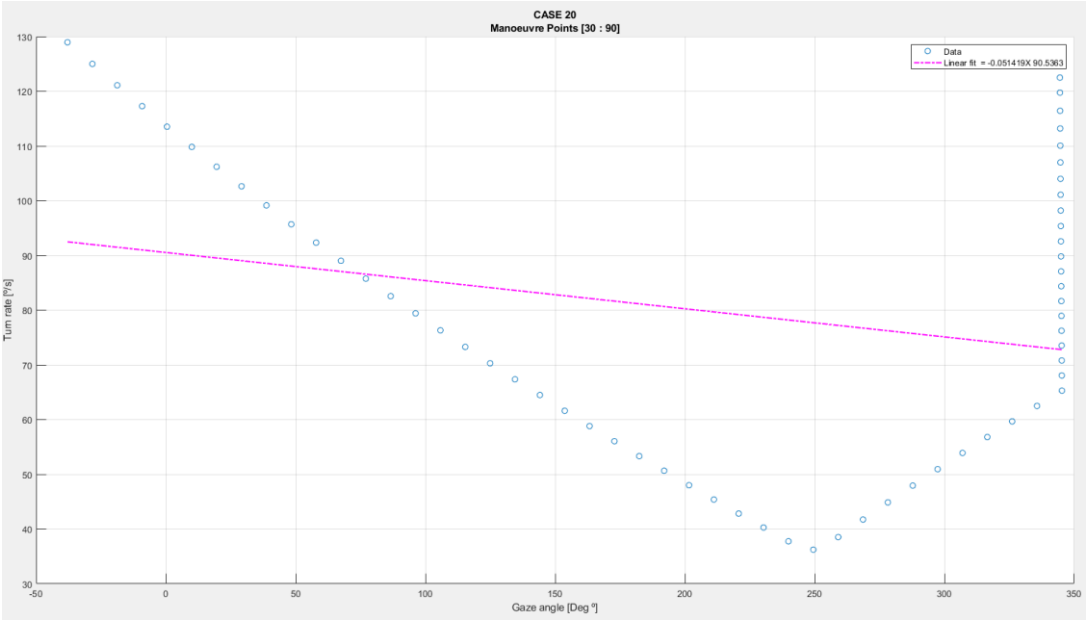

Figure 191Case 20 [90 90] Linear Regression

85 190

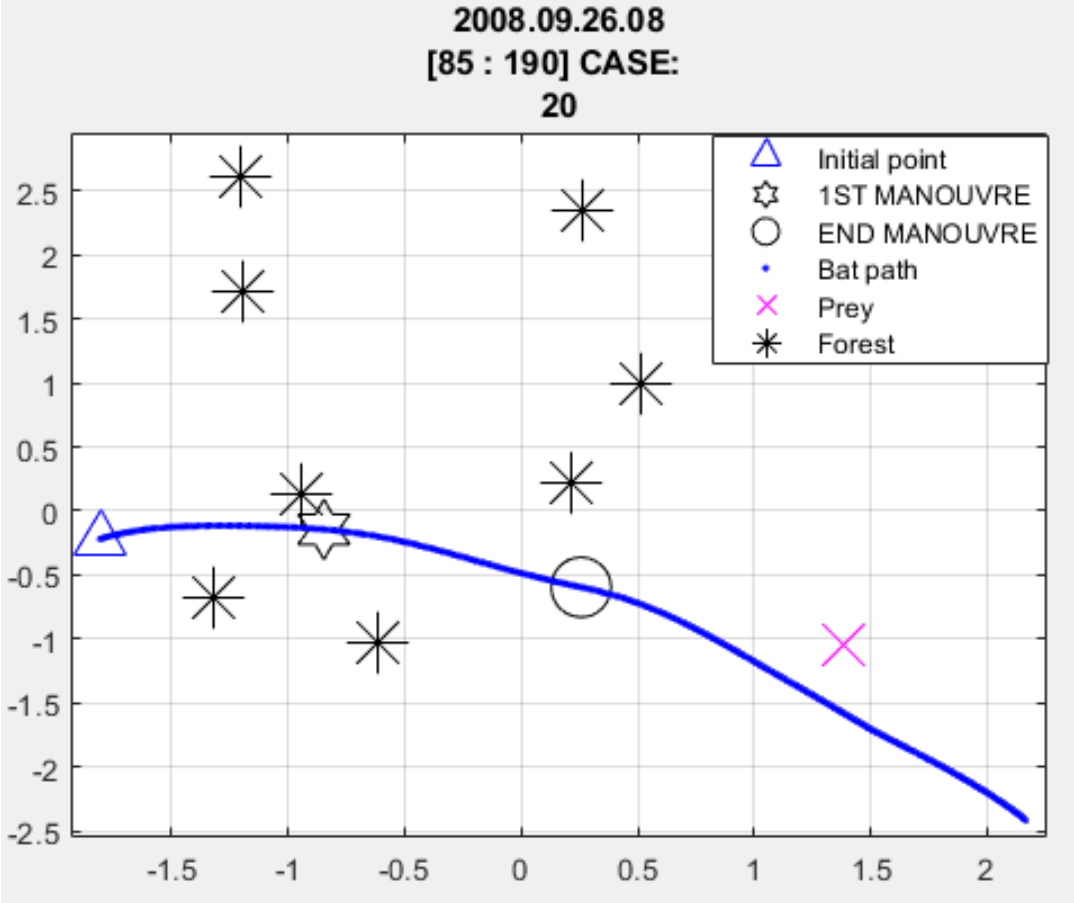

Figure 192Case 20 [85 190] Flight Path

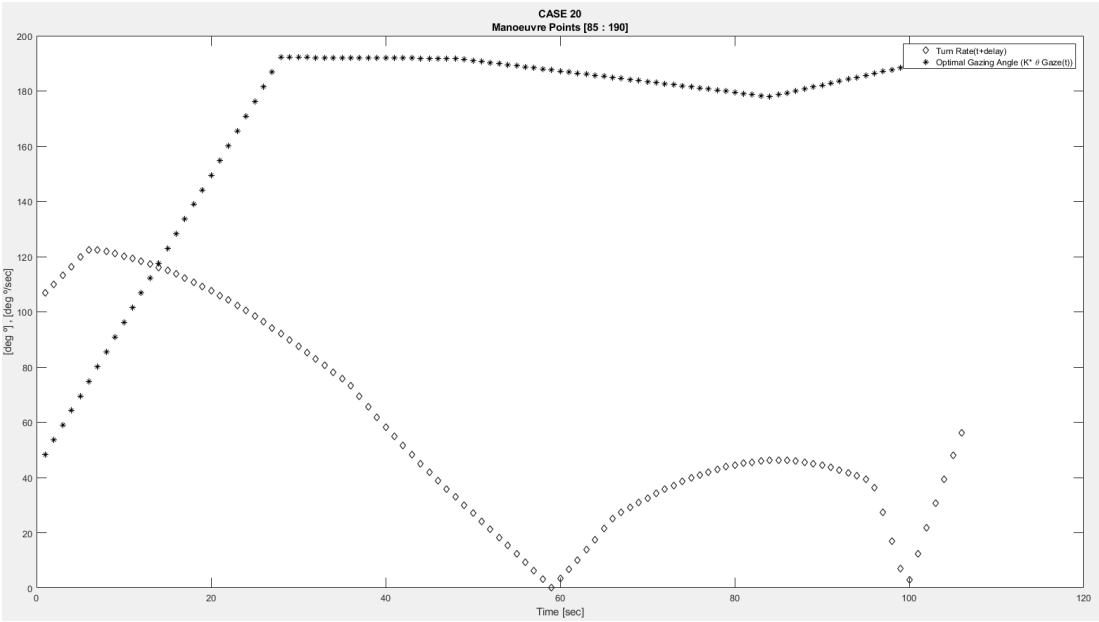

Figure 193Case 20 [85 190] Turn Rate Vs gazing Angle

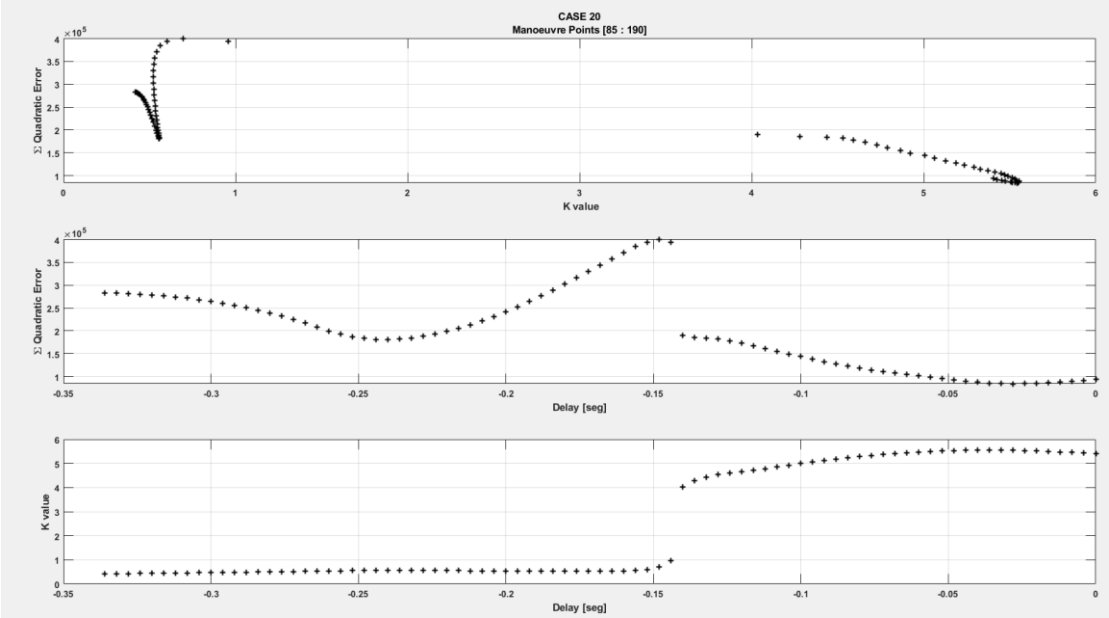

Figure 194Case 20 [85 190] Quadratic Error, Delay and K values

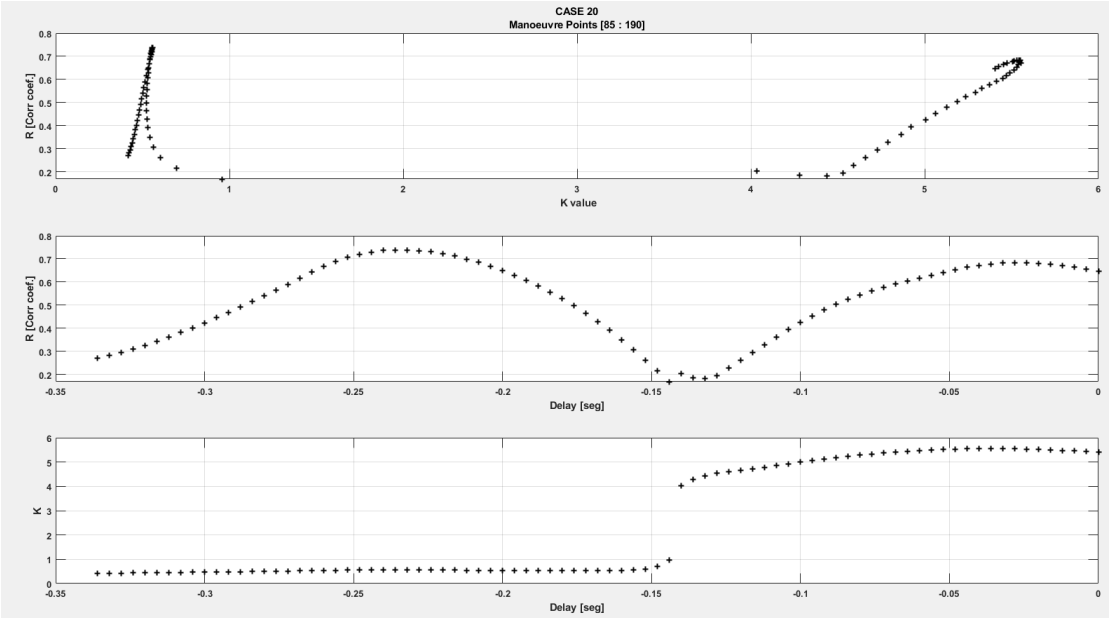

Figure 195Case 20 [85 190] R, Delay and K values

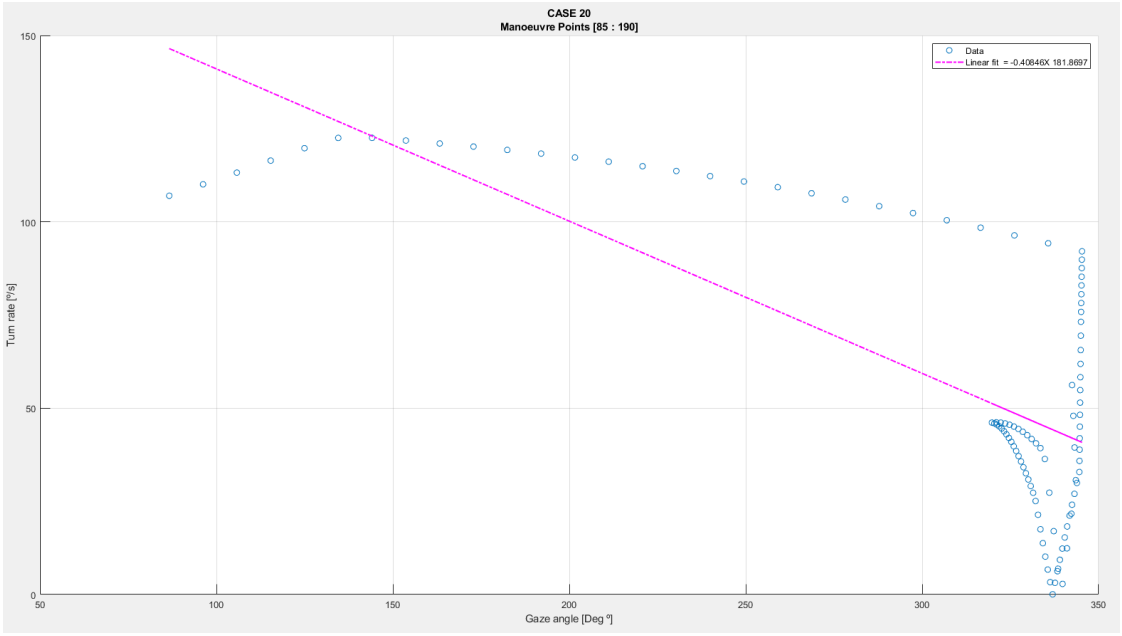

Figure 196Case 20 [85 190] Linear Regression

200 425

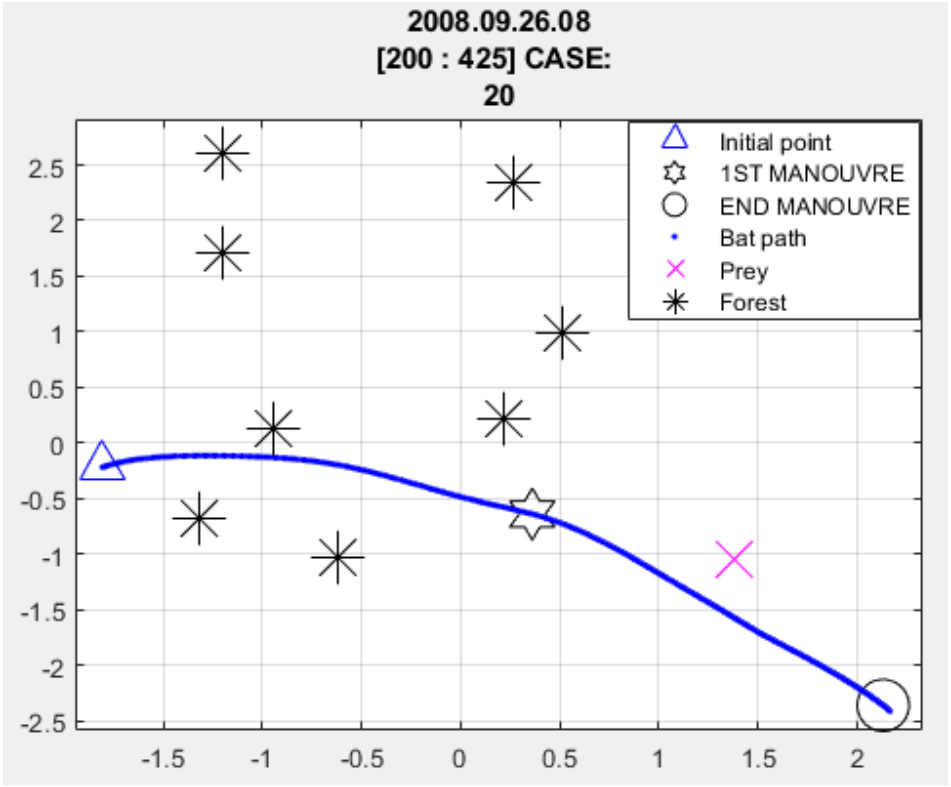

Figure 197Case 20 [200 425] Flight Path

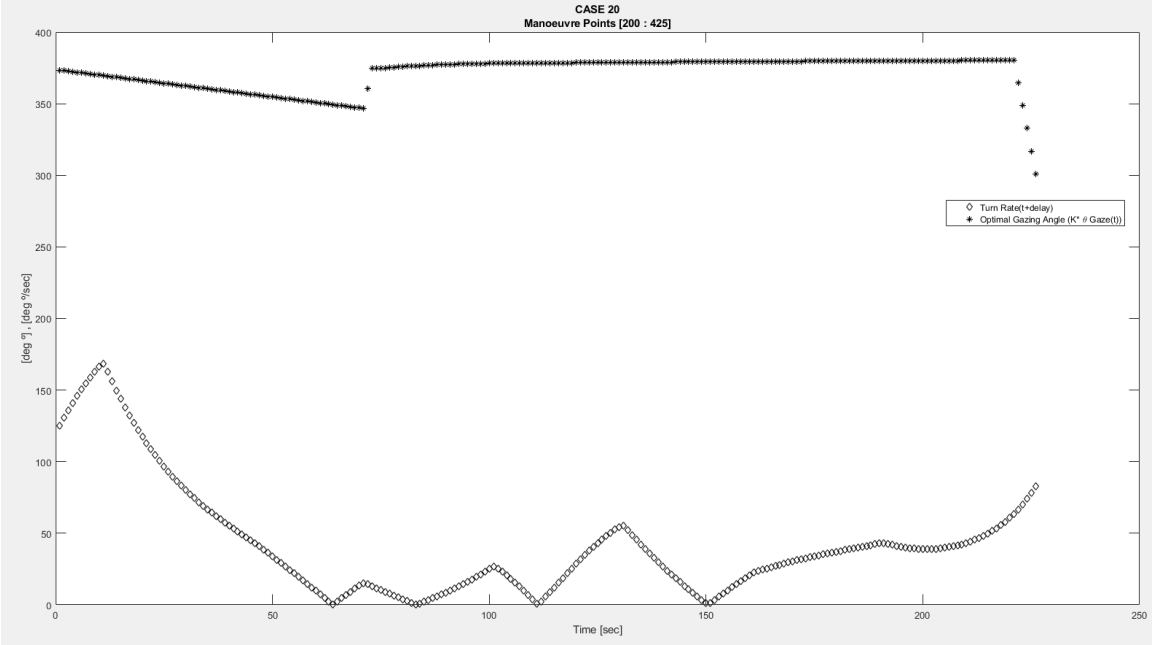

Figure 198Case 20 [200 425] Turn Rate Vs Gazing angle

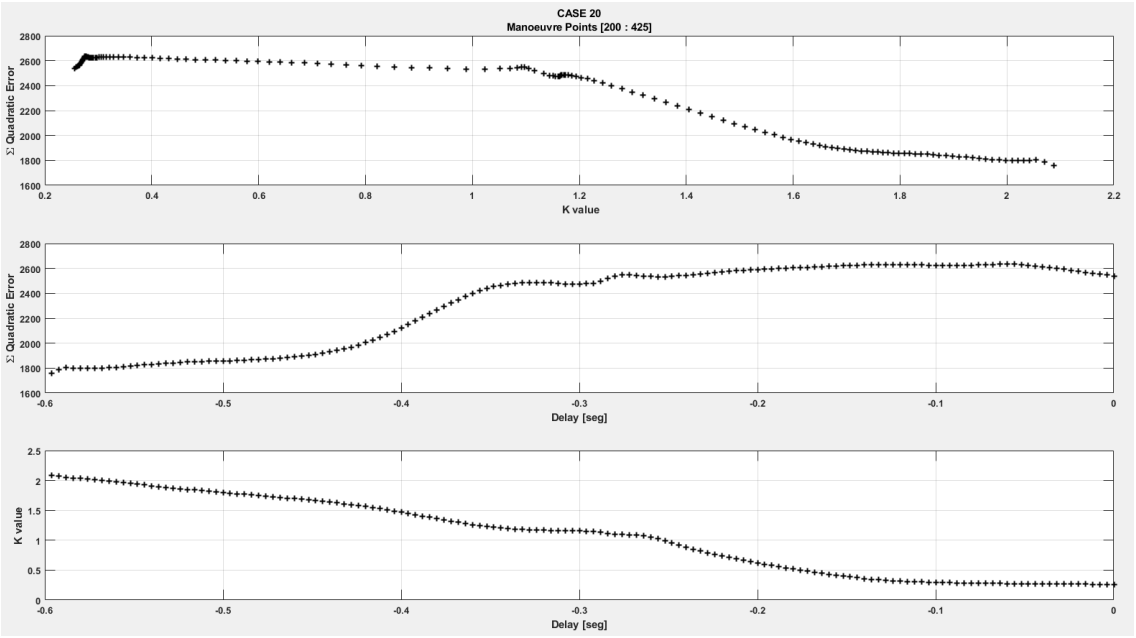

Figure 199Case 20 [200 425] Quadratic Error, Delay and K values

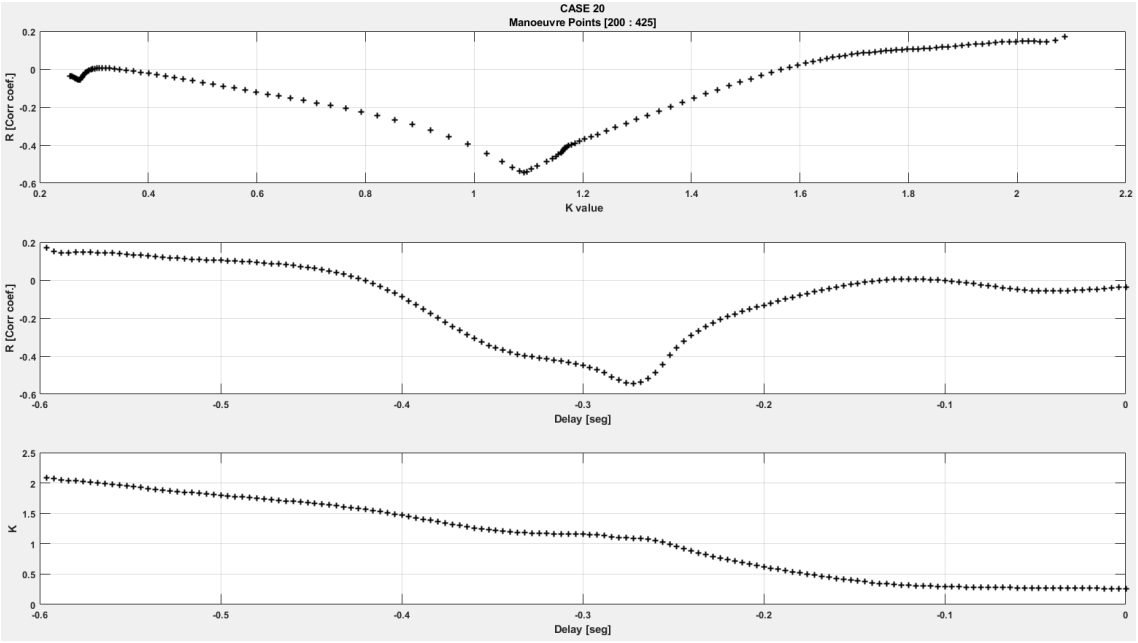

Figure 200Case 20 [200 425] R, Delay and K values

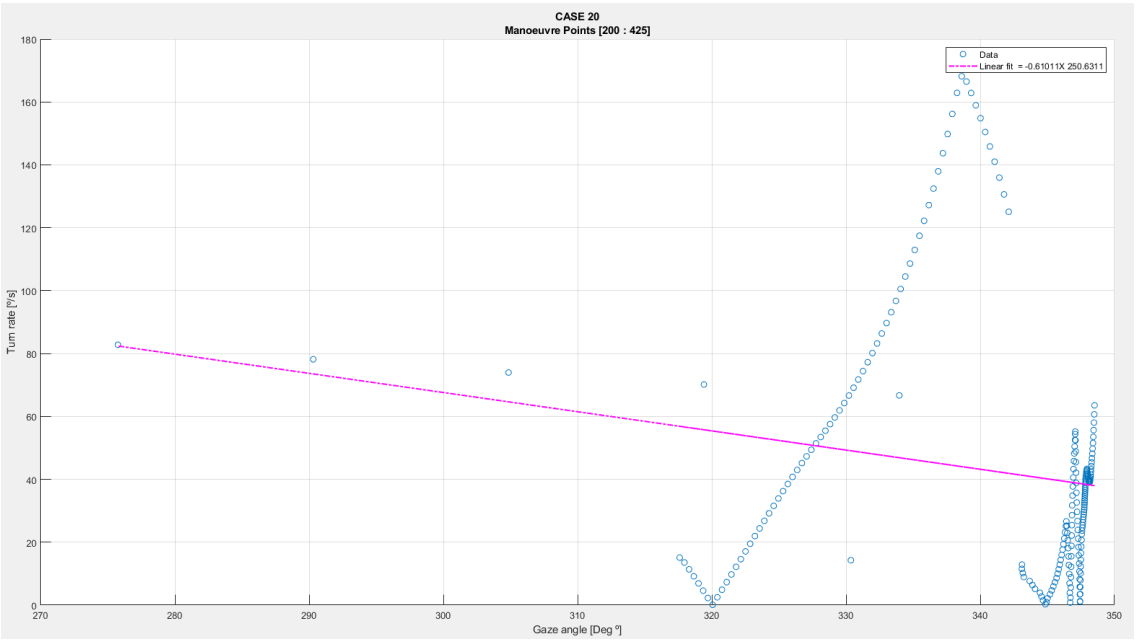

Figure 201Case 20 [200 425] Linear regression

350 425

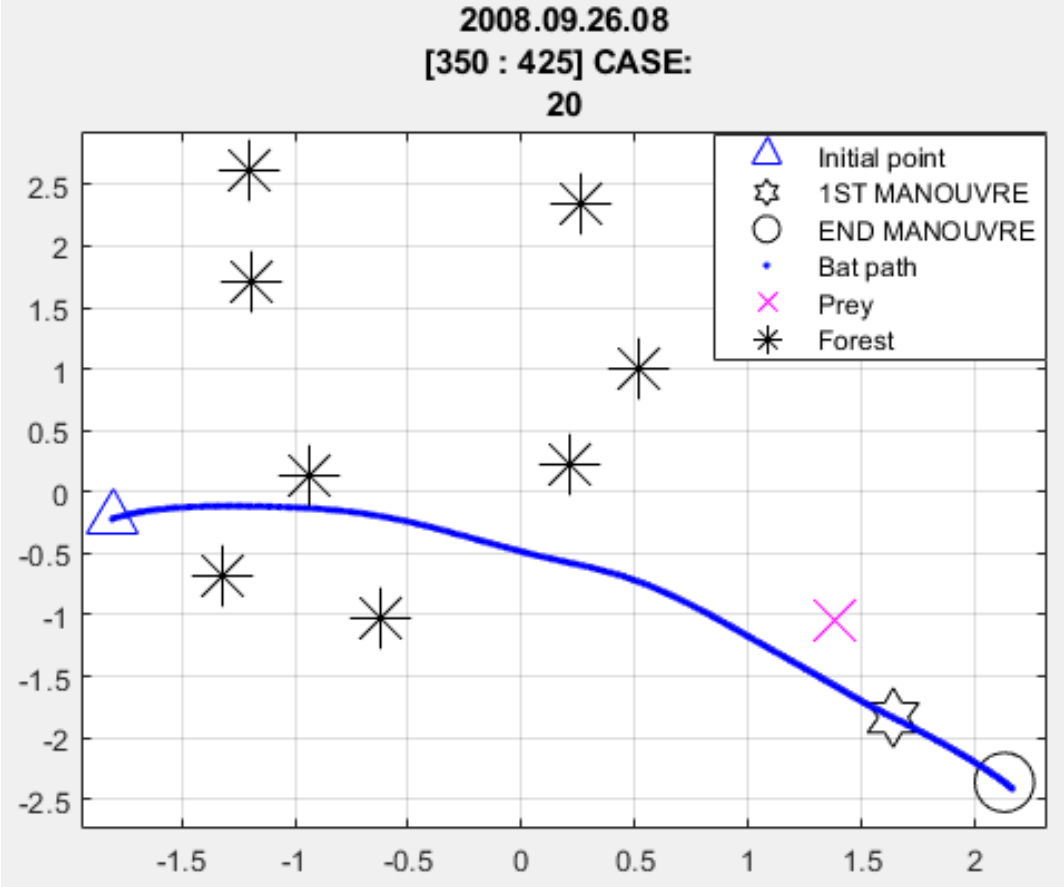

Figure 202Case 20 [350 425] Fligh path

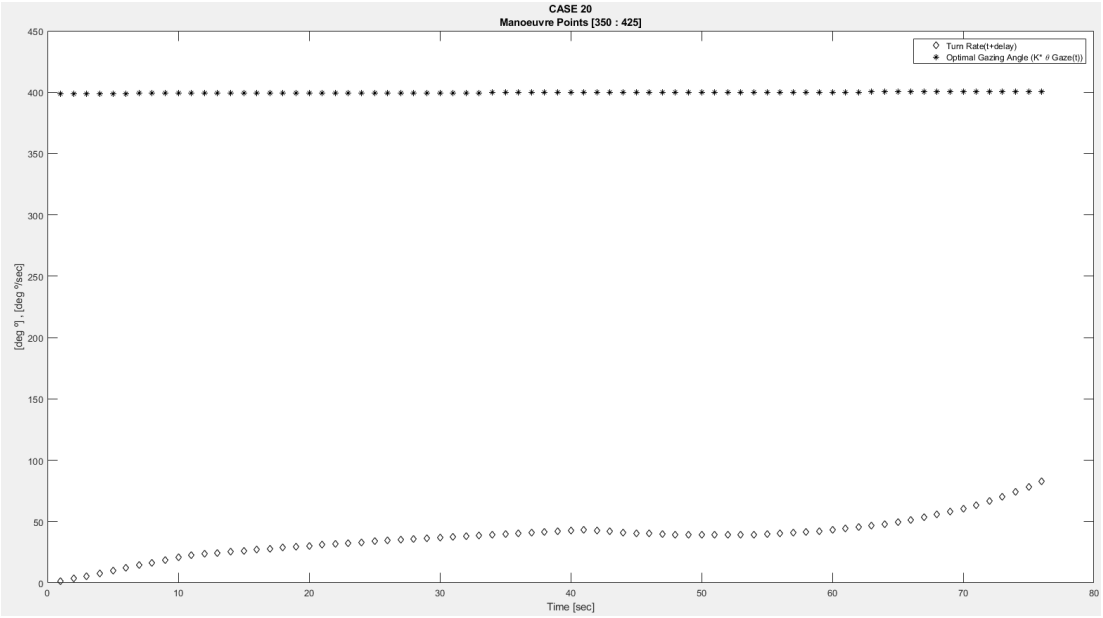

Figure 203Case 20 [350 425] Turn rate vs Gazing angle

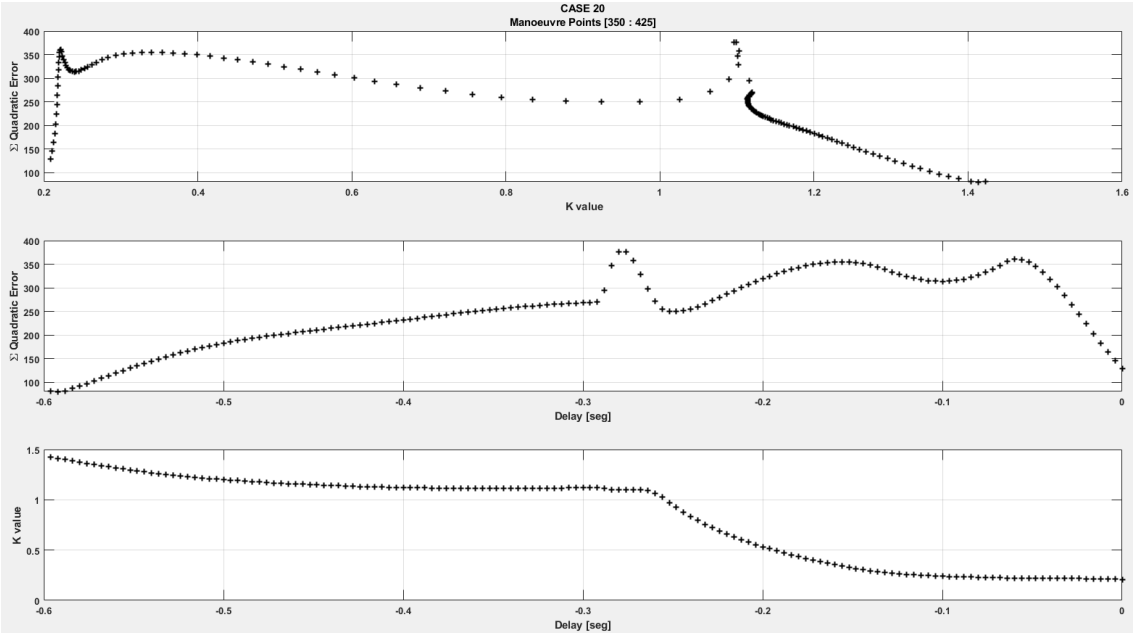

Figure 204Case 20 [350 425] Quadratic Error, Delay and K values

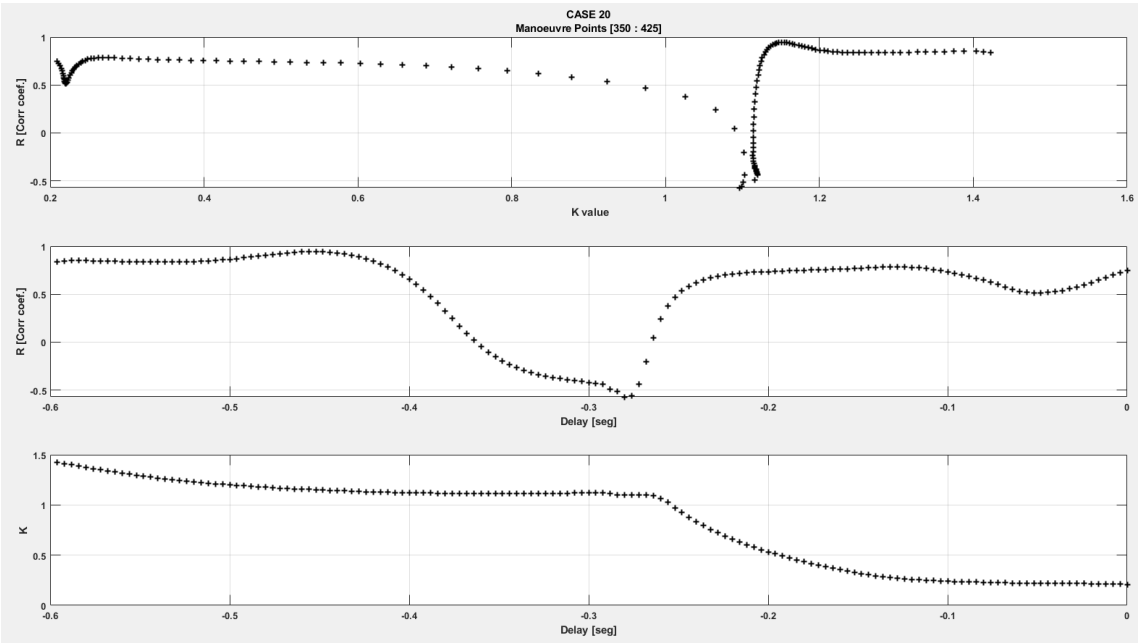

Figure 205Case 20 [350 425] R, delay and k values

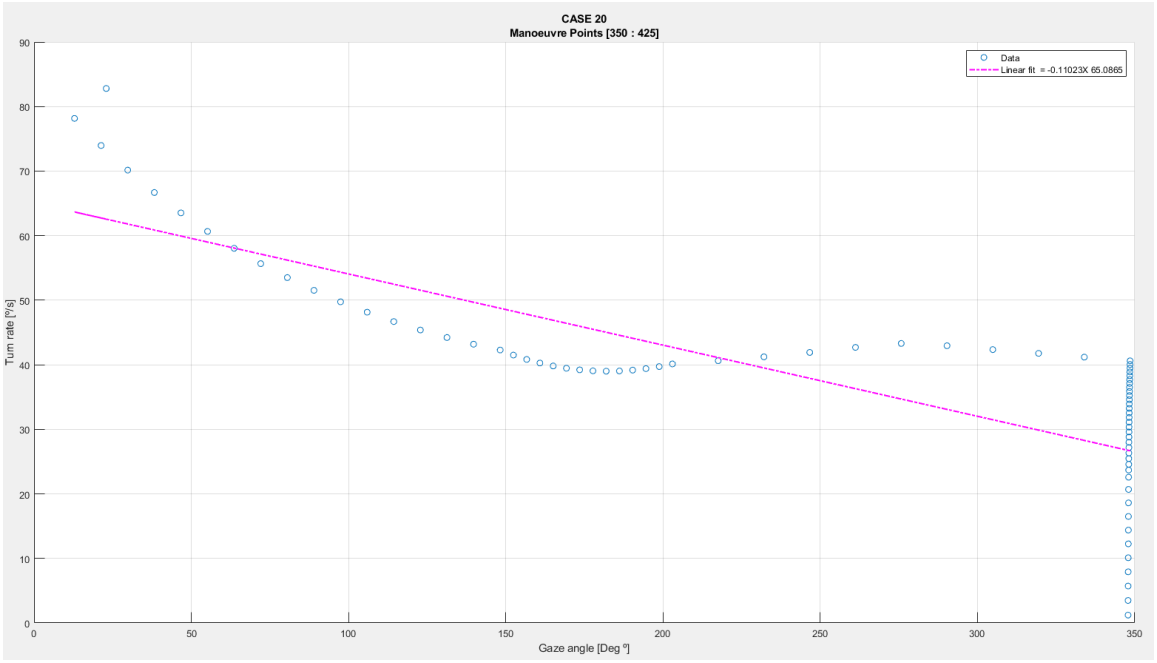

Figure 206Case 20 [350 425] Linear Regression

256 404

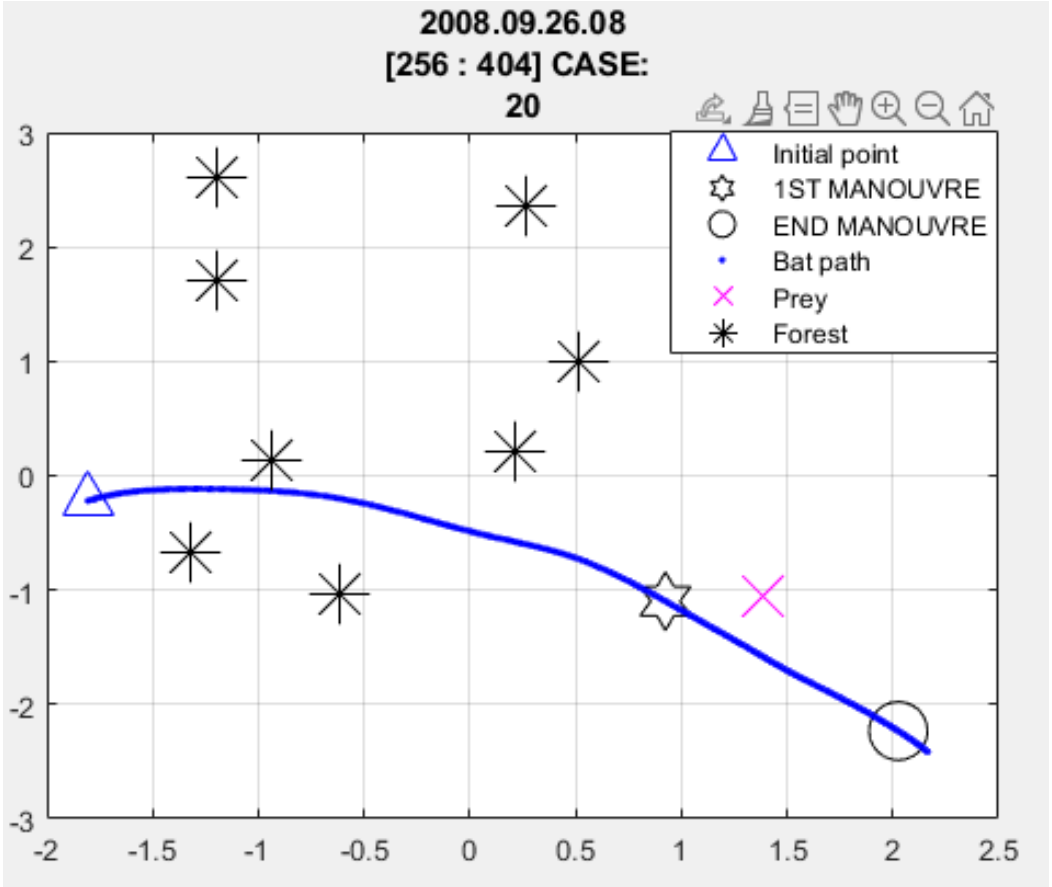

Figure 207 Case 20 [256 404] Flight path

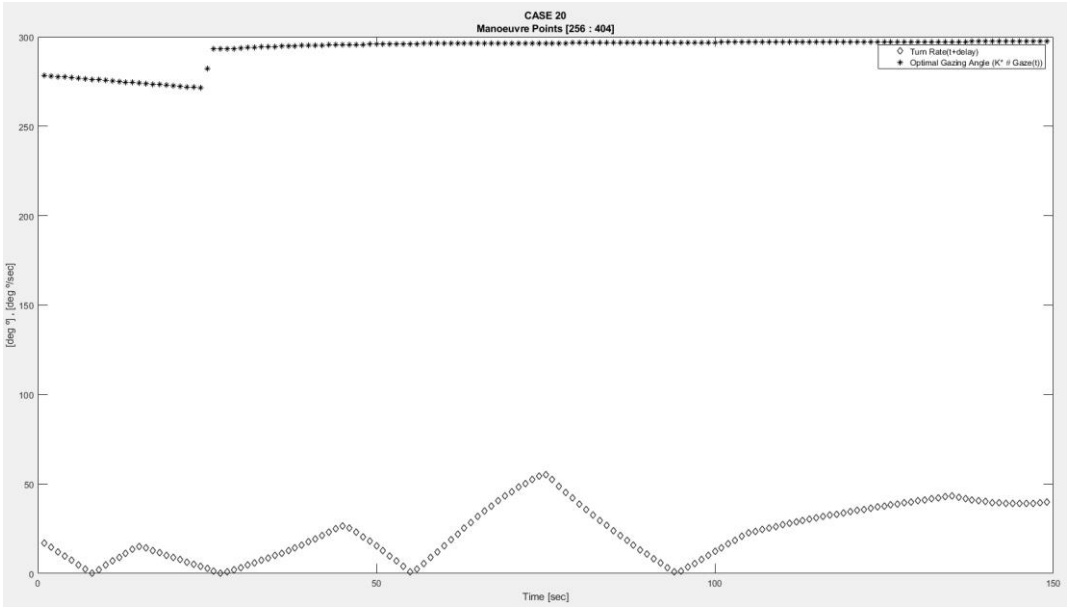

Figure 208Case 20 [256 404] Turn rate vs Gazing angle

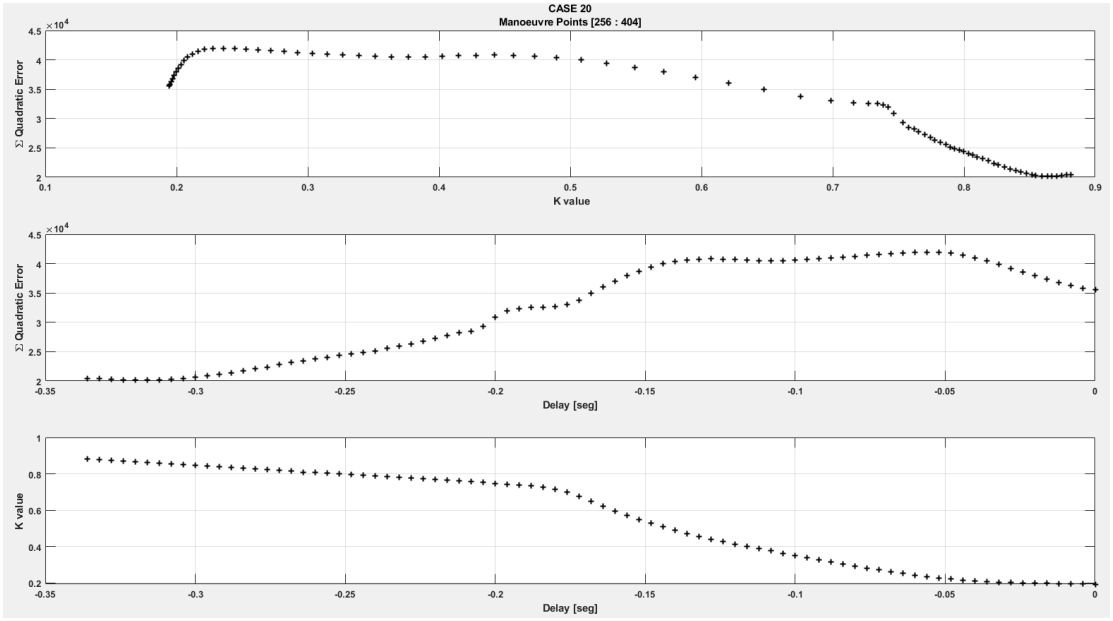

Figure 209Case 20 [256 404] Quadratic error, Delay, and K values

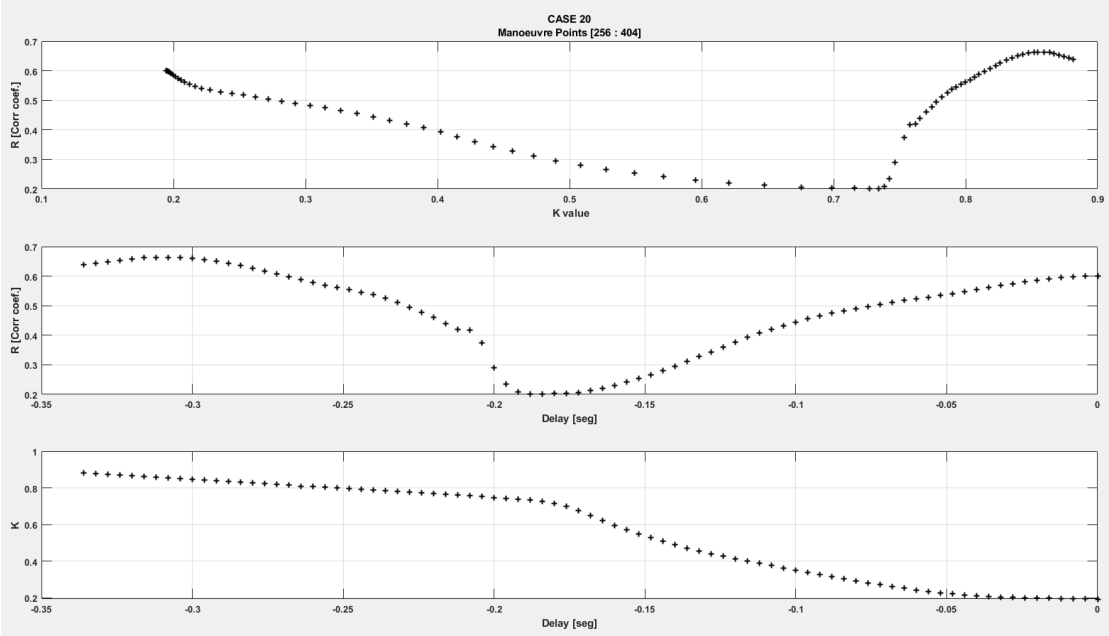

Figure 210Case 20 [256 404] R, Delay and K values

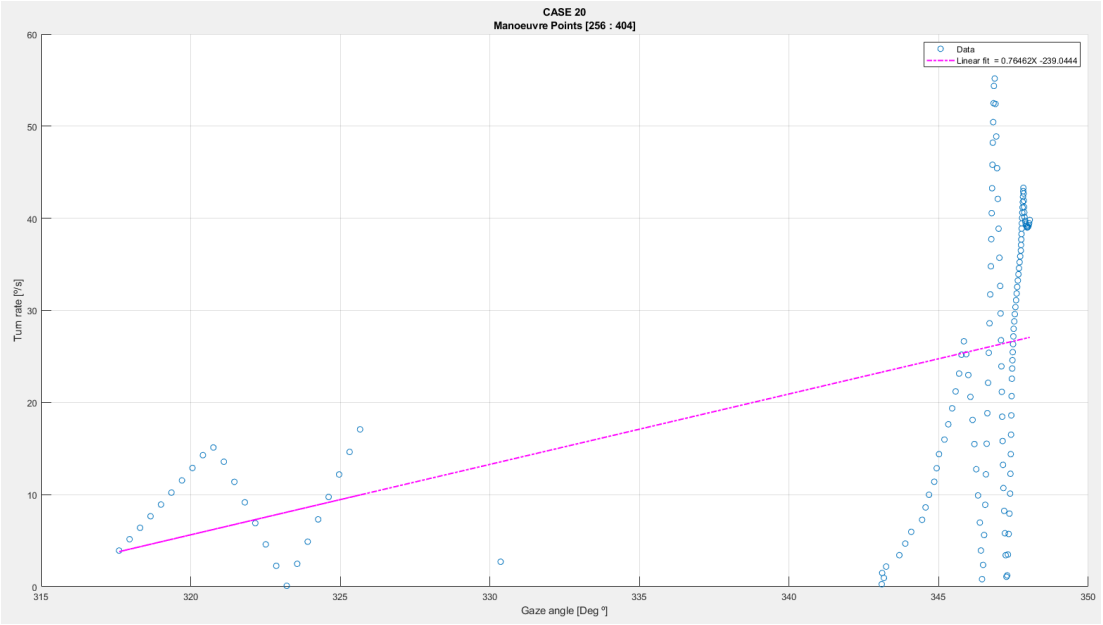

Figure 211Case 20 [256 404] Linear Regression

The previous analysis is summarized in the following table. The columns of $\boldsymbol{R}_{\boldsymbol{max}}$ and $\boldsymbol{k}_{\boldsymbol{opt}}$ were the results obtained from the optimization process while the colum containin $\boldsymbol{k}_{\boldsymbol{linear}}$ is the real linear paratemer when plotting gazing angle at time t , $\theta_{gaze}(t)$, and turn rate at time t plus delay for the $\boldsymbol{k}_{\boldsymbol{opt}}$, $\dot{\theta}_{flight}(t + delay)$.

Flight Case	*Manoeuvre Points*	R_{max}	k_{opt} *[1/s]*	k_{linear} *[1/s]*	$Delay_{opt}$ *[s]*
20	*[30: 90]*	*-0.78*	*0.3*	*-0.051*	*0.068*
20	*[85: 190]*	*0.74*	*0.55*	*-0.41*	*0.236*
20	*[200: 425]*	*-0.54*	*1.09*	*-0.61*	*0.276*
20	*[350: 425]*	*0.94*	*0.26*	*-0.11*	*0.124*
20	*[256: 404]*	*0.66*	*0.76*	*0.76*	*0.304*
13	*[100: 378]*	*0.1*	*0.61*	*-0.66*	*0.33*
13	*[200: 378]*	*-0.53*	*0.606*	*1.5*	*0.316*
13	*[200: 330]*	*0.81*	*0.45*	*-1.2*	*0.136*
11	*[50: 170]*	*0.73*	*10.17*	*7.0*	*0.192*
11	*[190: 359]*	*0.51*	*2.1*	*-0.49*	*0.46*
6	*[150:360]*	*-0.51*	*1.66*	*1.89*	*0.148*
6	*[150:190]*	*0.92*	*4.73*	*-22.35*	*0.476*
6	*[200:360]*	*0.74*	*1.41*	*0.68*	*0.364*
6	*[360:510]*	*0.91*	*0.5*	*0.19*	*0.044*
6	*[520: 608]*	*0.84*	*1.1*	*-0.7*	*0.152*
5	*[70: 180]*	*0.3*	*3.2*	*0.56*	*0.124*
4	*[50: 170]*	*0.35*	*0.74*	*2.44*	*0.196*
4	*[150: 280]*	*0.27*	*2.66*	*2.64*	*0.112*

4	*[220: 280]*	*0.978*	*8.1*	*95.51*	*0.06*
4	*[350: 480]*	*0.88*	*9.7*	*9.63*	*0.1*
4	*[450: 623]*	*0.76*	*5.4*	*7.93*	*0.572*
4	*[450: 553]*	*0.24*	*3.9*	*1.34*	*0.54*
4	*[570: 623]*	*0.71*	*7.7*	*2.78*	*0.436*
3	*[220: 350]*	*0.6*	*2.0*	*2.14*	*0.59*
3	*[220: 300]*	*0.6*	*1.05*	*0.77*	*1.05*
3	*[600:780]*	*0.79*	*0.6*	*-0.26*	*0.404*
3	*[950: 1050]*	*0.68*	*2.4*	*2.73*	*0.4*
3	*[1500: 1709]*	*0.3*	*1.6*	*-0.14*	*0.56*
3	*[1500: 1609]*	*0.6*	*1.4*	*-0.51*	*0.59*
3	*[1620: 1709]*	*0.11*	*1.2*	*-0.54*	*0.22*
2	*[80:170]*	*-0.87*	*6.5*	*12.7*	*0.288*
1	*[270:430]*	*0.87*	*1.7*	*-2.47*	*0.344*
1	*[350:425]*	*-0.83*	*0.77*	*0.6*	*0.116*

Table 2 Data analysis result

5 Discussions

From the table above the main conclusions were the following:

It can be stated that the $\boldsymbol{k}_{\boldsymbol{linear}}$ and $\boldsymbol{k}_{\boldsymbol{opt}}$ were not coincident. Those results indicated that there was a biased error in the analysis. A random time dependant term was included in the optimization cost function to simulate the expected biased error but the magnitude of it were lower than the real one.

The produced error between the optimization and the linear curve fit were due to the data density and the optimization process.

The sound data were interpolated to match the video frame data with a density of 250 frames per second, nevertheless, at least double the data density had to be included for further analysis. The low data density made the linear curve fitting process highly sensible o small data set variation. This way a error threshold was blurring the linear fit, and considering the expected $\boldsymbol{k}_{\boldsymbol{linear}}$ values were between the range of 0 to 1.5. Therefore, random noise was included in the results coming from the big, biased error. When this error were bigger than the k parameter, it made impossible to saw the real k parameter obtained via the optimization algorithm, $\boldsymbol{k}_{\boldsymbol{opt}}$ in the results.

From the table 2 it could be differentiated between the result blurred by a big, biased error and the one with lower biased term because those previous k parameter were almost the same.

All the regression parameter R_{max} with negative value must not be considered even for high values as the k parameter for the linear relationship between the turn rate and the gazing angle had to be positive based on the Tau theory. Therefore, for the negative values, the only explanation was, that in those snapshots of the manoeuvre the gazing angle were not leading the locomotion action. As with visual guided animals like humans, the gazing motor is not always connected to the mission planner with the objective to send the orders to guide the action motor, sometimes other reasons like for instance, pure joy, is leading the sensory motor.

By choosing only between optimized k values, $\boldsymbol{k}_{\boldsymbol{opt}}$, and considering the correlation parameter to be high enough to consider the linear relationship satisfied

the important cases to be considered are for the case number 20, the manoeuvre points between 85 to 190, the manoeuvre happening between 350 to 425, the manoeuvre of 256 to 404.

For the case 13 the flight constrained between 200 and 330.

For the case 6 the path corresponding to 150 to 190 for the high linear correlation value only, the manoeuvre taking place within the points 200 to 360, and the two best manoeuvre selection of this cases that are the one from 360 to 510 and the 520 to 608.

For the flight experiment number high positive correlation number were obtained but the k_{opt} were not as expected. Nevertheless, those cases need to be further analysed too.

For the test case 6 the best selection was the manoeuvre within frames 600 to 780 for both, a highly enough correlation value and expected optimal k parameter. The rest of the cases with a R_{max} around 0.6 could be interesting to revisit for further inspection specially the ones with k_{opt} of 1.05 and 1.4.

The case 1 results were not as good, but it could be good to include one manoeuvre from 270 to 430 frame number due to the high correlation parameter.

By choosing desired values based on the similarity between the optimized k value, k_{opt} , and the linear fit k value, $\boldsymbol{k_{linear}}$, the best analysed manoeuvres are the case 20 points from 256 to 404, the case 6 manoeuvre from 150 to 360, the 200 to 360 and the 360 to 510, the case 4 from 150 to 280 frames and the 350 to 480, the case 3 set of points from 220 to 300 , 220 to 300, and 950 to 1050 and for the case 1 the frames 350 to 425. The results from : case 3 points 950 to 1050, case 3 220 to 350, case 4 points 350 to 480 and 150 to 280, case 1 the frames 350 to 425, were out of the expected range either for a really high k value or really small linear regression coefficient thus, should not be considered for further analysis.

Flight Case	*Manoeuvre Points*	R_{max}	k_{opt} *[1/s]*	k_{linear} *[1/s]*	*Relative Error [%]*	$Delay_{opt}$ *[s]*
20	*[85: 190]*	*0.74*	*0.55*	*-0.41*	*174,54*	*0.236*
20	*[350: 425]*	*0.94*	*0.26*	*-0.11*	*142,30*	*0.124*
20	*[256: 404]*	*0.66*	*0.76*	*0.76*	*0*	*0.304*
13	*[200: 330]*	*0.81*	*0.45*	*-1.2*	*366,66*	*0.136*
6	*[200:360]*	*0.74*	*1.41*	*0.68*	*51,77*	*0.364*
6	*[360:510]*	*0.91*	*0.5*	*0.19*	*62*	*0.044*
6	*[520: 608]*	*0.84*	*1.1*	*-0.7*	*163,63*	*0.152*
3	*[220: 300]*	*0.6*	*1.05*	*0.77*	*26,66*	*1.05*
3	*[600:780]*	*0.79*	*0.6*	*-0.26*	*143,33*	*0.404*
1	*[350:425]*	*0.83*	*0.77*	*0.6*	*22,08*	*0.116*
Mean	*-*	*0,79*	*0,75*	*-*	*115,3*	*0,293*

Table 3 Summary most important results

The delays values obtained were plotted and averaged to obtain the mean value. It has seen that the value for the delay that better fits the formula proposed by Professor Moss was between 0.3 to 0.35 seconds or 300 to 350ms.

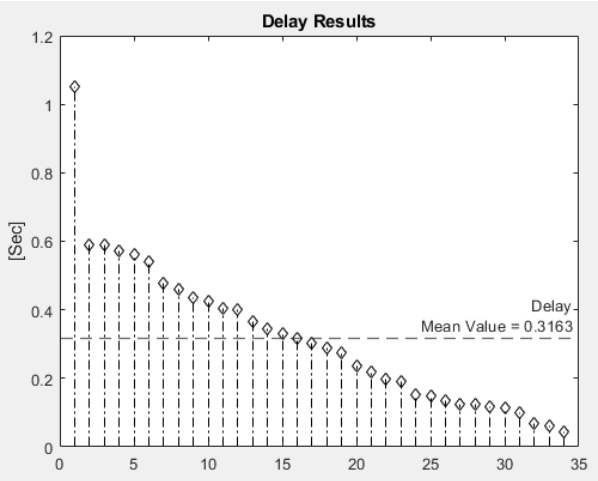

Figure 212 Delay computed from the Bat Lab Data

Those values were higher than the delays from her results thus, a review of the delay have to be done. The higher values for delay in case of her analysis were the search/approach with the highest values of 230ms.

6 Conclusions

The results obtained in the present research were aimed at developing a guidance strategy for a generic UAV. Before that, the results had to be validated with Moss results and connected to the Tau theory.

The main benefits of using the tau theory to derive a control strategy is the possibility to obtain it by using only the kinematic performance. Thus, without considering and neither the need of a dynamical model of the system. This way, the control strategy will be generic and could be implemented in a wide range of flying vehicles with few modifications to adapt the control system for optimal performance. This includes the outside conditions and the vehicle dynamics itself to compute the mass properties to obtain the maximum performance limits. When deriving the control strategy using Tau theory there are two parameter that are not considered the moment to start the movement and the limiting point to start the breaking procedure. Those two were avoided in the tau theory and presupposed.

Tau theory assumptions is that the actions are already started and the braking will occur with enough time to avoid a collision. Lee's research already suggested in the early 90's that an autonomous safe guidance could be achieve by leading a safety margin as the goal border in gap closure. The triggering reaction to star the movement is related with sensor study and the breaking procedure with vehicle dynamic performance. Those two could be a motivation for further research.

Sensors play a fundamental role in any UAV. The literature review has explained the connection that plays the role of sensory taus with the motion taus. The same connection needs to be derived for an autonomous guidance strategy.

A pure autonomous strategy using tau, could be understood as a two-level computing algorithm. The first, receive the desired information from the environment based on the sensors payload and process the information. From sensor data, environment cues will trigger, according to either a human accept input or a predefined function, an action to take. The intrinsic tau guidance will vary with time depending on the situation and desired action pre-programmed or inputs event of the human. This tau function could be understood as a time-varying value.

The procedure to derive a guidance strategy could follow two approaches. One based on an algorithm that output a specific result or following a heuristic process following a rule of thumb. Using neural networks, for example, this could be a threshold to fire an action and this threshold vary depending on the neuron. The action event will occur when the value from the sensor overpasses a desired threshold, e.g., a safety distance to a landing surface or two or more different measurements coordinates such as speed and distance. The motion-tau, or extrinsic tau, or actions to take, is coupled with the logical-tau, or intrinsic tau, that belongs to the decision system or mission planner. It was important to highlight that the previous with just a modest initial and basic suggestion as artificial intelligence is not the field of expertise of the author.

Following Lee's recommendations, the sensor logical function should be modelled as a second order system. [4]

After the results were reviewed not enough satisfactory proofs were found to sturdily stated that the bat followed a particular type of dynamics when

manoeuvring or in tau terms, closing the gaps. Nevertheless, it could be hypothesized that the animal followed a controlled collision manoeuvre to reach desired goal points. Those points have been chosen by the path planner, in an animal example is for instance, survival instincts, motivated from a specific task, in the research of Moss were prey capture. To accomplish that specific task and closure the gap the animal first, needed to navigate and scanned the environment. Thus, for most of the cases, to accomplish a guided task the action taken is not straightforward and the animal adapt its movement to the environment waiting for the final action or desired gap to close. It was for that reason that in some manoeuvres the linear parameter connecting the gazing activity for cue perception is higher than 1. That meant in tau terms, the animal is accelerating, and a collision will occur. For those actions with a $k > 1$, there were a proposed hypothesis. The animal was rushing, accelerating, to accomplish the final manoeuvre at soon as possible. At some point in the trajectory, the animal changes its dynamical pattern and accommodated to the decisive gap to close. In that moment, that could be a series of points, the bat changed its k parameter from $k > 1$ to $0.5 < k < 1$. By doing so, the animal was prepared to capture the prey controlling the break, or declaration process, of its flight dynamics to be corrected in the moment prior to capture the prey. Leading energy momentum on its flight dynamics could help the animal to corrected and redirect the flight in case the prey moved or if the prey was not static in the first place. Moreover, catching a prey is not a task an animal would perform with soft touch as it were a sculptor delicately finishing the details of its art. The animal would energize the movement to catch aggressively and faster as possible the prey.

For the previous reasons, it is fundamental to analyse data corresponding to other tasks that could accommodate the guidance strategy for other purposes.

In terms of data analyse and optimization of the current data. More flight cases and from different bats must be studied. Data analyses have to be done more detailed using as baseline the current research. Other statistical procedure could be used to derive the linear curve fitting function. For instance, more advance system identification procedures.

For the optimization analysis, the algorithm used ‘fminsearch’ from MATLAB is a really easy to use and fast computational tool, as it is a derivative free method, but it is recommended to use either for initial approximations or for cases with unconstrained multivariable function as stated in the MATLAB webpage. For more complex optimization procedure is recommended to use ‘fmincon’ algorithm instead. Moreover, another cost function to obtain the minimum error point is recommended to investigate.

From the personal recommendation of the author, the current research implies the study of a complex phenomenon. Even for trained bats, the analysis of its flight could be of great effort. For that reason, more powerful tool for data analysis is encouraged to use. As patterns with most possible different data set size was aimed to be found, artificial intelligence methods could be a solution that fits better the current data analysis.

For the data used, the heading angle of the flight was constrained to a two-dimensional space. Nevertheless, the author found interesting patterns by looking the three-dimensional trajectory of the animal. It was obvious that first, a two-dimensional guidance strategy needs to be derived to control the yaw angle. Also, including another space dimension not only include the control and guidance of pitch angle but also the roll angle. In any case, looking the three-dimensional space could help future research to recognize patterns to study a particular set from the trajectory, or gaps to be closed.

REFERENCES

[1] Common principle of guidance by echolocation and vision - David N. Lee , F.R. (Ruud) van der Weel , Tris Hitchcock , Eddie Matejowsky , and John D. Pettigrew z. 1992

[2] General Tau Theory: evolution to date- Lee D N, 1976

[3] A Theory of Visual Control of Braking Based on Information about Time-to- Collision. David Lee-1976

[4] Guiding Movement by Coupling Taus - David Lee ,1998

[5] The sonar beam pattern of a flying bat as it tracks tethered Insects- Kaushik Ghose and Cynthia F. Moss, 2003

[6] Adaptive Echolocation and Flight Behaviour in Bats Can Inspire Technology Innovations for Sonar Tracking and Interception - Clarice Anna Diebold, Angeles Salles and Cynthia F. Moss 2020

[7] Steering by Hearing: A Bat's Acoustic Gaze Is Linked to Its Flight Motor Output by a Delayed, Adaptive Linear Law. Kaushik Ghose and Cynthia F. Moss, 2006.

[8] Bats coordinate sonar and flight behaviour as they forage in open and cluttered environments. Benjamin Falk, Lasse Jakobsen, Annemarie Surlykke and Cynthia F. Moss, 2014.

[9] Spatial memory and stereotypy of flight paths by big brown bats in cluttered surroundings. Jonathan R. Barchi, Jeffrey M. Knowles and James A. Simmons, 2013*

[10] The tau of flight control. G. D. Padfield, 2011

[11] Survey of Advances in Guidance, Navigation, and Control of Unmanned Rotorcraft Systems. Farid Kendoul, 2011.

[12] Donald Redfield Griffin the Discovery of Echolocation. Raghuram, H. Marimuthu, G.

[13] Visual information during locomotion. D. Lee et al. 1974

[14] Timing an attacking for hand drive in table tennis. J Exp Psychol: Human Perception and Performance. Bootsma andvan Wieringen 1990

[15] Grasping "tau". Savelsbergh et al. 1991

[16] The Perception of the Visual World. Gibson J J, 1950

[17] Steering by echolocation: a paradigm of ecological acoustics. D. Lee 1995.

[18] The Co-ordination and Regulation of Movements. Bernstein, N

[19] The Future of Drones and their Public Acceptance. Macias, M., Barrado, C., Pastor, E.

[20] Commercial drones are here: The future of unmanned aerial systems. Cohn, P., Green, A., Langstaff, M., Roller, M.

[21] Air-mobility solutions: What they'll need to take off. Duvall, T., Green, A., Langstaff, M., Meie, K.

[22] Drones become even more insect-like. Young, J. ,Garr